A mouse model to study inducible oncogene cooperation *in vivo*

Thesis

UNRESTRICTED ·

Teresa Maria Elisa Modica

Laurea in Scienze Biologiche

A mouse model to study inducible oncogene cooperation *in vivo*

Thesis presented

to the Open University of London

for the Degree of Doctor of Philosophy

Discipline: Life and Biomolecular Science

Date: September 2011

Sponsoring establishment:

Stazione Zoologica Anton Dohrn, Naples (Italy)

Date of Submission : 28 September 2011
Date of Award: 16 Febmuary 2012

ABSTRACT

The current model for cancer development envisions cells undergoing a series of genetic mutations and/or alterations which result in their inability to respond normally to intracellular and extracellular signals that control proliferation, differentiation and death. The number of required genetic alterations varies for different types of cancer and it is likely that further changes occur during its progression to increased malignancy.

Thus, cancer is not a static disease but during the development and progression of tumour, multiple changes occur in two kinds of genes: oncogenes and tumour suppressor genes.

Oncogene-products can be classified as growth factors, growth factor receptors, Ras oncoproteins, cytoplasmic protein kinases, transcription factors, anti-apoptotic proteins.

In particular, the *ras* oncogene family includes three members: *N-ras*, *K-ras*, *H-ras*. In non-transformed cells, Ras protein, belonging to G-protein family, transduces growth signals from external to the internal environment. In fact, when activated, Ras exchanges GDP with GTP and this allosteric change allows binding of Ras effector molecules and transduction of signalling cascades. Ras activity is required for cell cycle progression.

In cancer it has been observed that this oncogene is constitutively activated by mutations and induces the cell to enter into cell-cycle also in the absence of growth signals.

Among the transcription factors, a gene involved in many tumours is *myc*. This transcription factor plays a key role in cell proliferation as its target proteins include many positive regulators of the cell-cycle. In tumour cells the protein product of this oncogene is overexpressed.

The cooperation between multiple oncogenes and/or loss of tumour suppressors from different functional classes is necessary for transformation to proceed.

In fact, it was observed that, although overexpression of a single oncogene does not transform wild-type mouse embryonic fibroblasts, combinations of *myc* and *H-ras*^{VAL12}, can induce cellular transformation and the cells expressing both oncogenes displayed a marked proliferative advantage.

In thyroid, neoplastic transformation generates several different histotypes of tumours, ranging from poorly aggressive and well-differentiated, to highly malignant and undifferentiated anaplastic cancers.

The aim of my thesis was to study the tumorigenesis induced by oncogenes and the oncogene cooperation *in vivo* during the gradual passage from a poorly aggressive to a much more aggressive tumour.

To this end a mouse model expressing the two oncogenes *H-ras*^{VAL12} and c-*myc* (referred as *ras* and *myc*) in a tissue-specific as well as in a conditional manner was generated.

For this purpose, the coding sequences of the two oncogenes were fused in a bicistronic construct and an IRES (Internal Ribosome Entry Sequence or Site) was inserted between them, to ensure the expression of the second oncogene. The construct was inserted under the control of the promoter of the ubiquitously expressed genes ROSA26 and Eef1α1.

In order to express these oncogenes in a tissue-specific manner, the transcription of the two oncogenes is prevented by a STOP sequence flanked by two LoxP sites. Such a STOP sequence can be removed by Cre recombinase protein.

The transgenic mice were crossed with mice expressing Cre in a tissue-specific manner. Two strains of transgenic mice expressing Cre in thyroid cells were used:

1. transgenic mice for TgCre, in which Cre is expressed under the control of Tg promoter after the development of the thyroid;

2. Pax8Cre, in which the Cre sequence is inserted in the Pax8 locus and is expressed during the early stages of the thyroid development.

In such a manner the oncogenes were expressed only in thyroid cells, but were still inactive.

In particular, *ras* was fused to the mutated ligand binding domain of the estradiol receptor that is sensitive to tamoxifen and not to endogenous estradiol; while *myc* was fused to the mutated ligand binding domain of the progesterone receptor (hPR891) that is sensitive to RU486 and not to endogenous progesterone.

With these fused oncogenes it is possible to activate only Ras (with tamoxifen) or only Myc (with RU486) or both (providing both tamoxifen and RU486).

Moreover the activity of two oncogenes might be used to immortalize mouse cell lines in culture.

INDEX

LIST OF ABBREVIATIONS pag.1

CHAPTER 1 INTRODUCTION

1.1 Neoplasms and oncogenes pag.6

1.2 The thyroid gland pag.7

1.2.1 Thyroid tumours and their molecular mechanisms pag.12

1.3 The *ras* proto-oncogene

1.3.1 The *ras* history pag.17

1.3.2 The *ras* family pag.18

1.3.3 Molecular mechanisms of Ras activity pag.21

1.3.4 The *ras* pathways pag.25

1.3.5 The *ras* oncogene pag.27

1.3.6 Molecular mechanisms of Ras activity

in thyroid cancerogenesis pag.29

1.4 The *c-myc* proto-oncogene

1.4.1 The *c-myc* history pag.32

1.4.2 The *myc* family pag.33

1.4.3 Molecular mechanisms of *c-myc* activity pag.35

1.4.4 The *c-myc* pathways pag.38

1.4.5 *c-myc*: between cell cycle and apoptosis pag.41

1.4.6 The *c-myc* oncogene pag.42

1.4.7 The *c-myc* oncogene in thyroid pag.44

1.5 Oncogenes and cancer development pag.45

1.5.1 *ras* and *myc* co-operation pag.47

1.6 Aim of the Ph.D. project and experimental strategy pag.52

CHAPTER 2 MATERIALS AND METHODS

Part A: Molecular Biology

A.1 Plasmid Manipulation

A.1.1 Digestion with restriction enzymes,
de-phosphorylation reaction, Klenow reaction pag.57

A.1.2 Purification of DNA pag.58

A.1.3 Agarose gel electrophoresis pag.58

A.1.4 Isolation of DNA from agarose gel pag.59

A.1.5 Ligation reactions pag.59

A.1.6 Transformation of *E.coli* with plasmid DNA pag.59

A.1.7 Isolation of plasmid DNA from *E.coli* pag.60

A.1.8 pCEFL vector pag.61

A.2 Western blot

A.2.1 Protein extraction, purification and quantification pag.61

A.2.2 Sodium Dodecyl Sulfate-PolyAcrylamide
Gel Electrophoresis (SDS-PAGE),
Protein transfer from gel to membrane
and membrane blocking pag.62

A.2.3 Primary and Secondary antibodies pag.63

A.2.4 Immune complexes detection pag.64

A.2.5 Membrane stripping pag.64

A.3 Processing of RNA

A.3.1 RNA extraction pag.65

A.3.2 RNA reverse transcription pag.65

A.3.3 mRNA quantification pag.66

Part B: Cell Culture

B.1 Cell lines maintaining and transfections and monitoring assays

B.1.1 HeLa, NIH3T3 and COS7 cell lines pag.67

B.1.2 FRTL-5 cell line pag.68

B.1.3 Cultures of mouse embryonic stem cells pag.68

B.1.4 Splitting pag.68

B.1.5 Freezing pag.69

B.1.6 Thawing pag.69

B.1.7 Transient and stable transfection pag.69

B.1.8 ATPlite assay pag.70

B.2 Electroporation of ES cells

B.2.1 DNA preparation pag.71

B.2.2 Cells preparation pag.71

B.2.3 Selection pag.72

B.2.4 Picking Colonies pag.72

B.2.5 Freezing electroporated ES cells pag.73

B.2.6 Thawing electroporated ES cells pag.73

B.2.7 DNA extraction from ES cells pag.74

B.2.8 Screening of the electroporated ES cells pag.74

B.2.9 Preparation of ES cells for blastocyst injection pag.75

Part C: Animal husbandry

C.1 *ROSA26c-myc-PR-ER-Hras^{V12}*

and Eef1α1c-*myc-PR-ER-Hras^{V12}* mouse strains pag.76

C.2 *ROSA26c-myc-PR-ER-Hras^{V12}*

or *Eef1α1c-myc-PR-ER-Hras*^{V12}/TgCRE-ER

or Pax8CRE mouse strains pag.76

C.3 Genotyping of mutant mice pag.77

C.4 Mice treatments pag.79

Part D: Hystological procedures

D.1 β-galactosidase staining pag.80

D.2 Immunohistochemistry pag.80

D.3 Histological staining pag.81

Part E: Vectors assembling

E.1 The RasMyc vector: cloning strategy pag.82

E.2 The MycRas vector: cloning strategy pag.84

CHAPTER 3 RESULTS

Part A: The vectors pag.89

A.1The RasMyc expression vector pag.90

A.2 The MycRas expression vector pag.98

Part B: Analysis of oncogenes expression

B.1 Transient transfections pag.104

B.2 Stable transfections pag.109

B.2.1 Analysis of genes involved in thyroid differentiation pag.113

B.2.2 Proliferation assays pag.116

B.2.2.1 Colony assay pag.117

B.2.2.2 ATPlite assay pag.125

B.2.3 The ERK protein phosphorylation pag.128

B.2.4 Analysis of *H-ras* and *c-myc* target genes pag.131

Part C: Studies in mice: conditional onco-mice

C.1 Generation of onco-mice

C.1.1 The targeting vectors pag.134

C.1.2 ES cells electroporation and screening pag.142

C.1.3 Genotyping of conditional onco-mice pag.145

C.1.4 Mouse strains expressing CRE pag.147

C.1.5 Treatments with the hormones pag.151

C.2 Phenotype of conditional onco-mice

C.2.1 Molecular phenotype pag.152

C.2.2 Histological phenotype pag.156

CHAPTER 4 DISCUSSION pag.160

BIBLIOGRAPHY pag.171

ACKNOWLEDGEMENTS pag.196

LIST OF ABBREVIATIONS

aa	amino acid
AP-1	Activating Protein-1
β-gal	β-galactosidase
βgeo	βgalactosidase-neomycin resistance sequence
bHLH	basic region helix-loop-helix
bZip	basic region leucine zipper
CDS	Coding Sequence
CIP	Calf Intestinal alkaline Phosphatase
Cl4	clone 4
Cl7	clone 7
Cl11	clone 11
Cre	Cyclization recombination
Ct	Threshold Cycle
DK	Kilo Dalton (kDa)
DMEM	Dulbecco's modified Eagle's medium
DMSO	Dimethylsulfoxide
E	embryonic day
Eef1α1	Eukaryotic translation elongation factor 1 alpha 1 *locus*
Eef1α1MycRas	Eef1α1-c-*myc*-PR-ER-H*ras*^{V12} allele
EMS	E box *myc* site sequence
EMCV	Encephalomyocarditis virus
E-Onc/PaxCRE	Eef1α1MycRas; Pax8CRE/Pax8+ mouse
E-Onc/TgCRE	Eef1α1MycRas; TgCRE-ER mouse

ER	murine Estrogen (estradiol) Receptor tamoxifene sensitive
ER-*ras* or ER-Ras^{V12}	ER-*H-ras*^{V12}
ER-ras-myc-PR cassette	ER-H*ras*^{V12}-c-*myc*-PR bicistronic cassette
ES	Embryonic Stem cells
EtOH	Ethanol
FRTL-5	Fischer Rat Thyroid Low serum 5%
FW	Forward primer
GAP	GTPase Activating Proteins
GDP	Guanosine Diphosphate
GDS	Guanine nucleotide Dissociation Stimulators
GEF	Guanine nucleotide Exchange Factors
GTP	Guanosine-5'-triphosphate
G418	Neomycin
HaMSV	Harvey Murine Sarcoma Virus
HAT	Histone Acetyltransferase complex
HRP	Horseradish Peroxidase
HVR	Hypervariable Region
IMP	Impedes Mitogenic signal Propagation
IRES	Internal Ribosome Entry Sequence
KSR	Kinase Suppressor of Ras
LBD	Ligand Binding Domain
loxP	locus of crossing [x-ing]-over
MbI	Myc-boxes I
MbII	Myc-boxes II
MCS	Multi Cloning Site

MEFs	Mouse Embryonic Fibroblasts
mw	Molecular Weight
myc-PR	c-*myc*-PR
myc-PR-ER-ras cassette	c-*myc*-PR-ER-H*ras*^{V12} bicistronic cassette
MycRas (clone/plasmid)	c-*myc*-PR-ER-H*ras*^{V12} (clone/plasmid)
NCF	Newborn Calf Serum
Neo	Neomycin resistance sequence
NIS	sodium (Na^+)/iodine (I^+) Symporter
ODC	Ornithine Decarboxylase
pCEFL-Ras vector	pCEFL-ER-H*ras*^{V12} vector
PCI	Phenol:Chloroform:Isoamyl Alcohol (25: 24: 1)
PR	Progesterone Receptor RU486 sensitive
RasMyc (clone/plasmid)	ER-H*ras*^{V12}-c-*myc*-PR (clone/plasmid)
REFs	Rat Embryo Fibroblasts
Rev	Reverse primers
R-Onc/PaxCRE	ROSA26MycRas; Pax8CRE/Pax8+ mouse
R-Onc/TgCRE	ROSA26MycRas; TgCRE-ER mouse
ROSA26	Reverse Orientation Splice Acceptor *locus*
ROSA26MycRas	ROSA26-c-*myc*-PR-ER-H*ras*^{V12} allele
RT	Room Temperature
RT-PCR	Real Time PCR
RU486	Mifepristone
SA	Splicing Acceptor sequence
SHE	Syrian Hamster Embryo
SOS	Son of Sevenless
SV40	Simian Virus 40

TAD	Trans Activation Domain
TAg	Tumor Antigen
TAM	Tamoxifene (for mice)
Tg	Thyroglobulin
THOX	Thyroid oxidase
TP	Tamoxifene (for mice) (or 4OHT-tamoxifene for cells) and Mifepristone
TPO	Thyroperoxidase
TRF	Thyroid-stimulating hormone Releasing Factor
TRRAP	TRansactivation/tRansformation Associated Protein
TSH	Thyroid-Stimulating Hormone
TSHR	TSH Receptor
T_3	triiodothyronine
T_4	thyroxine or tetra-idothyronine
T0	Time 0
T2gg	Time 2 days
T4gg	Time 4 days
T6gg	Time 6 days
wt	wild type
+ ctr	positive control
- ctr	negative control
3xpA	triple polyadenylation sequence
4H-TSH-INS	medium lacking both TSH and insulin
4OHT	4OH-tamoxifene
5H-INS	medium lacking insulin
5H-TSH	medium lacking TSH

6H	complete medium containing all the six hormones

CHAPTER 1

INTRODUCTION

1.1 Neoplasms and oncogenes

Neoplasm's, which literally means "new growths", can develop from normal cells of many tissues. Consequently, there are a wide variety of tumours differing with respect to their origin, growth and prognosis.

The most important biological distinction between tumours is that between benign and malignant neoplasms, only the latter is referred to as cancer. While the former remains confined to the site of its formation, the malignant one is capable of invading and destroying adjacent tissues as well as distant organs.

Studies on genes capable of inducing malignant transformation in normal cells, have led to the identification of *proto-oncogenes*, many of which are involved in the normal transmission of growth-promoting signals from the cell surface to the nucleus or are transcription factors and *tumour suppressor genes*, i.e. normal cellular genes that suppress malignant transformation.

Proto-oncogenes are a group of normal cell genes, functioning in a number of features of cell growth and differentiation that, if mutated, may acquire transforming activity. This kind of genes can be activated, to undergo a neoplastic transformation, by different mechanisms: insertional mutagenesis, chromosome translocation, gene amplification, point mutation.

1.2 The thyroid gland

The thyroid gland, a component of the endocrine system, derives its name from the Greek word 'thyreos' meaning 'shield'and 'eidos' meaning 'form'. In humans, the thyroid gland is located in front of the trachea, in the lower neck.

The thyroid gland, in all vertebrates, is responsible for producing thyroid hormones, known for their role in regulating metabolism in adults and required for many developmental processes.

The human thyroid gland is a brownish-red organ, in most cases having two lobes connected by an isthmus; normally weighs about 28g and consists of cuboidal cells arranged to form epithelial follicles, supported by connective tissue that forms a framework for the entire gland. In the normal thyroid gland, the follicles are usually filled with a colloidal substance containing the protein thyroglobulin (Tg) in high concentration. The thyroid hormones thyroxine (or tetra-idothyronine, T_4) and triiodothyronine (T_3) are covalently bound to Tg, as a results of a biochemical process involving several components of the thyroid cells machinery. Tg is eventually taken up by the follicular cells and proteolytically degraded in order to allow release of free T_3 and T_4 into the bloodstream.

Thyroglobulin is first detected at E16.5 in mouse development. At this stage also other genes specific of thyroid follicular cells, such as the thyroperoxidase *(TPO)*, *TSH* receptor (TSHR) and the sodium (Na^+)/iodine (I^+) symporter (*NIS*) are expressed. TPO drives iodide oxidation, its incorporation in tyrosine residues of the Tg molecule and catalyzes the coupling of iodinated tyrosine residues, to form T4 or T3. TSHR, a member of the glycoprotein G protein-coupled-receptor family able to respond to TSH, is secreted by the pituitary thyrotrophs and all steps in the formation and release of thyroid hormones are stimulated by TSH. NIS, present in the basolateral membrane of the thyroid cell, is responsible for the transport of iodide by an active process, in which

the downhill transport of two Na^+ ions results in the entry of one iodide atom against an electrochemical gradient. Their expression is governed by at least four transcription factors whose coexpression is a distinctive feature of the thyroid anlage. These genes involved at early stages of the thyroid morphogenesis are *Titf1/Nkx2.1*, *Foxe1*, *Pax8* and *Hhex*. They form a network of reciprocal cross-interactions changing as the thyroid primordium progresses from one developmental stage to another (Parlato et al., 2004).

In more detail, Titf1/Nkx2.1 is a homeodomain-containing transcription factor member of the Nkx2 family. In thyroid it is detectable around E9.5 but two additional domains of expression are the lung and restricted areas of the brain (Kimura et al., 1996; Lazzaro et al., 1991). This protein was initially identified for its ability to bind to specific DNA sequences present in the thyroglobulin and thyroid peroxidase gene promoters. The thyroid anlage is comparable in wild type and Nkx2.1-/- embryos up to E9. However, already at E10.5 the thyroid primordium shows a reduced expression of Pax8, Foxe1 and Hhex and appears much smaller compared to wild type (Parlato et al., 2004). Subsequently, thyroid cells disappear through apoptosis, which ultimately leads to the loss of primordial cells and absence of thyroid by E12-13 (Kimura et al., 1999). Moreover, embryos homozygous for a targeted disruption of the *Titf1/Nkx2.1 locus* develop and are born but die at birth due also to respiratory insufficiency, caused by severely hypoplastic lungs (Kimura et al., 1999). Hence, Nkx2.1 seems to act as a survival factor for developing thyroid progenitor.

Pax8 (paired box gene 8) is a member of a family of transcription factors characterized by the presence of a DNA binding domain called paired domain. During embryonic life, Pax8 is not only detected in the endodermal cells of the developing thyroid since E8.5 (Plachov et al., 1990) but also in the myelencephalon and in the kidneys. This factor recognizes and binds to specific sequences present in both *Tg* and *TPO* promoters and directly interacts with Nkx2.1 in differentiated thyroid follicular

cells. This interaction could be relevant in the expression of thyroid-specific genes. Pax8-/- embryos show a morphologically normal thyroid anlage. The thyroid bud evaginates from the endoderm and migrates into the mesenchyme. The absence of Pax8 causes that by E10.5 the thyroid primordium appears hypoplastic and negative for the expression of Foxe1 and Hhex (Parlato et al., 2004). At E11.5, the follicular cells are essentially undetectable. Pax8-/- mice are born with a low body weight, die within 2–3 weeks of birth and present a rudimentary gland, composed almost completely of calcitonin-producing C cells (Mansouri et al., 1998). According to these observations also Pax8 is required for the survival of thyroid cell precursors.

Foxe1 (formerly called TTF-2 for thyroid transcription factor-2) is a transcription factor member of the winged helix/forkhead family. At early stage of embryogenesis, Foxe1 mRNA is expressed in the endodermal layer of the foregut, in the thyroid anlage and in the ectoderm that will give rise to the anterior pituitary (Zannini et al., 1997). Homozygous *Foxe1*-/- mice are born at the expected ratio but die within 48 h after birth (De Felice et al., 1998). Analysis of these mutant mice shows that in the absence of this factor the specification of the thyroid anlage is correct. However, the migration of thyroid precursor cells is impaired: in E9.5 *Foxe1* null embryos, thyroid precursor cells are still on the floor of the pharynx, whereas in wild type embryos they are detached from the pharynx cavity and begin to descend (De Felice et al., 1998). E10 Foxe1-/- mutant mice exhibit either a small thyroid remnant still attached to the pharyngeal floor or no thyroid gland at all, while in wild type embryos it is already descending towards its final location. At later stages, *Foxe1* null thyroid cells either disappear or form an ectopic small thyroid remnant able to synthesize Tg (De Felice et al., 1998). These data indicate that Foxe1, in addition to cooperation in the control of the survival of thyroid cells, is specifically involved in the migration of the thyrocytes.

Hhex (formerly known as Hex for hematopoietically expressed homeobox or Prh for proline-rich homeobox) is a homeodomain-containing transcription factor, first identified in multipotent hematopoietic cells and widely expressed in early organogenesis. For this reason, *Hhex* null embryos show multiple malformations and are not viable after E15.5. Moreover, in *Hhex* null embryos at E9, the thyroid anlage is present and the expressions of Nkx2.1, Pax8 and Foxe1 are not affected. In these mutants at a later stage (E10), the thyroid primordium is represented only by a few nonmigrating cells which do not express Nkx2.1, Pax8 or Foxe1 mRNA. At later stages, the primordium disappears. These data strongly suggest that Hhex is involved in the survival of already determined thyroid precursors. Because Hhex is required to maintain Nkx2.1, Pax8 and Foxe1 expression in the developing thyroid, the thyroid phenotype displayed by Hhex-/- embryos might be due to the absence of these factors (Parlato et al., 2004).

Pendrin, a second protein involved in iodide transport, is the product of the PDS gene, responsible for the autosomal recessive disorder, *Pendred's syndrome*. This is a long-recognized inherited condition in which sensorineural hearing loss is combined with varying degrees of impaired thyroid hormone synthesis, leading to goiter. Pendrin is a transmembrane protein, a member of the sulfate transport protein family. Pendrin is expressed in the apical border of the thyroid cell, the inner ear, and the kidney (Heller N 1999). Mutations in pendrin cause an inner ear malformation, although not all patients have goiter. It is postulated that pendrin is required for iodide transport across the apical membrane of the thyrocyte into the follicular lumen, where it is then oxidized and coupled to tyrosine in Tg (Porra et al., 2002).

A schematic illustration of a thyroid follicular cell is depicted in figure 1.

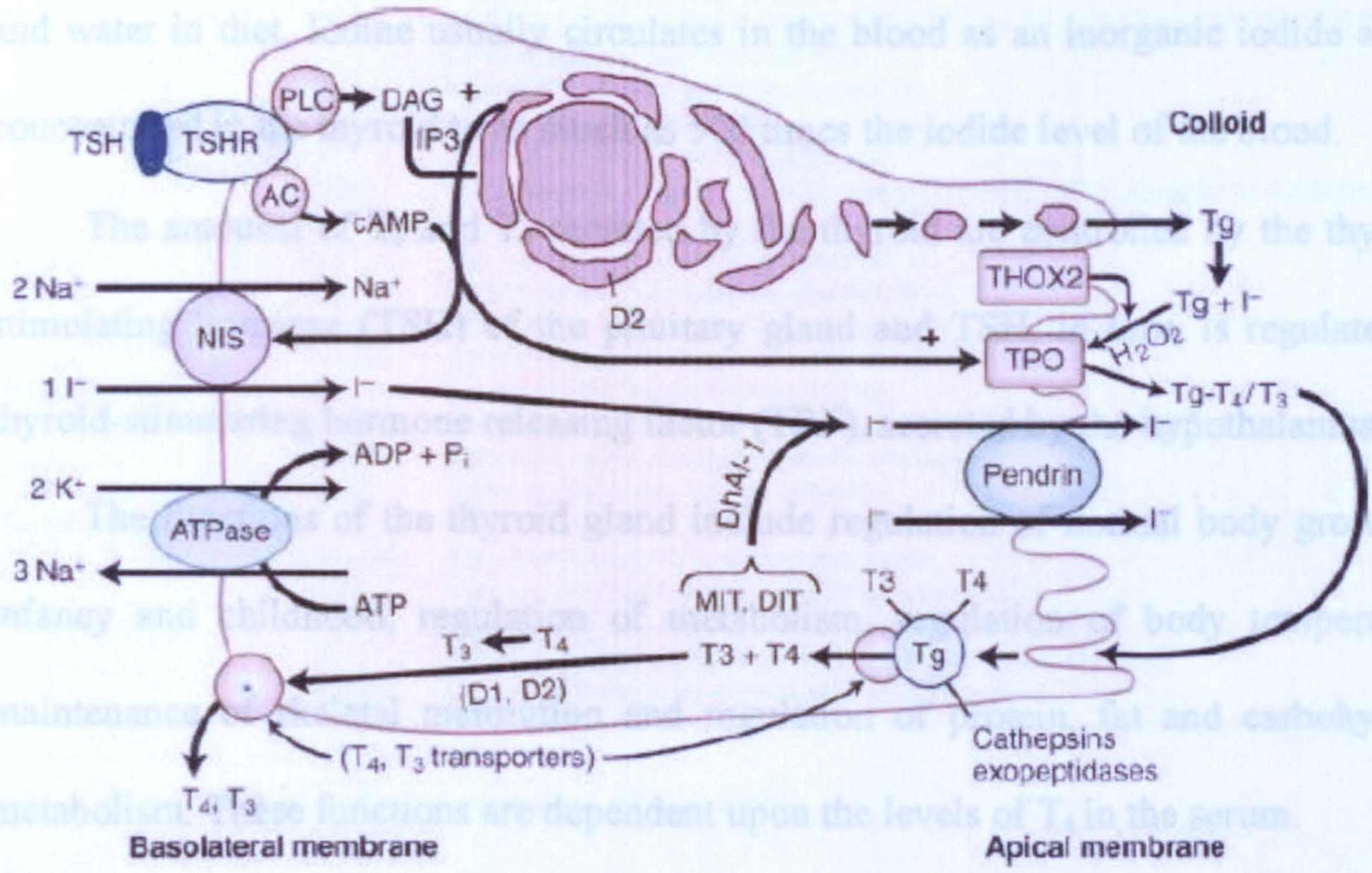

Figure 1. Schematic illustration of a follicular cell showing the key aspects of thyroid iodine transport and thyroid hormone synthesis. Sodium-iodide symporter (NIS); triiodothyronine (T3); thyroxine (T4); thyroglobulin (Tg); thyroid peroxidise (TPO); thyrotropin receptor (TSHR). Modified from (Spitzweg et al., 2000).

Although the thyroid gland constitutes about 0.5 percent of the total human body weight, it holds about 25 percent of the total iodine in the body, obtained from food and water in diet. Iodine usually circulates in the blood as an inorganic iodide and is concentrated in the thyroid to as much as 500 times the iodide level of the blood.

The amounts of T_3 and T_4 secreted by the thyroid are controlled by the thyroid-stimulating hormone (TSH) of the pituitary gland and TSH, in turn, is regulated by thyroid-stimulating hormone releasing factor (TRF), secreted by the hypothalamus.

The functions of the thyroid gland include regulation of normal body growth in infancy and childhood, regulation of metabolism, regulation of body temperature, maintenance of skeletal maturation and regulation of protein, fat and carbohydrate metabolism. These functions are dependent upon the levels of T_4 in the serum.

1.2.1 Thyroid tumours and their molecular mechanisms

In thyroid, neoplastic transformation generates several different histotypes of tumours, ranging from poorly aggressive and well differentiated, such as papillary thyroid carcinoma and follicular thyroid carcinoma, to highly malignant and undifferentiated anaplastic cancers.

Many oncogenes are implicated in this carcinogenetic process and among them also the *ras* oncogene (Gimm, 2001) (Tables 1 and 2).

Overview of genes implicated in the pathogenesis of thyroid carcinoma

Histological type	Gene	Comment
Papillary (PTC)	*RET/PTC*	Rearrangements are found in up to 40% (regional differences exist) At least eight rearrangements *RET/PTC1* most common in non-irradiated PTC and late post-Chernobyl PTC, *RET/PTC3* most common in early post-Chernobyl PTC
	TRK	Rearrangements may also be quite common At least three rearrangements
	P53	Involved in the dedifferentiation process
	PTEN	Underexpressed (cytoplasmic rather than nuclear expression), almost never mutations
	ras	Mutations may be early event in oncogenesis
	MET	May be overexpressed without mutations
	p16	May be mutated, methylation found in 33%
	c-erbB-2	Expressed in about 50% (cytoplasmic and nuclear expression)
	'mtDNA'	Somatic mitochondrial DNA mutations identified
Follicular (FTC)	*p53*	Involved in the dedifferentiation process
	ras	Mutations early event in oncogenesis and seemingly more common in tumours with metastases
	PPARγ	Seemingly only rearranged in cancers, not in adenomas
	PTEN	Underexpressed, almost never mutations
Undifferentiated (UTC)	*p53*	Overexpressed, often mutated
	β-Catenin	Mutations found in 61%, nuclear localisation
	PTEN	Very low levels of expression, high frequency of LOH
Medullary (MTC)	*RET*	Germline missense mutations in >95% of hereditary cases Somatic missense mutations in about 30–50% in sporadic cases
	c-erbB-2	Expressed in seemingly 100% (restricted to cytoplasm)

Table 1. Genes involved in thyroid carcinoma (Gimm, 2001).

Table 2. Mutation of genes involved in thyroid carcinoma (Gimm, 2001).

Mutation frequency, LOH frequency, and expression levels of genes mainly implicated in the pathogenesis of thyroid carcinoma[a]

		Normal/Adenoma	PTC	FTC	UTC	MTC
RET	Mutations	Negative (?)	Somatic mutation rearrangements 10–40%	Negative	Negative	hMTC Germline mutation >95%, sMTC Somatic mutation 30–50%
	LOH					
	Expression	Negative	Increased			Increased
TRK	Mutations	Negative	Somatic mutation rearrangements 5–25%	Negative	Negative	
	LOH					
	Expression	Negative	Increased			TrkC increased
p53	Mutations	0%	< 5%	< 5%	> 75%	Rare
	LOH					
	Expression	0%	High 11%	High 14%	High 64–71%	Rare
ras (Ha-, K-, N-)	Mutations	14–50%	5–20%	24–53%	20–60%	Negative
	LOH					
	Expression	0–56%	Increased 0–60%	Increased 0–53%	Increased 0–60%	33%
PTEN	Mutations	0%	2–3%	8%	0%	
	LOH	6–26%	5–21%	7–30%	35–59%	
	Expression	***	*/**	*/**	Negative/(*)	
PPARg	Mutations	Negative	Negative	Fusion with PAX8 (62%)		
	LOH					
	Expression					

[a] PTC, papillary thyroid carcinoma; hMTC, hereditary MTC; FTC, follicular thyroid carcinoma; sMTC, somatic MTC; UTC, undifferentiated thyroid carcinoma; MTC, medullary thyroid carcinoma; LOH, loss of heterozygosity; (*), expression almost absent; *, weak expression; **, moderate expression; ***, strong expression.

Constitutive activation of all the members of *ras* family, observed in the full range of thyroid malignancies (Sherman, 2003), suggests that it could be an early event (Garcia-Rostan et al., 2003) and its different frequencies depend on the tumour type (Table 3) (Tallini, 2002).

Table 3. Molecular alteration in thyroid tumours (Pallini, 2002).

Molecular Alterations in Thyroid Tumors of Follicular Cells

	Oncogene activation						Tumor suppression inactivation			
			TK							
	TSHr/GSα	H-, K-, N-Ras	RET rearrangement (RET/PTC)	NTRK1 (TRKA) rearrangement	MET overexpression	Wnt/ β-Catenin	CDK inhibitors[a]	p53	PTEN	PPARγ rearrangement
Adenoma	60% of toxic hyperplastic nodules and adenomas with TSHr or GSα mutations	10–20%	Absent	Absent	<10%	Absent	Decreased p27/Kip1 expression compared with normal thyroid	Absent	Loss of heterozygosity in 10–25% of cases; decreased nuclear expression but preserved cytoplasmic expression	Uncommon (10% of cases)
Follicular carcinoma	Rare	10–20%	Absent[b]	Absent	10%	Absent	Low p27/Kip1 expression (10–20% of cases)	Absent	Loss of heterozygosity in up to 30% of cases; decreased expression in 30–40% of cases	Common (60–70% of cases)
Papillary carcinoma	Rare	10%	35–50% (RET/PTC1: 30–40%; RET/PTC2: <5%; RET/PTC3: 5–10%)[c]	10%	70–80%	Absent	Low p27/Kip1 expression (10–20% of cases); p21/WAF1 gene deletion in 10% of cases	Absent	Gene mutations or loss of heterozygosity in 5% of cases; decreased expression in 30–40% of cases	Absent
Poorly differentiated carcinoma	Rare	50%	10–20%	Rare	70–80%	25%	Low p27/Kip1 expression (30% of cases)	Mutations in 20–30% of cases	Decreased expression	Rare?
Undifferentiated (anaplastic) carcinoma	Rare	50%	Rare	Rare	Rare?	60%	Low p27/Kip1 expression (50–60% of cases)	Mutations in 70–80% of cases	Loss of heterozygosity in 10% of cases; decreased expression in 50–60% of cases	Rare?

[a]The CDK inhibitors p15 INK4b and p16 INK4a are rarely mutated in thyroid tumors, although methylation of promoter or regulatory sequences may result in functional inactivation.
[b]Recent reports indicate that RET/PTC is present in a significant proportion of tumors with oncocytic features [103,104].
[c]Both RET/PTC1 and RET/PTC3 have a high prevalence in radiation-associated papillary carcinoma, with up to 60% of positive cases for each type of rearrangement according to different series.

Among the most common mutations in *ras*, there is the substitution of glycine with valine at position 12 in the first exon. The FRTL-5 cell line was transfected to stably express a constitutively active form of cellular *ras* carrying the mutation $HRas^{V12}$. A loss of differentiation of these cells was observed concomitantly with high levels of the protein, demonstrating the association between the *ras* oncogene and the most aggressive cancer of the thyroid gland showing no expression of the differentiated phenotype (De Vita et al., 2005).

As in many tumours, an increase in the levels of c-Myc has been found also in thyroid neoplasms including many thyroid carcinoma cell lines; the highest being in the more malignant, undifferentiated cell lines. Moreover, a block of c-Myc protein synthesis could inhibit the growth rate of the thyroid carcinoma cell lines, indicating that c-*myc* overexpression plays a critical role in the growth of thyroid cancer cells. These findings support the hypothesis that this proto-oncogene might be involved in thyroid neoplastic progression (Cerutti et al., 1996).

1.3 The *ras* proto-oncogene

1.3.1 The *ras* history

The first studies on the *ras* proto-oncogene date back to the beginning of the '60s, when some retroviruses, carrying murine leukaemia, were identified to induce sarcomas in rodents, thus leading to the acronym "*ras*" for rat sarcoma.

Later, these tumorigenic sequences derived from the rat genome and the cellular homologues of the well-characterized retroviral oncogenes were found related to the human oncogenes. The nucleotide sequences of the *H-ras* and *K-ras* were published in 1982 and later those of *N-ras*. In the following years, more light was shed on their

activity, function, structure and mutation as depicted in figure 2, (Malumbres and Barbacid, 2003).

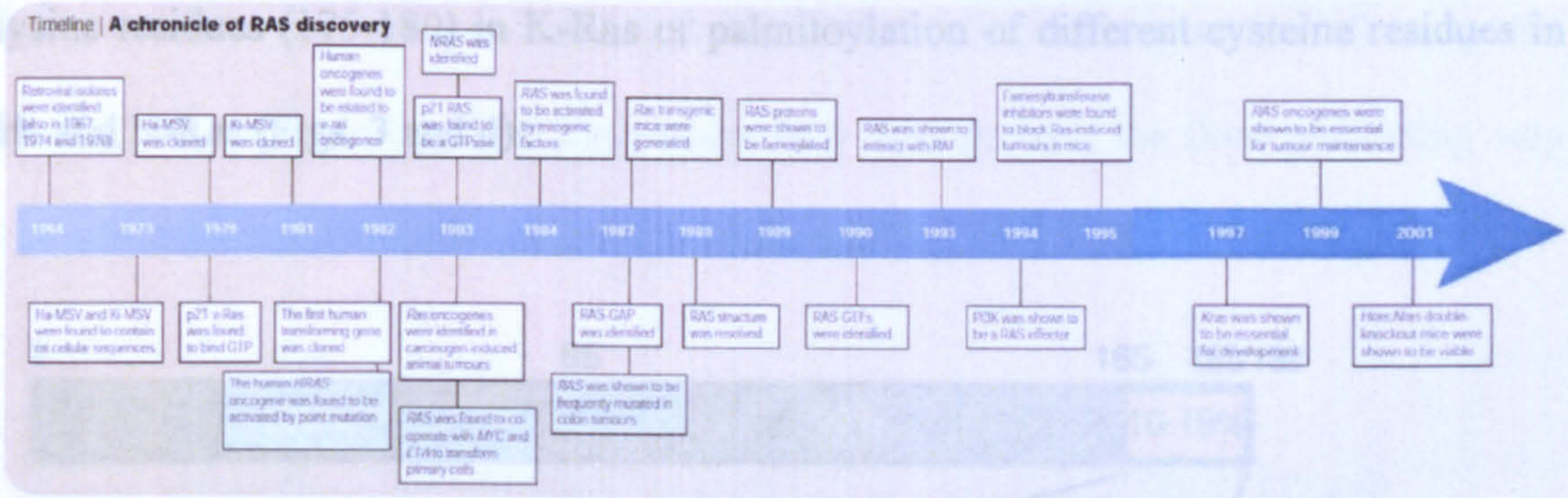

Figure 2. The *ras* history (Malumbres and Barbacid, 2003).

1.3.2 The *ras* family

In mammalians, the Ras family includes four isoforms tightly related among them: H-Ras, K-Ras4a, K-Ras4b and N-Ras. The *H-*, *K-* and *N-ras* genes are expressed in each tissue and cell type with a varying pattern depending on the organ, embryonic developmental stage and postnatal differentiation. All the three genes encode very similar products, the p21 proteins, which could be required in different amounts at different times in a tissue-specific manner (Leon et al., 1987).

The Ras family proteins undergo a series of post-translational modifications at the level of C-terminal region, to make it more hydrophobic. The three proteins share the same sequence for the first 85 residues at the N-terminal region and have a 90% degree of homology in the following 80 residues. The last 24 residues of the proteins exhibit significant sequence divergence. This hypervariable region (HVR), with about 10-15% conservation among the three isoforms, is composed of two domains: the membrane-targeting domain and the linker domain. The first one is divided in two subdomains: the C-terminal CAAX motif (C=cysteine, A=aliphatic amino acid,

X=serine or methionine) and the signal sequence. The cysteine of the CAAX sequence is farnesylated and then, after the proteolysis of the AAX sequence, carboxylmethylated. The second signal sequence consists of a polybasic stretch of six lysine residues (175-180) in K-Ras or palmitoylation of different cysteine residues in H- and N-Ras (Figs. 3 and 4).

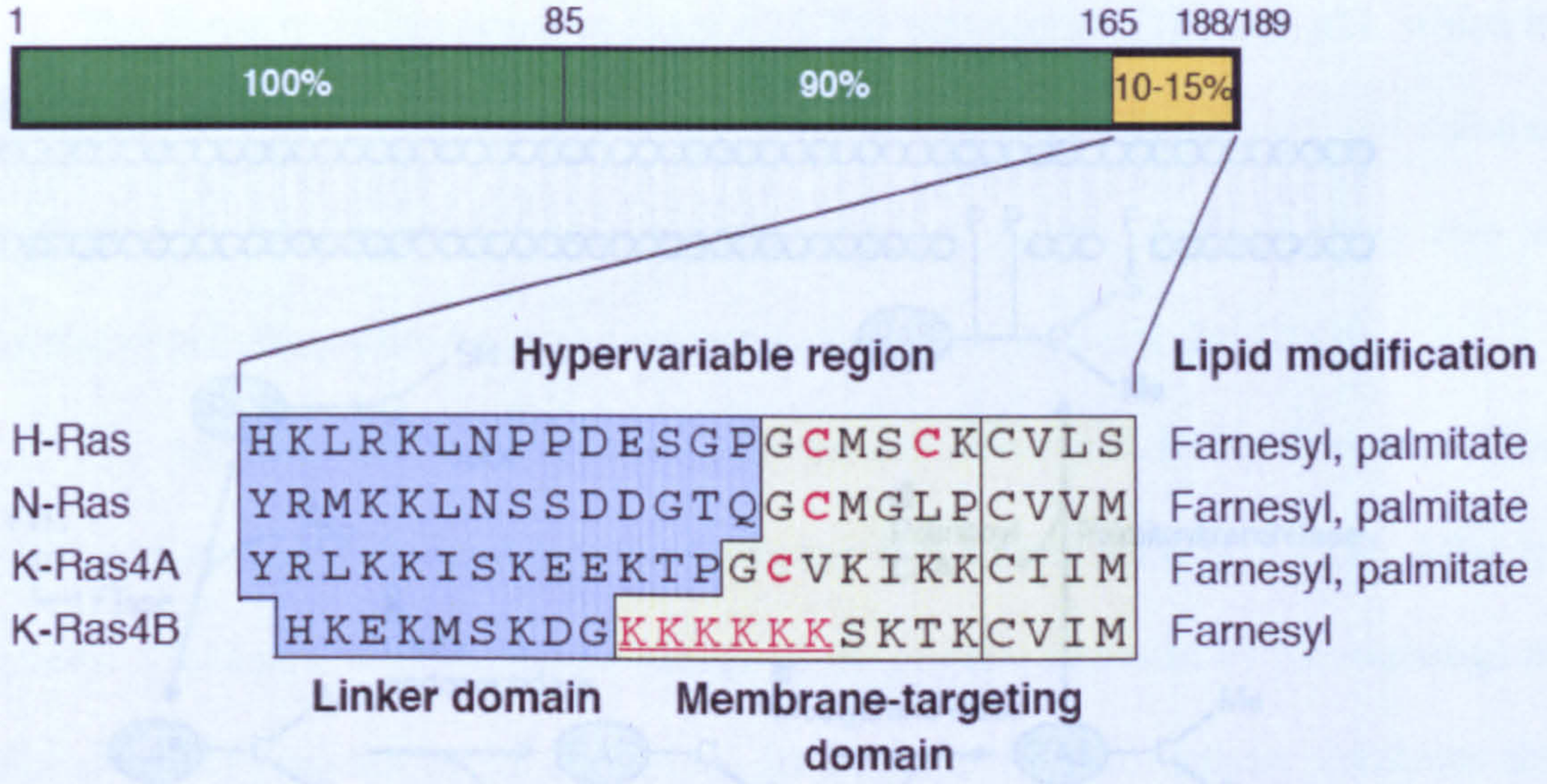

Figure 3. Ras hypervariable regions. The diagram shows the degree of sequence conservation between isoforms along the Ras protein; all of the effector, exchange factor and nucleotide-binding sites in the N-terminal conserved domains. The hypervariable region (HVR) is the only region of significant divergence between the Ras proteins and exhibits <10-15% sequence identity between any two isoforms. The HVR can be divided into two domains: the membrane-targeting domain and the linker domain. The membrane-targeting domain is made of the C-terminal CAAX motif, common to all Ras proteins, plus second signal sequences: cysteine palmitoylation sites (shown in red) in H-Ras, N-Ras and K-Ras4A or a polybasic domain in K-Ras4B (shown in red and underlined) (Prior and Hancock, 2001).

Newly synthesized Ras is a cytosolic protein and needs post-translational modifications to reach its final localization in the plasma membrane and to exert its function.

For H- and N-Ras, a farnesyltransferase catalyses the transfer of the 15-carbon isoprenoid chain from farnesyl pyrophosphate to a cysteine residue at the carboxyl

terminus and through its farnesyl group, Ras associates with the intracellular membranes (Fig. 4).

The three amino acids (AAX) at the carboxyl terminus are removed by an endopeptidase and the new carboxyl terminus is then methylated. Following the addition of two palmitoylated long-chain fatty acid groups, the final processing step consists in its transportation to the plasma membrane.

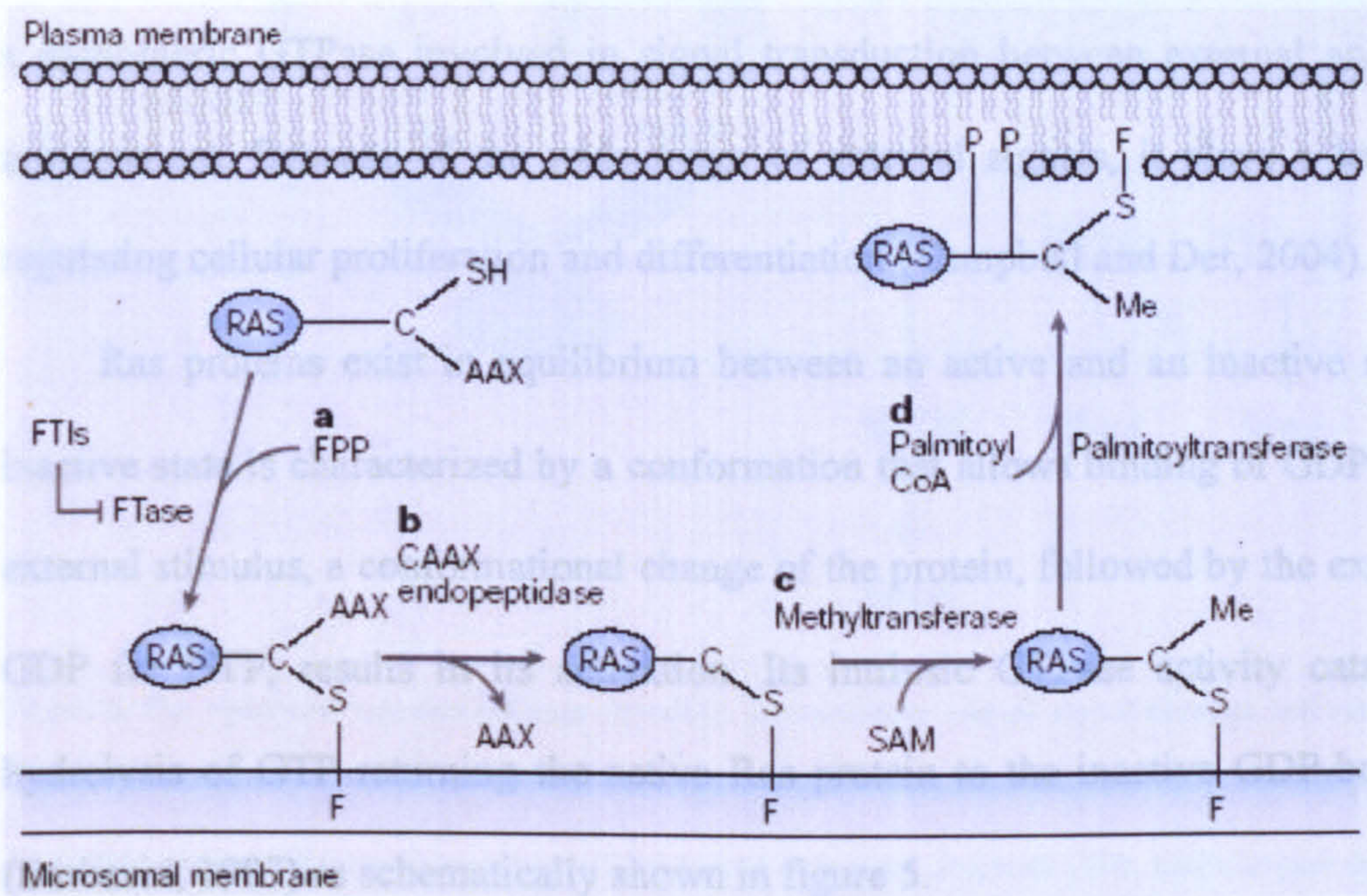

Figure 4. Post-translation processing of Ras proteins. Farnesyltransferase (FTase); farnesyl pyrophosphate (FPP); farnesyl group (F); palmitoyl long-chain fatty acid groups (P) (Downward, 2003).

Instead, K-Ras does not become palmitoylated and its movement towards the plasma membrane is promoted by an interaction between the negatively charged lipid and a group of lysine residues in its carboxyl terminus.

Since the three isoforms differ among themselves for the different post-translational modifications that confer different membrane anchors to the mature proteins, it seems possible that they have different functions because of their localization on the plasma membrane (Downward, 2003; Matallanas et al., 2003; Prior and Hancock, 2001).

In particular, the human *H-ras* gene is located on the minus strand p15.5 band of the chromosome 11 and consists of seven exons with the first as well as the last untranslated. The transcript encodes for a 189 aa long protein.

1.3.3 Molecular mechanisms of Ras activity

The *H-ras* proto-oncogene encodes a 21 KD polypeptide (188 aa), p21, which is a monomeric GTPase involved in signal transduction between external and cellular environment. Because of the wide range of external signals, it plays a key role in regulating cellular proliferation and differentiation (Campbell and Der, 2004).

Ras proteins exist in equilibrium between an active and an inactive state. The inactive state is characterized by a conformation that allows binding of GDP. After an external stimulus, a conformational change of the protein, followed by the exchange of GDP for GTP, results in its activation. Its intrinsic GTPase activity catalyses the hydrolysis of GTP returning the active Ras protein to the inactive GDP-bound state (Barbacid, 1987) as schematically shown in figure 5.

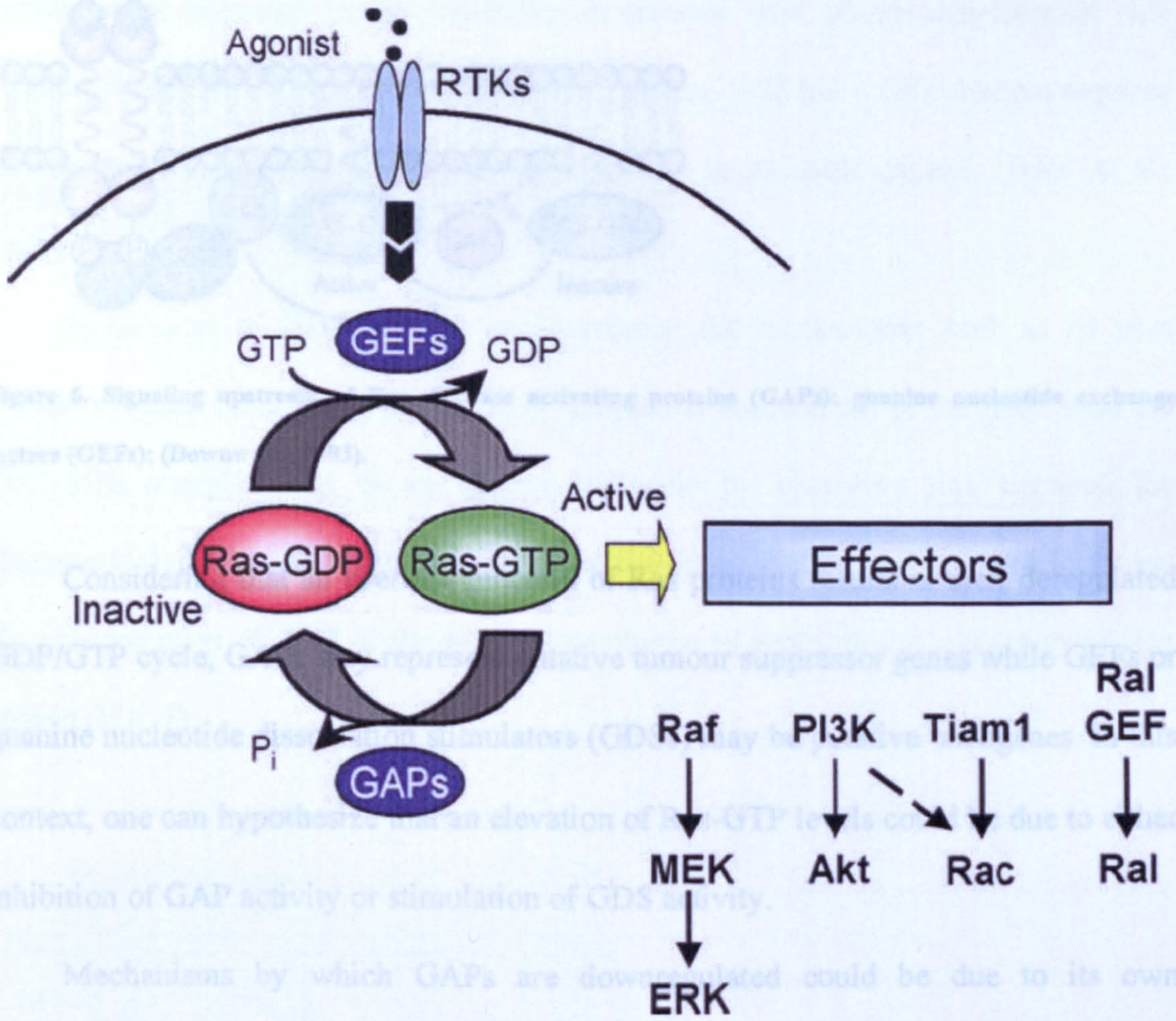

Figure 5. Ras upstream and downstream signaling. Extracellular stimuli signal through cell surface plasma membrane receptors, for example, RTKs. Through a variety of adaptor proteins, these signals cause guanine nucleotide exchange factors to replace the GDP-bound to inactive Ras with GTP. GAPs trigger the hydrolysis of GTP back to the inactive GDP-bound form. GTP-bound Ras binds to a plethora of downstream effector molecules to stimulate intracellular signaling of several pathways. Activation of these pathways and others cause changes in many mechanisms leading to transformation, invasion and metastasis (Campbell and Der, 2004).

The H-Ras protein, localized at the level of the inner face of the plasma membrane, carries out its function through the acivities of two distinct families of proteins: Guanine nucleotide Exchange Factors (GEFs) and GTPase Activating Proteins (GAPs). The GEFs facilitate the activation, whereas the GAPs the return of Ras back to the inactive state (Fig. 6). The balance between these proteins determines the activation state of Ras.

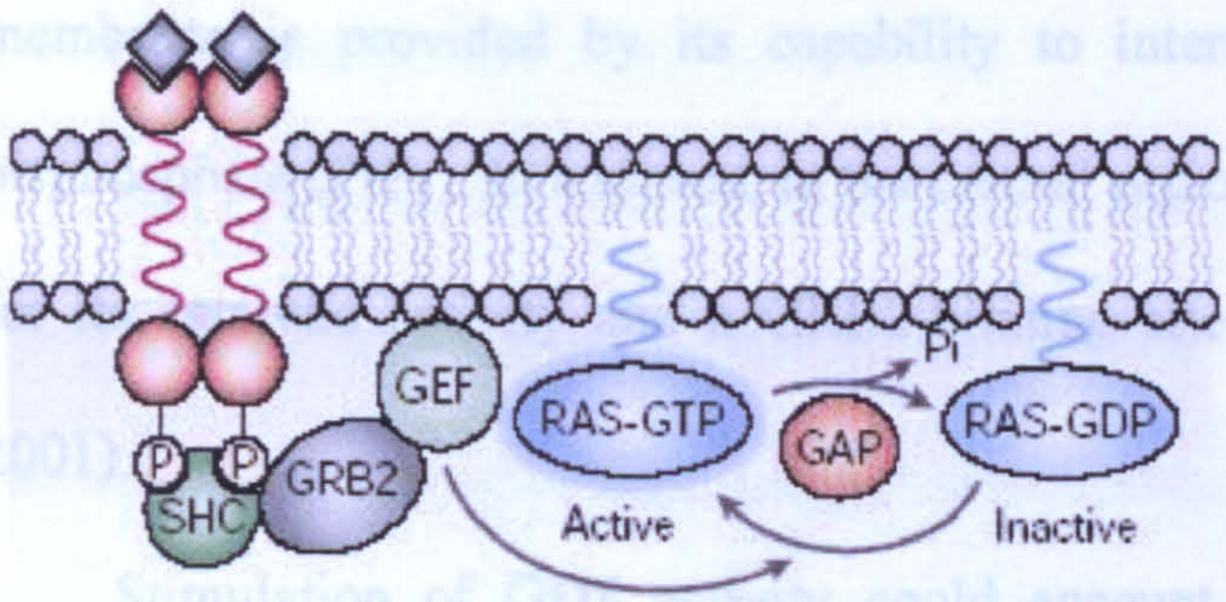

Figure 6. Signaling upstream of Ras. GTPase activating proteins (GAPs); guanine nucleotide exchange factors (GEFs); (Downward, 2003).

Considering that an aberrant function of Ras proteins results in their deregulated GDP/GTP cycle, GAPs may represent putative tumour suppressor genes while GEFs or guanine nucleotide dissociation stimulators (GDSs) may be putative oncogenes. In this context, one can hypothesize that an elevation of Ras-GTP levels could be due to either inhibition of GAP activity or stimulation of GDS activity.

Mechanisms by which GAPs are downregulated could be due to its own phosphorylation or the phosphorylation of two GAP-associated phosphoproteins p62 and p190. Another mechanism by which GAP activity may be regulated is because certainly mitogenically stimulated lipids may interact with p120 GAP or with its opposite GTPase inhibiting protein (Kazlauskas et al., 1990; Li et al., 1992; Medema et al., 1993; Tsai et al., 1990).

As regards GDSs, the best studied activation mechanism involves the assembly of complexes of activated, autophosphorylated growth-factor-receptor tyrosine kinases with the Son of Sevenless (SOS) GEF through the adaptor protein GRB2 resulting in the recruitment of SOS to the plasma membrane, where Ras is located (Downward, 2003).

Among the GEF family, SOS, the most studied and first identified in *Drosophila*, was cloned for one human and two murine homologs. SOS exerts its function downstream of a receptor tyrosine kinase. Its localization at the level of plasma

membrane is provided by its capability to interact with phosphatidylinositol 4,5-bisphosphate (PIP_2). In addition, in the central region, SOS has a GEF domain required for its catalytic activity and a GRB2-binding site in its carboxyl end (Takai et al., 2001).

Stimulation of GDS activity could account for mechanisms such as its own phosphorylation (Gulbins et al., 1993) or membrane association. In the latter case the Grb2-SOS complex acts as an adaptor molecule by providing link between the phosphorylated tyrosine receptor kinase and the membrane-bound Ras and increases the concentration of SOS at the plasma membrane to promote the activation of Ras protein (Fig. 7).

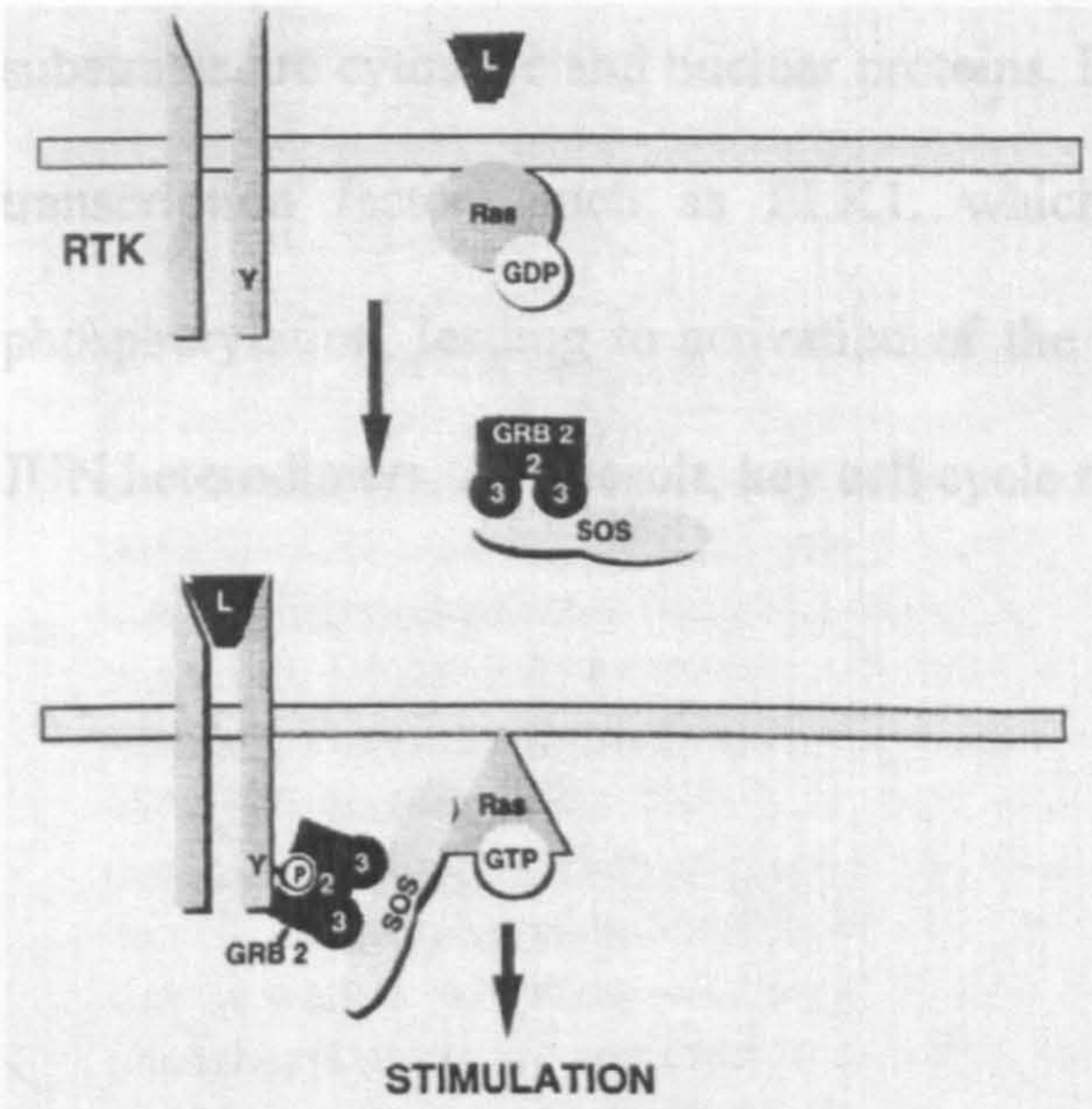

Figure 7. Grb2 mediates the translocation of SOS to the plasma membrane. Present evidence suggests that SOS activation of Ras protein is triggered by the translocation of the Grb2/SOS complex to the plasma membrane during the mitogenic stimulation via receptor tyrosine kinases (Khosravi-Far and Der, 1994).

1.3.4 The *ras* pathways

Ras is one of the proteins implicated in the transmission of extracellular stimuli from external environment to cellular environment by a signaling cascade that converts fast signals into long-term responses. When activated by a receptor tyrosine kinase, Ras in turn activates many proteins present in different pathways downstream. Among the most intensively studied mammalian pathways of Ras, is the MAP-kinase cascade involving three serine-threonine kinase referred as MAP-kinase kinase kinase, MAP-kinase kinase and MAP-kinase.

The first effector of this cascade is the protein serine/threonine kinase Raf, which, when activated, phosphorylates and activates mitogen-activated protein kinases (MAPKs) extracellular signal-regulated kinases 1 and 2, ERK1 and ERK2. Their substrates are cytosolic and nuclear proteins. In the latter case, they act on ETS family transcription factors such as ELK1, which regulates Fos expression and c-Jun phosphorylation, leading to activation of the AP1 transcription factor made by FOS-JUN heterodimers. As a result, key cell cycle regulatory proteins are expressed (Fig. 8).

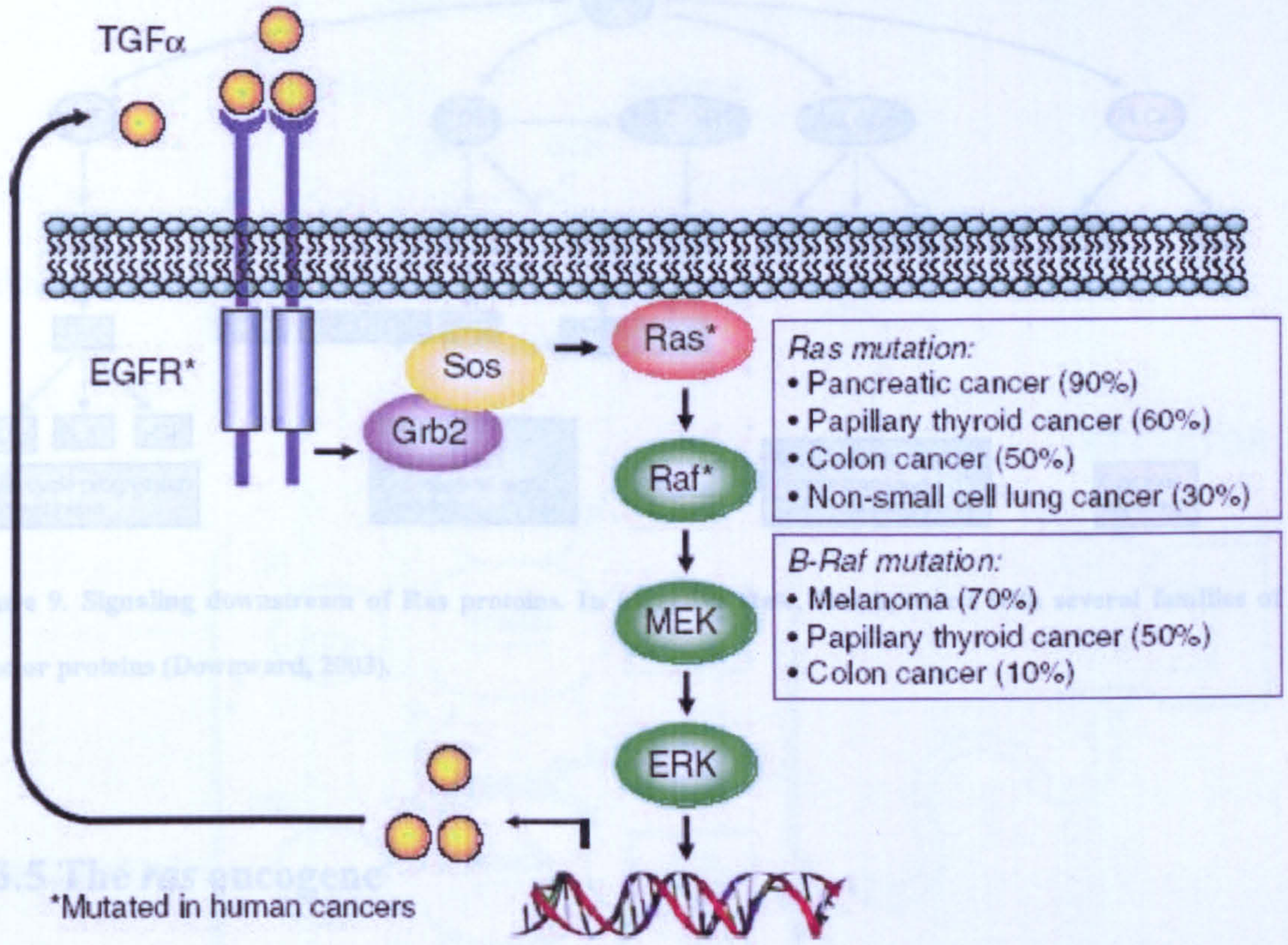

Figure 8. Signaling downstream of Ras proteins: activation of the ERK MAPK cascade (Der et al., 2007).

A second well-studied pathway involves the phosphatidylinositol 3-kinases (PI3Ks) as effector, whose action regulates cell survival.

When activated by the βγ complex of the G protein, this kinase leads the phosphatidylinositol phosphorylation at one or two residues. The resulting phosphorylated forms of this membrane lipid act as an anchor bringing downstream effectors of the cascade (such as AKT involved in cell survival regulation) to the inner face of the plasmatic membrane (Fig. 9).

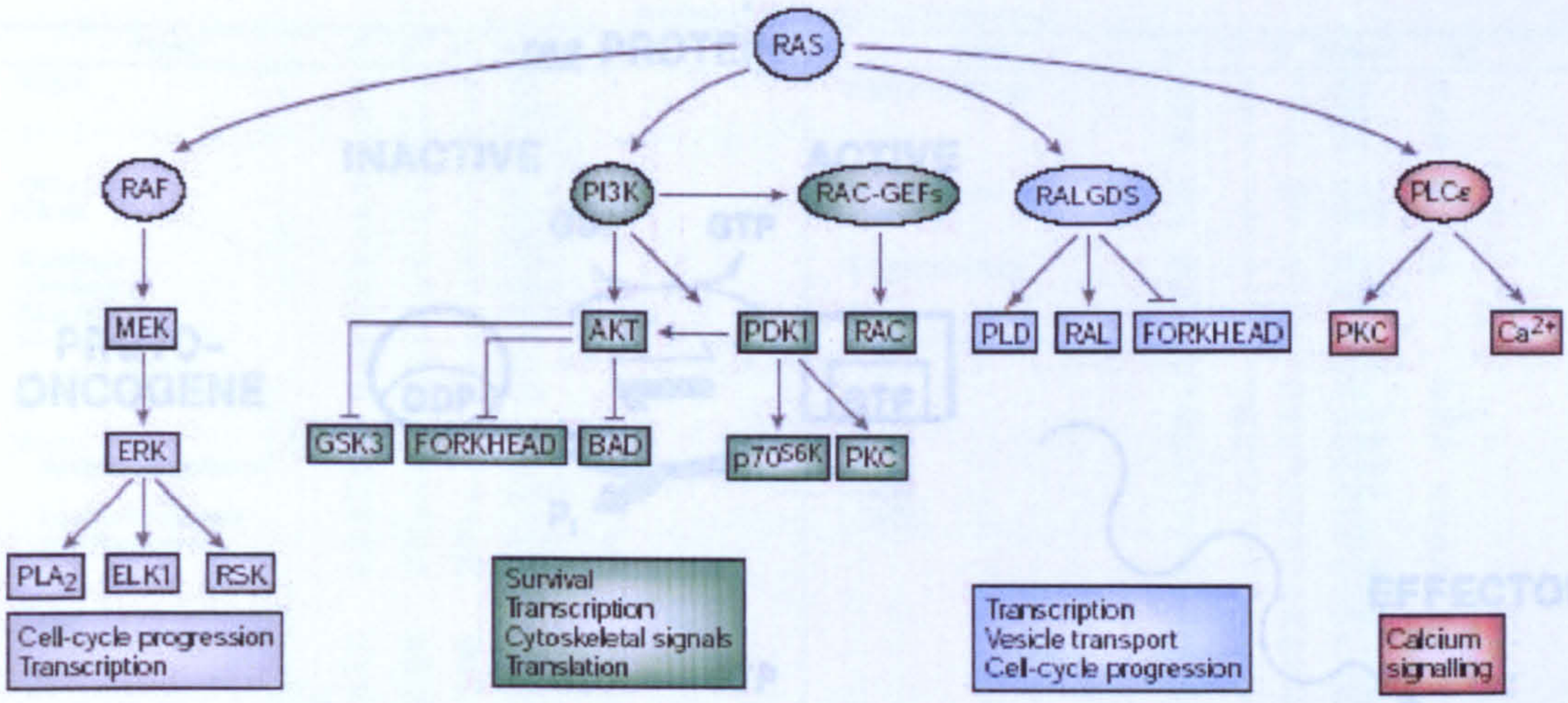

Figure 9. Signaling downstream of Ras proteins. In its active state, Ras interacts with several families of effector proteins (Downward, 2003).

1.3.5 The *ras* oncogene

From the figure 9, it is easy to understand how an aberrant Ras function can promote a malignant transformation.

ras genes can acquire transforming properties by qualitative and quantitative mechanisms. However, the neoplastic properties induced by highly overexpressed *ras* proto-oncogenes are weaker than those induced by their mutated alleles.

The most frequent mutations, rendering the Ras proteins constitutively active, occur in codons 12, 13 (affecting the guanosine triphosphate (GTP)-binding domain in exon 1) or 61 (affecting the GTPase domain in exon 2) of one of the three *ras* genes. These mutations are known to confer transforming properties to *ras* genes and reverse the normal equilibrium between the active and inactive forms, stabilizing Ras proteins in their active state (Barbacid, 1987), as it is depicted in figure 10.

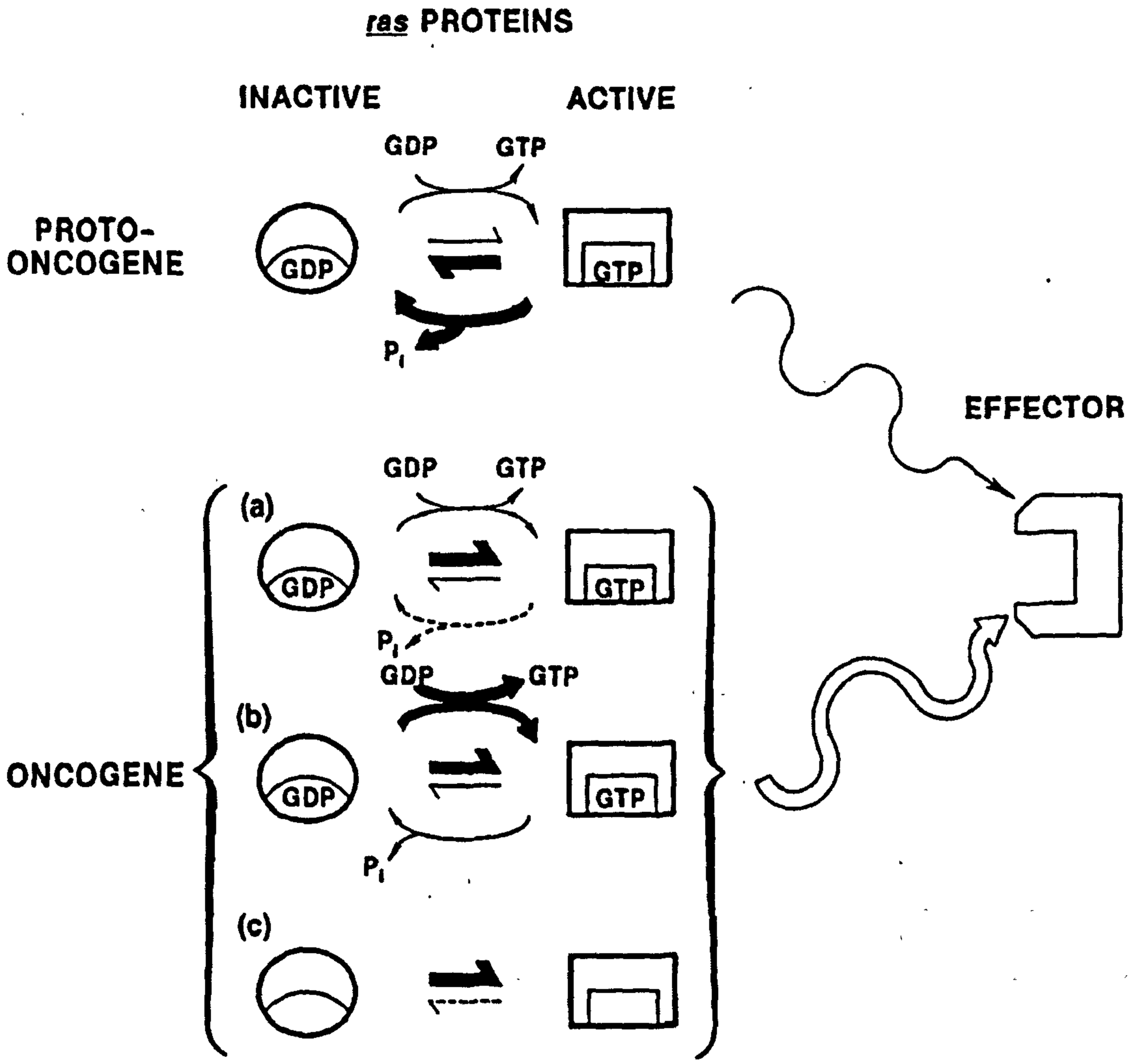

Figure 10. Current model of mechanism of action of normal and transforming ras proteins.

a) mutations that inhibit the intrinsic GTPase activity;

b) mutations that increase the exchange rate between GDP and GTP;

c) mutations that induce a constitutively active conformational change that does not require binding of guanine nucleotides (Barbacid, 1987).

The *ras* gene mutations are found in a variety of tumour types, such as adenocarcinomas of the pancreas, colon and lung, thyroid tumours and myeloid leukaemia, with different incidence (Bos, 1989) as in table 4.

Incidence of ras mutations in human cancer

Tumor	n[a]	+[b]	%[c]	Method[d]	ras[e]
Breast	16	0	0	3T3	
	34	0	0	ODN	
	24	2	8	ODN[f]	
	12	0	0	RMC[g]	
Ovary	37	0	0	ODN	
Cervix	30	0	0	ODN	
	76	7	9	RFLP[f]	
Esophagus	25	0	0	ODN	
Glioblastoma	30	0	0	ODN	
Neuroblastoma	25	0	0	ODN	
Stomach	26	0	0	3T3	
	7	0	0	3T3	
Skin: keratoacanthoma	10	1	10	3T3	
Lung					
Epidermoid carcinoma	20	0	0	ODN	
	21	1	5	RMC[g]	
Large cell carcinoma	10	0	0	ODN	
Adenocarcinoma	45	15	33	ODN	K
	18	4	22	RMC[g]	
Colon					
Adenocarcinoma	27	12	44	ODN	K
	158	64	40	RMC[g]	
	92	43	47	ODN	K
Adenoma	40	20	50	ODN	K
Adenoma (FAP)[h]	40	5	13	ODN	K
	75	5	7	ODN[i]	K
Pancreas: adenocarcinoma	63	53	84	RMC[g]	K
	30	28	93	ODN	K
	63	47	75	ODN	K
Thyroid					
Follicular carcinoma	15	8	53	ODN	H, K, N
Undifferentiated carcinoma	10	6	60	ODN	H, K, N
Papillary carcinoma	20	0	0	3T3	
	10	2	20	ODN	
Follicular adenoma					
Micro	16	8	50	ODN	H, K, N
Macro	10	0	0	ODN	
Seminoma	14	6	43	ODN	K, N
Melanoma	13	1	8	3T3	N
	37	7	19	ODN	N
Sarcoma	29	0	0	ODN	
Bladder carcinoma	28	2	7	3T3	H
	15	1	7	3T3	H
	24	4	17	3T3	H
Liver carcinoma	10	3	30	3T3	N
	21	0	0	ODN	
Kidney carcinoma	16	2	13	3T3	H
	14	1	7	RCM[k]	
Myeloid disorders					
MDS	19	1	5	ODN	
	8	3	38	3T3	N
	50	20	40	ODN	N/K
	27	11	41	ODN	N
	34	3	9	ODN	
IMF	9	2	22	ODN	N
AML	6	3	50	3T3	N
	8	5	63	3T3	N
	37	7	19	ODN	N
	52	14	27	ODN	N
	32	6	19	ODN	N
	9	5	56	3T3	N
	10	7	70	3T3	N
	18	5	28	ODN	N
	26	7	27	ODN	N
	57	15	26	ODN	N
	148	38	26	ODN	N
	9[m]	1	11	ODN	
CML					
Chronic phase	25	0	0	ODN	
	10	0	0	ODN	
	6	1	17	3T3	N
Acute phase	16	0	0	ODN	
	6	3	50	3T3	N
Lymphoid disorders					
ALL	19	2	11	ODN[n]	N
	14	0	0	ODN[n]	
	33	6	18	ODN	
NHL					
B-cell	68	0	0	ODN	
	64	0	0	ODN	
T-cell	20	0	0	ODN	
Hodgkin's	25	0	0	ODN	
	3	2		3T3	N
Hairy cell	6	0	0	ODN	

[a] n, number of samples tested.
[b] Number of samples containing a mutant *ras* gene.
[c] Percentage of samples with a mutated *ras* gene.
[d] Method used for the detection of mutated *ras* genes: 3T3, transfection assay with NIH/3T3 cells; ODN, oligodeoxynucleotide hybridization assay; RMC, RNase mismatch cleavage assay; RFLP, restriction fragment length polymorphism.
[e] *ras* gene preferentially found to be activated.
[f] Only tested for H-*ras* codon 12.
[g] Only tested for K-*ras* codon 12/13.
[h] FAP, familial adenomatous polyposis; IMF, idiopathic myelofibrosis; CML, chronic myeloid leukemia.
[i] Only tested for K-*ras*.
[j] 13 leiomyosarcomas, 10 histiocytomas, 2 schwannomas, 1 liposarcoma, 1 fibrosarcoma, 1 rhabdomyosarcoma (H. J. van Kranen, personal communication).
[k] See Footnote 5.
[l] See Footnote 3.
[m] Leukemias related to therapy with alkylating agents.
[n] Only tested for N-*ras*.

Table 4. Incidence of ras mutations in human cancer (Bos, 1989).

1.3.6 Molecular mechanisms of Ras activity in thyroid cancerogenesis

Tumours of the follicular epithelium of the human thyroid gland represent a multi-stage model of epithelial tumorigenesis proceeding from follicular adenomas. The follicular adenomas are divided into two groups: microfollicular and macrofollicular types. They are benign neoplasms, slowly progressive and well-differentiated, affecting young age groups. Undifferentiated or anaplastic thyroid

carcinoma is a rare tumour with a poor prognosis, highly malignant, occurring in the elderly, through differentiated carcinoma (Fig. 11).

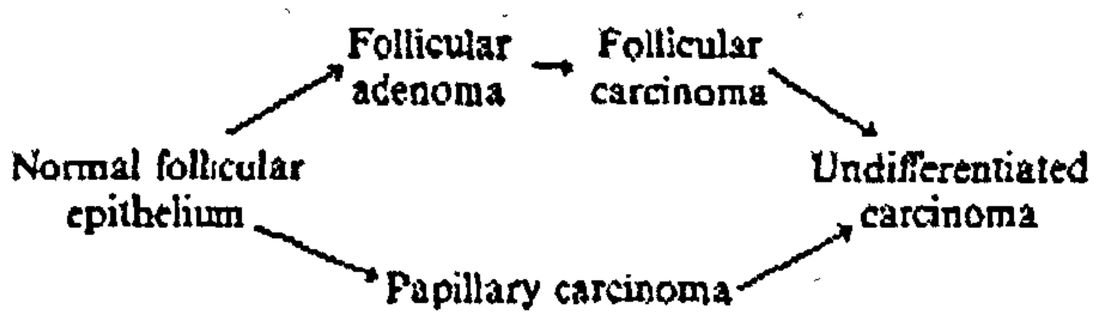

Figure 11. Tumours of the follicular epithelium of the human thyroid gland (Lemoine et al., 1989).

Some studies (tables 5, 6 and 7) indicate that active *ras* oncogenes (the predominant mutation being a valine for glycine substitution in codon 12 of H-*ras*) are found in all stages of human thyroid tumorigenesis and their activation by mutation occurs at an early stage of neoplastic progression (Fusco et al., 1987b; Hashimoto et al., 1990; Lemoine et al., 1988; Lemoine et al., 1989; Namba et al., 1990; Suarez et al., 1988).

Activated *ras* oncogenes in human thyroid adenomas

Case No.	*Age and sex*	*Histological type*	*Oncogene position mutated and amino acid substituted*	*Transfection assay*
1	24 F	Macrofollicular	–	n.d.
2	55 F	Macrofollicular	–	n.d.
3	40 F	Macrofollicular	–	n.d.
4	35 F	Macrofollicular	–	n.d.
5	36 F	Macrofollicular	–	n.d.
6	29 F	Macrofollicular	–	n.d.
7	33 F	Macrofollicular	–	n.d.
8	46 F	Macrofollicular	–	n.d.
9	30 F	Microfollicular	–	–
10	31 F	Microfollicular	N-*ras*, 61 CAA → CGA (gln → arg)	+ (N-*ras*)
11	42 F	Microfollicular	–	–
12	56 F	Microfollicular	Ki-*ras*, 12 GGT → AGT (gly → ser)	–
13	42 F	Microfollicular	–	–
14	55 F	Microfollicular	–	–
15	44 F	Microfollicular	–	–
16	55 F	Microfollicular	N-*ras*, 61 CAA → CGA (gln → arg)	+ (N-*ras*)
17	18 F	Microfollicular	–	–
18	38 F	Microfollicular	Ha-*ras*, 61 CAG → CGG (gln → arg)	+ (Ha-*ras*)
19	53 F	Microfollicular	Ha-*ras*, 61 CAG → CGG (gln → leu)	+ (Ha-*ras*)
20	16 M	Microfollicular	–	–
21	48 F	Microfollicular	N-*ras*, 61 CAA → CGA (gln → arg)	+ (N-*ras*)
22	42 F	Microfollicular	Ha-*ras*, 12 GGC → GTC (gly → val)	+ (Ha-*ras*)
23	33 F	Microfollicular	–	n.d.
24	49 F	Microfollicular	N-*ras*, 12 GGT → TGT (gly → cys)	n.d.

Mutations expressed as amino acid substitution produced in *ras* protein:
gln – glutamine; arg – arginine; gly – glycine; ser – serine; val – valine; cyst – cysteine; leu – leucine; asp – aspartate; lys – lysine.
Transfection assay: n.d., not done; +/– positive/negative assay; (identity of activated oncogene)

Table 5. Activated ras oncogenes in human thyroid adenomas (Lemoine et al., 1989).

Activated *ras* oncogenes in human thyroid carcinomas

Case No.	*Age and sex*	*Histological type*	*Oncogene position mutated and amino acid substituted*	*Transfection assay*
1	51 F	Differentiated, follicular	–	n.d.
2	39 F	Differentiated, follicular	–	n.d.
3	79 F	Differentiated, follicular	–	n.d.
4	70 M	Differentiated, follicular	Ha-*ras*, 12 GGC → GAC (gly → asp)	n.d.
5	78 F	Differentiated, follicular	–	n.d.
6	36 F	Differentiated, follicular	Ha-*ras*, 61 CAG → CGG (gln → arg)	n.d.
7	42 F	Differentiated, follicular	Ha-*ras*, 61 CAG → CGG (gln → arg)	n.d.
8	36 M	Differentiated, follicular	–	n.d.
9	66 F	Differentiated, follicular	N-*ras*, 61 CAA → CTA (gln → leu)	n.d.
10	74 F	Differentiated, follicular	–	n.d.
11	75 F	Undifferentiated (anaplastic)	Ki-*ras*, 12 GGT → AGT (gly → ser)	n.d.
12	46 F	Undifferentiated (anaplastic)	Ki-*ras*, 12 GGT → TGT (gly → cys)	+ (Ki-*ras*)
13	61 M	Undifferentiated (anaplastic)	Ha-*ras*, 12 GGC → GTC (gly → val)	+ (Ha-*ras*)
14	46 M	Undifferentiated (anaplastic)	Ha-*ras*, 61 CAG → AAG (gln → lys)	+ (Ha-*ras*)
15	72 M	Undifferentiated (anaplastic)	–	–
16	75 F	Undifferentiated (anaplastic)	–	n.d.
17	62 M	Undifferentiated (anaplastic)	–	n.d.
18	88 F	Undifferentiated (anaplastic)	–	n.d.
19	39 F	Undifferentiated (anaplastic)	N-*ras*, 12 GGT → GAT (gly → asp)	n.d.
20	62 F	Undifferentiated (anaplastic)	Ha-*ras*, 12 GGC → TGC (gly → cys)	n.d.

Table 6. Activated ras oncogenes in human thyroid carcinomas (Lemoine et al., 1989).

Activated *ras* oncogenes in human thyroid tumours*

	% Of cases with mutant ras oncogenes	*Cases with mutant ras/ total cases tested*	*Oncogene/position involved*		
			Ha-ras	*N*-ras	*Ki*-ras
ADENOMAS					
Macrofollicular	0	0/8			
Microfollicular	50	8/16	H_{12} val (1) H_{61} arg (1) H_{61} leu (1)	N_{12} cys (1) N_{61} arg (3)	K_{12} ser (1)
CARCINOMAS					
Follicular	53	8/15	H_{12} asp (1) H_{61} arg (4)	N_{61} arg (1) N_{61} leu (1)	K_{12} ser (1)
Undifferentiated (Anaplastic)	60	6/10	H_{12} val (1) H_{12} cys (1) H_{61} lys (1)	N_{12} asp (1)	K_{12} ser (1) K_{12} cys (1)

* Cumulative results of this study together with results published in Lemoine *et al.* (1988). *Cancer Research*, 48, 4459–4463.

Table 7. Activated ras oncogenes in human thyroid tumours (Lemoine et al., 1989).

Moreover, the mutation status of *ras*, is associated with poor prognosis. Among the patients of thyroid carcinoma, 74.3% die of ras mutated tumours with respect to 31.9% of those having tumours without mutations (Fig. 12) (Garcia-Rostan et al., 2003).

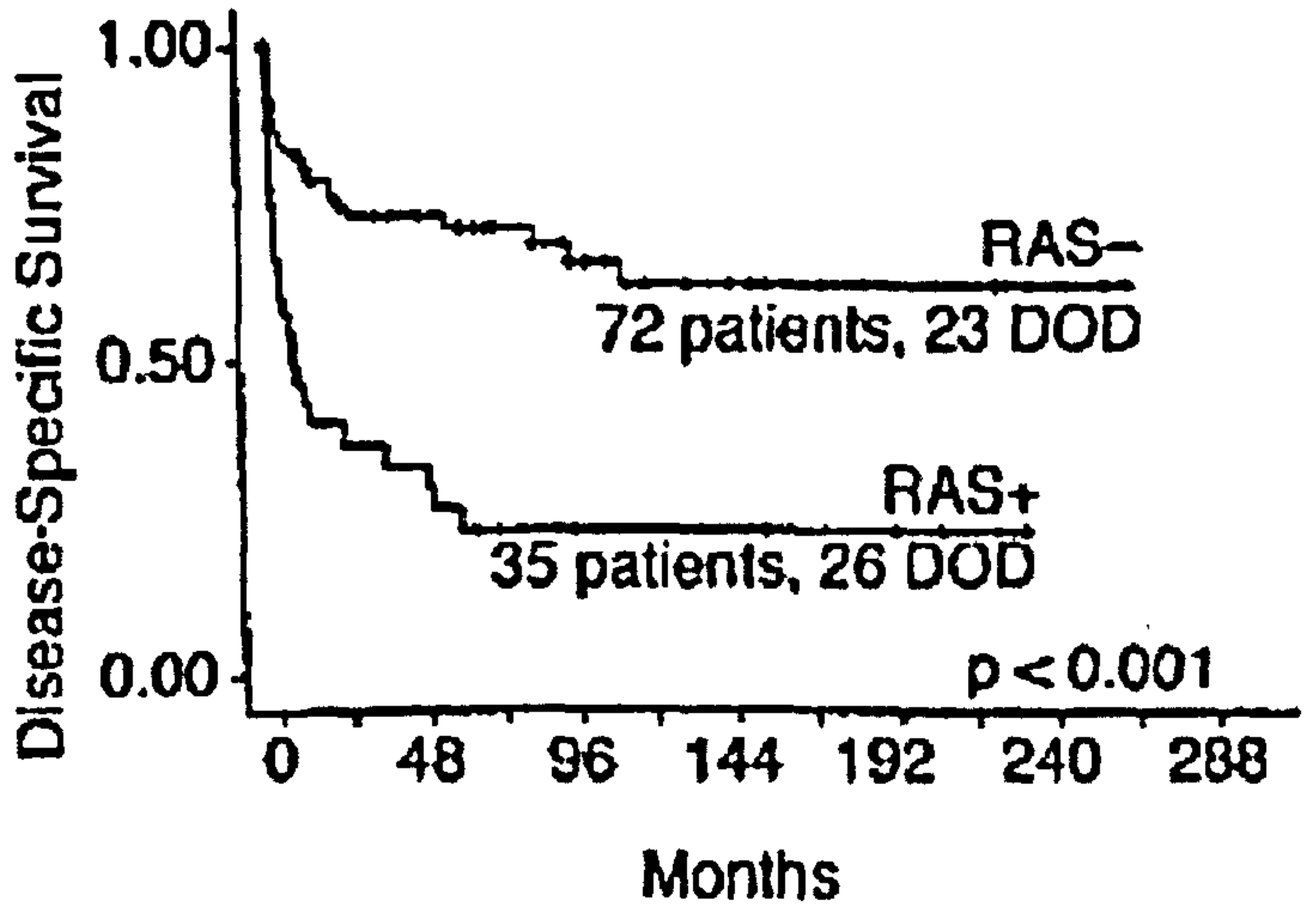

Figure 12. Survival of patients with thyroid carcinoma dichotomized according to the presence of activating H-, K- or N-*ras* mutations (RAS); dead of disease (DOD) (Garcia-Rostan et al., 2003).

1.4 The *c-myc* proto-oncogene

1.4.1 The *c-myc* history

The *c-myc* proto-oncogene was first described in 1982 as the cellular homologue to the transforming sequences of the avian myelocytomatosis retrovirus (Dalla-Favera et al., 1982b; Vennstrom et al., 1982). Oncogenic c-Myc is a key transforming agent in the etiology of human Burkitt's lymphoma. *c-myc* expression is altered in a wide variety of human tumours, which usually consists in an overexpression of the proto-oncogene leading to the repression or activation of several genes. In particular, many activated genes are those involved in cell growth, cell cycle (ODC) and cell proliferation, such as cyclins D1, D2 and CDK4. The genes that are silenced control processes such as inhibition of cell cycle (CDK inhibitors p21 and p15INK4A) or apoptosis. They also have a role in regulation of cell adhesion and structure formation i.e. they encode extracellular matrix proteins and cytoskeletal proteins such as β1-integrin or N-cadherin) (Brenner et al., 2005; Coller et al., 2000; Dang et al., 2006; Guo et al., 2000; Levens, 2003; Luscher and Eisenman, 1990; Menssen and Hermeking, 2002).

1.4.2 The *myc* family

The *c-myc* gene belongs to the *myc* family of proto-oncogenes including two other evolutionarily conserved members: *N-* and *L-myc*, with strong homology to *c-myc*. Each of the three mammalian *myc* family genes has the same characteristic three-exon structure with the major polypeptide open reading frame residing in the second and third exons. The first exon is not conserved.

The three members of the *myc* gene family are differentially expressed during the embryonic development (Facchini and Penn, 1998; Marcu et al., 1992; Patel et al., 2004; Ramsay et al., 1984). In mouse embryos, by *in situ* hybridization, the *c-myc* was shown to be preferentially expressed in endodermal and mesodermal tissues, while organs developing from ectoderm revealed low levels of *c-myc* RNAs (Pfeifer-Ohlsson et al., 1985; Schmid et al., 1989). *c-myc* expression varied with age in mice in a tissue-specific manner, with highest levels of expression in newborn and old animals. *N-* and *L-myc* expression was high in a more restricted set of perinatal and newborn tissues (Semsei et al., 1989).

Elevated *c-myc* expression has been associated with a wide variety of malignancies. On the other hand, *N-myc* is expressed in tumours such as neuroblastomas or retinoblastomas. *L-myc* expression is restricted to small cell lung carcinomas (SCLC) (Marcu et al., 1992).

In particular, the *c-myc* human gene is located on chromosome 8 and consists of three exons: a long, untranslated exon (exon I) and the two exons encompassing the protein coding sequences (exons II and III). The *c-myc* proto-oncogene encodes a transcription factor; which regulates the expression of many genes involved in the control of cell proliferation, differentiation and apoptosis (Askew et al., 1991; Cole, 1986; Evan et al., 1992; Spencer and Groudine, 1991). In fact, gene-targeting approaches have demonstrated that c-Myc function is critical for cell proliferation and

murine development. The *c-myc* expression seems to be necessary and sufficient for the entry of the cells into the S phase of the cell cycle (Hanson et al., 1994). Moreover, c-Myc-deficient mice die at embryonic day (E) 9.5 to 10.5 and are developmentally retarded (Davis et al., 1993).

Multiple transcription start sites exist within the gene, giving rise to four transcripts (P0, P1, P2 and P3 of ~3.1, 2.4, 2.25 and 2.0 kb respectively). P1 and P2 are the two most commonly used promoters and the mRNA transcripts initiated by them, have the capacity to encode the two major species of human c-Myc protein: Myc1 (66 KD protein) and Myc2 (64 KD protein) (Fig. 13).

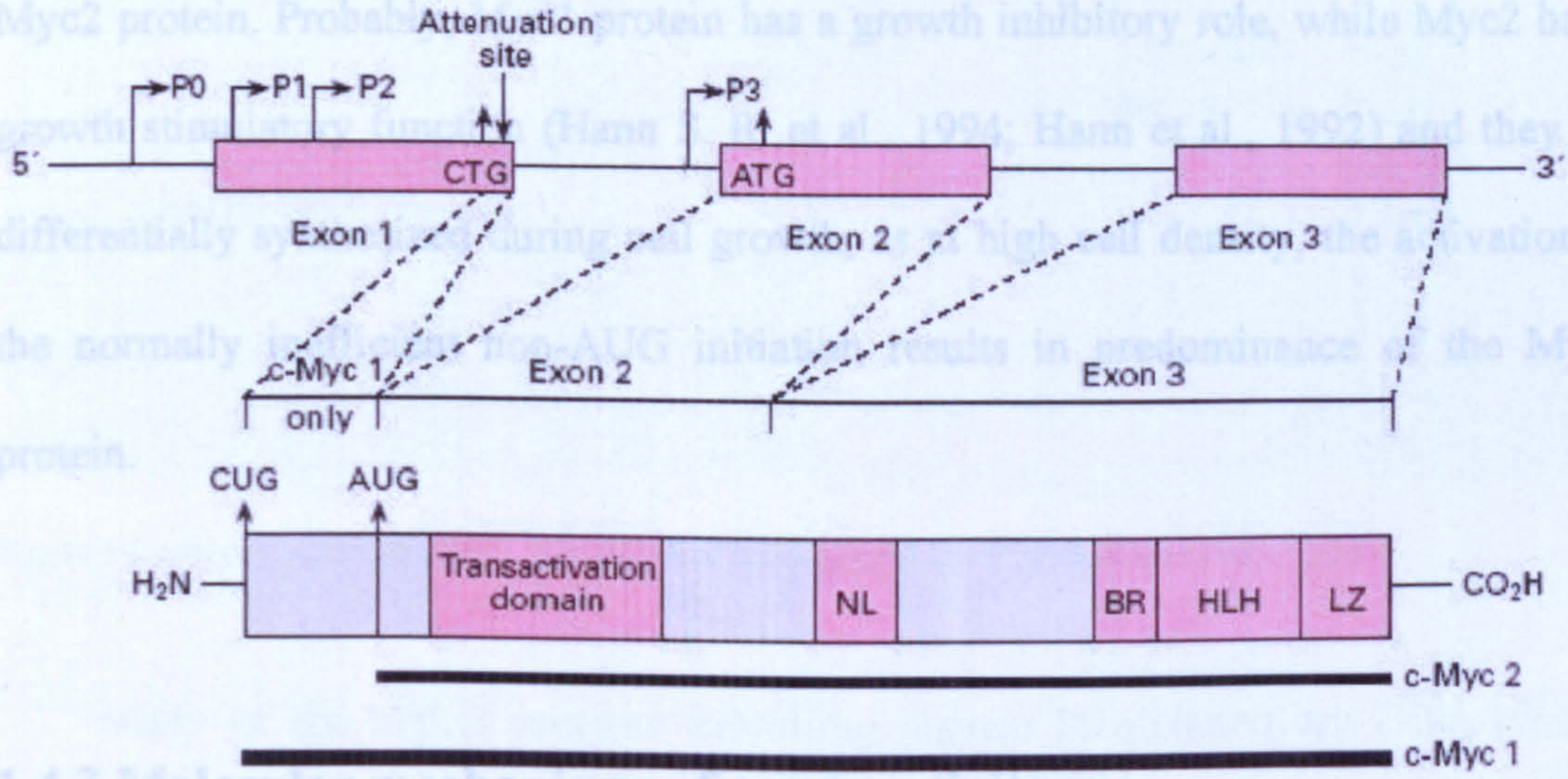

Figure 13. Schematic representation of the human c-*myc* gene and the two resultant protein products, c-Myc1 and c-Myc2 (Birnie, 1996).

Both proteins have relatively a short half-life (25-30 minutes) (Facchini and Penn, 1998; Hann and Eisenman, 1984), thus suggesting that the products of *c-myc* are regulatory rather than structural elements in the cell.

Myc proteins are rapidly degraded by ubiquitin-mediated proteolysis. In particular, two elements govern the Myc stability: an N-terminal element (degron), overlapping the Myc transactivation domain (TAD), is essential for Myc destruction

and a C-terminal element stabilizes Myc. Mutations within the Myc degron can determine cancer as a consequence of the protein stabilization and activation (Flinn et al., 1998; Salghetti et al., 1999). However, these controls, preventing its accumulation in normal cells, are lost in cancer cells, resulting in aberrantly high levels of Myc proteins. The strong selection for Myc overexpression in tumours appears to reflect its ability to provide constitutive signals that promote proliferation and angiogenesis.

The relative abundance of Myc2 vs. Myc1 protein varies among tissues and cell lines, with Myc2 species being the major isoform in most cases.

The Myc1 protein arises from an upstream non-AUG translational start site and thus contains an amino-terminal extension of 14 amino acids (aa) as compared to the Myc2 protein. Probably, Myc1 protein has a growth inhibitory role, while Myc2 has a growth stimulatory function (Hann S. R. et al., 1994; Hann et al., 1992) and they are differentially synthesized during cell growth, as at high cell density, the activation of the normally inefficient non-AUG initiation results in predominance of the Myc1 protein.

1.4.3 Molecular mechanisms of *c-myc* activity

The product of the *c-myc* proto-oncogene is a highly conserved nuclear phosphoprotein, functioning as a transcription factor, a region encoded in the third exon directing the translocation of polypeptides to the nucleus (NLS) (Eisenman et al., 1985; Hann and Eisenman, 1984; Stone et al., 1987)

The Myc2 protein is 439 aa long. Its amino terminus region probably regulates the protein-DNA interaction (Kato et al., 1992) and is capable of transcriptional activation (Kato et al., 1990). The carboxyl-terminal region (85 aa) shares significant sequence similarity with two classes of transcription factors: the basic region helix-

loop-helix (bHLH) and basic region leucine zipper (bZip) proteins, both having basic regions adjacent to their dimerization domains (Facchini and Penn, 1998) (Fig. 14).

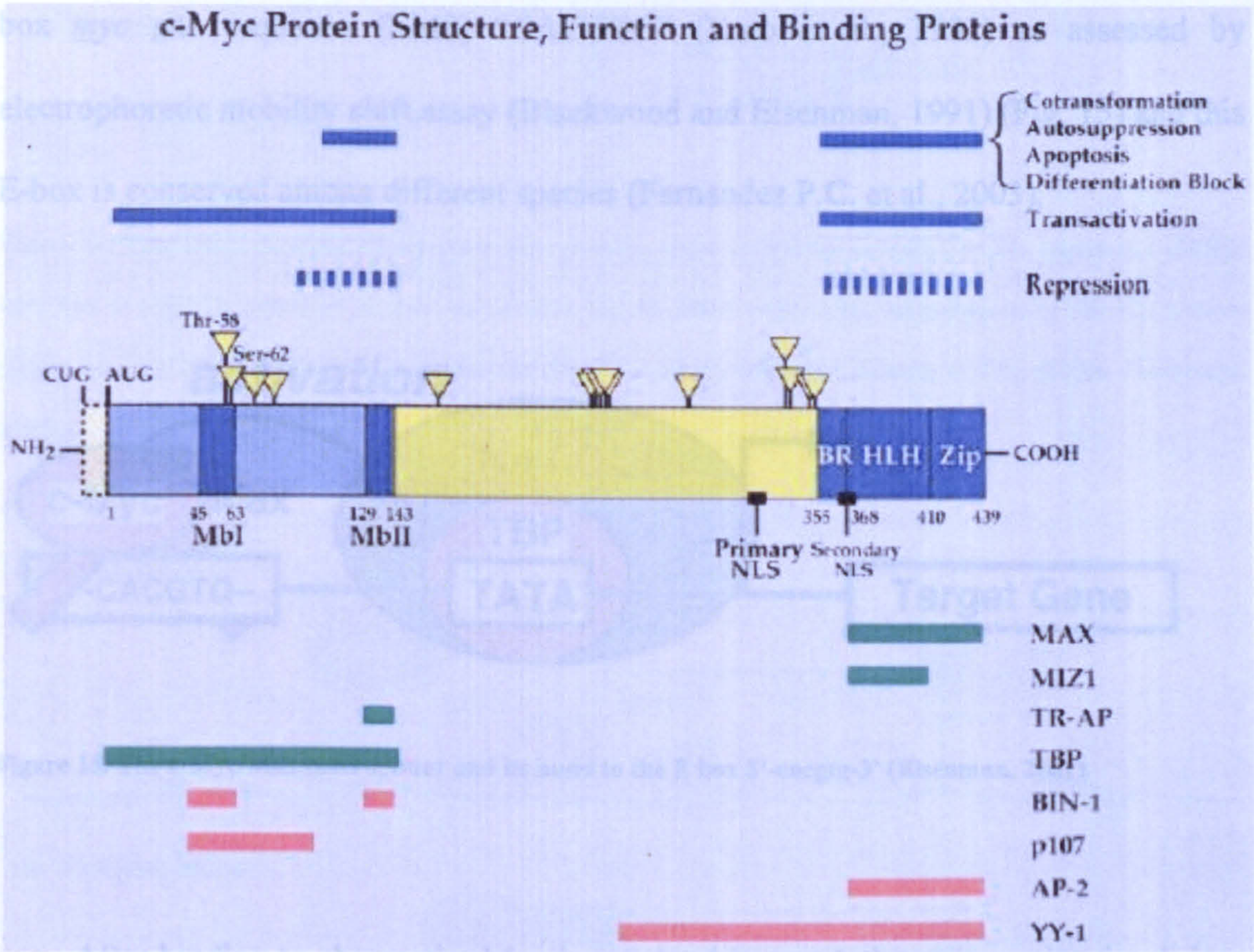

Figure 14. c-Myc protein structure, function and binding proteins (Facchini and Penn, 1998).

Many of the bHLH proteins exhibiting nuclear localization are DNA-binding proteins and function as transcriptional regulators (Blackwood and Eisenman, 1991). Moreover the HLH-Zip motif is responsible for specific heterodimeric formation between Myc and its binding partner, Max (Myc-associated factor "x"), which was identified during screening of a complementary DNA expression library.

Like Myc, also Max exhibits a basic region followed by HLH and Zip regions. By alternative splicing, *max* mRNAs encode 151- and 160-aa polypeptides containing the basic HLH-Zip domain and can oligomerize with Myc. Myc and Max can bind to each other by these two regions (HLH and Zip). Moreover, the integrity of these

regions in Myc is necessary for its binding with Max and the bond between the cMyc-Max complex and the DNA.

As a transcriptional regulator, c-Myc/Max complex specifically binds to the E box *myc* site sequence (EMS) "CACGTG" (Kato et al., 1992) as assessed by electrophoretic mobility shift assay (Blackwood and Eisenman, 1991) (Fig. 15) and this E-box is conserved among different species (Fernandez P.C. et al., 2003).

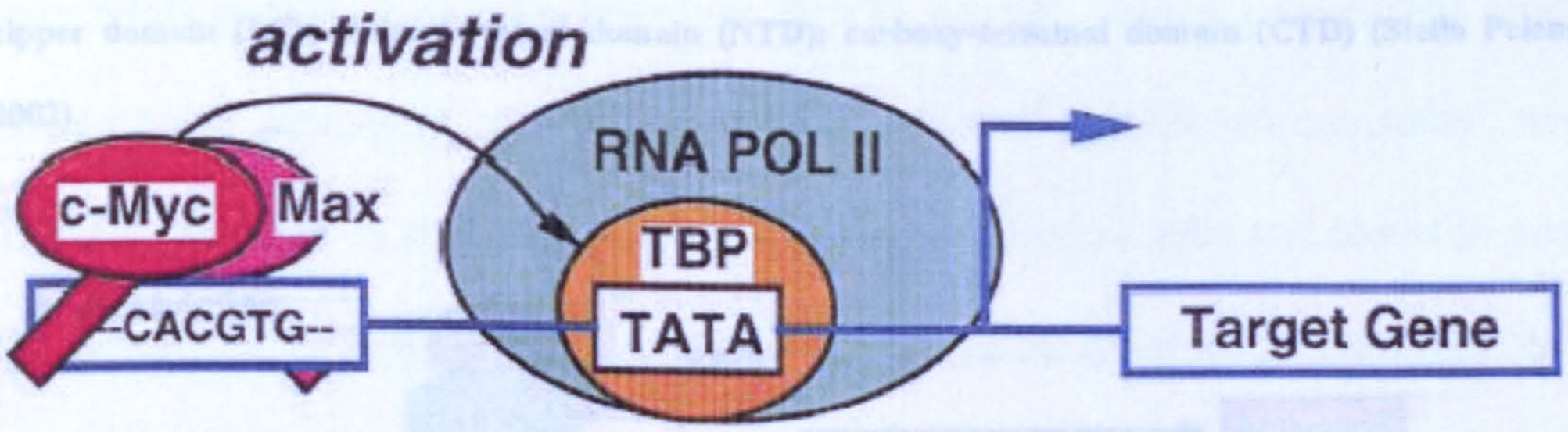

Figure 15. The c-Myc/Max heterodimer and its bond to the E box 5'-cacgtg-3' (Eisenman, 2001).

After binding to chromatin, Myc is involved in translating mitogenic stimuli into chromatin modifications (Amati et al., 2001; Grandori et al., 2000; McMahon et al., 1998). It induces histone H4 acetylation (near E-box site) by recruitment of TRansactivation/tRansformation Associated Protein (TRRAP), its interaction with Myc is depicted in figures 16 and 17 and described in the "1.4.4 The *c-myc* pathways" paragraph. This complex, capable of acetylating proteins involved in transcription, is known to acetylate Myc, leading to a dramatic increase in protein stability (from 41 to 132 min). Following acetylation at lysines 323 and 417, that alters its rate of degradation, Myc protein is stabilized (Frank et al., 2001; Patel et al., 2004) and the Myc-targeted genes transcriptionally activated. Myc regulates cyclin D2 by a similar mechanism (Bouchard et al., 2001) (Figs. 16 and 17).

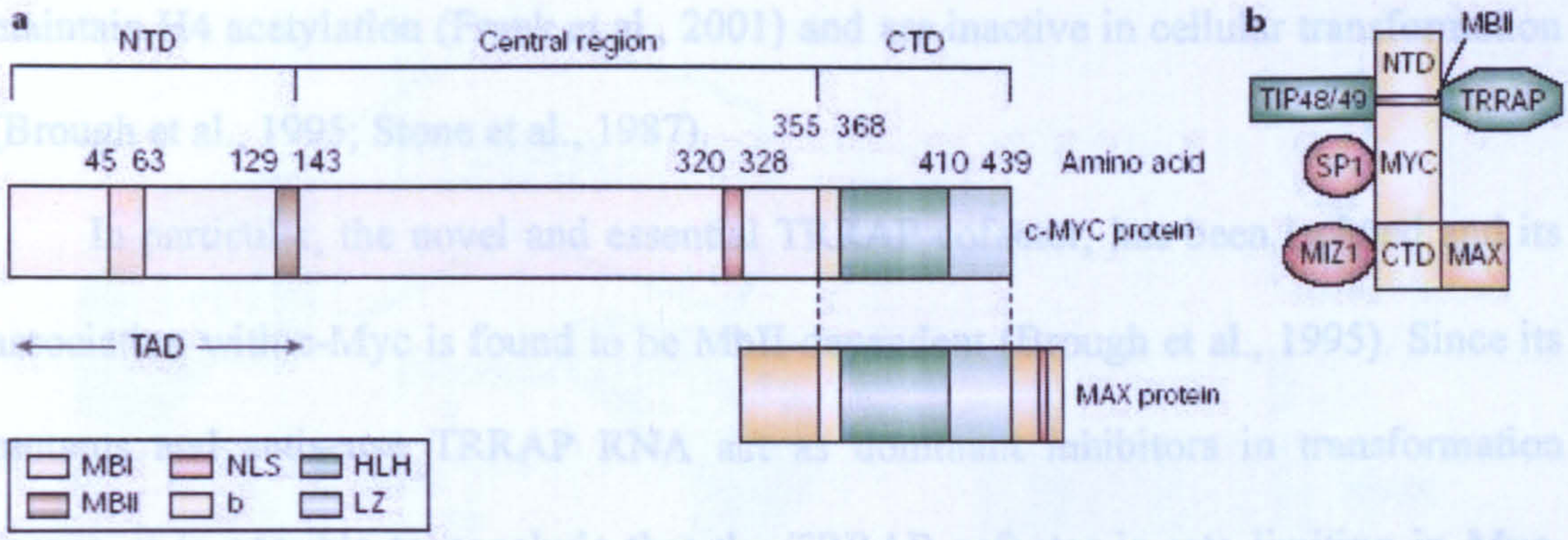

Figure 16. Functional domains of human c-Myc protein, trans-activation domain (TAD); Myc box I (MBI); Myc box II (MBII); signal of nuclear localization (NLS); basic region (b); helix-loop-helix (HLH); leucine zipper domain (LZ); amino-terminal domain (NTD); carboxy-terminal domain (CTD) (Stella Pelengaris, 2002).

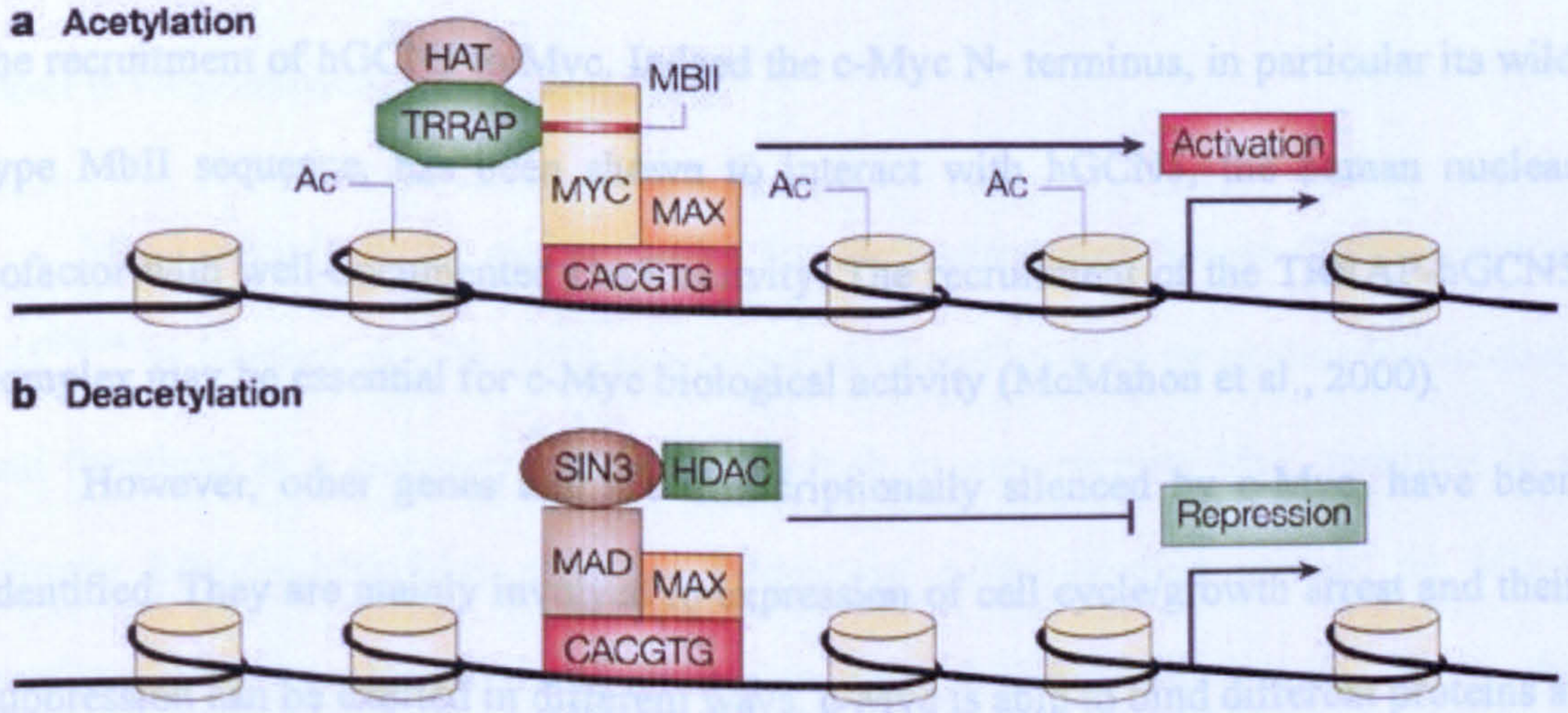

Figure 17. Myc-Max and Mad-Max complexes regulate gene activation through chromatin remodelling (Pelengaris et al., 2002).

1.4.4 The *c-myc* pathways

Several genes activated by Myc, are identified. One or more nuclear proteins are able to associate with the c-Myc N terminus to exert this activation. These proteins or cofactors interact with conserved blocks of approximately 20 aa referred to as Myc-boxes I and II (MbI and MbII). Deletion mutants of these two regions are unable to

maintain H4 acetylation (Frank et al., 2001) and are inactive in cellular transformation (Brough et al., 1995; Stone et al., 1987).

In particular, the novel and essential TRRAP cofactor, has been isolated and its association with c-Myc is found to be MbII-dependent (Brough et al., 1995). Since its mutants and antisense TRRAP RNA act as dominant inhibitors in transformation assays, it is possible to conclude that the TRRAP cofactor is rate limiting in Myc-dependent transformation (McMahon et al., 1998). This new nuclear factor interacting with MbII possesses histone acetylase (HAT) activity, which presumably modifies nucleosomal packaging to facilitate transcription at specific chromosomal targets. TRRAP pre-exists in a complex with hGCN5 in mammalian cells and seems to mediate the recruitment of hGCN5 to Myc. Indeed the c-Myc N- terminus, in particular its wild type MbII sequence, has been shown to interact with hGCN5, the human nuclear cofactor with well-documented HAT activity. The recruitment of the TRRAP-hGCN5 complex may be essential for c-Myc biological activity (McMahon et al., 2000).

However, other genes that are transcriptionally silenced by c-Myc, have been identified. They are mainly involved in expression of cell cycle/growth arrest and their suppression can be exerted in different ways. c-Myc is able to bind different proteins at its C terminus domain apart from Max (Fig. 18). By interacting with transcription factors (YY-1 (Ying Yang-1), TFII-I or Miz-1), c-Myc can repress some genes having the transcriptional initiator (Inr) element in their promoter. Particularly Miz-1 is a zinc-finger protein playing a major role in controlling the expression of genes, Inr-containing promoter and is involved in cell-cycle arrest, inducing G1 arrest. These genes are repressed by c-Myc (in a c-Myc dependent manner) (Li et al., 1994; Peukert et al., 1997).

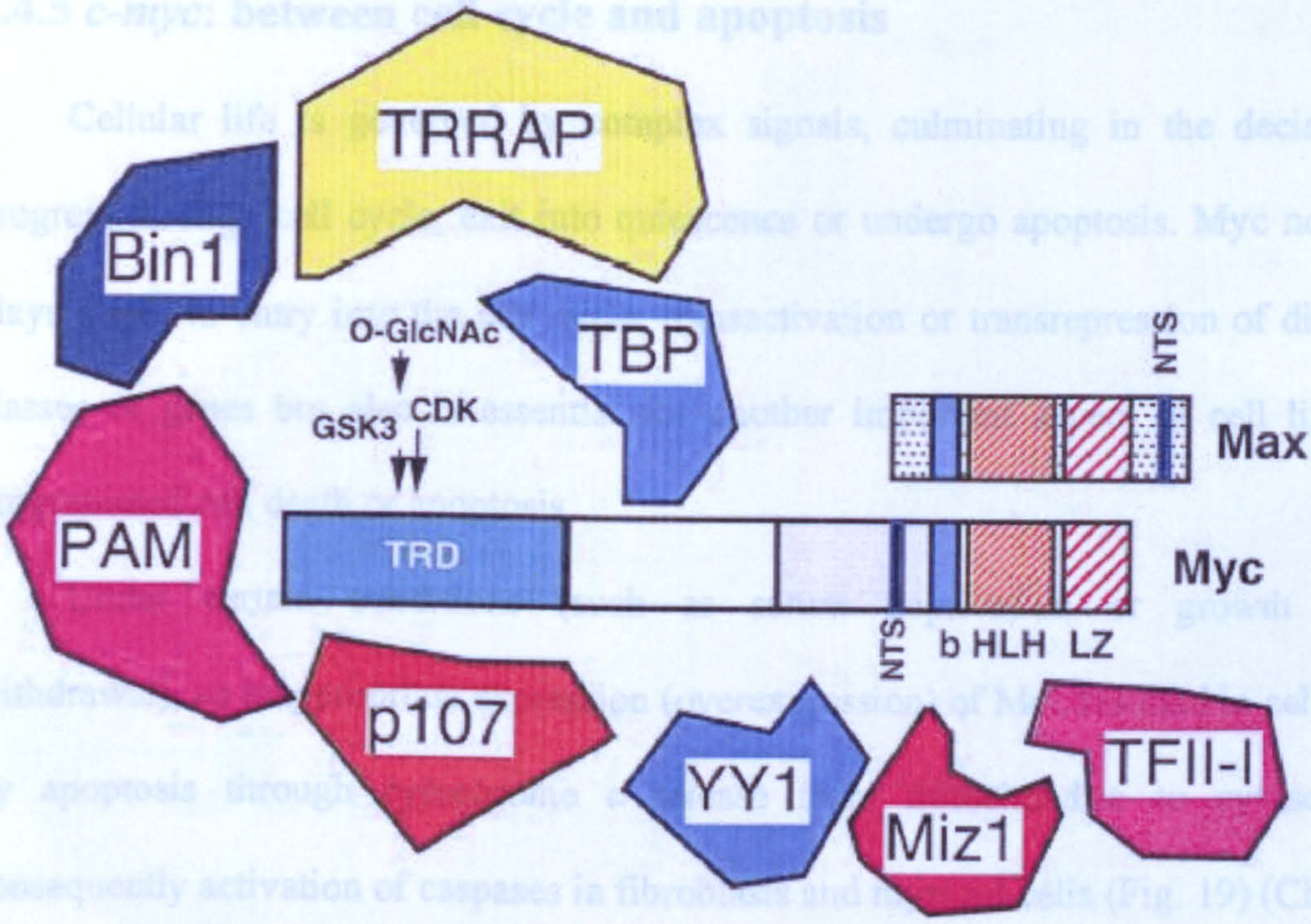

Figure 18. c-Myc interacting proteins (Dang, 1999).

Miz-1 stimulates the expression of the cyclin-dependent kinase (Cdk) inhibitor $p15^{INK4b}$ by interaction with p300 as a co-activator and leads to its nuclear localization and functions as a complex with c-Myc, which in turn recruits Max, resulting in a trimeric Miz-1-c-Myc-Max complex. Moreover, c-Myc-binding surface on Miz-1 overlaps with its transcriptional activation and p300-binding domain. Thus, the transcriptional activation by Miz-1 is inhibited by c-Myc interfering with the formation of a Miz-1 – p300 complex (Staller et al., 2001).

Alternatively, repression by c-Myc can occur through an Inr-independent mechanism, such as by interaction with proteins like Sp1, as in the case of $p21^{(WAF1/CIP1)}$ (Gartel et al., 2001), or Smad, as in the model in which $p15^{INK4b}$ is silenced following the binding between c-Myc and the Smad complex (Seoane et al., 2001). Moreover, the Myc/Max complex can directly interact with the Inr element of many genes to interfere with their repression rather than with their expression (Gartel and Shchors, 2003).

1.4.5 *c-myc*: between cell cycle and apoptosis

Cellular life is governed by complex signals, culminating in the decision to progress through cell cycle, exit into quiescence or undergo apoptosis. Myc not only plays a role in entry into the cell cycle, transactivation or transrepression of different classes of genes but also is essential for another important aspect of cell life: the programmed cell death or apoptosis.

Under certain conditions (such as serum deprivation or growth factor withdrawal), an inappropriate expression (overexpression) of Myc resulted in cell death by apoptosis through cytochrome *c* release from mitochondria to cytosol and consequently activation of caspases in fibroblasts and myeloid cells (Fig. 19) (Chang et al., 2000; Conzen et al., 2000; Juin et al., 1999; Packham and Cleveland, 1994; Thompson, 1998). This behaviour could safeguard cells from cancer as it eliminates cells that accumulate high levels of this oncoprotein.

Apoptosis is known to be a function of myc separable from transactivation and induction of cell cycle but it correlates with transrepression. Between the two evolutionarily conserved regions, MbI and MbII, just the latter is required for transcriptional repression and plays a critical role in Myc-induced apoptosis. Even a reduced transrepression in mutant form of the phosphoprotein correlates with a diminished ability in accelerating apoptosis caused by reduced ability to release of cytochrome *c* (Conzen et al., 2000).

Some anti-apoptotic genes such as Bcl2, when expressed in cells ectopically expressing *myc*, block c-Myc-induced apoptosis (Wagner et al., 1993). However, other genes, capable of transforming cells and providing protection from apoptosis, such as *H-Ras*^{V12}, enhanced or unblocked apoptosis rather than suppressing it in serum-deprived fibroblasts (Kauffmann-Zeh et al., 1997; Kennedy et al., 1997).

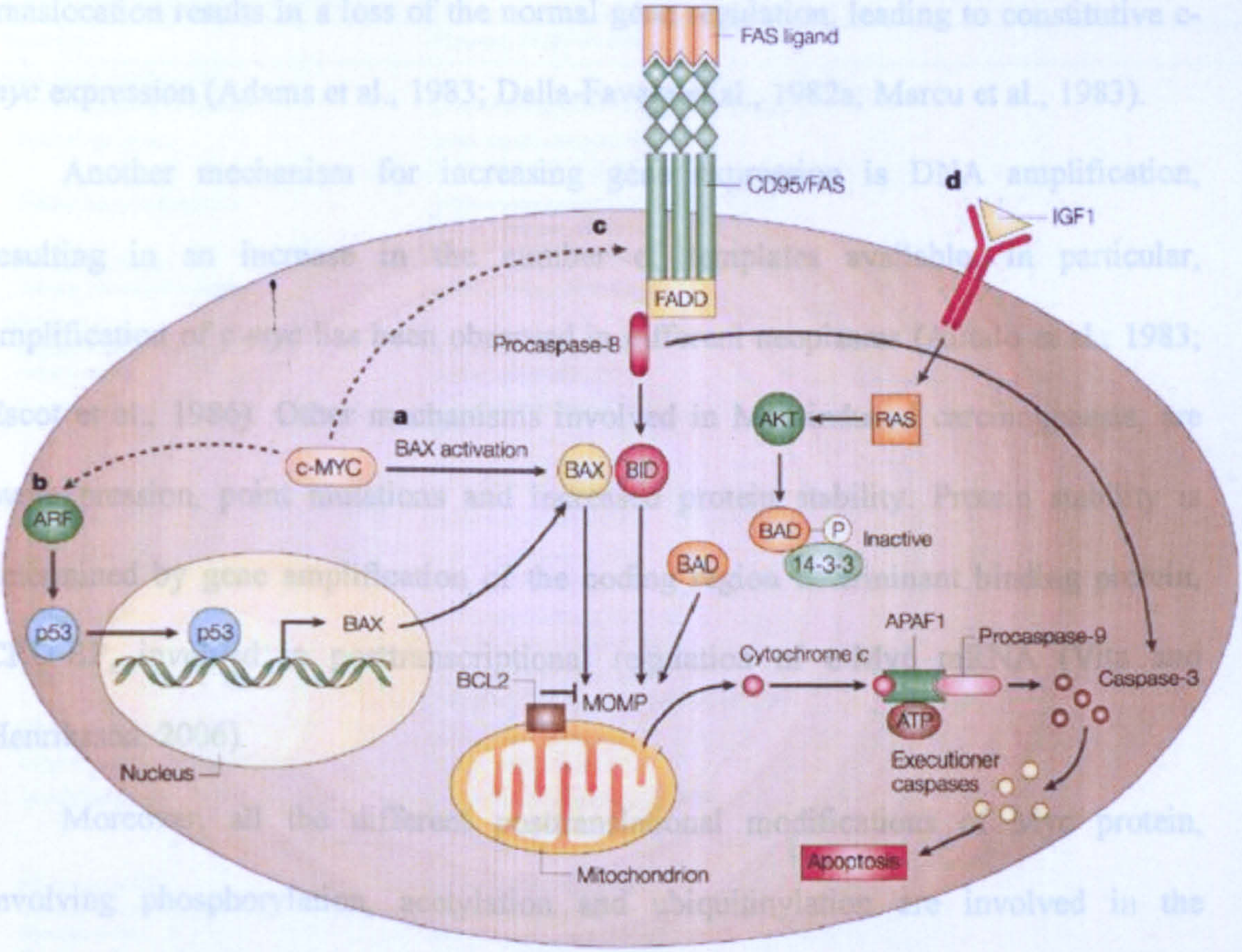

Figure 19. Pathways involving c-MYC and apoptosis (Pelengaris et al., 2002).

1.4.6 The *c-myc* oncogene

The c-*myc* oncogene is among the most frequently overexpressed genes in human cancer (Nesbit et al., 1999).

As proto-oncogene, *myc* family genes can be activated to become an oncogene in different ways. It could be the target for insertional mutagenesis due to retroviral integration between exons 1 and 2 in bursal lymphomas. This is usually followed by deletion of the 5' portion of the provirus and expression of the normal Myc protein, enhanced by the 3' LTR of the virus (Li et al., 1984; Steffen, 1984).

A second activation of the same proto-oncogene could be the abnormal constitutive expression of its unaltered coding sequence due to a translocation as in Burkitt's lymphoma, between the *myc* locus and the immunoglobulin gene loci. Such a

translocation results in a loss of the normal gene regulation, leading to constitutive c-*myc* expression (Adams et al., 1983; Dalla-Favera et al., 1982a; Marcu et al., 1983).

Another mechanism for increasing gene expression is DNA amplification, resulting in an increase in the number of templates available. In particular, amplification of c-*myc* has been observed in different neoplasms (Alitalo et al., 1983; Escot et al., 1986). Other mechanisms involved in Myc-induced carcinogenesis, are overexpression, point mutations and increased protein stability. Protein stability is determined by gene amplification of the coding region determinant binding protein, CRD-BP, involved in posttranscriptional regulation of c-Myc mRNA (Vita and Henriksson, 2006).

Moreover, all the different posttranslational modifications of Myc protein, involving phosphorylation, acetylation and ubiquitinylation are involved in the regulation of Myc stability (Vervoorts et al., 2006; Westermarck and Hahn, 2008). The frequency of the most common Myc alterations observed in human tumours is summarized in table 8.

Summary of *Myc* deregulation in human tumors

Tumor type	Frequency of *Myc* aberrations
Hematological malignancies	
B-acute lymphocytic leukemia	c-*Myc* rearrangement/amplification (47–52%)
Burkitt's lymphoma	c-*Myc* translocation (100%) c-*Myc* overexpression (91%)
Diffuse large cell lymphoma	c-*Myc* rearrangement/translocation (6–16%) c-*Myc* overexpression (10%)
Multiple myeloma	c-*Myc* translocation (15%)
Primary plasma cell leukemia	c-*Myc* rearrangement (13%)
Solid tumors	
Atypical carcinoid lung cancer	c-*Myc* amplification (17%)
Bladder cancer	c-*Myc* amplification (33%)
Breast cancer	c-*Myc* amplification (9–48%) c-*Myc* overexpression (45%) *MYCN* overexpression (25%) CRD-BP amplification (18%)[a]
Cervix cancer	c-*Myc* amplification (29%)
Colon cancer	c-*Myc* amplification (17%) c-*Myc* overexpression (67%)
Gastric cancer	c-*Myc* amplification (15–30%) c-Myc overexpression (47%)
Glioblastoma	*MYCN* amplification (<5%) c-*Myc*/*MYCN*/*L-Myc* overexpression (57–78%)
Hepatocellular carcinoma	c-*Myc* amplification (33%)
Large cell neuroendocrine carcinoma	c-*Myc* amplification (23%)
Medulloblastoma	c-*Myc*/*MYCN* amplification (5–15%) c-*Myc* overexpression (31%) *MYCN* overexpression (68%)
Melanoma, nodular	c-*Myc* amplification (61%)
Melanoma, superficial spreading	c-*Myc* amplification (28%)
Neuroblastoma	*MYCN* amplification (25–30%)
Oesophageal squamous cell carcinoma	c-*Myc* amplification (10–30%)
Osteosarcoma	c-*Myc* amplification (7–78%)
Ovarian cancer	c-*Myc* amplification (40%) c-*Myc* overexpression (44%) *L-Myc* amplification (15%) *L-Myc* overexpression (40%)
Prostate cancer	c-*Myc* amplification (30–50%) c-*Myc* overexpression (70%)
Renal clear cell carcinoma	c-*Myc* amplification (8%)
Retinoblastoma	*MYCN* amplification (10–20%)
Rhabdomyosarcoma	*MYCN* amplification (43–67%)
Small cell lung carcinoma	c-*Myc* amplification (20%) *L-Myc* amplification (13%) *MYCN* amplification (10%)

The major genetic aberrations of *Myc* in human tumors include gene amplification in solid tumors and chromosome translocation in lymphoma and leukemia. Mutation of the *Myc* gene has also been reported in some lymphomas.

[a] CRD-BP: c-*Myc* mRNA stabilizing protein, associated with Myc protein stabilization.

Table 8. *myc* activation mechanisms (Marina Vita, 2006).

1.4.7 The *c-myc* oncogene in thyroid

Different studies have led to discordant conclusions concerning the role of Myc in thyroid carcinogenesis. The *c-myc* expression level was compared between normal and tumorigenic thyroid cells. There is a higher amount of *c-myc* mRNA in adenoma cells as compared to the normal ones. Moreover, in normal thyroid cells, *c-myc* mRNA

is visible just after TSH stimulation in a time-dependent manner (Yamashita et al., 1986).

However, further studies confirmed that *c-myc* proto-oncogene expression occurs in benign cancer as well as in normal thyrocytes (Burman et al., 1987). Moreover, high levels of c-*myc* and c-*fos* transcripts were observed in thyroid carcinomas with unfavourable prognosis (Table 9) (Hashimoto et al., 1990; Terrier et al., 1988; Wyllie et al., 1989; Yamashita et al., 1986).

Expression of c-*myc* and c-*fos* proto-oncogenes in human thyroid carcinomas

Histological type of thyroid specimens	*No. of patients with elevated levels of c-*onc *RNA*[a]*/No. of patients analyzed*	
	*c-*myc *RNA*	*c-*fos *RNA*
Carcinomas		
Follicular well differentiated	0/1	1/1
Follicular moderately differentiated	4/6	3/6
Papillary	6/13	7/13
Anaplastic	1/1	1/1
Medullary	2/2	2/2
Total	13/23	14/23
Benign tissues		
Adenoma	1/22	20/22
Graves' disease	1/3	0/3
Normal thyroid tissues	2/8	2/8

[a]Elevated levels of c-*myc* and c-*fos* transcripts corresponding to ≧3 fold the levels found in normal human tissues and cells (thyroid, lymphocytes).

Table 9. Activated *c-myc* and *c-fos* oncogenes in human thyroid tumours (Terrier P, 1988).

1.5 Oncogenes and cancer development

According to the current model for cancer development envisions, cells undergo a series of genetic mutations and/or alterations, which result in their inability to respond

normally to intracellular and extracellular signals that control proliferation, differentiation and death. The number of required genetic alterations varies for different types of cancer and it is likely that further changes occur during its progression toward increased malignancy.

The co-operation between multiple oncogenes and/or loss of tumour suppressors from different functional classes and altered expression of cancer-associated molecules (Bergers et al., 1998) is a necessary path for transformation to proceed. In fact, it was observed that, although over-expression of a single oncogene does not transform wild type mouse embryonic fibroblasts, combinations of *myc* and *H-ras*^{V12}, could induce cellular transformation resulting in a marked proliferative advantage (Land et al., 1983b).

Transformation of cultured cells is itself a multistep process: rodent cells require at least two introduced genetic changes before they acquire tumorigenic competence (Fusco et al., 1987a).

From observations on human cancers and animal models, it appears that tumour development goes ahead via a process formally analogous to Darwinian evolution, in which a succession of genetic changes, each conferring one or another type of growth advantage, leads to the progressive conversion of normal human cells into cancer cells.

A powerful system to investigate tumorigenesis has resulted from the ability to manipulate the mouse germ line through the introduction of new genetic information (Hanahan, 1989) and through the targeted disruption of existing genes by homologous recombination (Capecchi, 1989; Zimmer, 1992). In addition, the colorectal tumours provide an excellent system for the search and study of the genetic alterations involved in the development of a common human neoplasm. Its salient features include the fact that mutation in at least four to five genes are required for the formation of a malignant form and few changes suffice for benign tumorigenesis. One important type of somatic

alteration identified in colorectal tumour is *ras* gene mutation. In addition to somatic alteration by point mutation, oncogenes may be activated by amplification, although, only in few cases, as observed in karyotypic analyses. These cases include examples of *c-myc* (Alitalo et al., 1983; Fearon and Vogelstein, 1990; Rothberg et al., 1985; Stewart et al., 1986).

1.5.1 *ras* and *myc* co-operation

The aim of this work is to study the multistep process of the thyroid tumorigenesis due to the oncogenic interaction. In particular, the work focuses on the interaction between two oncogenes: *Hras* and *c-myc*.

In transforming primary cells, nuclear oncogene such as *myc* is known to cooperate with those genes acting in the cytoplasm such as *ras*. The first type belongs to the immortalizing genes, whereas the second one to the transforming oncogenes.

It was proposed that the *myc* gene leads to the establishment of rodent cell lines, considering that it does not induce any morphological or proliferative changes in 3T3 cells or in primary rat embryo fibroblasts. Hence the changes caused by the *myc* gene alone in *in vitro* transformed cells are not sufficient to generate neoplastic lesions and that additional changes are necessary (Palmieri et al., 1983).

Introduction of the *ras* and *myc* oncogenes simultaneously through retroviral vectors, into midgestation mouse embryos, led to the formation of malignant tumours in a great variety of tissues (Table. 10). To asses the transforming potential of the *ras* and *myc* oncogenes in the developing embryo, embryos were exposed to *ras* or *myc* single infection or to their simultaneous introduction. Only when jointly infected, the oncogenes induced a wide spectrum of neoplasms, the majority of which were malignant or premalignant. These results indicate that many cells of the developing embryo are highly susceptible to the combined expression of both oncogenes and are

consistent with the hypothesis that the *ras* and *myc* oncogenes act synergistically *in vivo* in cellular transformation (Compere et al., 1989). In addition, rat embryo fibroblasts were found to have tumorigenic conversion following the *ras*-plus-*myc* cotransfection. They observed that a *ras* oncogene was not able to force an REF to expand into a tumorigenic clone when this gene was expressed at low levels within a cell growing in the presence of adjacent normal cells and required a collaborating oncogene like *myc* to achieve this result. Moreover, also a DNA clone that induced high levels of *myc* expression was able to immortalize cells and to cooperate with *ras* more efficiently than clones with lower expression levels of a *myc* protein (Land et al., 1986).

Summary of histologic analysis of lesions after *ras/myc* double infection	No. observed
Benign (all skin)	
Surface epithelial hyperplasia with severe dysplasia, premalignant	9
Mixed appendage tumor	2
Mesenchymal proliferation	1
Malignant	
Brain	
Neoplasm exhibiting prominent angiocentric pattern and epithelial papillary configurations (consistent with meningeal origin)	6
Primitive neoplasm (? neural, lymphoid, germ cell origin)	1
Skin	
Squamous cell carcinoma	3
Kidney	
Malignant neoplasm replacing renal medulla	1
Spindle cell neoplasms in heart, skin, and subcutaneous tissue, chest wall (poorly differentiated carcinomas, high grade sarcomas)	7

Table 10. Summary of histologic analysis of lesions after *ras/myc* double infection (Compere et al., 1989).

It is known that specific combinations of oncogenes can transform, whereas the same oncogenes are impotent individually. In particular, the *ras* and *myc* oncogenes

collaborate in transformation of primary cells (Weinberg, 1989). When alone, these two oncogenes were unable to induce foci formation in rat embryo fibroblasts, whereas in combination, they achieved the formation of quickly growing foci with altered phenotype. Moreover, these cells were tumorigenic when introduced into the nude mice (Land et al., 1983b).

It is also noteworthy that the functional domains of *c*-Myc protein required for c-Ha-Ras cotransformation of rat embryo fibroblasts overlap with those regulating its own autosuppression during transcription (Fig. 20) (Penn et al., 1990; Stone et al., 1987).

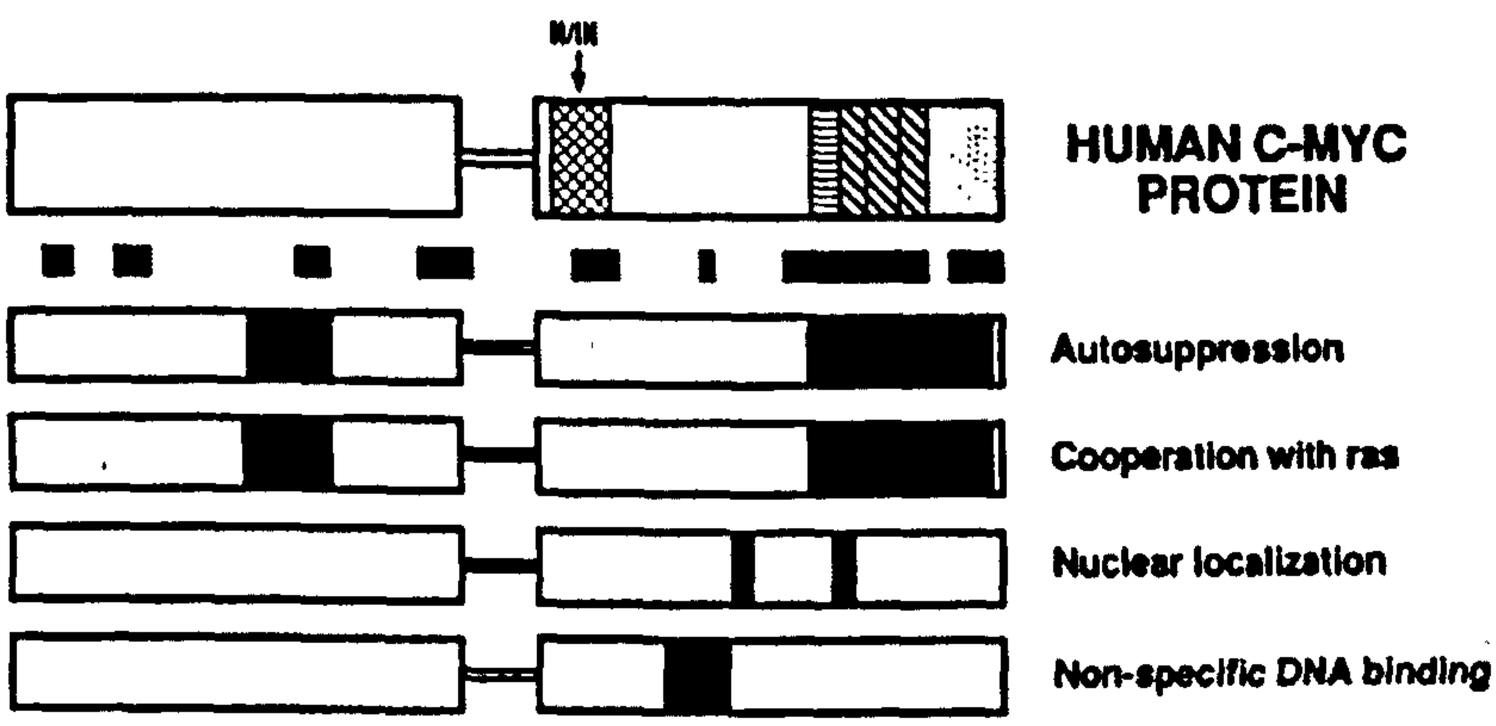

Structural and functional domains of human c-*myc* protein. Secondary-structure predictions based on amino acid sequence information suggest that the 439-amino-acid nuclear phosphoprotein may be composed of an α-helix–β-sheet domain (amino acids 1 to 203) and a predominantly α-helical domain at the carboxyl end (amino acids 238 to 439) which are separated by a less-structured hinge region (amino acids 204 to 237). Additional structural motifs include a highly acidic domain ( ), a basic region ( ), a helix-loop-helix domain ( ), and a leucine zipper ( ). Regions most highly conserved among the members of the *myc* gene family ( ) are also indicated. The functionally essential domains of c-*myc* identified to date are represented by the solid black boxes in the specified schematic diagrams and map as follows: autosuppression, residues 106 to 143 and 353 to 433; cooperation with *ras* oncogenes in rat embryo fibroblasts, residues 106 to 143 and 353 to 433; nuclear localization, residues 320 to 328 and 364 to 374; and nonspecific DNA binding, residues 290 to 318. *II/III*, Border of exon II- and exon III-encoded sequences.

Figure 20. Structural and functional domains of human c-Myc protein (Penn et al., 1990).

In thyroid cell lines, as well as in fibroblasts and other tissues, more than one step is required for the complete transformation of cells to achieve the fully malignant phenotype (Table 11) (Fusco et al., 1987a)

Transformation markers of PC Cl 3 cells after interaction with two different oncogenes

Cell type[a]	Colony-forming efficiency (%)[b]	Tumor incidence[c]	Latency period (wks)	Histology
PC Cl 3	0	0/5		
PC-HaMSV	0	0/4		
PC-*myc*	0	0/5		
PC-*myc* + HaMSV	1–2	4/4	3–4	Carcinoma
PC-HaMSV + *myc*	1–2	4/4	4–5	Carcinoma
PC-Homer 6 + HaMSV	0	0/4		

[a] PC-HaMSV, PC Cl 3 cells infected with HaMSV; PC-*myc*, PC Cl 3 cells transfected with the pMCGM1 plasmid bearing the human c-*myc* gene; PC-*myc* + HaMSV, PC-*myc* subsequently infected with HaMSV; PC-HaMSV + *myc*, PC-HaMSV subsequently transfected with pMCGM1; PC-Homer 6 + HaMSV, PC Cl 3 transfected with the vector Homer 6 and then infected with HaMSV.

[b] Colony-forming efficiency was measured in agar as indicated in Table 2, footnote *a*.

[c] Tumorigenicity was assayed by injecting 2×10^6 cells into athymic nude mice. Number of animals with tumors/number of animals tested.

Table 11. Transformation markers of cells from rat thyroid gland after interaction with two different oncogenes (Fusco et al., 1987a).

One aspect of their collaboration is the ability of Ras to stabilize Myc protein by inhibiting its proteosome-dependent degradation. Sears et al. (1999) observed an increase in the level of Myc protein following a growth stimulation of the cells. Since Ras activation is the main event following mitogenic stimulation, they hypothesized that Ras and its pathway were involved in the increase of Myc. Their experiments demonstrated that the expression of an activated form of H-*ras* gene contributed to the Myc stabilization and, in contrast, a dominant negative mutant form of H-*ras* gene led to a dramatic decrease in the level of Myc in serum-stimulated cells. The Ras/Raf/MAPK pathway might be involved in Myc protein stabilization through the inhibition of the proteosome-mediated proteolysis, since either the MAPK inhibitor or the dominant negative mutant form of H-*ras* gene did not affect the *myc* RNA levels, induced by serum stimulation (Sears et al., 1999).

In order to understand how the pathways, downstream these two proteins, interact to drive cell growth, Sears et al (1999) focused their attention on the two

phosphorylation sites located in the N-terminal domain of Myc: Thr 58 and Ser 62, which are regulated by mitogen stimulation.

It was observed that the Ser 62 phosphorylation is required for the stabilization of Myc and is mediated by ERK kinase; whereas Thr 58 phosphorylation, following that of Ser 62, controls the c-Myc ubiquitin-mediated degradation and the glycogen synthase kinase (GSK-3, whose activity is held check by that of the AKT) plays a crucial role in such a phosphorylation event.

Thus, Ras activation elicits two responses: a direct effect of ERK on Myc protein stabilization and an indirect effect on GSK-3, on which depend ubiquitination and degradation (Sears et al., 1999) (Fig. 21).

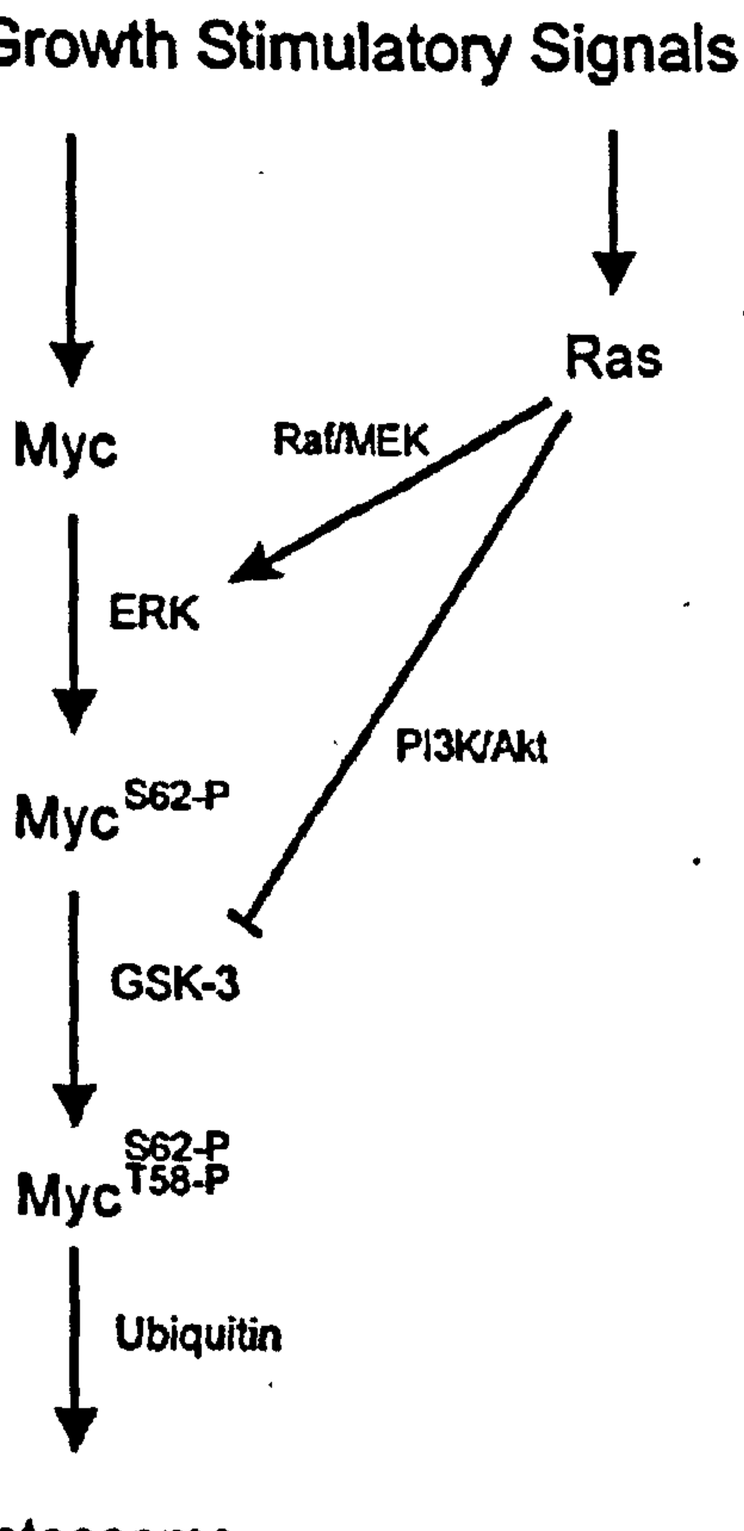

Pathways controlling Myc phosphorylation and accumulation.

Figure 21. Pathways controlling Myc phosphorylation and accumulation (Sears et al., 2000).

1.6 Aim of the Ph.D. project and experimental strategy

The aim of this Ph.D. project is to study the molecular basis of thyroid cancerogenesis induced by oncogenes and their interaction by synchronous activation.

Three were the main steps of this work:

1. To generate an oncogenic construct suitable for creating a transgenic mouse strain.

A novel conditional onco-mouse expressing two oncogenes, *c-myc* and *H-ras*^{V12}, in a tissue-specific as well as in a conditional manner, would be useful for such a study.

We have focused on two oncogenes: *H-ras*^{V12} and *c-myc*. To induce their combined action in the same cell, we generated a targeting construct containing the inducible alleles of the oncogenes, cited above. Each oncogene was fused to a mutated Ligand Binding Domain (LBD) of a steroid receptor. In particular, chimeric alleles of *H-ras*^{V12} (fused to the mutated LBD of the Estradiol Receptor -ER-) and *c-myc* (fused to the mutated LBD of the Progesterone Receptor -PR-) were used. In such a manner, the chimeric gene product would be post-translationally and temporally regulated by the administration of the cognate ligand. Just after addition of the corresponding drug, the protein would change its conformation and become activated to exert its function. In both cases, it was used as a mutagenized LBD which permits the binding of synthetic drugs like tamoxifene (Juin et al., 1999) and mifepristone or RU486 (Kellendonk et al., 1996), but not that of the natural ligands such as estradiol and progesterone respectively. Since the inducer drugs differ between them, it would be possible to activate only ER-Ras^{V12} (with tamoxifene for the *in vivo* or 4OHT for the *in vitro* system, respectively) or only c-Myc-PR with RU486 or both simultaneously in the presence of two drugs: tamoxifene (or 4OHT) and RU486.

To allow that the two oncogenes are expressed simultaneously and to work on oncogene cooperation, in order to induce tumorigenesis, a bicistronic construct was made in which, an Internal Ribosome Entry Sequence (IRES) was inserted between the

sequences encoding the two oncogenes, to allow the translation of two consecutive open reading frames from the same messenger RNA.

The IRES mechanism involves the formation of a complex structural element in the 5'-untranslated region of the mRNA. IRESs were first discovered in picornavirus RNAs but there are now many examples of cellular mRNAs containing IRESs. In general, these have been identified in genes whose function is associated with cellular processes such as cell growth or cell death, cell cycle or apoptosis.

It seems that cellular IRESs are required to maintain the expression of critical proteins when cap-dependent translation is reduced.

The capacity of different IRESs to induce efficiently, high levels of exogenous cDNA expression, changes based on the cell type. Among the different IRESs or the different approaches for co-expressing two genes, the encephalomyocarditis virus (EMCV) IRES induces high levels of DNA translation (Ghattas et al., 1991). However, even its activity differs dramatically according to the cell line or tissue used (Borman et al., 1997). It has emerged from studies on site-directed mutagenesis, that a specific region of EMCV comprising nucleotides between 403 and 811, is required for efficient translation and that a region 400 nucleotides upstream of the initiation codon assumes a stem-loop structure. Moreover, a 57 KD cellular protein has been found to interact with this stem-loop structure (Jang and Wimmer, 1990). On the basis of these observations, it is possible to explain the different activities in different cell lines assuming that cell type-specific and spatiotemporally controlled trans-acting factors might exist, interacting with that region. Such proteins could be involved in the positive or negative control of the IRES-mediated translation based on the accessibility of this structure (Creancier et al., 2001).

IRES-mediated bicistronic expression is successful *in vivo* (Fenske et al., 2004; Mountford and Smith, 1995; Vincent and Robertson, 2003).

A powerful approach for a tissue-specific and at a chosen time expression of the oncogenes is the Cre-loxP strategy (Brenner et al., 2005), in which P1 bacteriophage Cre recombinase (Cyclization recombination) is a 38 KD protein recognizing and mediating site-specific recombination between two loxP (locus of crossing [x-ing]-over of bacteriophage P1) sequences. LoxP sequence (34bp) consists of two 13 bp inverted repeats interrupted by an eight nonpalindromic sequence which dictates the orientation of the entire sequence. The Cre protein acts on two loxP sequences on the basis of their orientation. This Cre/loxP system can be used to make gene insertion or replacement, large genomic deletion or inversion or chromosomal translocation.

Sometimes it would be useful that the transcription of the target gene does not occur until it becomes necessary to study its function or its effects (in case of integration in the genome of additional copies of a target gene). This is possible using a STOP sequence upstream of the target gene, flanked by two loxP sequences. After the Cre action, the floxed STOP cassette can be removed and the target gene can be transcribed.

The Cre/loxP recombination system requires two mouse strains: the first one harbouring a loxP-flanked segment of a target gene and the second one expressing Cre recombinase in specific cell types. After crossing these two mouse strains, the modification of the loxP-flanked target gene is restricted in a spatial and temporal manner according to the pattern of Cre expression in the particular strain, used.

This kind of construct, in which the target proteins are regulated after translation by the corresponding drugs and containing a STOP cassette preceding the oncogenic coding sequences, will allow us to generate mice in which the activity of oncogenes is tightly controlled in a spatio-temporal manner.

2. To evaluate the expression of the construct and its biological effects in thyroid cell lines.

To test the effects of these two oncogenes in cell systems, the bicistronic cassette was cloned under the control of EF1α promoter into a eukaryotic expression vector.

The construct was transfected in a thyroid cell line. Different assays were performed on the positive selected clones in order to verify the expected co-operation between the two oncogenes. The main purpose was to assess the ability of the targeting vector to induce TSH-independent growth of thyroid cells or induce their dedifferentiation.

3. To evaluate the expression of the construct and its biological effects in transgenic mice.

The transgenic construct was used as targeting vector to modify, by homologous recombination, Embryonic Stem (ES) cells to generate a mouse model.

To obtain a flexible model carrying the oncogenes in any tissue, a targeting vector was designed carrying the two oncogenes inserted into ROSA26 *locus*, which is ubiquitously expressed throughout mouse development and adulthood. ROSA26 is the acronym for the complete noun Reverse Orientation Splice Acceptor. It maps to mouse chromosome 6 and displays ubiquitous expression during embryonic development (starting at the morula-blastocyst stage) and in adult. Both DNA strands of the genomic region are transcribed producing three different transcripts, two noncoding and one coding. Two of the transcripts with a sense-antisense relationship share the sequence of the exon 3. Following a gene insertion, usually into the first intron of the locus, the antisense transcript is the only one present in the mutant mice and the loss of the two noncoding transcripts does not give any abnormal phenotype (Friedrich and Soriano, 1991; Vooijs et al., 2001; Zambrowicz et al., 1997).

A second *locus*, broadly expressed throughout mouse development and adulthood, is the Eef1α1 (Eukaryotic translation elongation factor 1 alpha 1). Eef1α1 is located on chromosome 9 in mouse. This cytoplasmic protein promotes the GTP-dependent binding of aminoacyl-tRNA to the A-site of ribosomes during protein biosynthesis. Thus, it belongs to the GTP-binding elongation factor family and is ubiquitously expressed during embryonic development and adulthood.

In both these cases, the transgenic sequence was placed downstream to a splice acceptor site and targeted into the first intron between exons 1 and 2 of ROSA26 *locus* or between the first intron and the second exon of Eef1α1.

Mice harbouring the targeting vector, integrated into the two *loci* mentioned above, were then mated with mice expressing CRE to allow the Cre/loxP recombination.

CHAPTER 2

MATERIALS AND METHODS

Part A: Molecular Biology

A.1 Plasmid Manipulation

A.1.1 Digestion with restriction enzymes, de-phosphorylation reaction, Klenow reaction

In this work many plasmids have been generated or modified to obtain the constructs and the targeting vectors of interest described below.

In general:

for qualitative analysis, 500 ng of DNA were digested; for quantitative preparations, 2 μg of sample were used. All the restriction enzymes were from New England Biolabs or Roche, and the reactions were performed in the appropriate buffers, supplied by the manufacturer. The separation of the resulting fragments was achieved by agarose gel electrophoresis.

After enzymatic digestion, the 5'-phosphate group was removed in order to avoid self-ligation and circularization of plasmid DNA. The de-phosphorylation reaction of 500 to 2000 ng DNA was carried out with 5 Units calf intestinal alkaline phosphatase (CIP) (New England Biolabs) for 1h at 37°C in a final volume of 50 μl. The modified DNA was then extracted with phenol-chloroform.

The sticky plasmid ends were made blunt by Klenow reaction, which was set up in a final volume of 50 μl with 20 μl digested DNA, 5 Units of Klenow enzyme, 100 μM dNTPs in 1X reaction Buffer and carried out at 16°C for 20 minutes.

A.1.2 Purification of DNA

After each enzymatic reaction, the DNA was purified by phenol:chloroform:isoamyl alcohol (PCI) (25: 24: 1) extraction before proceeding to the next step of cloning.

An equal volume of PCI was added to the DNA sample, mixed well to form an emulsion and centrifuged at 12000 *g* for 15 minutes at room temperature (RT).

The aqueous phase was saved and 0.1 volume of 3M Sodium acetate (pH 6) and 2.5 volumes of absolute ethanol were added to the same and left at -20°C for 20 minutes. The sample was then centrifuged at 12000 *g* for 15 minutes at 4°C; the DNA pellet obtained, was washed with 70% ethanol and suspended in appropriate amount of mQ water.

A.1.3 Agarose gel electrophoresis

Depending on the size of the DNA fragments to be resolved, gels of different concentrations were cast in TBE buffer (45 mM Tris-Borate pH 7.5, 1 mM EDTA) using the fluorescent dye ethidium bromide, at a concentration of 0.5 μg/ml. The fragment of interest was detected corresponding to the molecular weight of the DNA ladder-marker .

The samples, prepared by adding 0.1 volume of 10X dye (0.5% bromophenol blue, 40% glycerol, 5.5mM Tris, 55 μM EDTA pH 7.5) were run on gels at 100V in 0.5X TBE buffer and DNA was visualized on UV transilluminator.

A.1.4 Isolation of DNA from agarose gel

Following agarose gel electrophoresis, the DNA gel slices were excised under UV light. DNA was extracted from them by QIAquick Gel Extraction Kit (Qiagen) following the protocol supplied by the manufacturer. The gel was solubilized in the appropriate buffer, isopropyl alcohol was added and then loaded on a chromatographic column, which was washed with ethanol. The DNA was then eluted from the resin using 30 µl of mQ water.

A.1.5 Ligation reactions

The ligation reactions with 400 Units T4 DNA Ligase in a volume of 10 µl were generally set up as follows:

X ng vector DNA : Y ng insert DNA = 1: 3 (on the basis of their dimension)

and carried out 16°C over night.

They were then purified with phenol-chloroform and the DNA pellet was dissolved in 10 µl of mQ water, out of which, 5µl were used for transformation of electro-competent XL1Blue *E.coli* cells. The resulting clones were analyzed by restriction digestion and sequencing.

A.1.6 Transformation of *E.coli* with plasmid DNA

E.coli XL1Blue cells were prepared for transformation as follows: cells were grown to mid-log phase (A_{600}=0.6) in 200 ml of Luria Broth (LB: 1% bactotryptone, 1% NaCl and 0.5% Bacto-yeast extract) at 37°C with shaking. Cells were divided into four 50 ml tube, harvested by centrifugation at 3500 *g* at 4°C for 15 min, resuspended

into 25 ml (for each 50 ml of culture) of ice cold 10% glycerol solution. This suspension was then centrifuged at 3500 *g* for 15 min at 4°C. The resulting pellet was resuspended in 25 ml (for each 50 ml of culture) of ice cold 10% glycerol solution. After further centrifugation, the pellet was resuspended in 5 ml (for each 50 ml of culture) of ice cold 10% glycerol solution and centrifuged again as above. Each final pellet was resuspended in 1 ml of 10% glycerol solution, aliquoted and stored at -80°C. For each transformation, DNA was added to 40 µl of competent cells, incubated on ice for 5 min; then, cells were electroporated using gene pulser (Biorad) (25 µF, 1,7 kV, 200 Ohm), and successively grown in 1 ml of LB for 1h at 37°C. After plating on LB-agar containing appropriate antibiotics, the cells were incubated at 37°C overnight.

A.1.7 Isolation of plasmid DNA from *E.coli*

Colonies picked up from plates were incubated in LB, supplemented with the appropriate antibiotic in a final concentration of 100 µg/ml, at 37°C overnight with shaking.

Large-scale (maxi-preps) and little-scale (mini-preps) plasmidic DNA preparations were carried out using the Qiagen maxi and mini prep kits, respectively. Both procedures are based on the alkaline lysis method; following centrifugation, debris precipitate while plasmid DNA remains in solution. That solution is loaded on a column to purify isolated plasmid DNA. After the first centrifugation, the column is washed with ethanol 70% before DNA elution in 30-50 µl of elution buffer or mQ water.

Purified DNA was always quantified and checked by enzymatic digestion with appropriate enzymes.

The concentration of isolated DNA was determined by spettrophotometry

according to the following formula: absorbance of one A_{260} unit indicates a DNA concentration of approximately 50 µg/ml.

A.1.8 pCEFL vector

pCEFL vector is an eukaryotic expression vector containing the Ef1α1 (eukaryotic elongation factor) promoter upstream of the multi cloning site (MCS). The vector carries two origins of replication: the fist one of *E.coli* (ColE1) to permit its replication into bacteria and the second one of the virus SV40 in order to allow its replication into eukaryotic cells.

Moreover, the vector contain two antibiotic resistance coding genes: the first one is a procariotic gene (Ampicillin), the second one is an eukaryotic gene (Neomycin), preceded by the SV40 promoter and followed by the SV40 polyA signal.

A.2 Western blot

A.2.1 Protein extraction, purification and quantification

The cells were washed twice with PBS 1X, covered with 60 µl of Lyses Buffer (50 mM Tris buffer pH 8.0, 150 mM NaCl, 0,1% SDS, 1% Triton, 5 mM $MgCl_2$, 0,5% Deoxycholic Acid) supplemented with protease inhibitors (1X protease inhibitors Cocktail Sigma, 0.5 mM $Na_4P_2O_7$, 0.5 mM PMSF, 1 mM DTT, 50 mM NaF, 0.5 mM Na_3VO_4) and incubated at 4°C for 5-10 minutes.

After centrifugation, the proteins were contained in the supernatant phase.

The isolated proteins were quantified using BCA™ Protein Assay Kit by Pierce following the protocol supplied by the manufacturer. After the reduction of the Cu^{2+} ion, due to the presence of the proteins, the absorbance values at 562 nm (proportional

to the amount of proteins) were interpolated among the values of a standard curve made by known concentrations of Albumin (BSA).

A.2.2 Sodium Dodecyl Sulfate-PolyAcrylamide Gel Electrophoresis (SDS-PAGE), Protein transfer from gel to membrane and membrane blocking

Proteins were separated by electrophoresis on denaturing acrylamide gel containing a polyacrylamide gradient ranging from 4% to 12%. The kit used was ''NuPAGE Bis-Tris electrophoresis system kit'' from Invitrogen following the protocol supplied by the manufacturer.

About 30 µg of total proteins extracted were supplemented with NuPAGE LDS-sample buffer 1X (Invitrogen) and NuPAGE reducing agent 1X (Invitrogen) and heat treated before loading.

The running buffer was MOPS SDS Running Buffer 1X (Invitrogen) supplemented with NuPAGE Antioxidant 1X (500 µl/200 ml) in the inner (cathode) buffer chamber.

Gels were generally run at 200V for about 1 h.

Proteins, separated on a gel, were transferred to a Polyvinylidene difluoride (PVDF, Immobilion^{TM}-P from Millipore) membrane by electroblotting.

A sandwich composed by gel and membrane in touch, flanked by 3 mm Whatman paper and sponges, was placed into a transfer chamber within transfer buffer (20% Methanol, Towbin 1X composed of 25 mM Tris, 190 mM Glycine, 0,03% SDS).

Transfer was generally run at 100V for about 1 h and 30 minutes.

To block every non-specific binding sites on the membrane, after transfer the membrane was incubated for 1 hour at room temperature with a solution containing

PBS (or TBS), 0,05% (or 0.1%) Tween 20 and 5% Non-Fat Dry Milk from Biorad.

A.2.3 Primary and Secondary antibodies

A primary antibody has a specific epitope to recognize the protein of interest and was diluted in the blocking solution following the protocol supplied by the manufacturer.

Primary antibody used according to manufacturer's instructions:

- Anti-Ras clone RAS10 monoclonal antibody was by Upstate Cell Signaling Solutions
- Anti-c-Myc (9E10) monoclonal antibody was by Santa Cruz Biotechnology
- Anti-phospho-p44/42 MAP Kinase polyclonal antibody was by Cell Signaling
- Anti-p44/42 MAP Kinase polyclonal antibody was by Cell Signaling
- Anti-phospho-Akt (Ser473) polyclonal antibody was by Cell Signaling
- Anti-Akt polyclonal antibody was by Cell Signaling
- Anti-β-Actin monoclonal antibody was by Sigma
- Anti-Tubulin a monoclonal antibody was by Sigma
- Rabbit polyclonal anti-Pax8, previously produced in our laboratory, was used at approximately 1 μg/ml.

The membrane was dip into the antibody solution for 1 h at room temperature or at 4°C overnight on an oscillating motion.

After treatment, the membrane was washed with a solution containing PBS (or TBS) and Tween 20 0.05% (or 0.1%) to remove the exceeding antibody.

Secondary antibody (ECL™ Anti-mouse Ig Horseradish peroxidise-linked whole antibody (from sheep) or ECL™ Anti-rabbit Ig Horseradish peroxidise-linked whole

antibody (from donkey) Amersham Biosciences) were diluted in the blocking solution following the protocol supplied by the manufacturer.

The membrane was dip into the antibody solution for 1 h at room temperature on an oscillating motion.

After treatment, the membrane was washed with a solution containing PBS (or TBS) and Tween 20 0.05% (or 0.1%) to remove the exceeding antibody.

A.2.4 Immune complexes detection

The ECL Western Blotting detection reagents from Amersham Biosciences was used to detect the proteins of interest bound to a membrane by the detection of immobilized specific antigens conjugated to Horseradish Peroxidase (HRP) labelled antibody.

The reaction solution was placed on the membrane for 1 minute at room temperature. The reaction consists in the oxidation of luminol carried out by the Horseradish Peroxidase (HRP) linked to secondary antibody.

The emitted light is proportional to the amount of protein of interest and was detected by autoradiography or by ChemiDoc™ XRS (Biorad).

A.2.5 Membrane stripping

Membrane stripping is a treatment allowing the complete removal of primary and secondary antibodies from membrane.

The membrane was dip into the stripping solution (62.5 mM Tris/HCl pH 6.8, 2% SDS, 0.07% β-Mercaptoethanol) and incubated at 50°C for 30 minutes.

After treatment, the membrane was washed with a solution containing PBS (or

TBS) and Tween 20 0.05% (or 0.1%).

A.3 Processing of RNA

A.3.1 RNA extraction

Total RNA was extracted from cells using the TRIzol Reagent (Invitrogen) following the protocol supplied by the manufacturer.

The cells were washed twice with sterile PBS 1X, covered with 1 ml of TRIzol for each plate and incubated at room temperature for 5 minutes. After genomic DNA fragmentation, chloroform addiction and centrifugation, RNA was contained in the upper aqueous phase. RNA was isolated and precipitated by addiction of isopropyl alcohol and further centrifugation. The RNA pellet was washed with 75% ethanol, dried and resuspended in a proper amount of mQ water.

RNA extraction from tissues, after complete mechanical disruption of the tissue, follows the protocol described above.

The RNA quality was checked by electrophoresis in a denaturing gel (1% w/v agarose, MOPS buffer 1X (20 mM MOPS, 20 mM sodium acetate, 1 mM EDTA pH8), 2.2M formaldehyde) following addition of loading buffer (50% glycerol, 1 mM EDTA pH8, 0.25% bromophenol blue, 0.25% xylene cyanol FF, 0.1 ng BrEt) to each sample and heat denaturation.

Electrophoresis was generally run at 100V in running buffer composed by MOPS 1X.

A.3.2 RNA reverse transcription

In order to obtain the cDNA synthesis, 1 μg of total RNA was used as template

for the synthesis of the first strand cDNA reverse starting from random examers, using the QuantiTect Reverse Transcription kit (Qiagen) according to manufacturer's instructions.

A.3.3 mRNA quantification

RT-PCR amplifications were conducted using 12.5 µl of Power SYBR Green PCR master mix (Applied Biosystem), 0.5 µM of each primers a final volume of 25 µl. Thermocycling was performed using ABI Prism 7300 Real Time PCR System (Applied Biosystems Foster City, USA) initiated by a 10 min incubation at 95 C°, followed by 40 cycles (95 C°, 15 sec; 60C°, 1min). Each run was completed with a dissociation curve analysis to confirm the specificity of amplification and lack of primer dimers. Threshold cycle (Ct) values were determined by Applied Biosystems software and analyzed using MS Excel program.

Reactions were carried out in triplicate and each one was internally normalized against the α-1 tubulin mRNA in each sample.

The mathematical expression describing such PCR amplification process is:

$$Q_n = q \times (1+k)^n \qquad \text{(Eq.1)}$$

or in other words

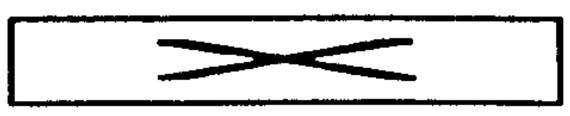

(Eq.2)

where

Q_n = molecules number following n amplification cycles
q = molecules number at the beginning of the reaction
k = amplification process efficiency ($k \in [0-1]$)
n = reaction cycles number

At a particular threshold cycle (a cycle chosen in the linear phase of the amplification) it becomes:

$$Q\text{threshold} = q \times (1+k)^{C_t} \qquad \text{(Eq. 3)}$$

For the amplification of the same gene in two different samples 1 and 2, using the same *Q*threshold the expression will be:

$$\frac{q_1}{q_2} = \frac{(1+k_2)^{C_{t2}}}{(1+k_1)^{C_{t1}}} \qquad \text{(Eq. 4)}$$

For each primer-pair, amplifications were carried out with different amount of each primer of the pair (300nM, 600nM and 900nM) in all the possible combinations. The best primer-pair was chosen on the basis of its dissociation curve and Ct value.

Reactions for quantification of mRNAs were performed in the same conditions, using 10 ng cDNA for each template, in three independent samples (as technical triplicates). The expression of the genes of interest was normalized by the expression of a housekeeping gene (α1-tubulin) measured under the same condition.

Part B: Cell Culture

B.1 Cell lines maintaining, transfections and monitoring assays

B.1.1 HeLa, NIH3T3 and COS7 cell lines

HeLa cells, NIH3T3 and COS7 cells were cultured in Dulbecco's modified Eagle's medium supplemented with 10% FBS, 1% penicillin/streptomycin and 4 mM glutamine and were maintained at 37°C in an atmosphere of humidified air containing 5% CO_2.

B.1.2 FRTL-5 cell line

FRTL-5 cells were cultured in Coon's modified F12 medium supplemented with 5% Newborn Calf Serum (NCF), 1% penicillin/streptomycin and a 1X mix composed by 6 hormones: Thyroid Stimulating Hormon (TSH) 1 mU/ml (Sigma), Insulin 10 mg/L (Sigma), Somatostatin 10 μg/L (Sigma), Transferrin 5 mg/L (Sigma), Hydrocortisol 3,7 μg/L (Sigma), Tripeptide gly-his-lys 20 μg/L (Sigma).

B.1.3 Cultures of mouse embryonic stem cells

ES cells were grown according to standard conditions. After thawing, ES cells were routinely passed each two days. Cells were cultured on mitotically inactivated primary mouse embryonic fibroblasts (MEFs), carrying neomicin resistance, prepared and cultured by the ES facility at BIOGEM. The ES culture medium consisting of Dulbecco's modified Eagle's medium (DMEM) with 4500 mg/l D-glucose and L-glutamine, 15% foetal bovine serum-FBS tested for ES cells, 2 mM glutamine, 0.1 μM β-mercaptoethanol, 1X non-essential amino acids, 50 mg/ml penicillin/streptomycin, 1.2 mM Sodium Pyruvate and 1000 U/ml leukaemia inhibitory factor (LIF).

The ES cells used for transfection were R1 ES cells, derived from wild type SV129 mice strain and bought from Nagy Lab.

B.1.4 Splitting

When cells were confluent it was necessary to dilute them. The plates were washed twice with phosphate-buffered saline PBS to eliminate the medium, were added with 1 ml of Trypsin-EDTA (2 ml for ES cells) and incubated at 37°C for 2-3 minutes (8-10 minutes for ES cells). The cells were separated into single cells by

pipetting up and down. To stop the trypsin reaction, 5 ml of medium were added to each plates. The trypsinized cells were collected into a centrifuge tube, spinned down by centrifugation at 1000 *g* for 5 minutes and resuspended in a proper amount of medium on the basis of the desired dilution.

B.1.5 Freezing

Each plate was washed twice with PBS and then the cells were incubated with 1 ml of Trypsin-EDTA (2 ml for ES cells) for 2-3 minutes (10 minutes for ES cells) at 37°C. The cells were centrifuged, resuspended in 1 ml freezing medium (90 % FBS or NCS, 10% dimethylsulfoxide -DMSO-) (50% ES-DMEM, 40% FBS, 10% dimethylsulfoxide -DMSO- for ES cells) and stored at -80°C or at -195°C into 2 vials.

B.1.6 Thawing

The cells contained into freezing medium in each vial were diluted with 10 ml of 37°C pre-heated culture medium, transferred into a centrifuge tube and spinned down by centrifugation at 1000 *g* for 5 minutes. The cells collected in a pellet were resuspended in 20 ml of culture medium and plated into two plates (or resuspended in 10 ml of culture medium and plated on a dish with feeders for ES cells). The day after the medium was changed to remove floating dead cells.

B.1.7 Transient and stable transfection

The cells were transiently transfected with 2 μg of plasmidic DNA carrying the coding sequence (CDS) of the oncogenes of interest (H-*ras*^{V12} and c-*myc*), subcloned

into the pCEFL vector downstream of the Ef1α1 (eukaryotic elongation factor) promoter.

One day before transfection, the cells were harvested by trypsinization, counted and then plated into 100 mm plate at a cell density of 20%. After cell adhesion, transfectinon was carried out by using the cationic lipid FuGENE 6 Transfection Reagent (Roche) according to the manufacturer's instructions. The transfection solution was prepared mixing Dulbecco's modified Eagle's medium (DMEM), FuGENE and plasmidic DNA in a ratio of 20:3:1 μg respectively. After 40 minutes of incubation at room temperature, the transfection solution was diluted into the appropriate cell culture medium and distributed into the plates. 48h later the cells were collected and lysed to extract the proteins.

Stable transfection was carried out following the procedure mentioned above, but 48h after transfection the cells were maintained for two weeks in a selective medium (medium containing 400 μg/ml of G418 antibiotic). In such a manner only the cells that express the gene providing the neomicyn resistance were able to grow and to form colonies. These colonies were isolated by picking up and transferred into one well of a clean 96-well dish to continue their culture individually.

B.1.8 ATPlite assay

ATPlite assay was used for the quantitative evaluation of proliferation and cytotoxicity of cultured mammalian cells and it is based on the production of the light caused by the reaction of ATP with added luciferase and D-luciferin.

The ATPlite procedure for 96-well microplate was as follow:

- To lyse the cells and stabilize the ATP, 50 μl of mammalian cell lysis solution were added to 100 μl of cell suspension per well and the plate

was shaked for 5 minutes in a orbital sheker at 700 rpm;

- 50 µl of substrate solution were added to the wells and the plate was shaked for 5 minutes in a orbital sheker at 700 rpm;
- The plate was dark adapted for 10 minutes before measuring the luminescence.

B.2 Electroporation of ES cells

B.2.1 DNA preparation

30 µg of the targeting vector were linearized by enzymatic digestion with Asp EI (from Roche), at 37°C for 5 hours. The digested DNA was extracted with phenol-chloroform, precipitated with ethanol, and the pellet resuspended in 30 µl of sterile 1mM Tris-HCl pH 7.4/ 0.1 mM EDTA pH 8.

B.2.2 Cells preparation

Two to four 100 mm plates of ES cells (approximately 2-3 x 10^7 cells) were fed 3-4 hours before harvesting. The cells were washed with phosphate-buffered saline PBS and single cell suspension was generated as follow: 2 ml of Trypsin/EDTA were added per plate and incubated at 37°C and 5% CO_2 for 10 minutes. 5 ml of ES medium were added to each dish to stop the trypsin reaction. The separation into single cells was achieved by pipetting up and down. The cells counted and resuspended in an appropriate volume to obtain 10^7 cells. The cells were spinned down by centrifugation at 800 *g* for 5 minutes. The pellet was washed twice with 10 ml PBS to remove all serum to avoid altering the electroporation conditions. The ES cells were resuspended in 800 µl of ice cold PBS, the 30 µg of linear DNA, purified as described in the previous paragraph, were added to the cells. The solution (ES cells + DNA) was

transferred into electroporation cuvette and electroporated. The BioRad GenePulser was set at 250 V, 500μF and the time constants obtained ranged between 6 and 7. After the electroporation, the cells were incubated for 10 minutes at room temperature, then transferred into 40 ml of ES medium. The cells were cultured onto four 100 mm dishes pre-seeded with mitotically inactivated MEFs. The medium was changed the next day. The electroporated cells were grown in ES medium without selection agent for 48 hours.

B.2.3 Selection

After allowing the electroporated cells to grow for 48 hours, selection was started. ES selection medium contains Neomycin (400 μg/ml) in doses lethal to all ES cells except to those that express the gene providing the resistance. Selection was carried out for 5-6 days.

B.2.4 Picking Colonies

The dish containing ES cells was washed once with PBS and then the cells were kept in PBS. Single colony was isolated under a microscope by aspiration with the tip of p20 pipette. The colony was placed into one well of a clean (no feeders) 96-well dish, containing 50 μl of trypsin and kept in ice until its complete filling. The colonies were trypsinized for 10 minutes at 37°C and 5% CO_2. The colonies were mechanically dissociated by pipetting up and down. The reaction was stopped by adding 100 μl of ES cell medium (without antibiotics) to each well of the dish. The cell suspension was transferred into 96-well dish containing fresh MEFs.

Once the cells reached 70% confluence, they were splitted in three. Two third of the colture was plated into two 96-well dishes containing fresh MEFs. The remaining one third was plated into gelatin coated 96-well dish. After two days, the ES cells grown on MEFs were cryopreserved. The ES cells on gelatin were splitted in half and plated again on gelatin coated 96-well dish. Once they reached high confluence, they were lysed for DNA extraction and PCR analysis.

B.2.5 Freezing electroporated ES cells

Each well was washed twice with PBS and then the cells were incubated with 50 µl of trypsin for 5' at 37°C. The cells were resuspended in 50 µl 2X freezing medium (20% dimethylsulfoxide-DMSO, 45% FBS, 35% ES culture medium). 100 µl of mineral oil were put on the top of each well to prevent sublimation.

The plates were placed at -80°C for two days and then stored at -195°C

B.2.6 Thawing electroporated ES cells

The 96-well dish was placed into the incubator (37°C, 5% CO_2) and the lower aqueous phase was transferred into one well of a 24-well dish containing fresh MEFs.

The colonies were expanded to freeze down several vials of cells.

B.2.7 DNA extraction from ES cells

The cells were washed twice with PBS and then each well was incubated with 50 µl of Lyses Buffer (10 mM Tris pH 7.5, 10 mM EDTA pH 8, 10 mM NaCl, 0.5% SDS with 1.0 mg/ml Proteinase K) over night at 60°C. The next morning, the DNA was extracted by adding ice cold absolute ethanol with 75 mM NaCl. After incubation for 2-3 days at 4°C, the plates were inverted on paper towel to drain the liquid. The DNA was rinsed three times with cold 70% ethanol and was stored at 4°C in 70% ethanol.

B.2.8 Screening of the electroporated ES cells

After a preliminary positive selection of electroporated ES cells by growth in a medium containing G418, a second screening on positive clones has been carried out by PCR.

For the Eef1α1MycRas/Eef1α1+ ES clones these PCR were performed using three primers in which one of them, the forward (FW1) was complementary on the 5' arm of the targeting vector. One of the two reverse primers (Rev1) annealed on the 3' arm of the targeting vector; while the second one (TransgLongR5 rev) annealed at the end of the splicing acceptor sequence (SA), on the construct.

The PCR was set up so that in one reaction both the wild type and recombinant locus could be identified, using all the three primers in the same reaction.

The primers used for the amplification were as follows:

FW1: 5' GGCAAACTGGGAAAGCGGTGTCGTGTGC 3'

Rev1: 5' CCGAGAATTAGCTCCGCTCAAAACTCAAGG 3'

TransgLongR5 rev: 5' CGGCCTCGACTCTACGATACCGTCGATCC 3'

The annealing temperature was 63°C.

On the Eef1α1 allele, primers FW1 and Rev1 amplify a 1058 bp product specific for the wild type allele; whereas the primers FW1 and TransgLongR5 rev amplify a 1115 bp product specific for the transgenic allele.

For the ROSA26MycRas/ROSA26+ ES clones these PCR were performed using four primers: two of them to amplify the wild-type allele (D3 fw and WT3 Rev annealing at the 5' and at the 3' arm of the targeting vector respectively and amplifying a 3800 bp product) and the other two for the transgenic one (LongD5 fw and TransgLongR5 rev annealing on the 5' arm of the targeting vector and on the construct at the end of the splicing acceptor sequence (SA) respectively, amplifying a 3650 bp product).

The primers used for the amplification were as follows:

D3 fw: 5' TGGACCCTTACCTTGACCCAGG 3'

WT3 Rev: 5' GCCACATCCATAGTGGCTCATTAGG 3'

LongD5 fw: 5' GGTCGTGTGGTTCGGTGTCTCTTTTCTGTTGG 3'

TransgLongR5 rev: 5' CGGCCTCGACTCTACGATACCGTCGATCC 3'

After the first step of DNA denaturation, the next two steps of each cicle, annealing and extension of both PCR, were carried out together at 68°C for 6 minutes.

B.2.9 Preparation of ES cells for blastocyst injection

One vial of recombinant ES cells was thawed and cultured as described previously. On the day of injections, cells were fed two hours before harvesting by trypsinization. The single cell suspensions was plated onto a new dish (without MEFs) and placed into the incubator for 20 minutes to completely remove the MEFs.

The medium containing the floating cells was collected and spinned at 1000 rpm for 5 minutes. The ES cells were counted and 10^6 cells were sent to BIOGEM

transgenic core facility to be processed for injection into blastocysts from C57BL/6 females. The same facility also dealt with re-implantation of blastocysts into uteri of CD1 pseudopregnant females.

Part C: Animal husbandry

C.1 *ROSA26c-myc-PR-ER-Hras^{V12}* and Eef1α1c-*myc-PR-ER-Hras^{V12}* mouse strains

All procedures on animals were carried out in accordance with the "DECRETO LEGISLATIVO 27 gennaio 1992 n.116", its application attachment "CIRCOLARE N. 8, 22 aprile 1994" and the "FELASA" guidelines.

Several chimeras were obtained after blastocysts re-implantation. Chimeras were bred with wild type C57BL/6 females to ascertain contribution of recombinant ES cells to the germline. The recombinant strains were spread by crossing heterozygous animals to C57BL/6 females.

C.2 *ROSA26c-myc-PR-ER-Hras^{V12}* or *Eef1a1c-myc-PR-ER-Hras^{V12}*/TgCRE-ER or Pax8CRE mouse strains

The mice harbouring *c-myc-PR-ER-Hras^{V12}*-cassette under the control of ROSA26 or Eef1α1 promoter (R-Onc and E-Onc respectively) were crossed with TgCRE-ER transgenic mice or Pax8CRE heterozygous mice in order to obtain mice heterozygous for the oncogenic cassette and for *cre* alleles. The floxed *neo* cassette was removed from the targeting vector following the CRE recombinase action.

C.3 Genotyping of mutant mice

All the mouse strains were genotyped by polymerase chain reaction (PCR).

On the day of weaning, the mice were numbered and DNA extracted from tail tips. The tail tips were incubated over night at 55°C in 750 µl of lyses buffer (50 mM Tris pH 7.5, 100 mM EDTA pH 8, 100 mM NaCl, 1% SDS) and 1.0 mg/ml Proteinase K.

The following day the DNA was extracted adding 0.3 volumes of 6M NaCl and precipitated with isopropanol. After washing with 70% ethanol, the DNA pellet was drain at room temperature and resuspended in 150-200 µl mQ H_2O.

For both the transgenic mouse strains, the PCR was set up so that in the unique reaction both the wild type and recombinant locus could be identified, using three different primers in the same reaction: one common reverse primer (ROSARevWT3 for the R-Onc mice or Eef1aRev2 for the E-Onc mice) and two forward primers (one specific for ROSA26 -ROSA FW- or Eef1α1 -Eef1a FW2- wild-type allele and the other one specific for the transgenic cassette -βglobin FW-) (for schematic representation see figures 101 and 103).

The primers used for the amplification were as follows:

ROSA FW: 5' CCATCTGTAATGGGATCTGATGCCC 3' (into the first intron of the ROSA26 gene)

ROSARevWT3: 5' GCCACATCCATAGTGGCTCATTAGG 3' (into the first intron of the ROSA26 gene)

βglobin FW: 5' TAGGGCGAATTCGGATCC 3' (into the βglobin intron sequence of the construct)

Eef1a FW2: 5' CTAACTAGGGTGAGGCCATCCC 3' (into the first intron of the Eef1α1 gene)

Eef1aRev2: 5' CTAAGAAGCCCGAGAATTAGCTCCGCTCA 3' (into the first intron of the Eef1α1 gene)

The annealing temperature was 53°C.

On the ROSA26 allele, primers ROSA FW and ROSARevWT3 amplify a 730 bp product specific for the wild type allele; whereas the primers βglobin FW and ROSARevWT3 amplify a 530 bp product specific for the transgenic allele.

On the Eef1α1 allele, primers Eef1a FW2 and Eef1aRev2 amplify a 398 bp product specific for the wild type allele; whereas the primers βglobin FW and Eef1aRev2 amplify a 266 bp product specific for the transgenic allele.

For of Pax8CRE alleles, genotyping was performed using one common forward primer (I2) and two reverse primers: one specific for *Pax8* wild type (E3) and the other specific for *Pax8* null allele (*Pax8cre*) (CG), respectively.

The following primers were used for the amplification:

I2: 5' TCTCCACTCCAACATGTCTGC 3' (into the intron 2)

E3: 5' CCCTCCTAGTTGATTCAGCCC 3' (into the exon 3)

CG: 5' AGCTGGCCCAAATGTTGCTGG 3' (into the *cre* gene)

The annealing temperature was 61°C.

Primers I2 and E3 amplify a 389 bp product specific for the wild type allele; whereas the primers E3 and CG amplify a 700 bp product specific for the mutated allele.

TgCRE-ER transgene was identified using the following primers:

K7: 5' AGTCCCTCACATCCTCAGGTT 3' (into the *cre* coding sequence)

K8: 5' ATGCCAACCTCACATTTCTTG 3' (into the *cre* coding sequence)

that amplify a 450 bp product specific for CRE. The annealing temperature was 58°C.

PCR setup

All PCR reactions were conducted using 100-500 ng of genomic DNA, 1X PCR buffer (10 mM Tris-HCl pH 8.3, 50 mM KCl, 1.5 mM $MgCl_2$) 600 nM of common primer, 300 nM of each specific primer, 200 µM of each dNTP, and 0.5 units of Taq polymerase in a final volume of 25 µl. Reactions were performed with the following cycling parameters: 35 cycles of 94°C for 1 min, annealing ranging from 53 to 61°C (depending on the primers couple) for 1 min and 72°C for 1 min.

C.4 Mice treatments

The E-Onc/TgCRE, R-Onc/TgCRE, E-Onc/PaxCRE and R-Onc/PaxCRE double heterozygous mice (see chapter 3 part C section C.1.3) were treated at about two months of age with tamoxifene and RU486 to activate ER-Ras^{V12} and c-Myc-PR recombinant proteins respectively.

For tamoxifene the vehicle was composed by ethanol 96% and vegetal oil in a ratio 1:9 to obtain a final concentration of 10 mg/ml of tamoxifene. The solution was then sonicated.

RU486 was resuspended in the proper amount of PEG400 (Sigma), to obtain a final concentration of 25 mg/ml. 1-2 hours of constant temperature (45°C) was needed until the solution was completely homogeneous.

The drugs were administrated to *c-myc-PR-ER-*$Hras^{V12}$*/cre* double heterozygous mice by intraperitoneal injections. Each injection was performed at a dose of 1 mg/day of tamoxifene and 2.5 mg/day of RU486, repeated for 5 days, both together or one per week.

Part D: Hystological procedures

D.1 β-galactosidase staining

The embryos were dipped into fixative solution (0.1 M phosphate buffer pH 7.6; 0.2% glutaraldehyde; 5 mM EGTA; 2 mM $MgCl_2$) at room temperature, for a time depending on their size, after dissecting them free of their extraembryonic membranes. The fixed embryos were rinsed with a detergent solution (0.1 M phosphate buffer pH 7.6; 2 mM $MgCl_2$; 0.01% sodium deoxycholate; 0.02% NP-40). The samples were incubated at 30°C for at least 2 hours in the dark in the staining solution (0.1 M phosphate buffer pH 7.6; 2 mM $MgCl_2$; 0.01% sodium deoxycholate; 0.02% NP-40; 5 mM potassium ferricyanide; 5 mM potassium ferrocyanide; 1 mg/ml X-gal in DMSO).

D.2 Immunohistochemistry

Thyroids were fixed in 4% paraformaldehyde and dissected 5 μm thick. They were incubated 2-3 times in xylene for 10 minutes each, twice in 100% ethanol for 2 minutes each and hydrated by placing in 95%, 70%, 50%, 30% ethanol for 2 minutes each.

To inactivate the endogenous peroxidase, the sections were incubated for 20 minutes in hydrogen peroxide and methanol in a ratio of 4 ml:1 ml. Afterwards, the tissues were washed in running water for 20 minutes. Slides were placed twice in PBS for 5 minutes each and blocked with 10% serum from the species from which the secondary antibody was taken for 30 minutes at room temperature in a humidified chamber. Then, slides were incubated overnight at 4°C with primary antibody diluted in PBS from 1:1000 to 1:500.

The slides were rinsed twice in PBS for 5 minutes each before incubating them with secondary antibody in a humidified chamber for 20 minutes and washed again

twice in PBS.

To amplify and detect the signal, after removing the secondary antibody by washing in PBS, 2 drops Vectastain "A" and 2 drops Vectastain "B" were mixed in 10 ml PBS 30-60 minutes before use and added to the sections for 1h at room temperature. The slides were washed with PBS and overlaid with fresh, filtered DAB solution (10 mg DAB + 20 µl 38% H_2O_2 in 20 ml 0.1 M Tris pH 7.2). The reaction was stopped by washing in running water when a uniform brown color first becomes visible on the sections.

The slides were left to dry by placing them in 30%, 50%, 70%, 95% ethanol and then mounted with Eukitt.

D.3 Histological staining

Thyroids were fixed in 4% paraformaldehyde and dissected 5 µm thick. They were incubated 2-3 times in xylene for 10 minutes each, twice in 100% ethanol for 10 minutes each and hydrated by placing in 95%, 80%, 50% ethanol for 5 minutes each.

Staining was carried out as follows:

- incubation in hematoxylin for 20 minutes,
- washing in running water for 30 minutes,
- incubation in eosin for 1-2 minutes,
- washing in distilled water for 5 minutes

The slides were left to dry by placing them into 50%, 80%, 95% and 100% ethanol and then incubated in Xilene for 10 minutes and mounted with Eukitt.

Part E: Vectors assembling

E.1 The RasMyc vector: cloning strategy

The cloning strategy of the RasMyc plasmid was according to the following scheme:

1) Cloning of the plasmid SA-βgeo-STOP composed of a splice acceptor site (SA), a βgalactosidase-neomycin resistance (βgeo) and a triple polyadenylation sequence (3xpA). The entire cassette was flanked by two LoxP sites.

A fragment BamHI–BamHI (containing 3xpA) was cut from pSAloxneotpA and cloned into pBS. In the EcoRV site of this plasmid, was then inserted a HindIII-XbaI fragment (containing βgeo) excised from IRES-βgeo and blunt ended by Klenow treatment.

Then an oligonucleotide containing the LoxP sequence flanked by SpeI and NotI restriction sites was cloned in the same sites of the construct (called βgeo-STOP).

A fragment PstI-HindIII (containing SA) was cut from pSAloxneotpA and cloned in pBS.

An oligonucleotide containing the LoxP sequence flanked by HindIII-ClaI restriction sites was cloned in the same sites of this construct. Then a sequence containing restriction sites for SalI-PmeI was inserted upstream of SA. Finally, the SalI-SalI fragment was excised and cloned in the XhoI site of βgeo-STOP plasmid to obtain the following construct, SA-βgeo-STOP.

This first cassette is depicted in figure 84 in chapter 3 part C section C.1.1.

2) Cloning of a plasmid (*myc-PR*) containing the sequence coding for the c-*myc* fused to the progesterone receptor (*myc-PR*).

An 870 bp fragment contaning PR-polyA sequence was amplified by PCR (PCR-a) from pSG5-CrePR2 plamid. The 5' primer used for the amplification included a 20 bp sequence corresponding to 3' end of c-*myc*. The 3' primer containing the AscI and NotI sites facilitated cloning. A BamHI–NotI fragment of 1320 bp containing the coding sequence of c-*myc* was excised from pcDNA3Myc and cloned into pBS (pBS *myc*). This construct was used as a template in a PCR reaction (PCR-b) to amplify a 180 bp fragment coding the 3' end of c-*myc* sequence.

Finally, the products of the two PCR reactions (PCR-a and PCR-b) were used as a template for a new PCR (PCR-c). The 5' primer of PCR-b reaction and the 3' primer of PCR-a reaction, were used as primers. The amplicon was cut StyI-NotI and inserted into the same sites of pBS *myc*. In such a manner, a plasmid containing the sequence coding for c-*myc* oncogene fused to the PR (pBS *myc*-PR), was obtained. Figure 28 in chapter 3 part A section A.1 is a schematic representation of the three PCR.

The structure of the pBS *myc*-PR plasmid is drawn in figure 31 in chapter 3 part A section A.1.

3) Assembling a construct (ER-ras-myc-PR) containing *H-ras*^{V12} fused to estrogen receptor (ER-Ras^{V12}), IRES, *myc-PR* (Fig. 39 in chapter 3 part A section A.1).

A 640 bp XhoI-BamHI fragment corresponding to ECMV-IRES excised from pIRES, was cloned into the same sites of pBS *myc*-PR. Then, the BamHI site downstream of IRES was disrupted and another BamHI site was inserted upstream to IRES. In this BamHI site of the plasmid BamHI-BamHI fragment of 1700 bp was cloned corresponding to the sequence coding ER-Ras^{V12} excised from pCEFL ER^{TM}-

RAS to obtain ER-ras-myc-PR (RasMyc plasmid Fig. 39 in chapter 3 part A section A.1).

The 4500 bp NotI-NotI fragment, excised from pER-ras-myc-PR, was subcloned into pCEFL plasmid downstream of the strong EF1α promoter (pCEFL-RasMyc Fig. 42 in chapter 3 part A section A.1).

E.2 The MycRas vector: cloning strategy

The cloning strategy followed the scheme described below:

1) Removal of the IRES from the IRES-*myc*-PR plasmid obtained in one of the previous subcloning steps.

A 650 bp XhoI-BamHI fragment corresponding to ECMV-IRES was excised from

a BlueScript plasmid containing the IRES and the myc-PR-polyA sequences (pBS IRES-*myc*-PR), that was obtained during the work, to obtain pBS *myc*-PR plasmid. After destroying the BamHI site, an oligonucleotide was subcloned in the same sites of pBS *myc*-PR.

A MunI-NotI fragment containing the polyA sequence, downstream of PR, was excised and a PCR reaction was performed to restore the 3' end of PR.

The 5' primer used for the amplification included the MunI site, while the 3' primer containing the NotI site facilitated the cloning of the amplicon. The *myc*-PR-polyA plasmid was used as a template for the PCR.

The MunI-NotI amplicon was cut and inserted in the same sites of pBS *myc*-PR.

The structure of the *myc*-PR plasmid obtained and used for the following cloning is depicted in figure 31 in chapter 3 part A section A.2.

2) Insertion of the IRES downstream of the Myc-PR fusion protein (Fig. 32 in chapter 3 part A section A.2).

A 650 bp EcoRI-NotI fragment corresponding to ECMV-IRES excised from pIRES, was cloned into the same sites of pBS *myc*-PR, to obtain pBS *myc*-PR-IRES. An AscI site was inserted between the IRES and the NotI site. A NotI site was inserted upstream of the c-*myc* sequence to facilitate the next cloning (Fig. 43 chapter 3 part A section A.2).

3) Cloning of the *H-Ras*^{V12} fused to estrogen receptor (ER-Ras^{V12}) downstream of the last *myc*-PR-IRES plasmid, to obtain the vector drawn in figure 50 in chapter 3 part A section A.2.

Then, a BamHI-BamHI fragment containing the ER-Ras^{V12} sequence was subcloned into the BamHI site of pBS *myc*-PR-IRES, to obtain pBS-MycRas.

Then, the 4500 bp NotI-NotI fragment, excised from pBS-MycRas, was subcloned into the NotI site into pCEFL vector (pCEFL-MycRas Figs. 50 and 54 in chapter 3 part A section A.2), downstream of EF1α promoter to test the MycRas construct by cell transfection.

In figures 22 to 26 are represented some fragments of sequences performed to verify the integrity of the plasmids obtained in this work.

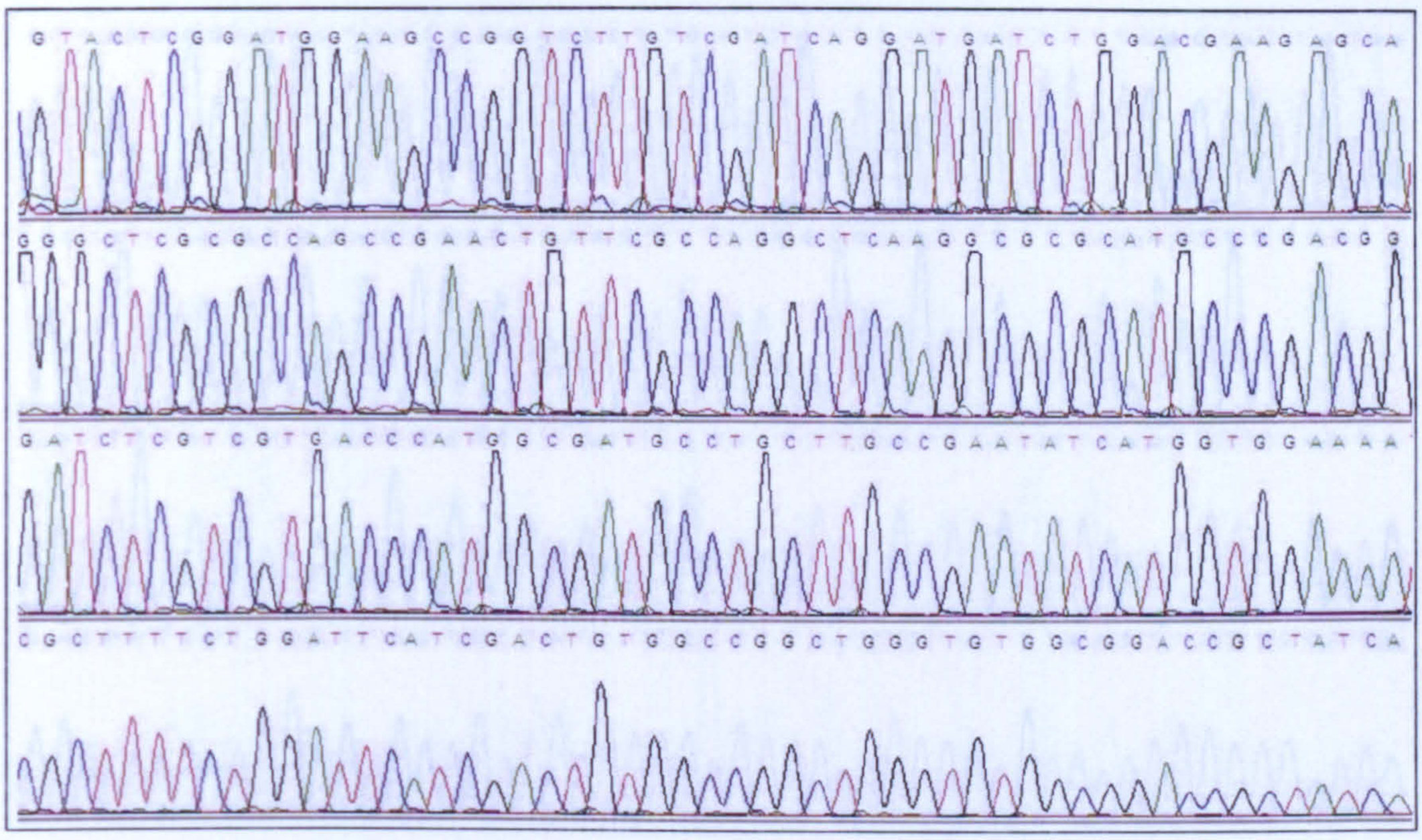

Figure 22. Neo Fw sequence of the SA-βgeo-MycRas-βglobin intron pA plasmid.

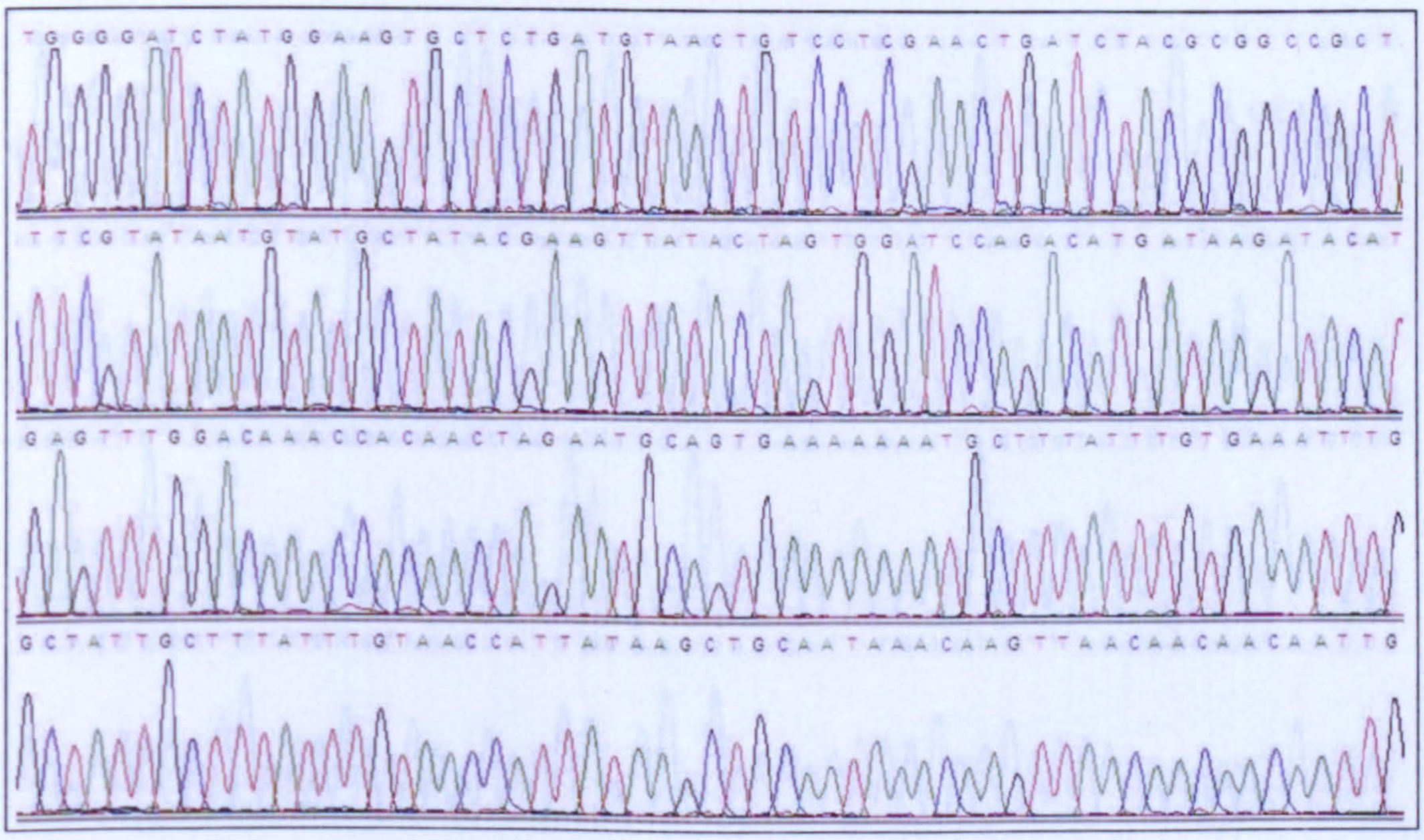

Figure 23. Myc Rev sequence of the SA-βgeo-MycRas-βglobin intron pA plasmid.

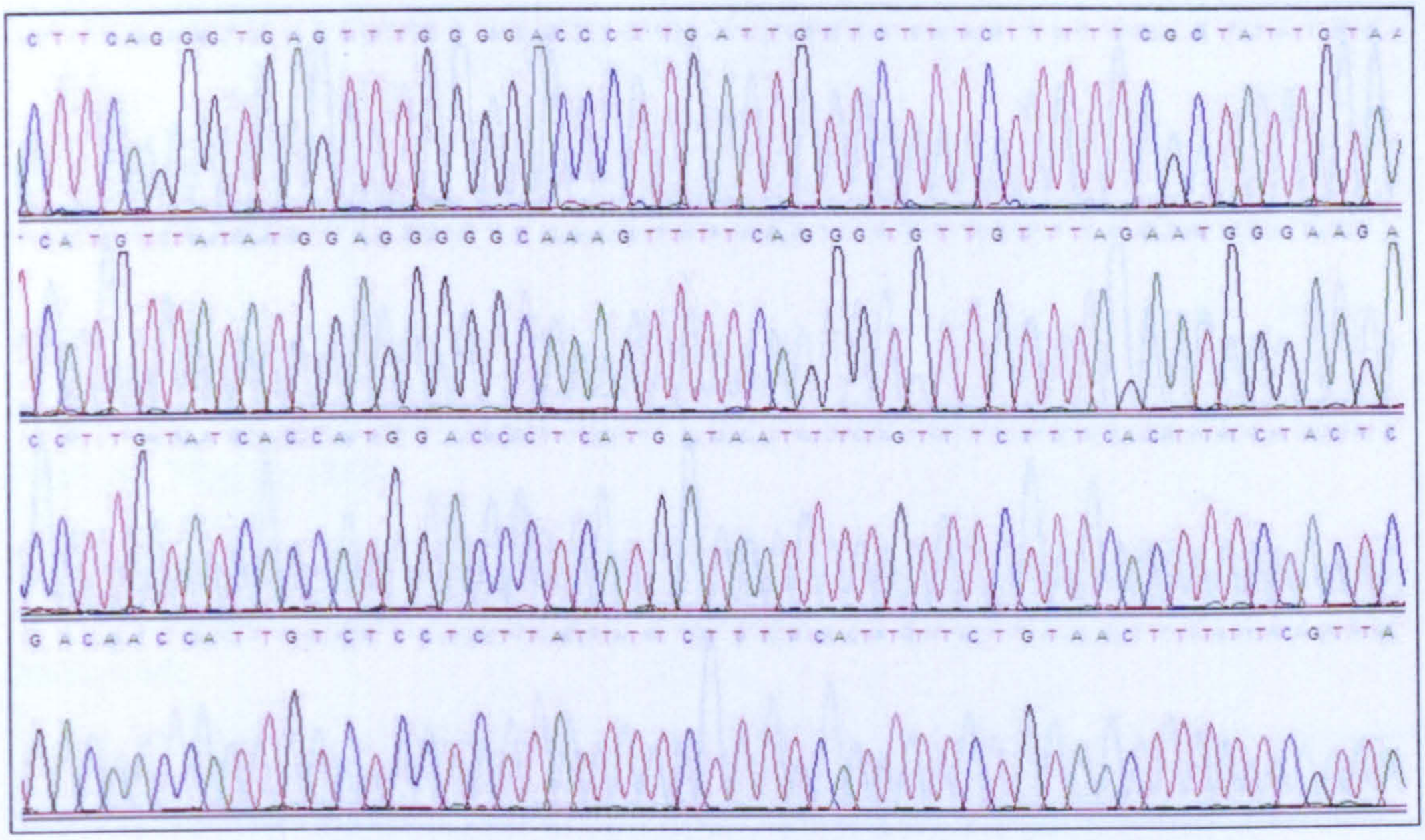

Figure 24. Ras Fw sequence of the SA-βgeo-MycRas-βglobin intron pA plasmid.

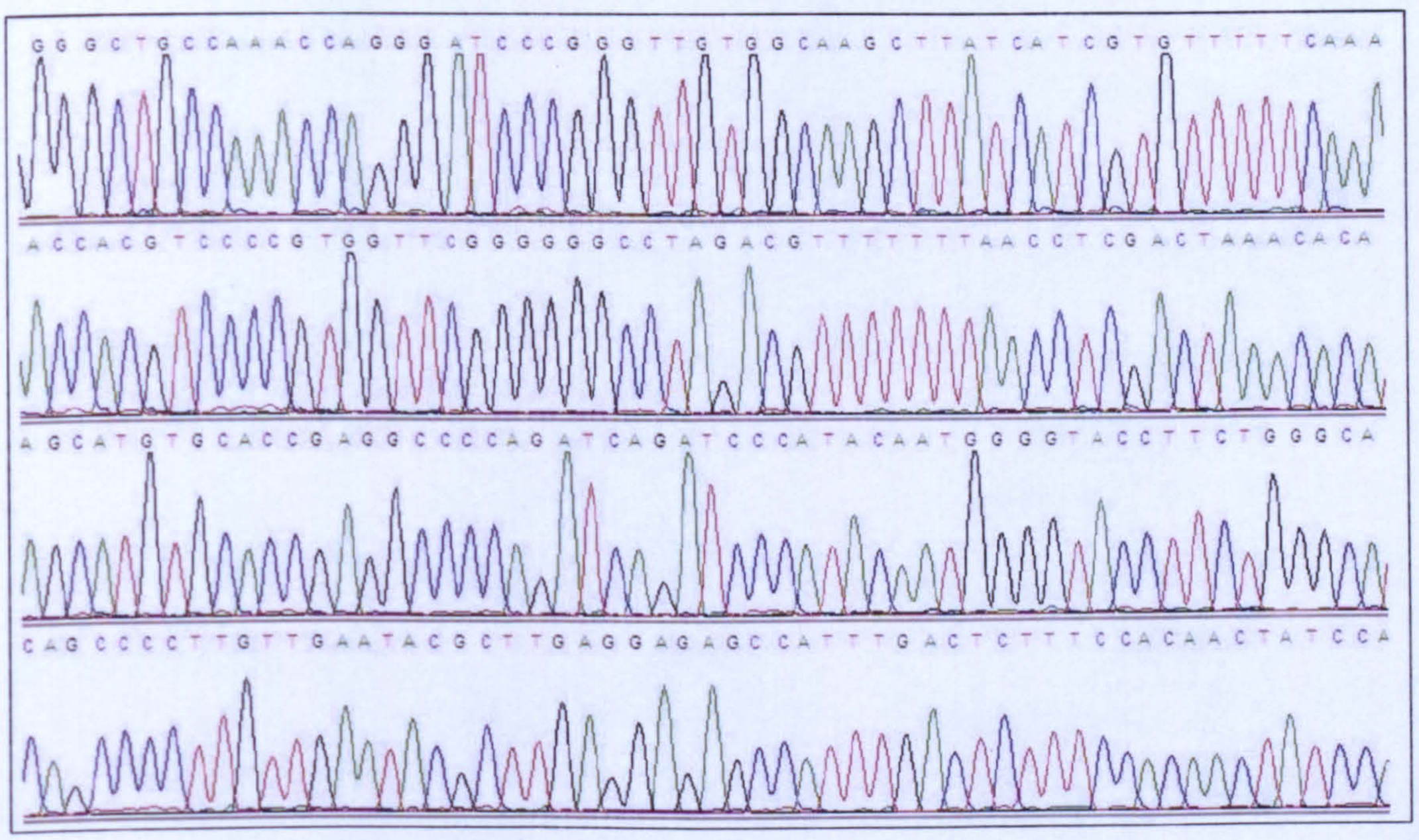

Figure 25. Ras Rev sequence of the SA-βgeo-MycRas-βglobin intron pA plasmid.

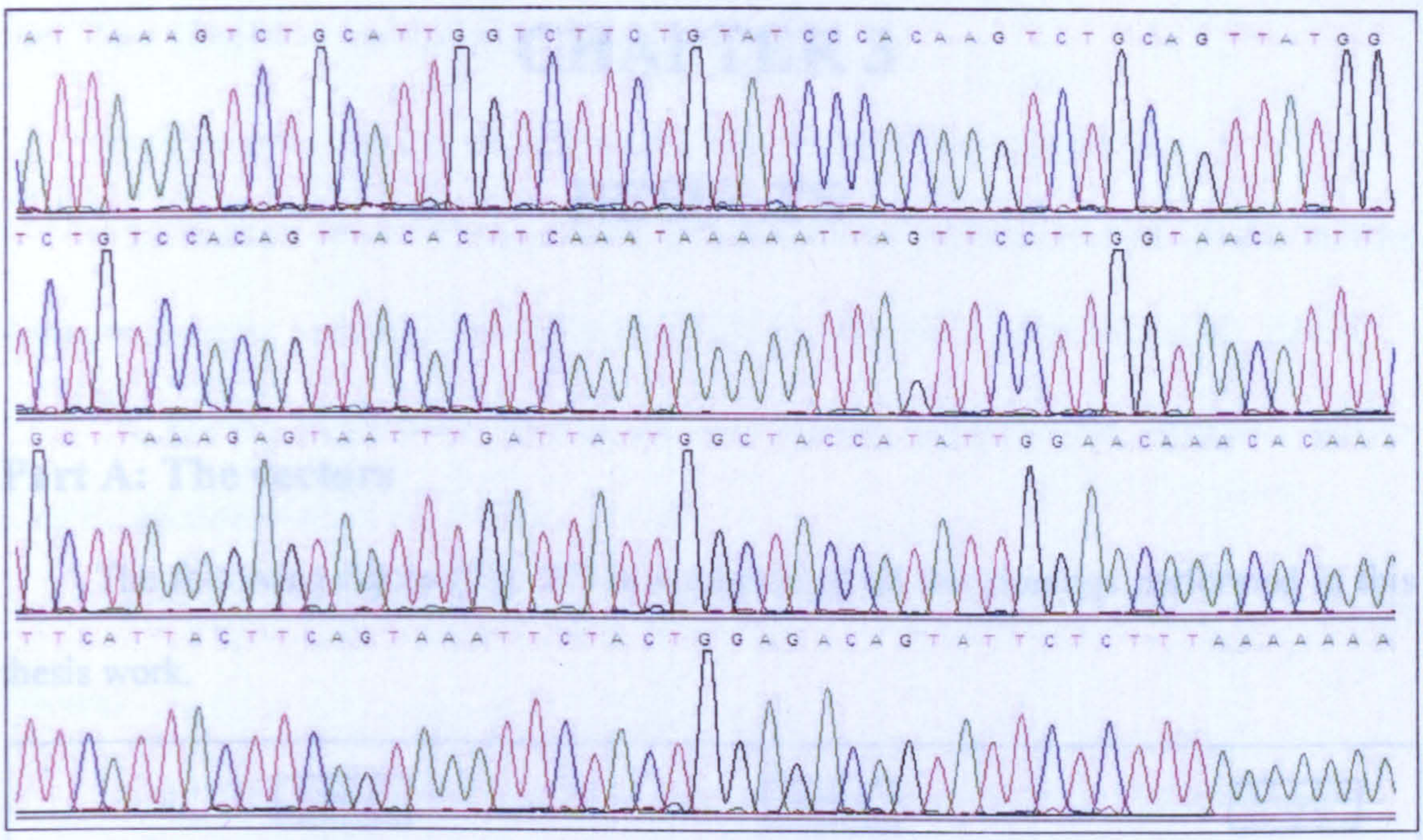

Figure 26. SA Rev sequence of ROSA26 targeting vector.

CHAPTER 3

RESULTS

Part A: The vectors

The following figure (Fig. 27) is a scheme of all the clonings performed in this thesis work.

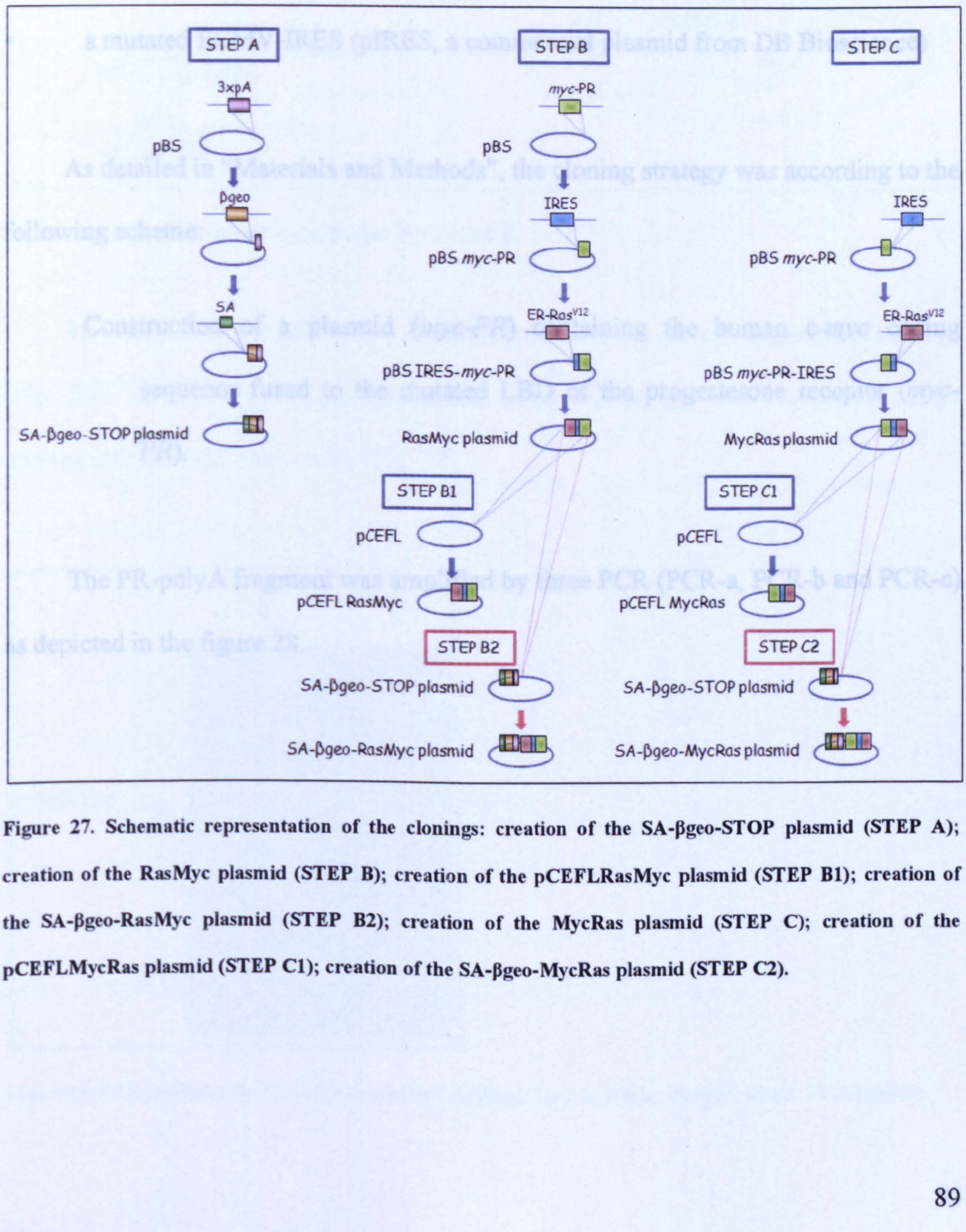

Figure 27. Schematic representation of the clonings: creation of the SA-βgeo-STOP plasmid (STEP A); creation of the RasMyc plasmid (STEP B); creation of the pCEFLRasMyc plasmid (STEP B1); creation of the SA-βgeo-RasMyc plasmid (STEP B2); creation of the MycRas plasmid (STEP C); creation of the pCEFLMycRas plasmid (STEP C1); creation of the SA-βgeo-MycRas plasmid (STEP C2).

A.1 The RasMyc expression vector

To prepare the vector, the following DNA fragments were used:

- the human *H-ras*^{V12} fused to a tamoxifene-responsive mutant of the murine estrogen receptor Ligand Binding Domain (LBD), ER-Ras^{V12}, (De Vita et al., 2005);
- a RU486 responsive mutant of the murine progesterone receptor, pSG5-CrePR2,(Kellendonk et al., 1996);
- the coding sequnce of human c-*myc* (pcDNA3Myc, kindly provided by R. Dalla Favera)
- a mutated ECMV-IRES (pIRES, a commercial plasmid from DB Bioscience)

As detailed in "Materials and Methods", the cloning strategy was according to the following scheme:

Construction of a plasmid (*myc-PR*) containing the human c-*myc* coding sequence fused to the mutated LBD of the progesterone receptor (*myc-PR*).

The PR-polyA fragment was amplified by three PCR (PCR-a, PCR-b and PCR-c) as depicted in the figure 28.

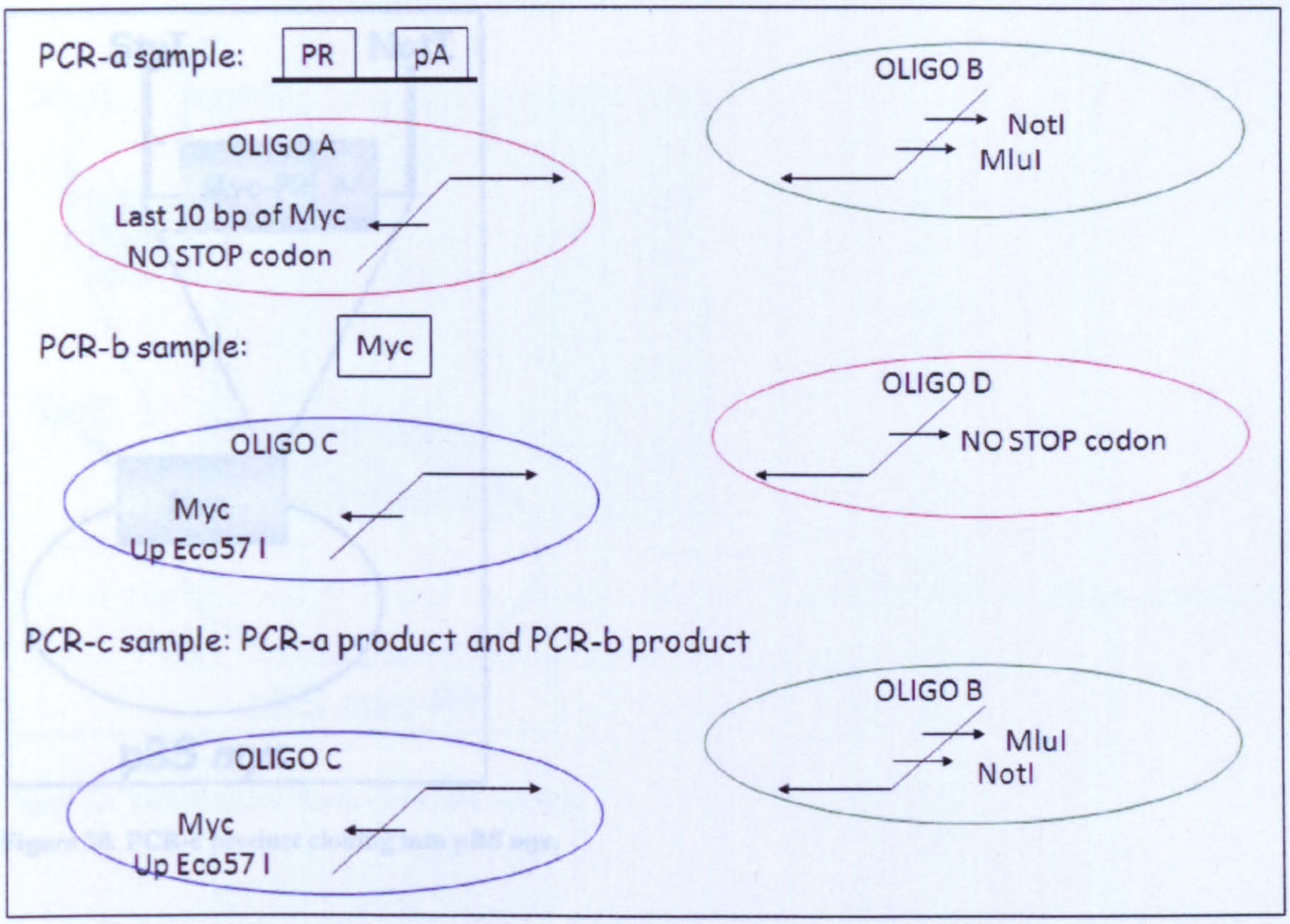

Figure 28. PR-polyA fragment amplification by three PCR.

To verify the structure of the construct, the *myc*-PR-polyA fragment (1100 bp) (Fig. 29), amplified by PCR, was eluted from agarose gel and sequenced before cloning into the pBS *myc* vector (Fig. 30).

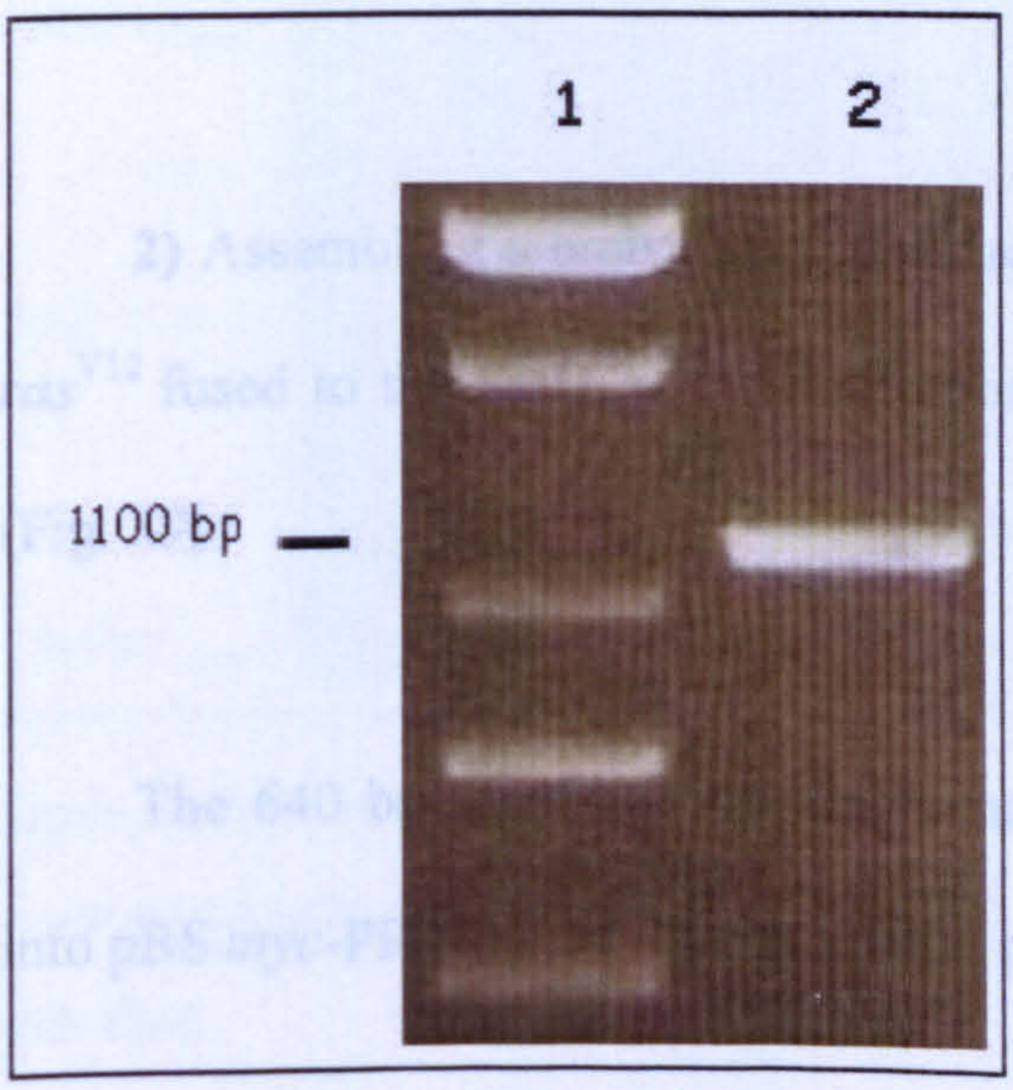

Figure 29. PCR product *myc*-PR-polyA fragment (1100 bp). Lane 1: 100 bp marker; lane 2: PCR product.

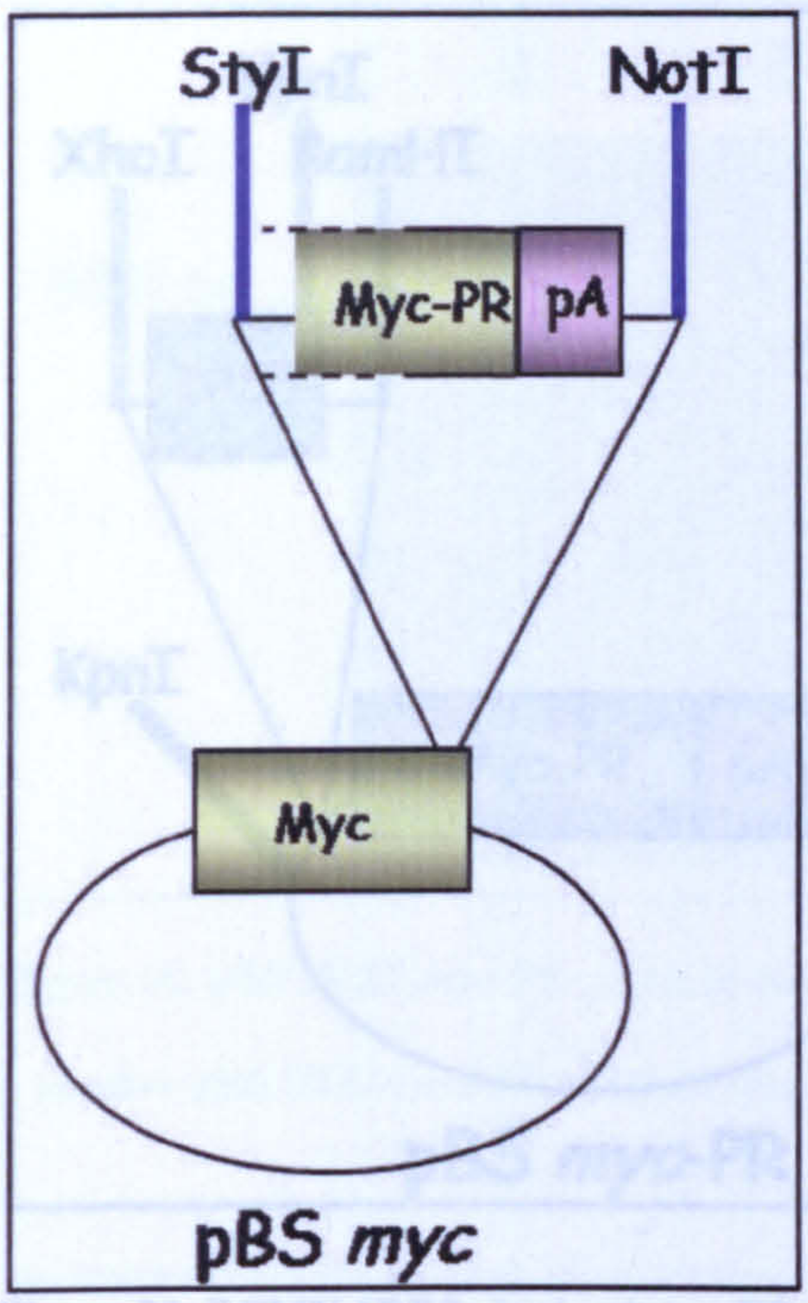

Figure 30. PCR-c product cloning into pBS *myc*.

The structure of the pBS *myc*-PR plasmid is as in figure 31.

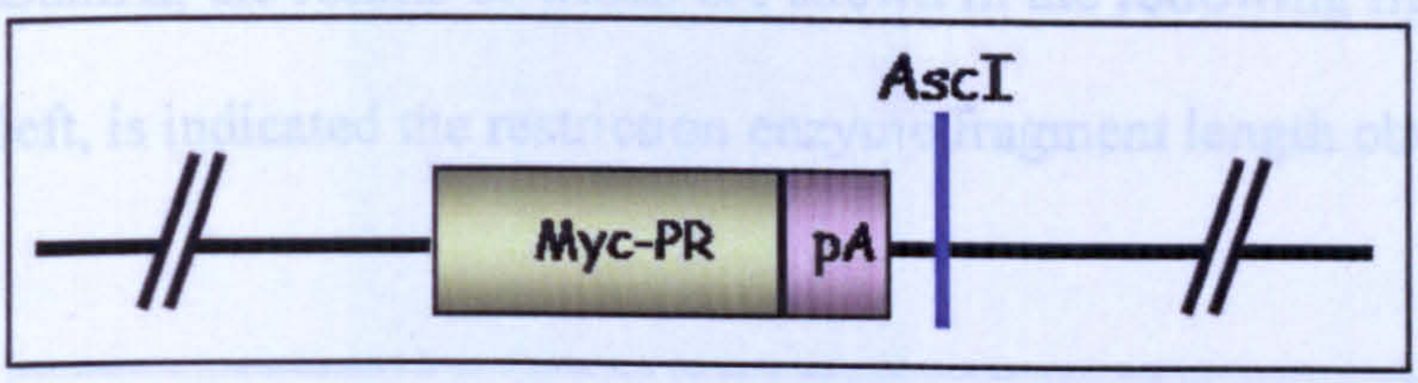

Figure 31. pBS *myc*-PR plasmid. c-Myc-Progesterone Receptor fusion protein (Myc-PR); polyadenylation sequence (pA); AscI restriction site (AscI).

2) Assembling a bicistronic construct (ER-ras-myc-PR) containing the human *H-ras*^{V12} fused to the LBD of the murine estrogen receptor (ER-Ras^{V12}), IRES, *myc-PR* (Fig. 39).

The 640 bp XhoI-BamHI fragment corresponding to ECMV-IRES was cloned into pBS *myc*-PR (Fig. 32) (to obtain the pBS IRES-*myc*-PR plasmid).

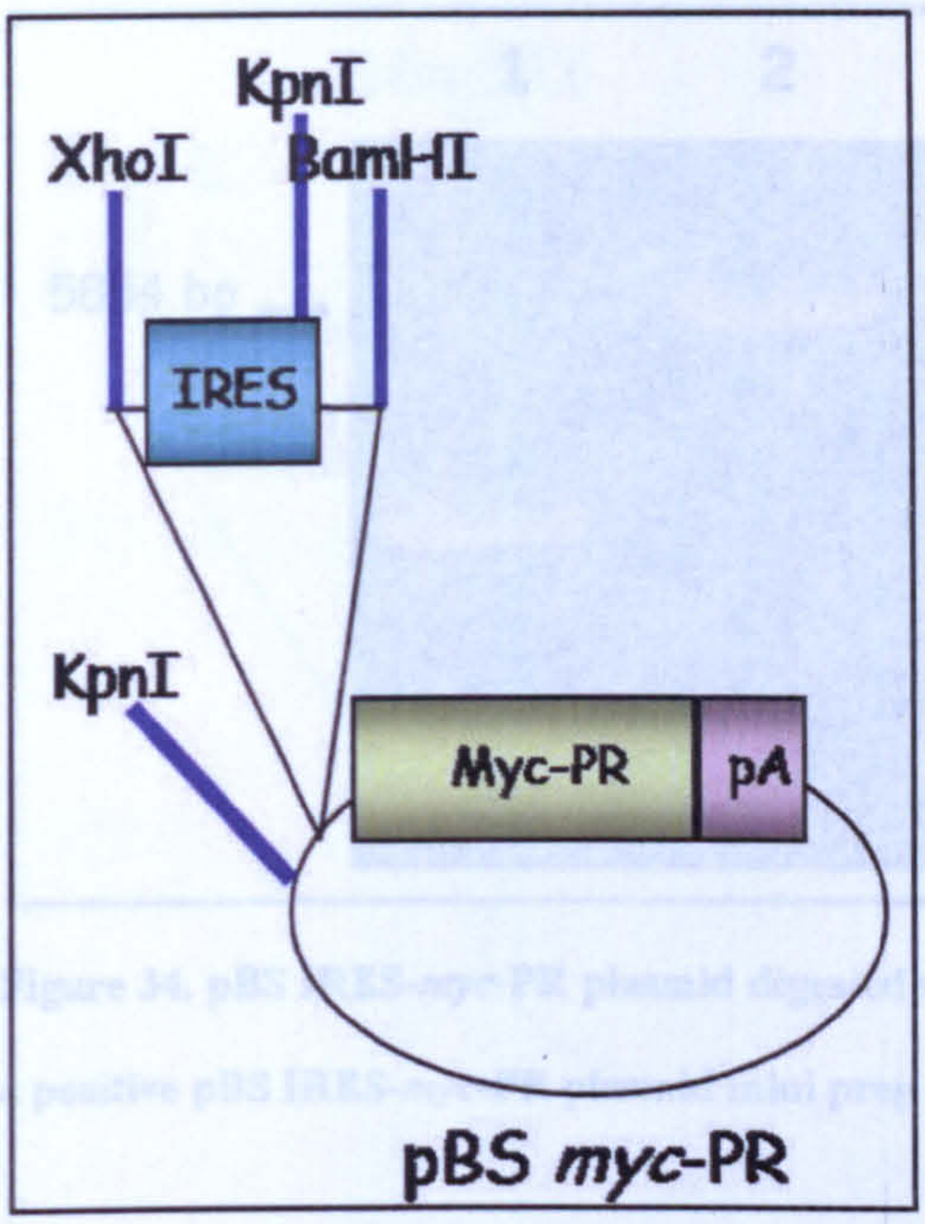

Figure 32. ECMV-IRES cloning into pBS *myc*-PR.

The plasmid was checked by analysis with the restriction enzymes KpnI, XhoI or BamHI, the results of which are shown in the following figures (33, 34 and 35). On the left, is indicated the restriction enzyme fragment length obtained.

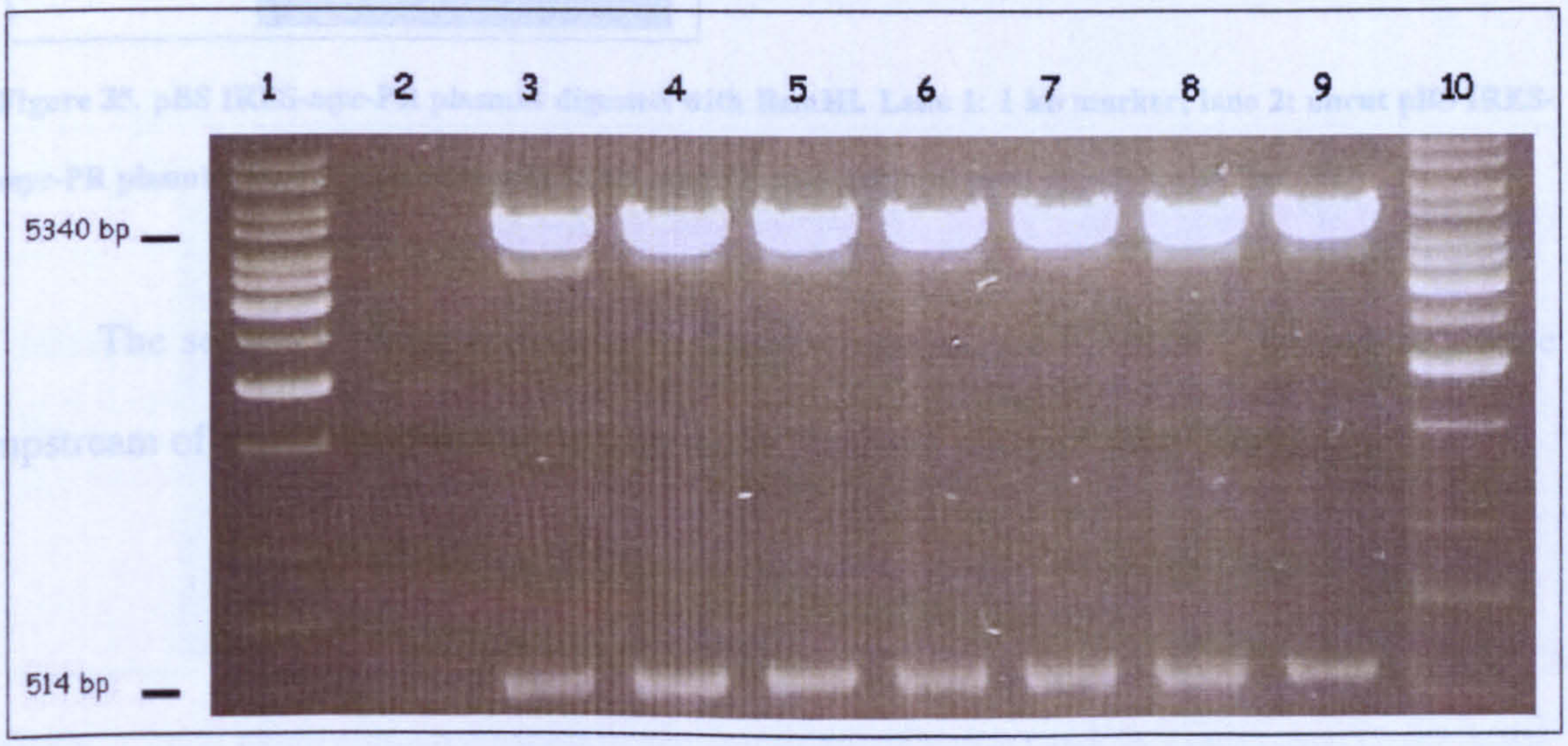

Figure 33. MINI PREP of pBS IRES-*myc*-PR plasmid digested with KpnI. Lanes 1 and 10: 1 kb marker; lane 2: uncut pBS IRES-*myc*-PR plasmid; lanes 3 to 9: 7 positive pBS IRES-*myc*-PR plasmid mini preps digested with KpnI.

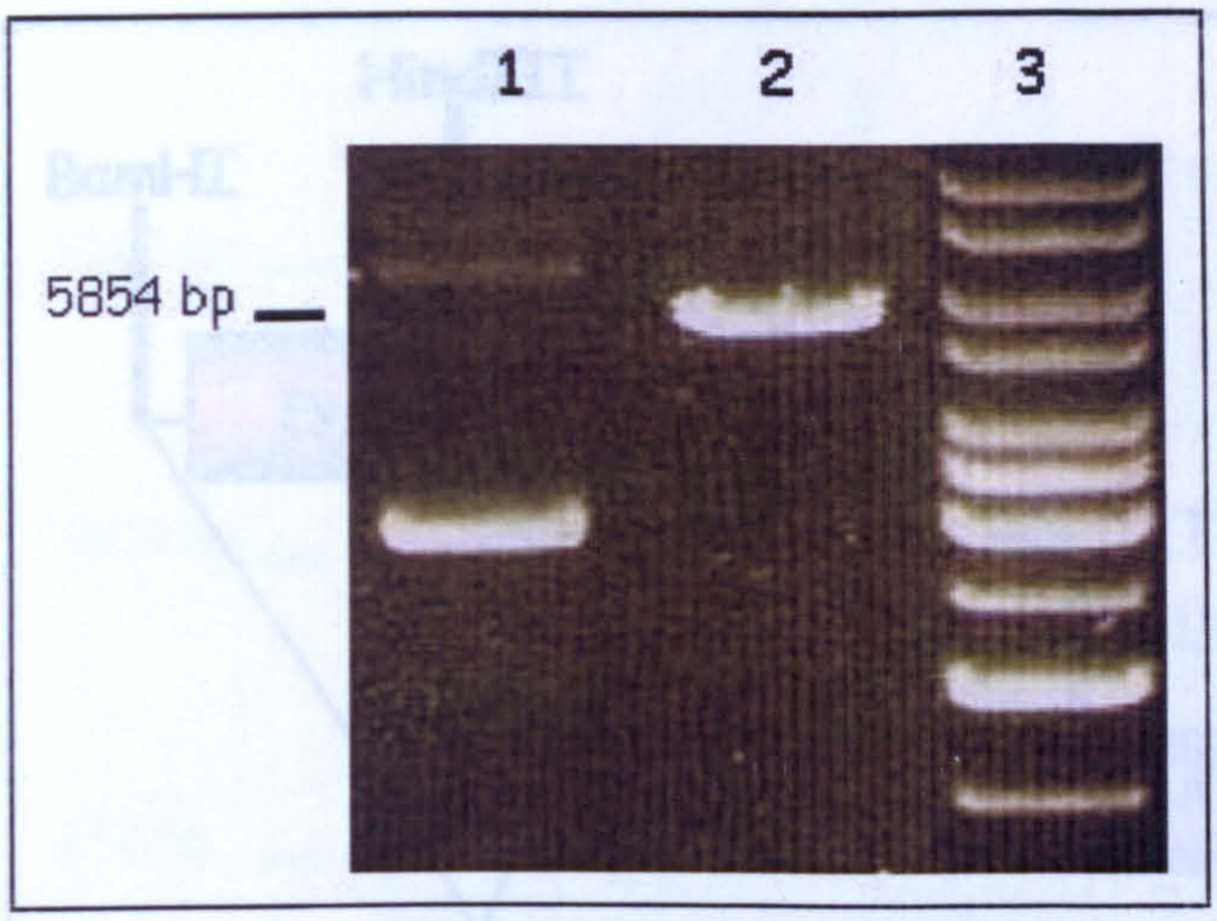

Figure 34. pBS IRES-*myc*-PR plasmid digested with XhoI. Lane 1: uncut pBS IRES-*myc*-PR plasmid; lane 2: a positive pBS IRES-*myc*-PR plasmid mini prep digested with XhoI; lane 3: 1 kb marker.

Figure 35. pBS IRES-*myc*-PR plasmid digested with BamHI. Lane 1: 1 kb marker; lane 2: uncut pBS IRES-*myc*-PR plasmid; lane 3: a positive pBS IRES-*myc*-PR plasmid mini prep digested with BamHI.

The second cloning consisted in the insertion of the ER-Ras^{V12} coding sequence upstream of the IRES (Fig. 36) to obtain the RasMyc plasmid (Fig. 39).

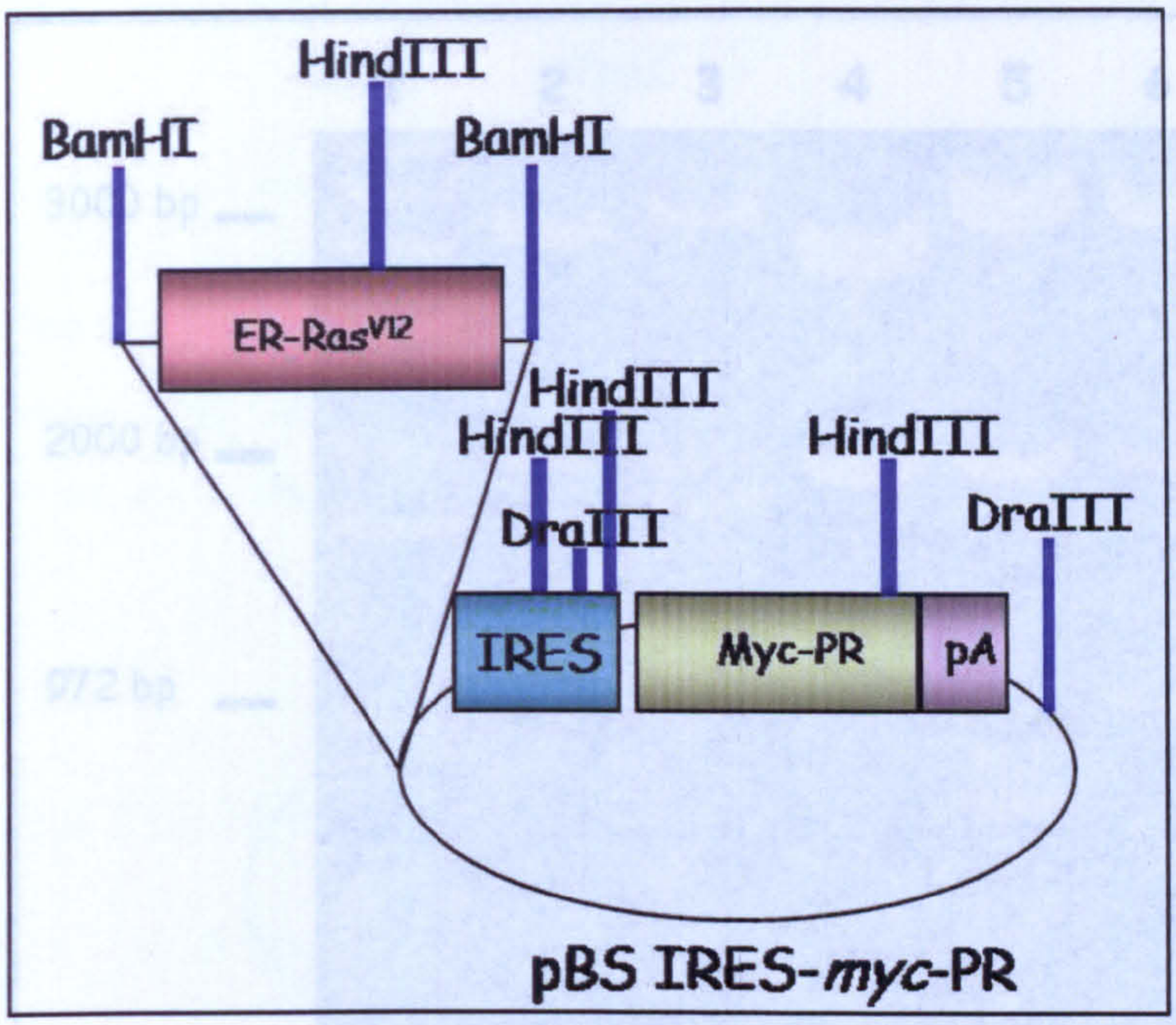

Figure 36. ER-Ras^{V12} cloning into pBS IRES-*myc*-PR.

It was ascertained by analysis with the restriction enzymes DraIII or HindIII and the results are shown in the figures 37 and 38.

The resulting positive clones, whose bands obtained by restriction, are indicated on the left, were further confirmed by sequencing analysis.

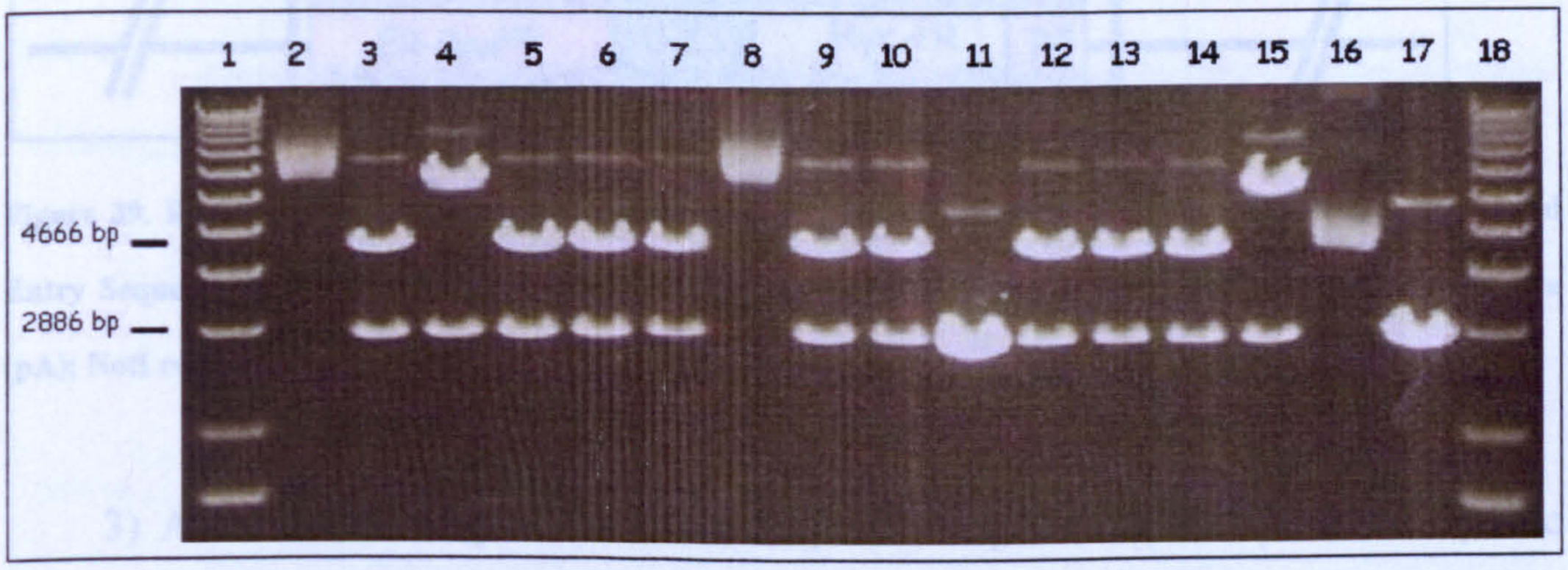

Figure 37. MINI PREP of RasMyc plasmid digested with DraIII. Lanes 1 and 18: 1 kb marker; lanes 2 and 8: uncut RasMyc plasmid; lanes 3, 5, 6, 7, 9, 10, 12, 13 and 14: 9 positive RasMyc plasmid mini preps digested with DraIII; lanes 4, 11, 15, 16 and 17: 5 negative RasMyc plasmid mini preps.

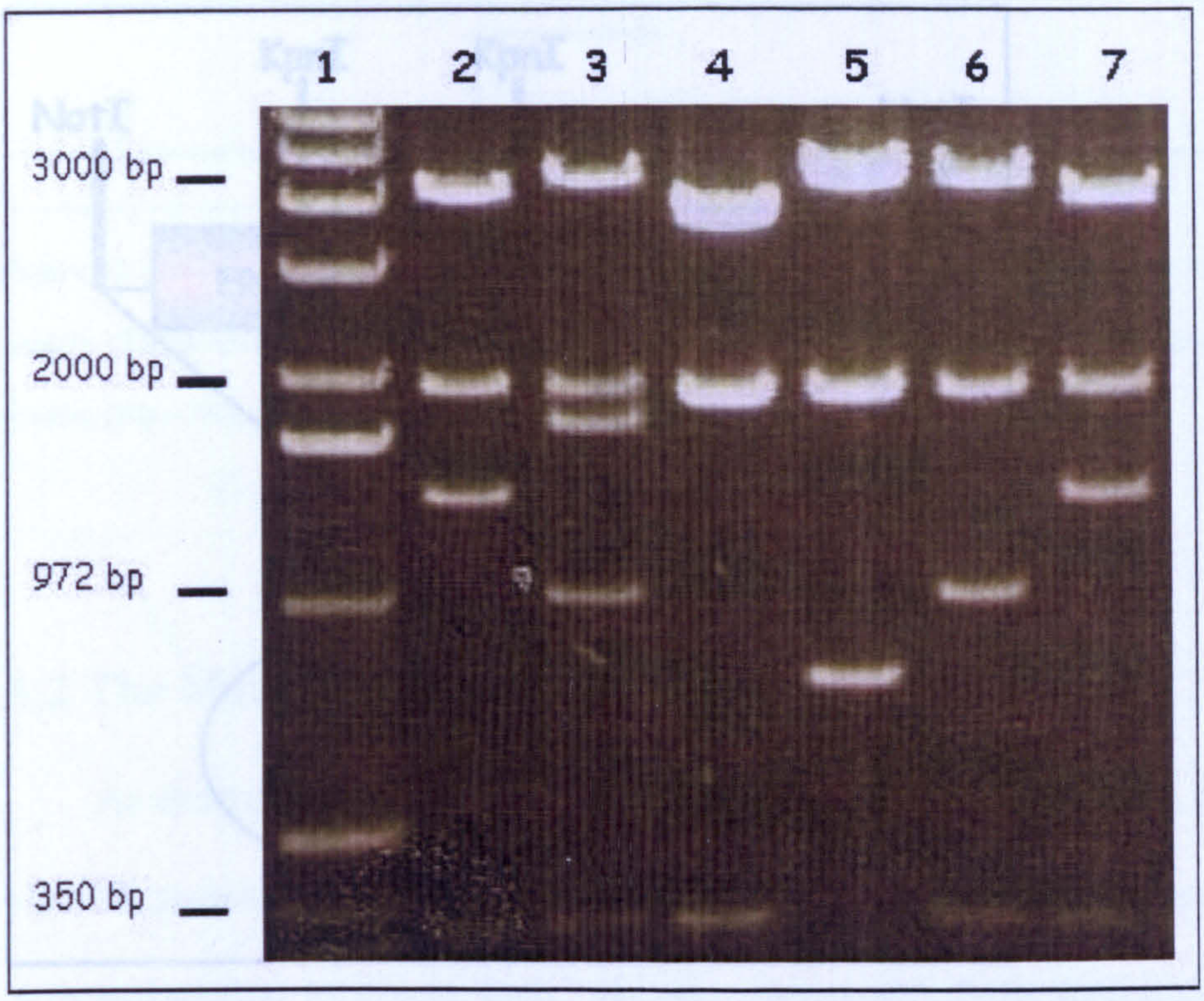

Figure 38. MINI PREP of RasMyc plasmid digested with HindIII. Lane 1: 1 kb marker; lanes 2 to 5 and lane 7: 5 negative RasMyc plasmid mini preps; lane 6: 1 positive RasMyc plasmid mini prep digested with HindIII.

The structure of the RasMyc plasmid is depicted below (Fig. 39).

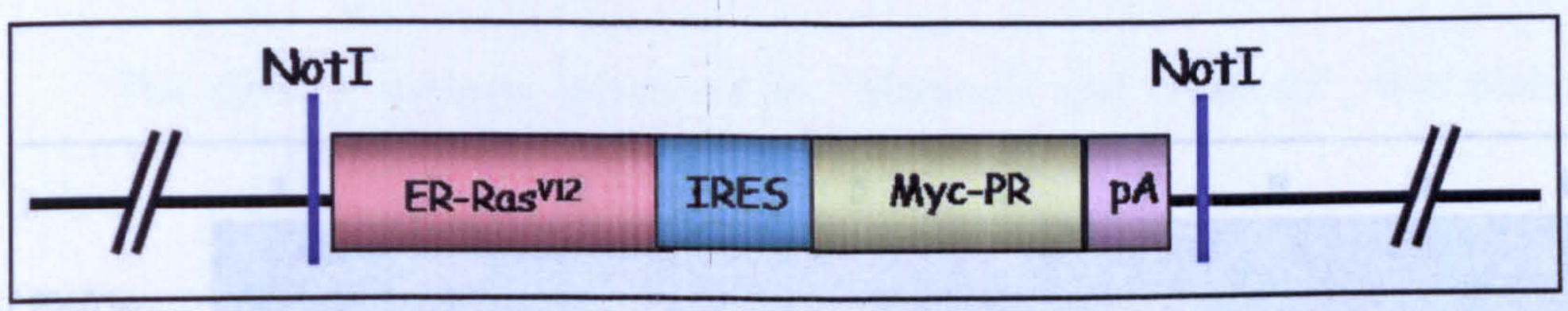

Figure 39. RasMyc plasmid. Estrogen Receptor-HRas^{V12} fusion protein (ER-H-ras^{V12}); Internal Ribosomal Entry Sequence (IRES); c-Myc-Progesterone Receptor fusion protein (Myc-PR); polyadenylation sequence (pA); NotI restriction site (NotI).

3) A further cloning of the ER-ras-myc-PR sequences (RasMyc cassette) into pCEFL vector (Fig. 40) was done, to obtain the plasmid depicted in figure 42 (pCEFL-RasMyc plasmid. EF1α).

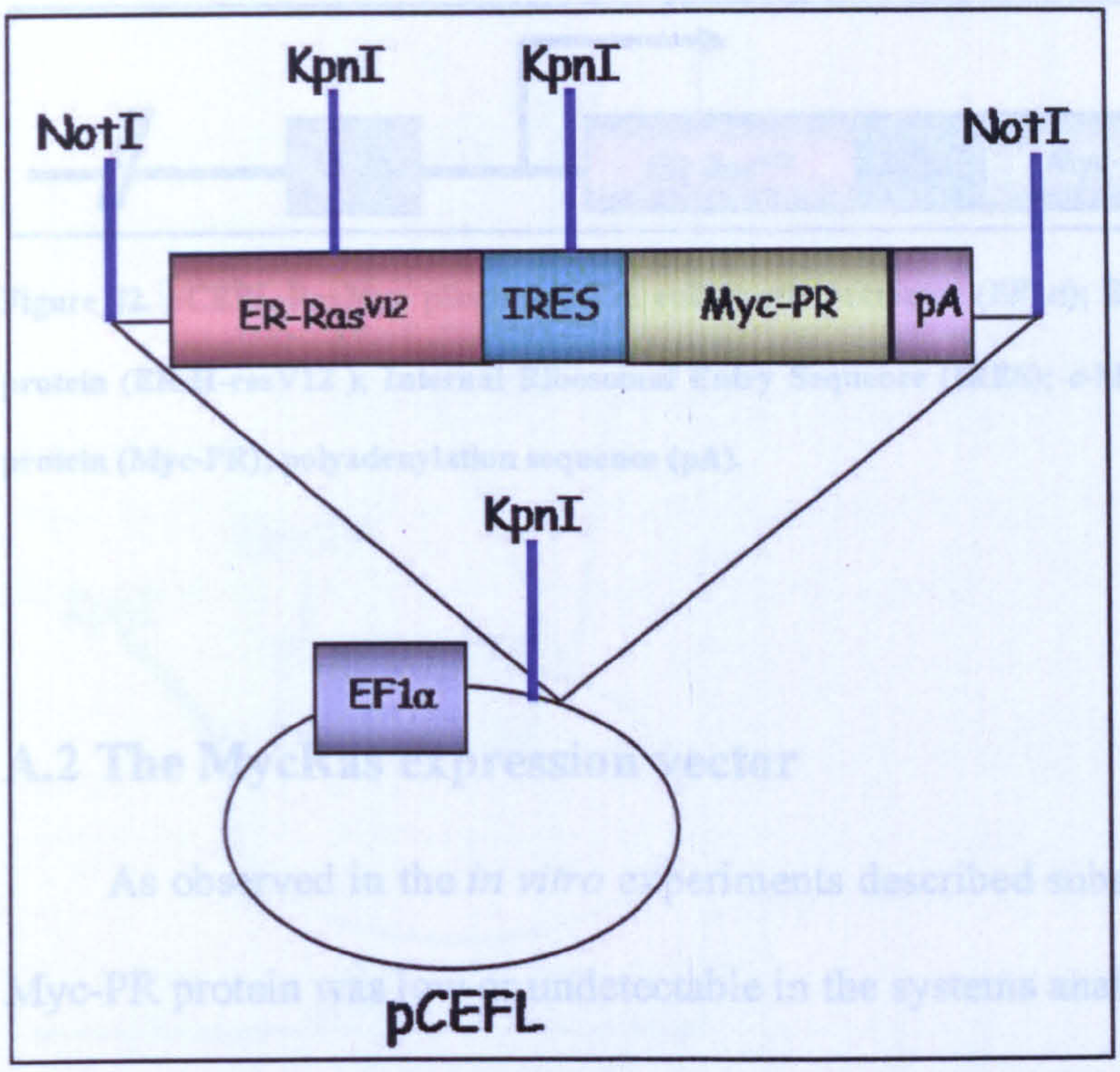

Figure 40. ER-ras-myc-PR (RasMyc cassette) cloning into pCEFL.

After this cloning, the analysis by restriction enzyme KpnI, gave us the expected fragments (Fig. 41).

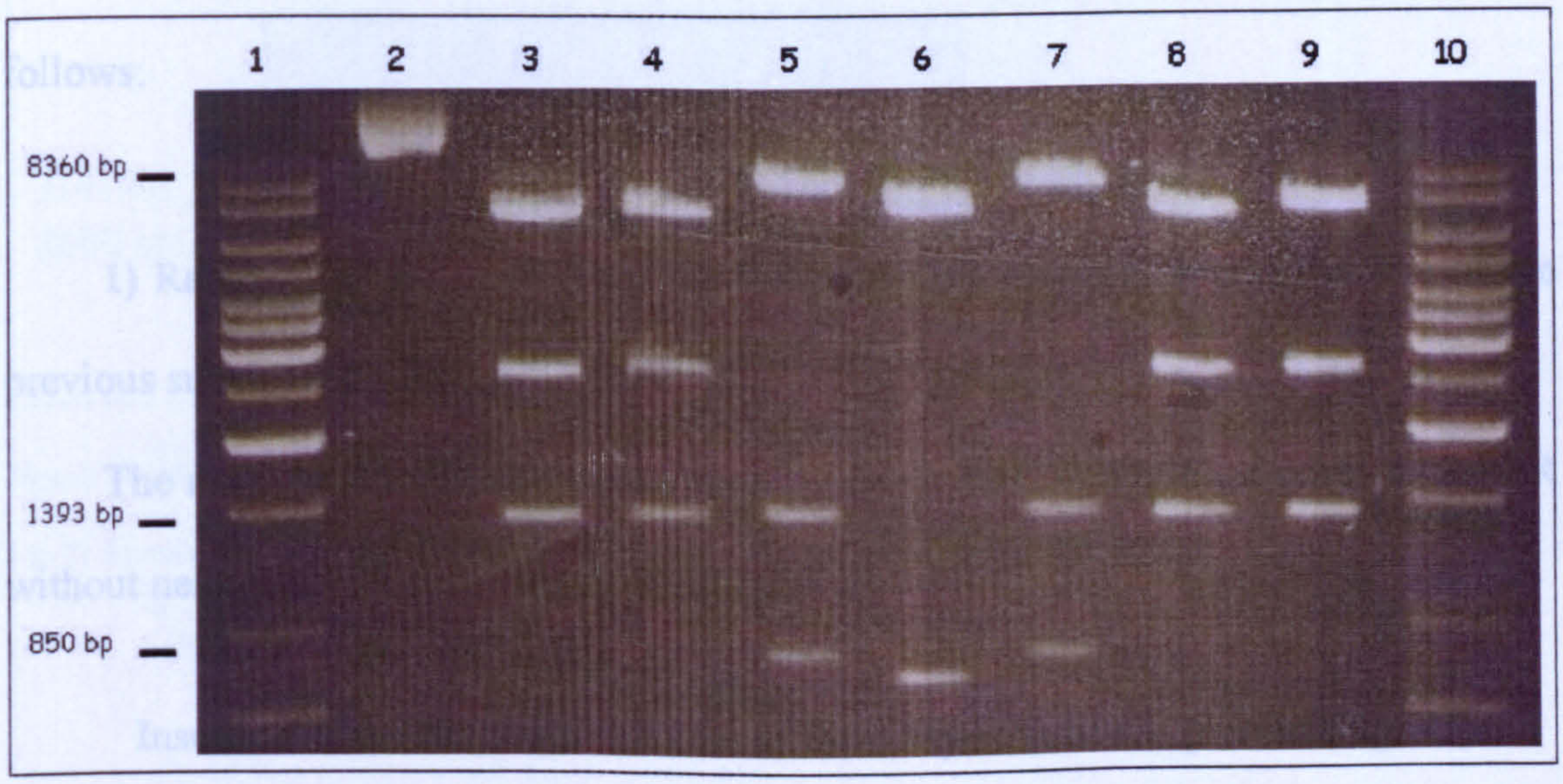

Figure 41. MINI PREP of pCEFL-RasMyc plasmid digested with KpnI. Lanes 1 and 10: 1 kb marker; lane 2: uncut pCEFL-RasMyc plasmid; lanes 3, 4, 6, 8 and 9: 5 negative pCEFL-RasMyc plasmid mini preps; lanes 5 and 7: 2 positive pCEFL-RasMyc plasmid mini preps digested with KpnI.

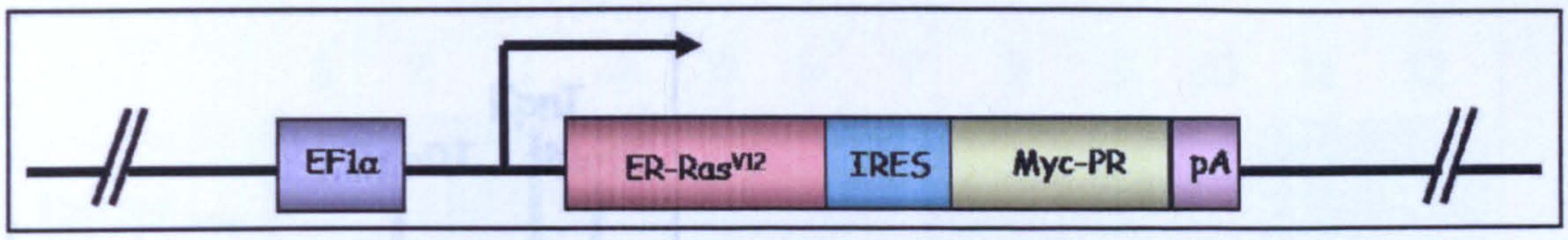

Figure 42. pCEFL-RasMyc plasmid. EF1α eukaryotic promoter (EF1α); Estrogen Receptor-HRas^{V12} fusion protein (ER-H-rasV12); Internal Ribosomal Entry Sequence (IRES); c-Myc-Progesterone Receptor fusion protein (Myc-PR); polyadenylation sequence (pA).

A.2 The MycRas expression vector

As observed in the *in vitro* experiments described subsequently, the amount of c-Myc-PR protein was low or undetectable in the systems analyzed. Moreover, since *myc* is overexpressed in cancer cells, the two oncogenes of the targeting construct were inverted to obtain the MycRas plasmid (Fig. 50) to have a more efficient cap-dependent translation of c-*myc-PR*.

The cloning strategy, described in "Materials and Methods", was planned as follows:

1) Removal of the IRES from the IRES-*myc*-PR plasmid obtained in one of the previous subcloning steps.

The result was a plasmid containing the c-*myc* coding sequence fused to the PR without neither polyA sequence or IRES (pBS *myc*-PR).

Insertion of the IRES downstream of the c-Myc-PR fusion protein (Fig. 43).

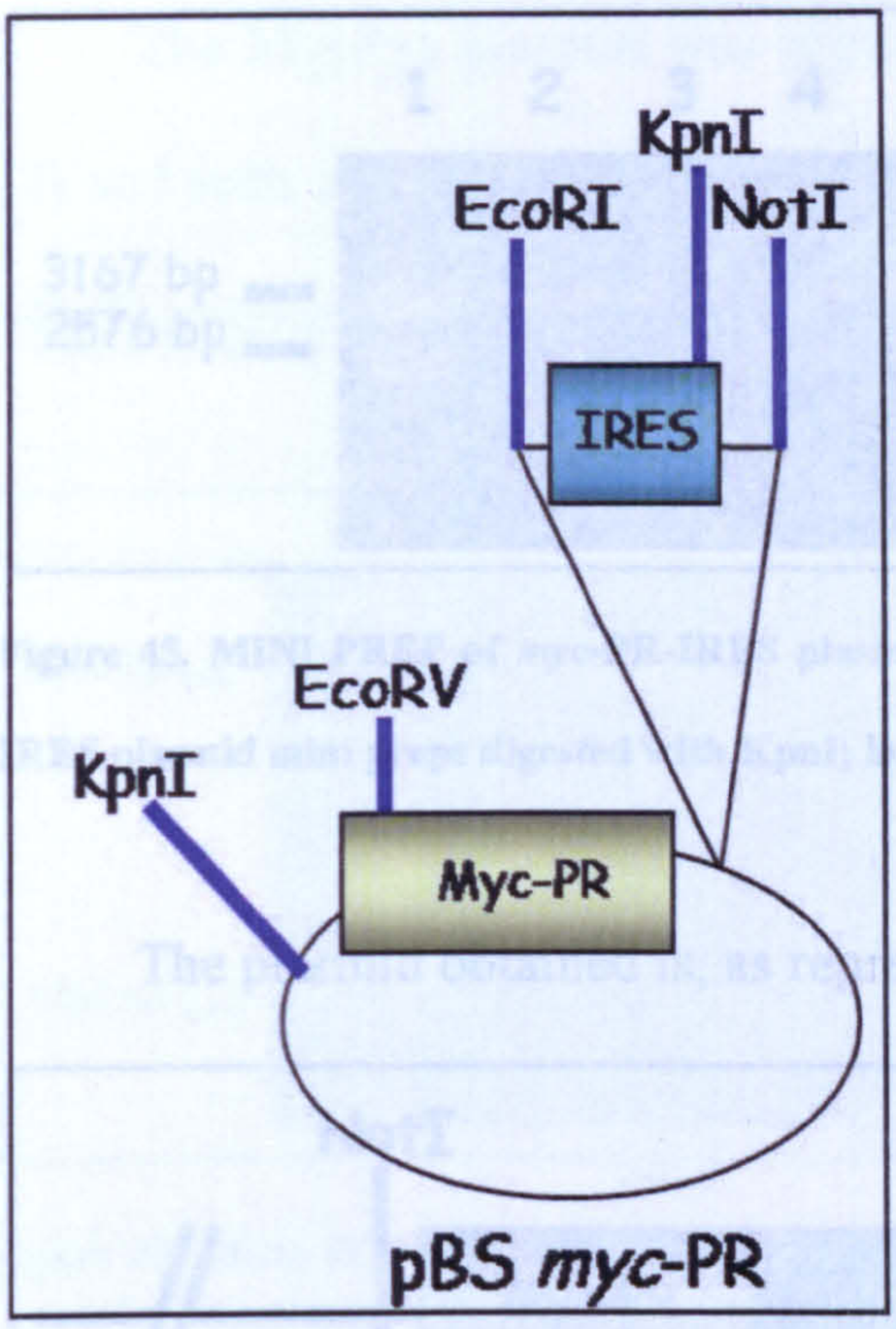

Figure 43. ECMV-IRES cloning into pBS myc-PR.

The digestions of the *myc*-PR-IRES plasmid were carried out coupling EcoRV and NotI (Fig. 44) restriction enzymes or with KpnI (Fig. 45).

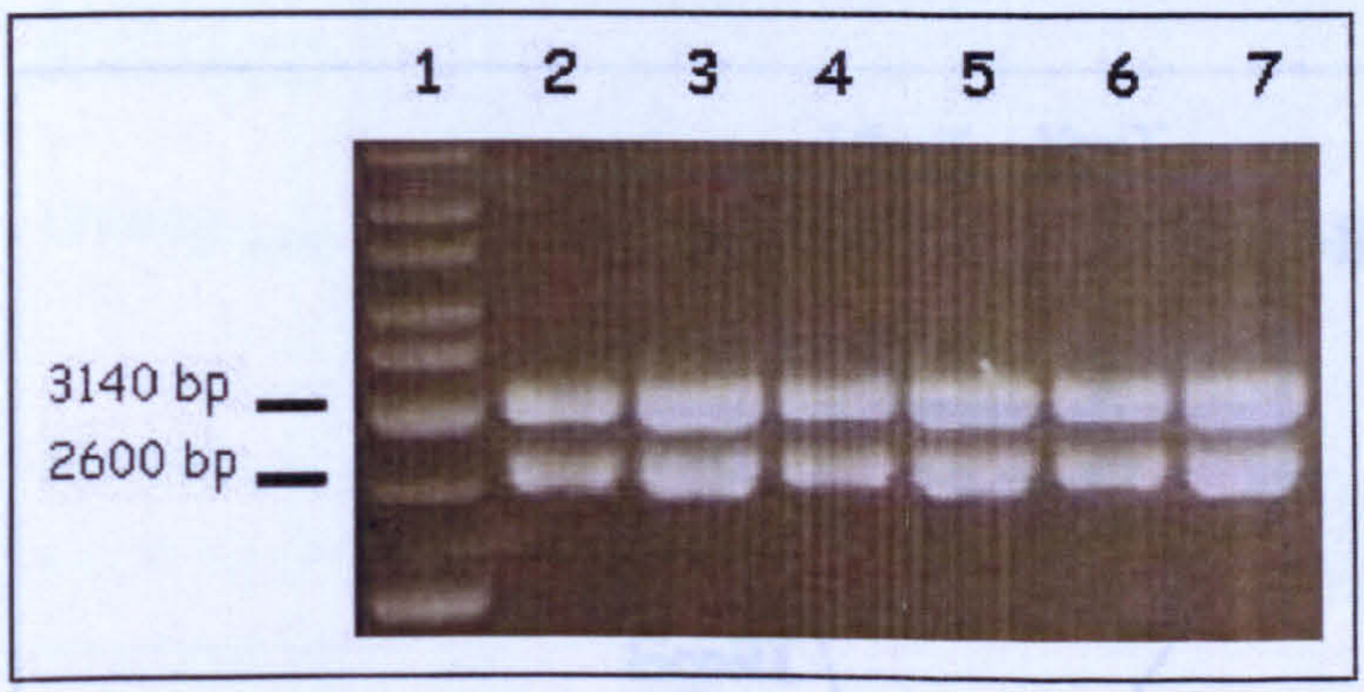

Figure 44. MINI PREP of *myc*-PR-IRES plasmid digested with EcoRV and NotI. Lane 1: 1 kb marker; lanes 2 to 7: 6 positive Myc-PR-IRES plasmid mini preps digested with EcoRV and NotI.

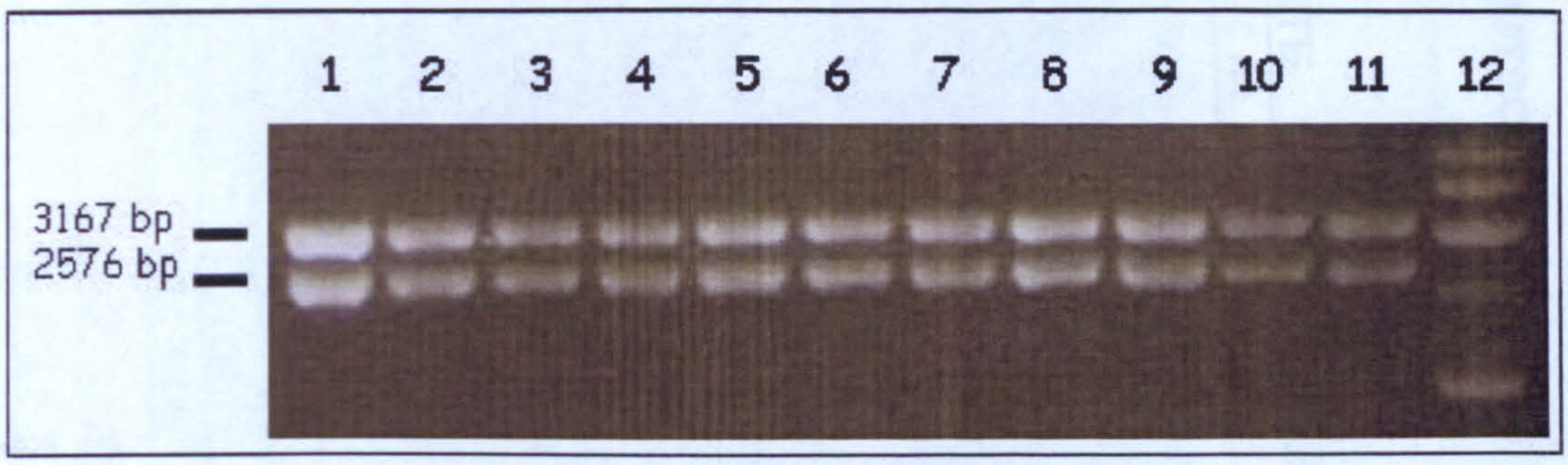

Figure 45. MINI PREP of *myc*-PR-IRES plasmid digested with KpnI. Lanes 1 to 11: 11 positive Myc-PR-IRES plasmid mini preps digested with KpnI; lane 12: 1 kb marker.

The plasmid obtained is, as represented below (Fig. 46).

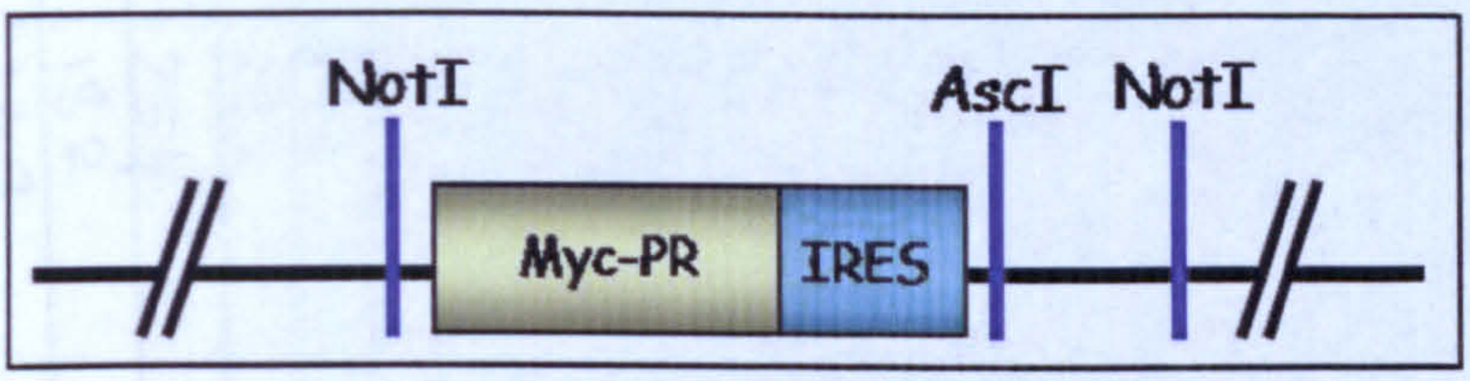

Figure 46. *myc*-PR-IRES plasmid. c-Myc-Progesterone Receptor fusion protein (Myc-PR); Internal Ribosomal Entry Sequence (IRES); NotI restriction site (NotI); AscI restriction site (AscI).

3) Cloning of the *H-ras*^{V12} fused to estrogen receptor (ER-Ras^{V12}) downstream of the last *myc*-PR-IRES plasmid (Fig. 47).

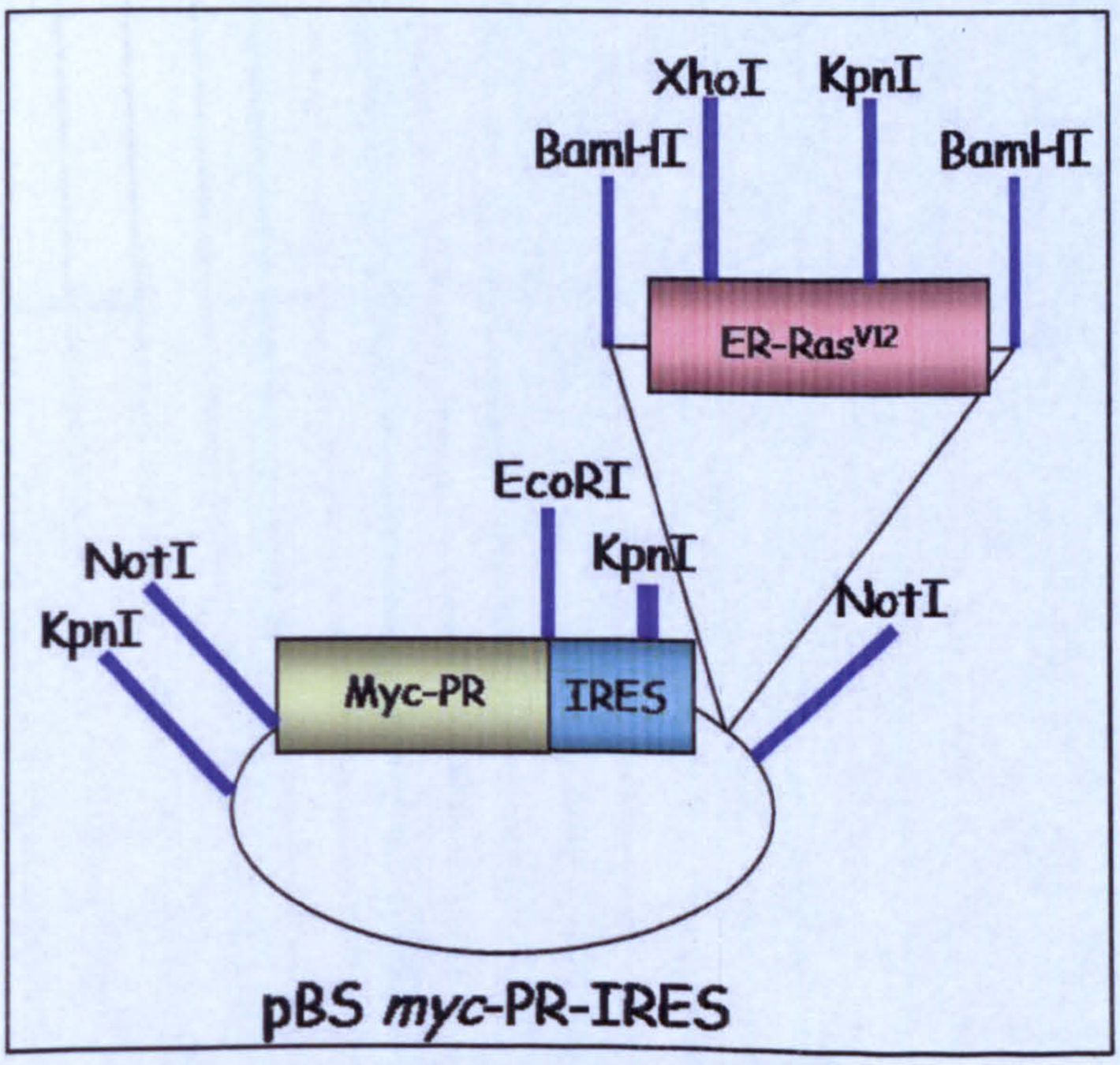

Figure 47. ER-Ras^{V12} cloning into pBS *myc*-PR-IRES.

The MycRas plasmid was digested simultaneously with EcoRI and XhoI (Fig. 48) and with other three restriction enzymes separately: NotI, BamHI and KpnI (Fig. 49). The expected resulting bands are indicated in the figures below (Figs. 48 and 49).

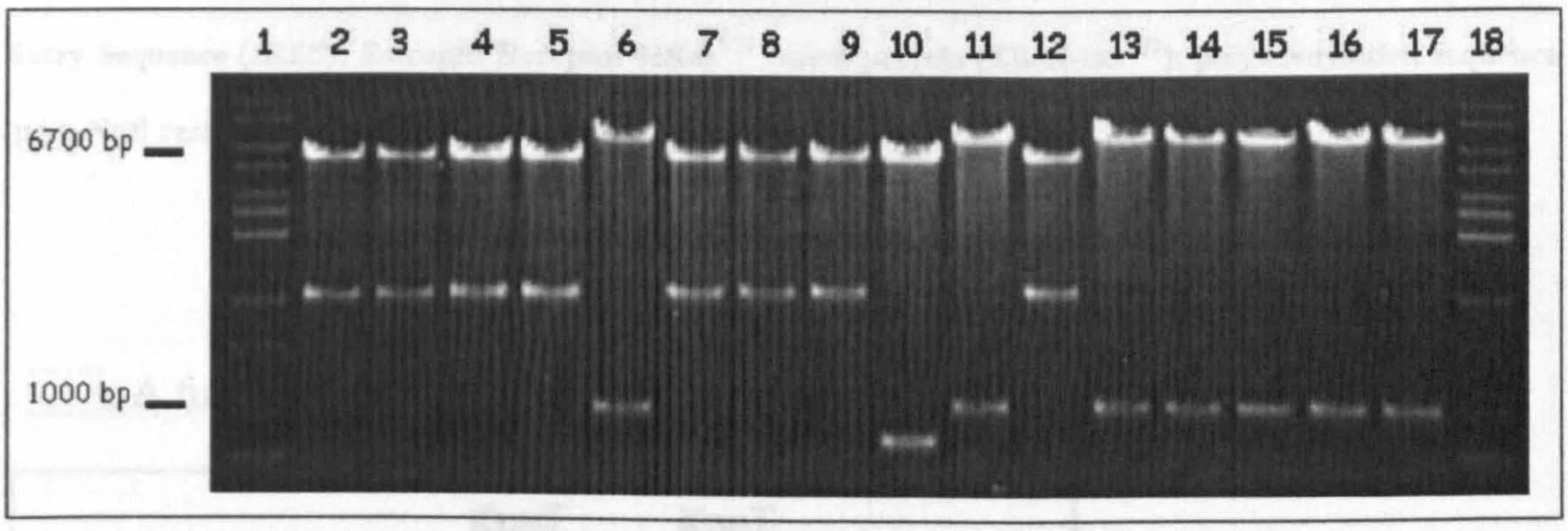

Figure 48. MINI PREP of MycRas plasmid digested with EcoRI and XhoI. Lanes 1 and 18: 1 kb marker; lanes 2 to 5, 7 to 9 and 12: 8 positive MycRas plasmid mini preps digested with EcoRI and XhoI; lanes 6, 10, 11, 13 to 17: 8 negative MycRas plasmid mini preps.

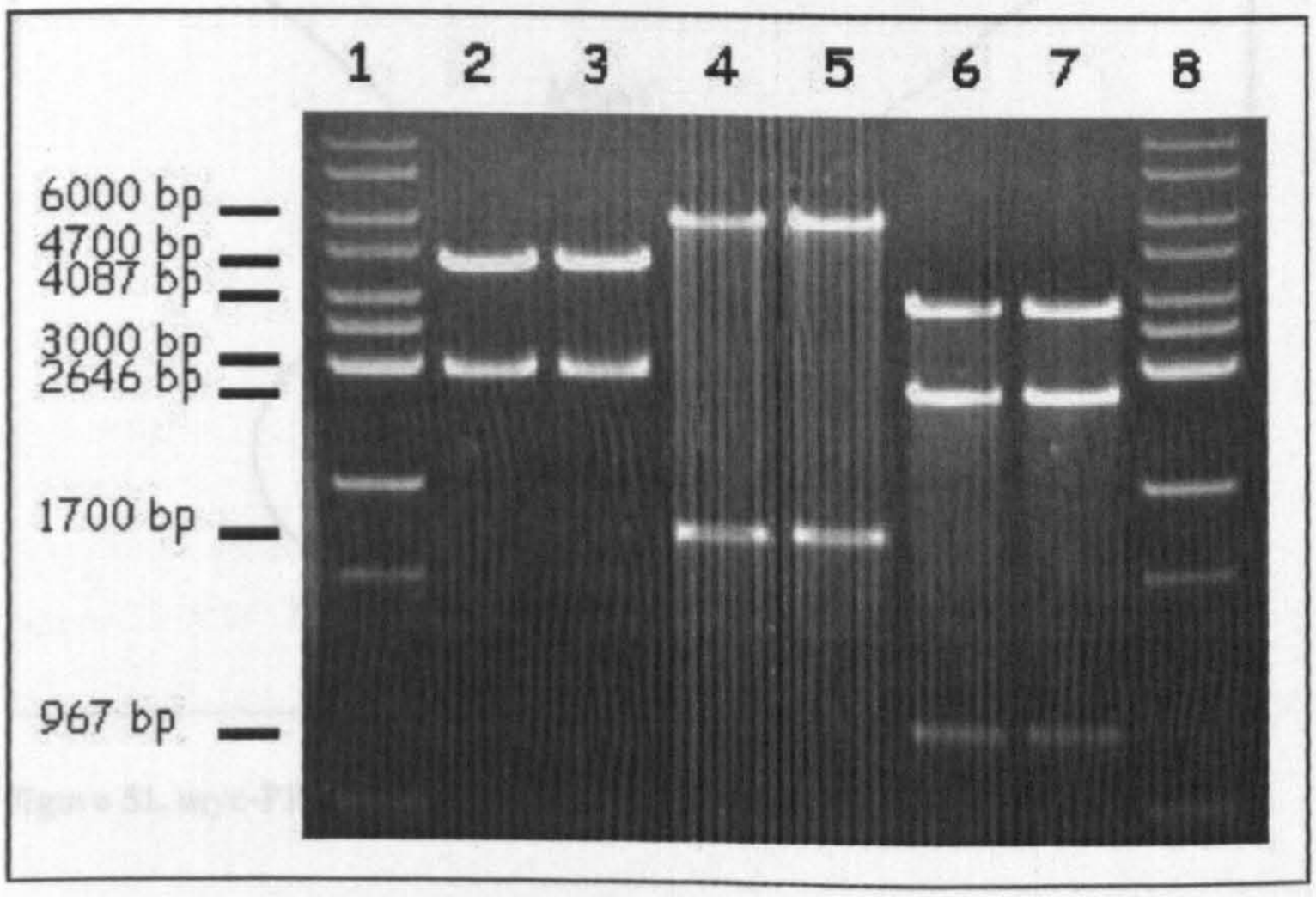

Figure 49. MINI PREP of MycRas plasmid digested with NotI, BamHI and KpnI. Lanes 1 and 8: 1 kb marker; lanes 2 and 3: 2 positive MycRas plasmid mini preps digested with NotI; lanes 4 and 5: 2 positive MycRas plasmid mini preps digested with BamHI; lanes 6 and 7: 2 positive MycRas plasmid mini preps digested with KpnI.

The final plasmid is shown in the following figure 50:

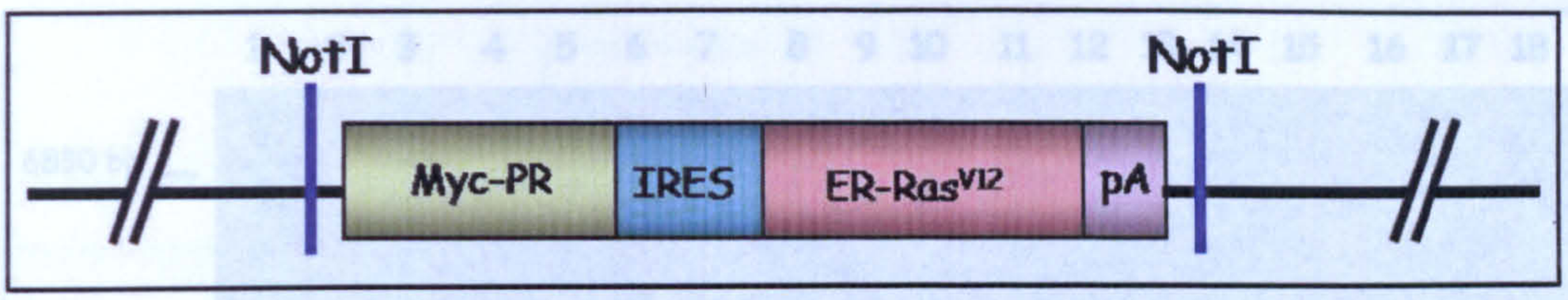

Figure 50. MycRas plasmid. c-Myc-Progesterone Receptor fusion protein (Myc-PR); Internal Ribosomal Entry Sequence (IRES); Estrogen Receptor-HRas^{V12} fusion protein (ER-H-ras^{V12}); polyadenylation sequence (pA); NotI restriction site (NotI).

A further cloning of the MycRas construct into pCEFL vector (Fig. 51).

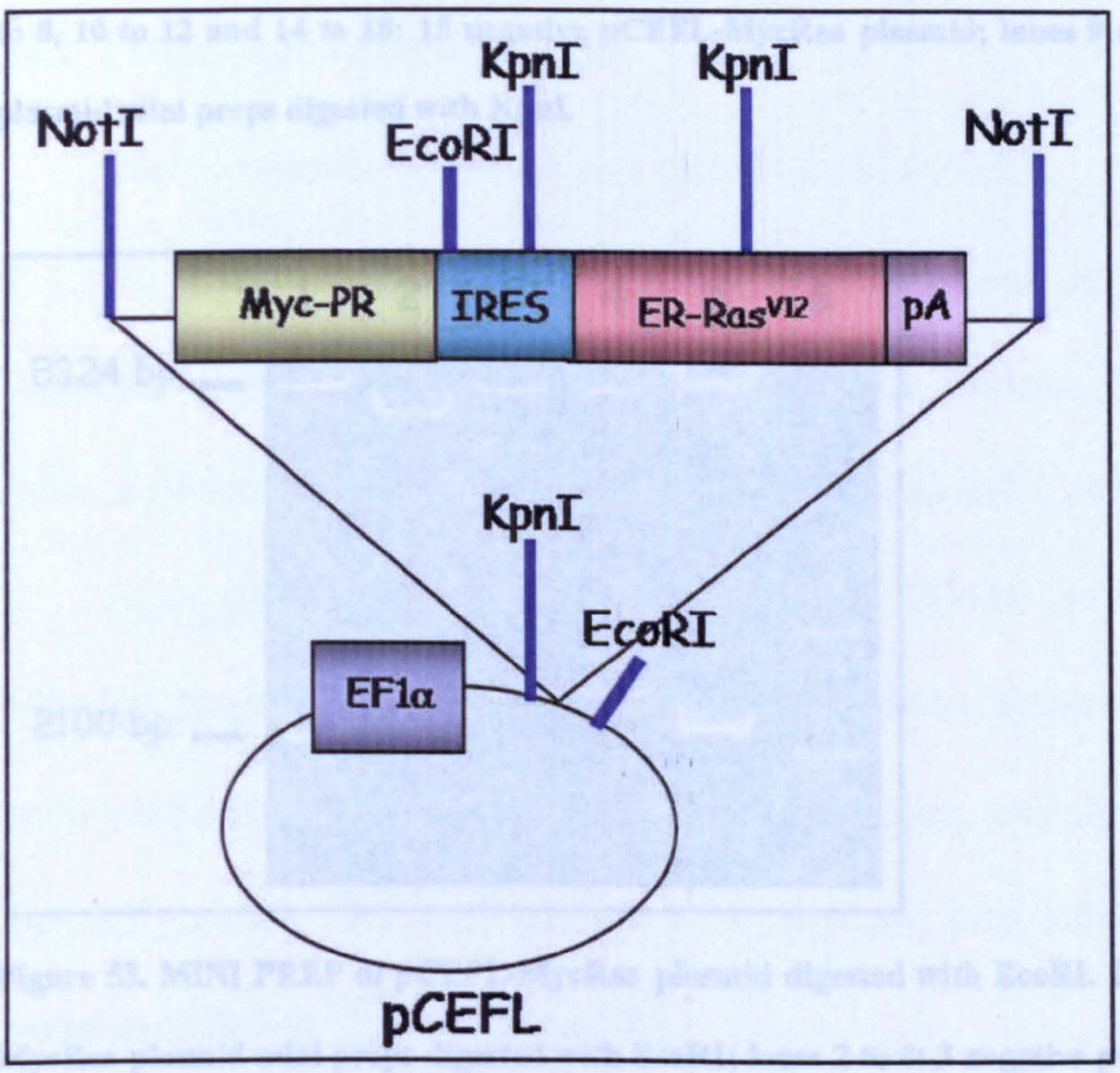

Figure 51. myc-PR-ER-ras (MycRas cassette) cloning into pCEFL.

The analysis of this vector was carried out by digestion with KpnI or EcoRI restrictions enzymes (Figures 52 and 53).

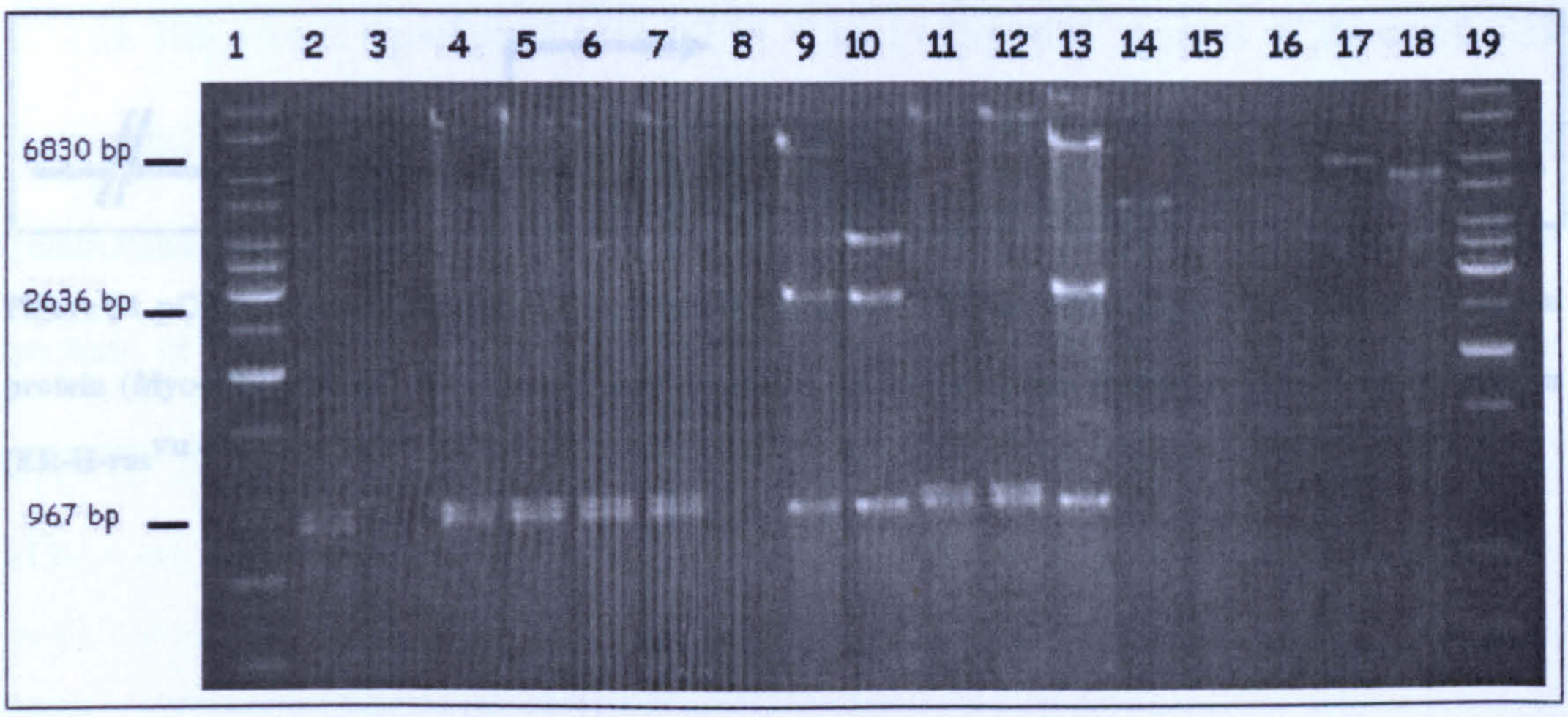

Figure 52. MINI PREP of pCEFL-MycRas plasmid digested with KpnI. Lanes 1 and 19: 1 kb marker; lanes 2 to 8, 10 to 12 and 14 to 18: 15 negative pCEFL-MycRas plasmid; lanes 9 and 13: positive pCEFL-MycRas plasmid mini preps digested with KpnI.

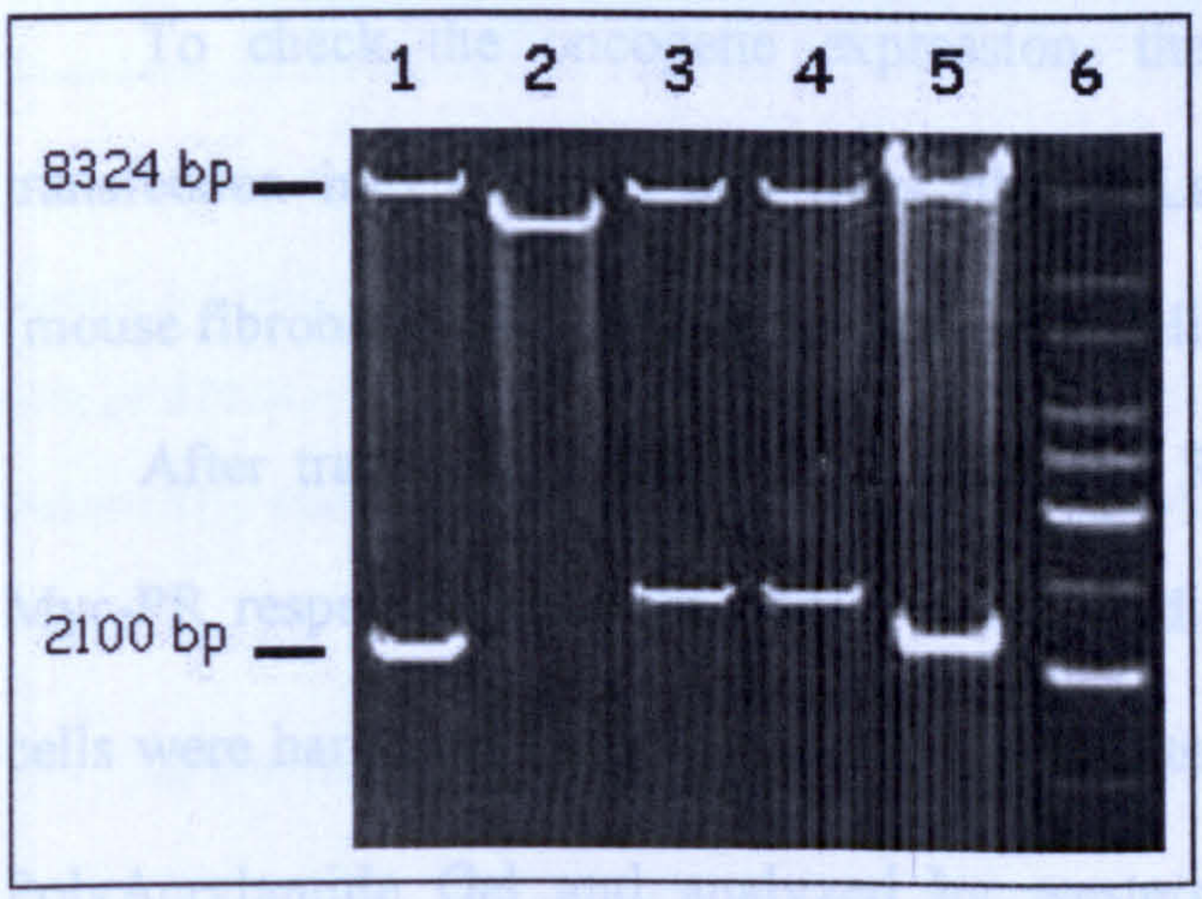

Figure 53. MINI PREP of pCEFL-MycRas plasmid digested with EcoRI. Lanes 1 and 5: 2 positive pCEFL-MycRas plasmid mini preps digested with EcoRI; lanes 2 to 4: 3 negative pCEFL-MycRas plasmid; lane 6: 1 kb marker.

The Eukaryotic expression vector carrying the MycRas bicistronic cassette is as follows (Fig. 54).

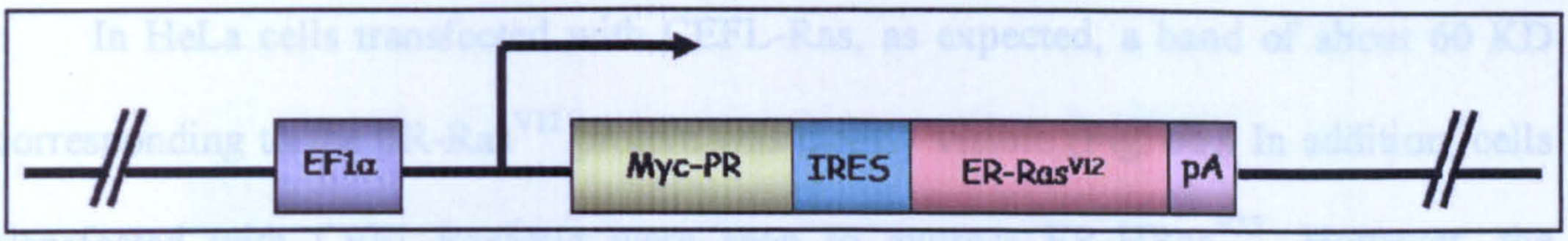

Figure 54. pCEFL-MycRas plasmid. EF1α eukaryotic promoter (EF1α); c-Myc-Progesterone Receptor fusion protein (Myc-PR); Internal Ribosomal Entry Sequence (IRES); Estrogen Receptor-HRas^{V12} fusion protein (ER-H-ras^{V12}).

Part B: Analysis of oncogenes expression

B.1 Transient transfections

The bicistronic construct was tested in cell systems.

To check the oncogene expression, the construct was tested by transient transfection into different cell lines like HeLa (human epithelial cells), NIH 3T3 (mouse fibroblast cells), FRTL-5 (rat thyroid cells) and Cos7 (monkey kidney cells).

After transfection, 4OH-tamoxifene and RU486 (to activate ER-Ras^{V12} and c-Myc-PR respectively), were added to the medium. After 48 hours of treatment, the cells were harvested for extraction of total proteins, which were fractionated on SDS-PolyAcrylamide Gel and analyzed by western blot using antibodies against both proteins (ER-Ras^{V12} and c-Myc-PR).

HeLa cells were transiently transfected, either with the pCEFL empty vector (CEFL), or with the pCEFL vector carrying the ER-Ras^{V12} coding sequence downstream of the eukaryotic promoter (CEFL-Ras) as controls or with the same vector carrying the RasMyc construct (CEFL-RasMyc). Hormones were added as described above.

The expressions of ER-Ras^{V12} and c-Myc-PR were analyzed by western blot (Figs. 55 and 56).

In HeLa cells transfected with CEFL-Ras, as expected, a band of about 60 KD corresponding to the ER-Ras^{V12} protein was clearly visible (Fig. 55). In addition, cells transfected with CEFL-RasMyc were seen to express ER-HRas^{V12}. However, the amount of the protein was lower when expressed by the bicistronic construct as compared to the same protein expressed by the CEFL-Ras vector (Fig. 55, lanes 6 to 11).

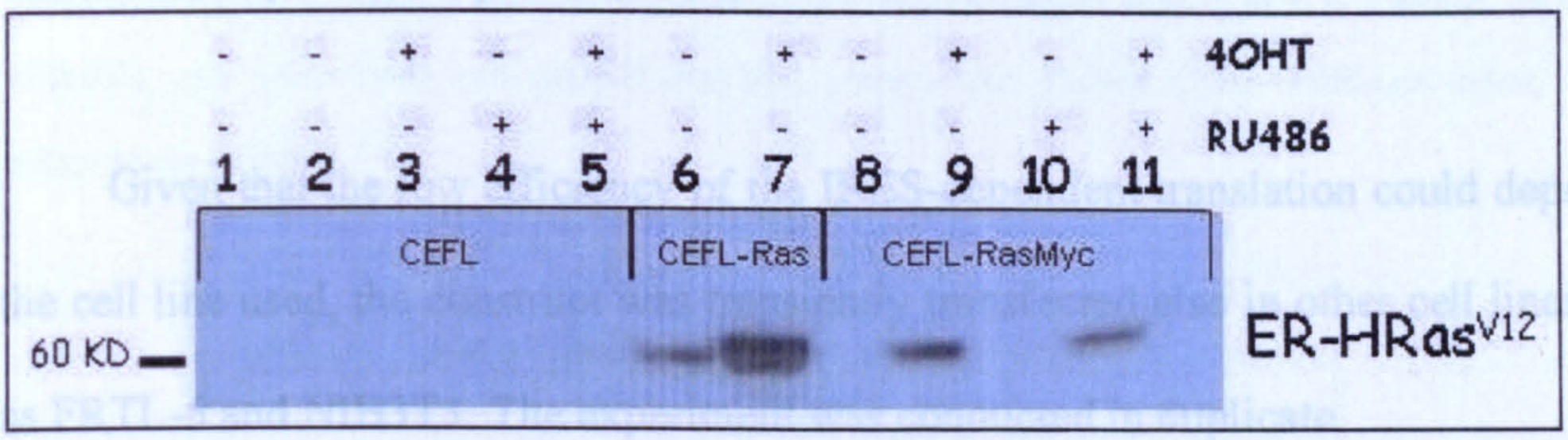

Figure 55. ER-Ras^{V12} (ER-HRas^{V12}) expression in transfected HeLa cells. Lane 1: un-transfected HeLa cells; lanes 2, 3, 4 and 5: HeLa cells transfected with pCEFL wild type vector; lanes 6 and 7: HeLa cells transfected with pCEFL-Ras vector; lanes 8, 9, 10 and 11: HeLa cells transfected with pCEFL-RasMyc vector. Kilo Dalton (KD); 4OH-tamoxifene (4OHT); mifepristone (RU486).

In western blot analysis of HeLa transfected either with the pCEFL empty vector (CEFL), or with the pCEFL vector carrying the c-Myc-PR coding sequence (CEFL-Myc) as controls or with the same vector carrying the RasMyc construct (CEFL-RasMyc) (Fig. 56), the c-Myc-PR band was detected in the extract of HeLa transfected with pCEFL-c-Myc-PR. However, no band corresponding to the expected 87 KD c-Myc-PR of the bicistronic construct was visible (Fig. 56, lanes 6 to 11).

Thus, these results showed that there was a cap-dependent translation of ER-Ras^{V12}, whereas the cap-independent translation of the second cistron was not observed. This could be explained either by its complete absence or by its presence in such a low amount, almost below the threshold value of the system, to render it undetectable.

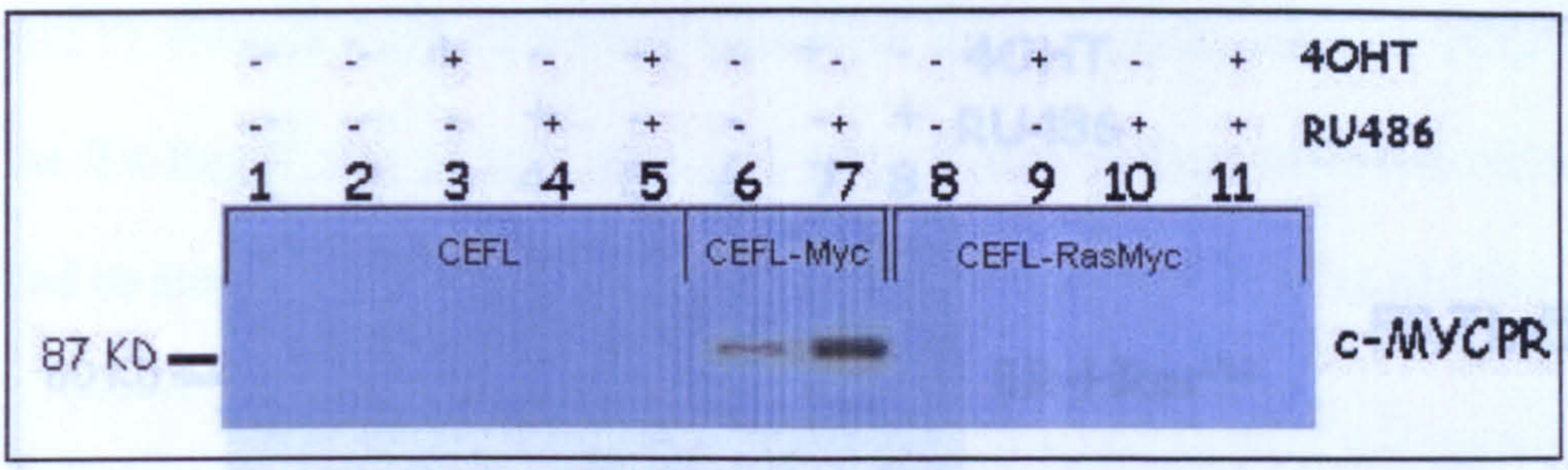

Figure 56. c-MycPR expression in transfected HeLa cells. Lane 1: un-transfected HeLa cells; lanes 2, 3, 4 and 5: HeLa cells transfected with pCEFL wild type vector; lanes 6 and 7: HeLa cells transfected with pCEFL-Myc vector; lanes 8, 9, 10 and 11: HeLa cells transfected with pCEFL-RasMyc vector. Kilo Dalton (KD); 4OH-tamoxifene (4OHT); mifepristone (RU486).

Given that the low efficiency of the IRES-dependent translation could depend on the cell line used, the construct was transiently transfected also in other cell lines, such as FRTL-5 and NIH3T3. The experiment was conducted in duplicate.

The ER-Ras^{V12} 60 KD protein, translated in a cap-dependent fashion, was the unique protein detected after addition of the 4OH-tamoxifene in both FRTL5 and NIH3T3 cell lines (Fig. 57). In fact, in the extracts from FRTL5 and NIH3T3 cells transfected with pCEFL-RasMyc, a band corresponding to the expected 87 KD c-Myc-PR was detected (Fig. 58). Thus, only the cap-dependent ER-HRas^{V12} translation was observed.

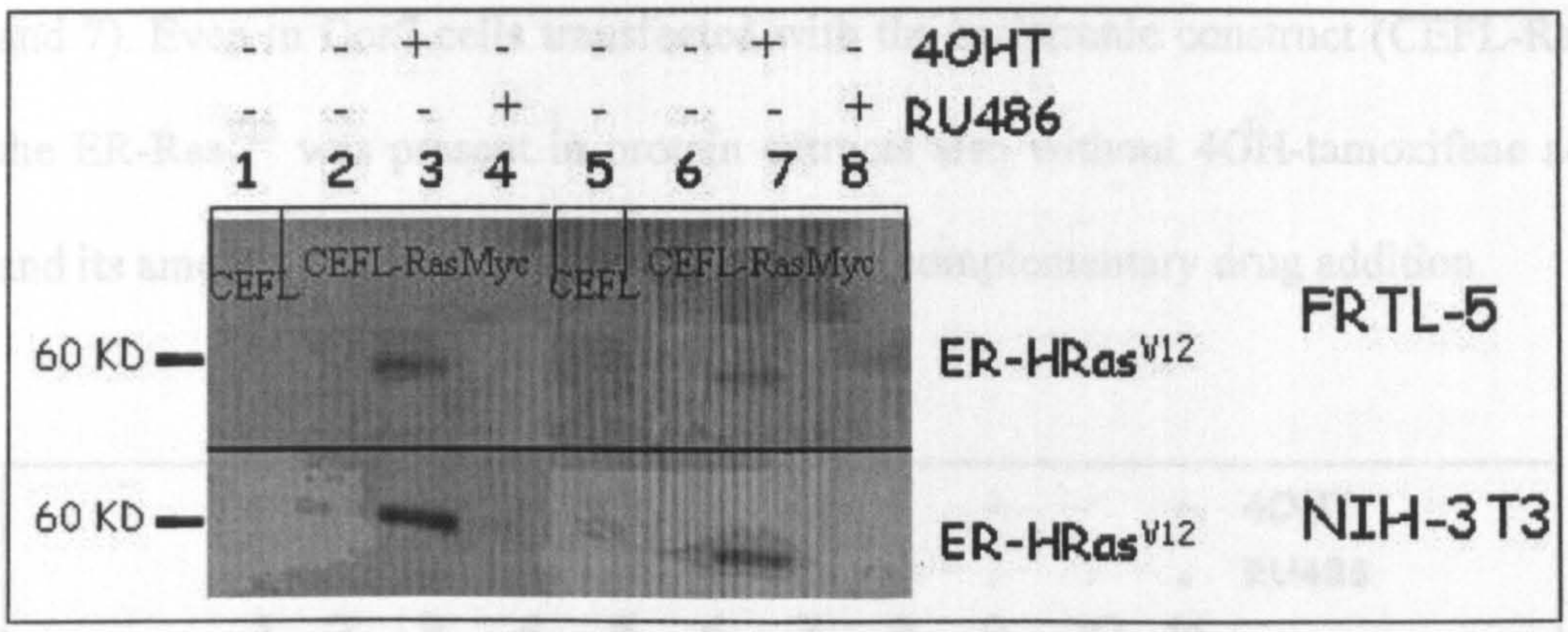

Figure 57. ER-Ras^{V12} (ER-HRas^{V12}) expression in transfected FRTL-5 and NIH-3T3 cells. Lanes 1 and 5: FRTL-5 and NIH-3T3 cells transfected with pCEFL wild type vector; lanes 2, 3, 4, 6, 7 and 8: FRTL-5 and NIH-3T3 cells transfected with pCEFL-RasMyc vector. Kilo Dalton (KD); 4OH-tamoxifene (4OHT); mifepristone (RU486).

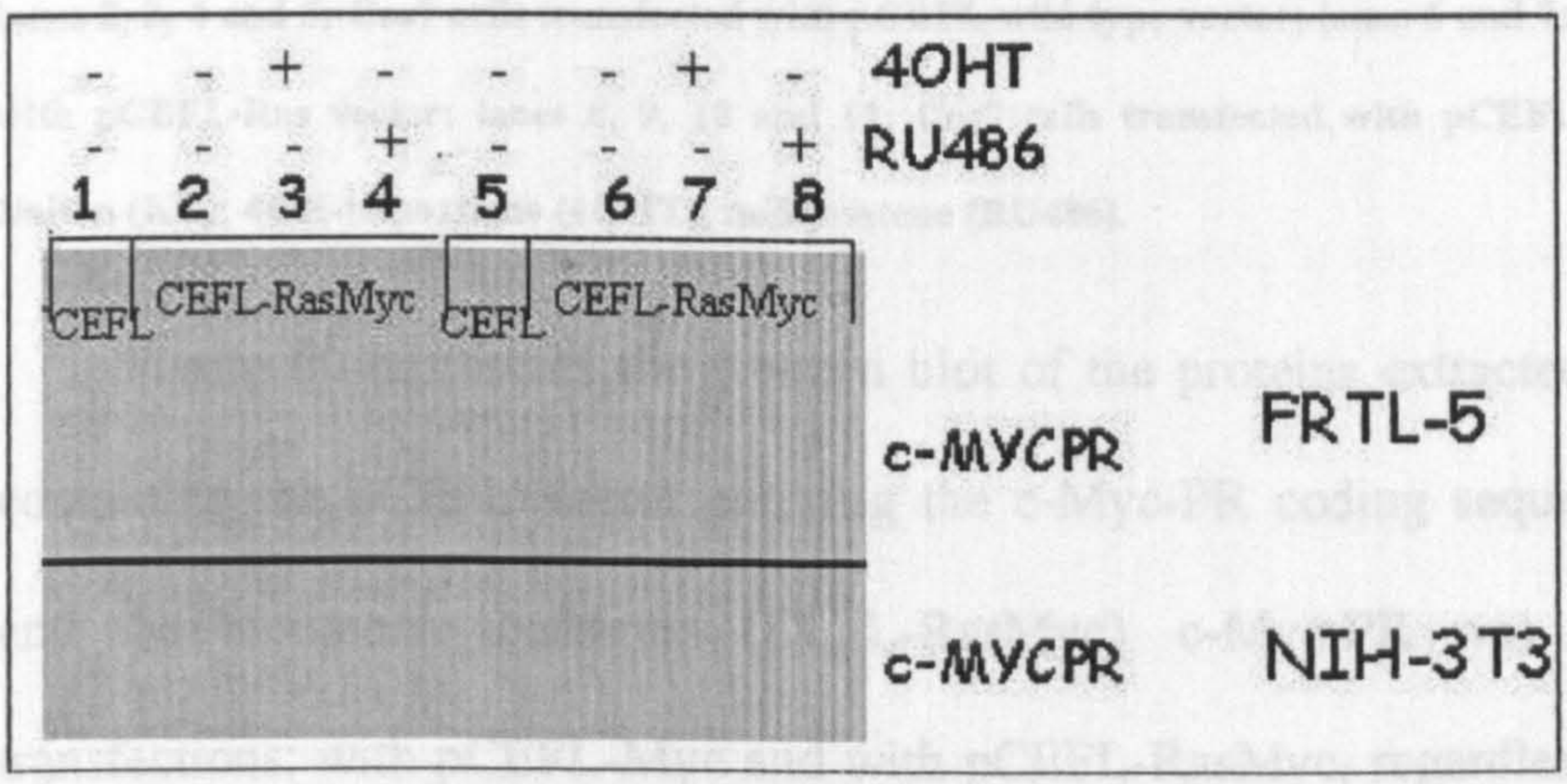

Figure 58. c-Myc-PR expression in transfected FRTL-5 and NIH-3T3 cells. Lanes 1 and 5: FRTL-5 and NIH-3T3 cells transfected with pCEFL wild type vector; lanes 2, 3, 4, 6, 7 and 8: FRTL-5 and NIH-3T3 cells transfected with pCEFL-RasMyc vector. Kilo Dalton (KD); 4OH-tamoxifene (4OHT); mifepristone (RU486).

In addition, Cos7 cells were transfected with either the pCEFL empty vector (CEFL) or the pCEFL vector carrying the ER-Ras^{V12} coding sequence (CEFL-Ras) or the c-Myc-PR coding sequence (CEFL-Myc) as controls or with the same vector carrying our construct (CEFL-RasMyc). The proteins were extracted and analyzed by western blot after cell treatment with 4OH-tamoxifene and RU486 for 48 hours.

Figure 59 indicates that the ER-Ras^{V12} protein was detected in control cells (transfected with CEFL-Ras) treated with 4OH-tamoxifene or left untreated (lanes 6

and 7). Even in Cos7 cells transfected with the bicistronic construct (CEFL-RasMyc), the ER-Ras^{V12} was present in protein extracts also without 4OH-tamoxifene addition, and its amount was found to increase after its complementary drug addition.

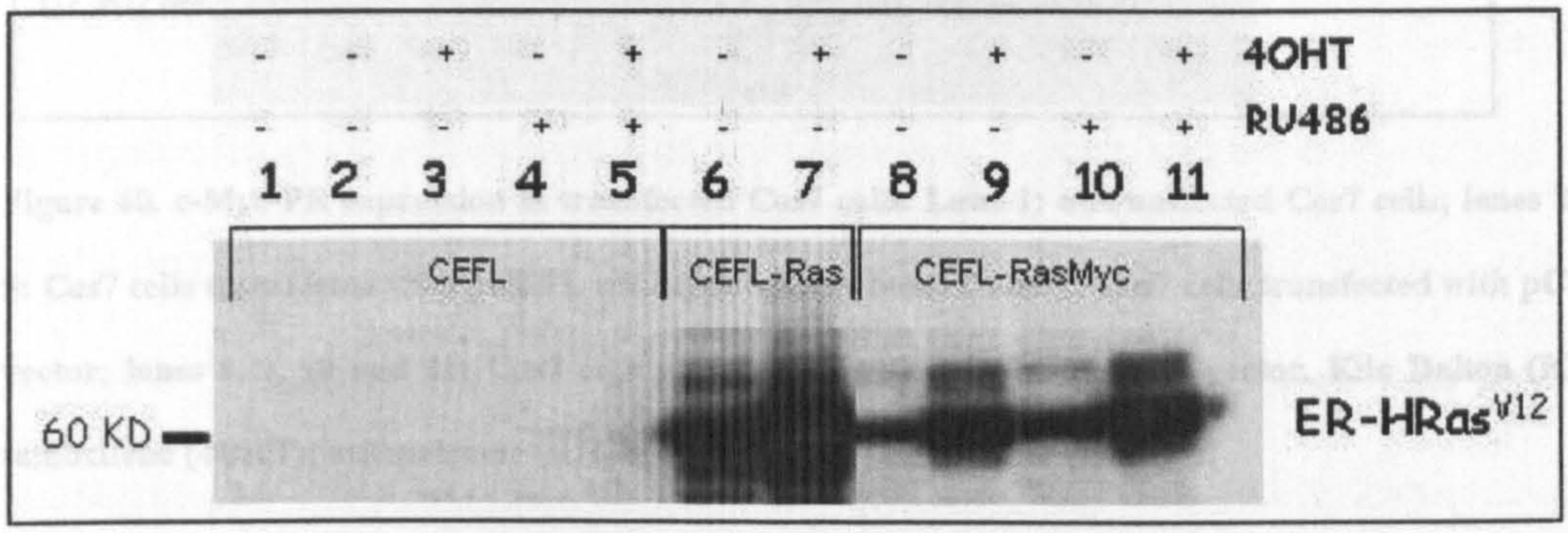

Figure 59. ER-Ras^{V12} (ER-HRas^{V12}) expression in transfected Cos7 cells. Lane 1: untransfected Cos7 cells; lanes 2, 3, 4 and 5: Cos7 cells transfected with pCEFL wild type vector; lanes 6 and 7: Cos7 cells transfected with pCEFL-Ras vector; lanes 8, 9, 10 and 11: Cos7 cells transfected with pCEFL-RasMyc vector. Kilo Dalton (KD); 4OH-tamoxifene (4OHT); mifepristone (RU486).

Figure 60 represents the western blot of the proteins extracted from Cos7 cells containing the pCEFL vector carrying the c-Myc-PR coding sequence (CEFL-Myc) and the bicistronic construct (CEFL-RasMyc). c-Myc-PR was detected in both transfections: with pCEFL-Myc and with pCEFL-RasMyc, regardless of the treatment (lanes 6 to 11).

Thus, Cos7 cells transfected with pCEFL-RasMyc showed a cap-dependent ER-Ras^{V12} translation and IRES-dependent translation of c-Myc-PR was also observed. Even though, the amount of c-Myc-PR protein was low, it was possible to conclude that the bicistronic construct can work in Cos7 cells. This result could be explained assuming that the IRES activity was cell type-specific, presumably due to the reasons described previously. However, Cos7, are known to be the cells expressing transfected genes very efficiently; hence the absence of c-Myc-PR in other cell lines and its presence in Cos7 cells could be attributed to the transfection or expression efficiency of these cells.

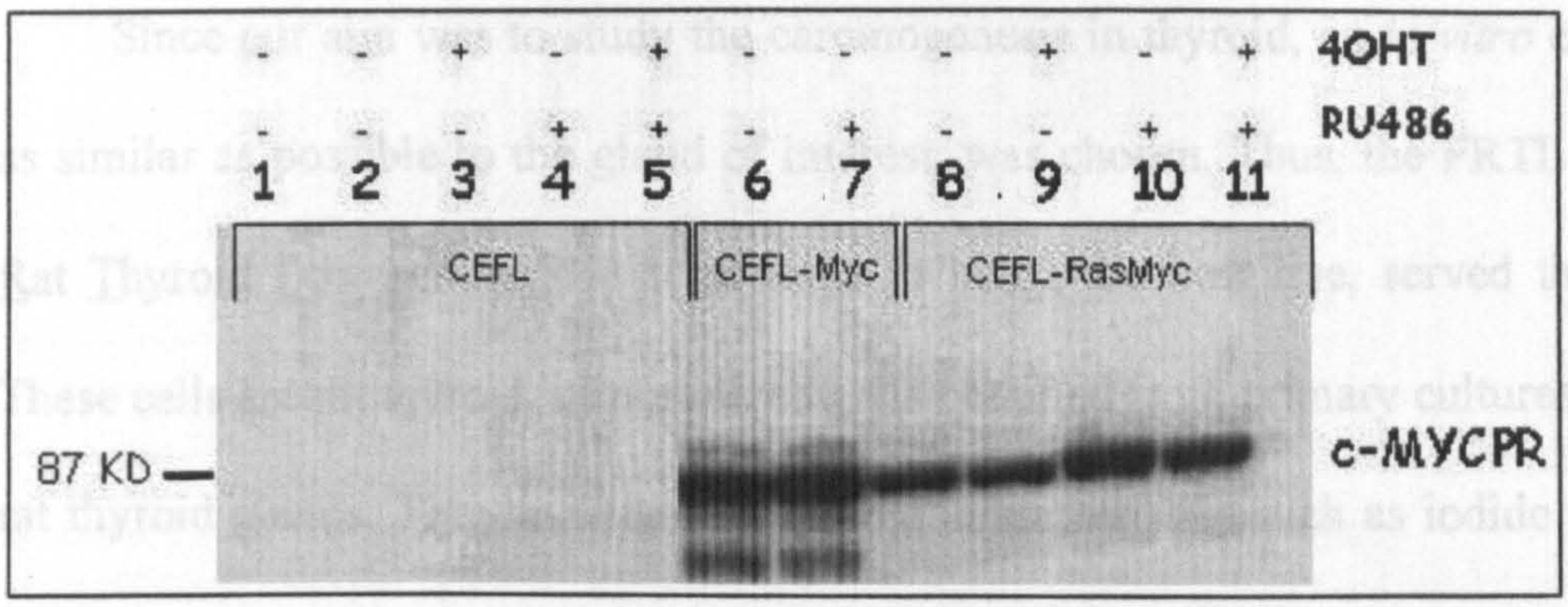

Figure 60. c-Myc-PR expression in transfected Cos7 cells. Lane 1: untransfected Cos7 cells; lanes 2, 3, 4 and 5: Cos7 cells transfected with pCEFL wild type vector; lanes 6 and 7: Cos7 cells transfected with pCEFL-Myc vector; lanes 8, 9, 10 and 11: Cos7 cells transfected with pCEFL-RasMyc vector. Kilo Dalton (KD); 4OH-tamoxifene (4OHT); mifepristone (RU486).

B.2 Stable transfections

The c-Myc protein has been found overexpressed in the majority of the tumours in which it is involved. Therefore our aim was to obtain c-Myc-PR protein levels higher than that obtained with the RasMyc vector transiently transfected, to reach a suitable amount of protein able to co-operate with the second oncoprotein during its transforming activity. For this purpose, the MycRas vector was created inverting the two oncogenes up- and downstream of the IRES, to obtain a 5'cap-dependent c-Myc-PR translation.

Based on the results obtained with the transient transfections of the RasMyc vector described in the previous paragraph, for the MycRas construct we decided to carry out a stable transfection. As compared to the transient transfections, in which only a small number of cells result transfected and in which the vector can insert randomly in different regions of the genome creating a pool of different cells, with stable transfection, it is possible to obtain a clone of selected cells fully identical and homogeneously transfected.

Since our aim was to study the carcinogenesis in thyroid, an *in vitro* cell system, as similar as possible to the gland of interest, was chosen. Thus, the FRTL-5 (Fischer Rat Thyroid Low serum 5%) considered to being the best line, served the purpose. These cells are rat thyroid immortalized cells obtained from primary cultures of Fischer rat thyroid glands. They maintain functional characteristics such as iodide uptake and thyroglobulin synthesis over prolonged periods of culture and are cultured in a medium containing approximately 5 percent calf serum supplemented with a mixture of hormones. The FRTL-5 cells were subjected to stable transfection with the MycRas construct and then to selection with G418, after which, 59 stable neomycin resistant clones were picked up and expanded separately. The expression of both chimeric proteins in the positively selected clones was checked by western blot analysis in the presence of either 4OH-tamoxifene or RU486 or both or without them.

Among the 59 G418 positively selected FRTL-5/MycRas clones, at least four were found to express both proteins, out of them two were expanded for further analyses (Figs. 61 and 62) and named as clone 4 (Cl4) and clone 7 (Cl7). A clone (Cl11) obtained from FRTL-5 cells stably transfected with pCEFL-ER-Ras^{V12} vector (De Vita et al., 2005) was used as ER-Ras^{V12} positive control clone. This clone has been found to express high ER-Ras^{V12} levels conferring to the clone, the ability to grow in a TSH-independent manner when induced with 4OH-tamoxifene. Moreover, the expression of some thyroid-specific genes including thyroglobulin was appreciably reduced in the same clone.

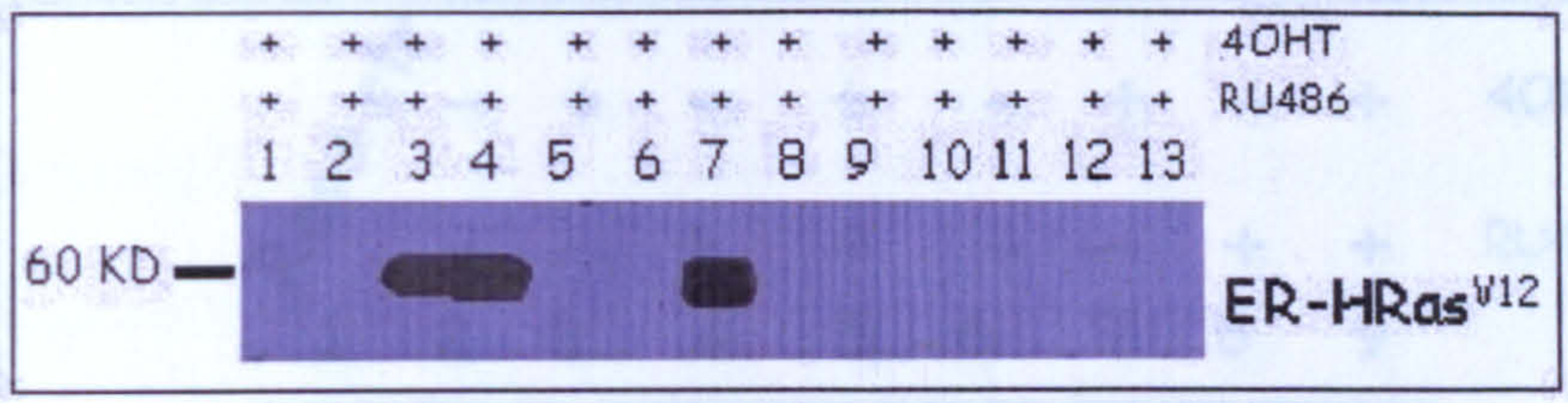

Figure 61. ER-Ras^{V12} (ER-HRas^{V12}) expression in 13 out of 59 FRTL-5/MycRas screened clones. Lanes 1 to 13: clones 1 to 13. Kilo Dalton (KD); 4OH-tamoxifene (4OHT); mifepristone (RU486).

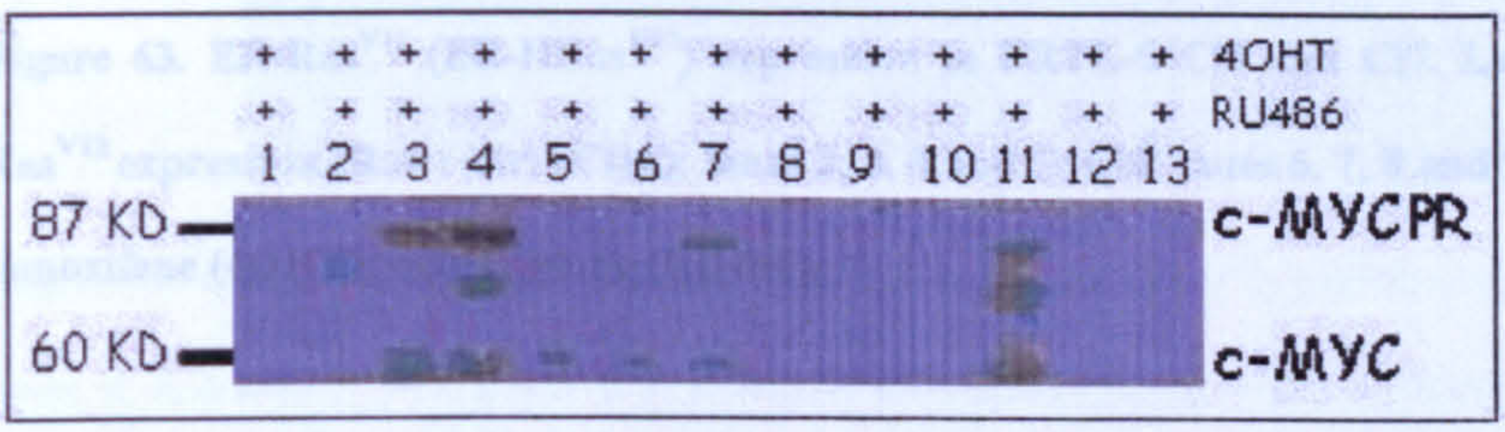

Figure 62. c-Myc-PR expression in 13 out of 59 FRTL-5/MycRas screened clones. Lanes 1 to 13: clones 1 to 13. Kilo Dalton (KD); 4OH-tamoxifene (4OHT); mifepristone (RU486).

The whole cell lysates of the two stable FRTL-5/MycRas clones (Cl4 and Cl7) were obtained and a 30 µgs of protein samples were resolved on a precast SDS-PAGE gel.

The ER-Ras^{V12} expression (the gene downstream of the IRES in the MycRas construct) was found to be higher in Cl4 than in Cl7 (Fig. 63) but about 30 fold lower than that of Cl11, figure 64 lane 6 (Cl4 15 µg) and lane 2 (Cl11 0.5 µg).

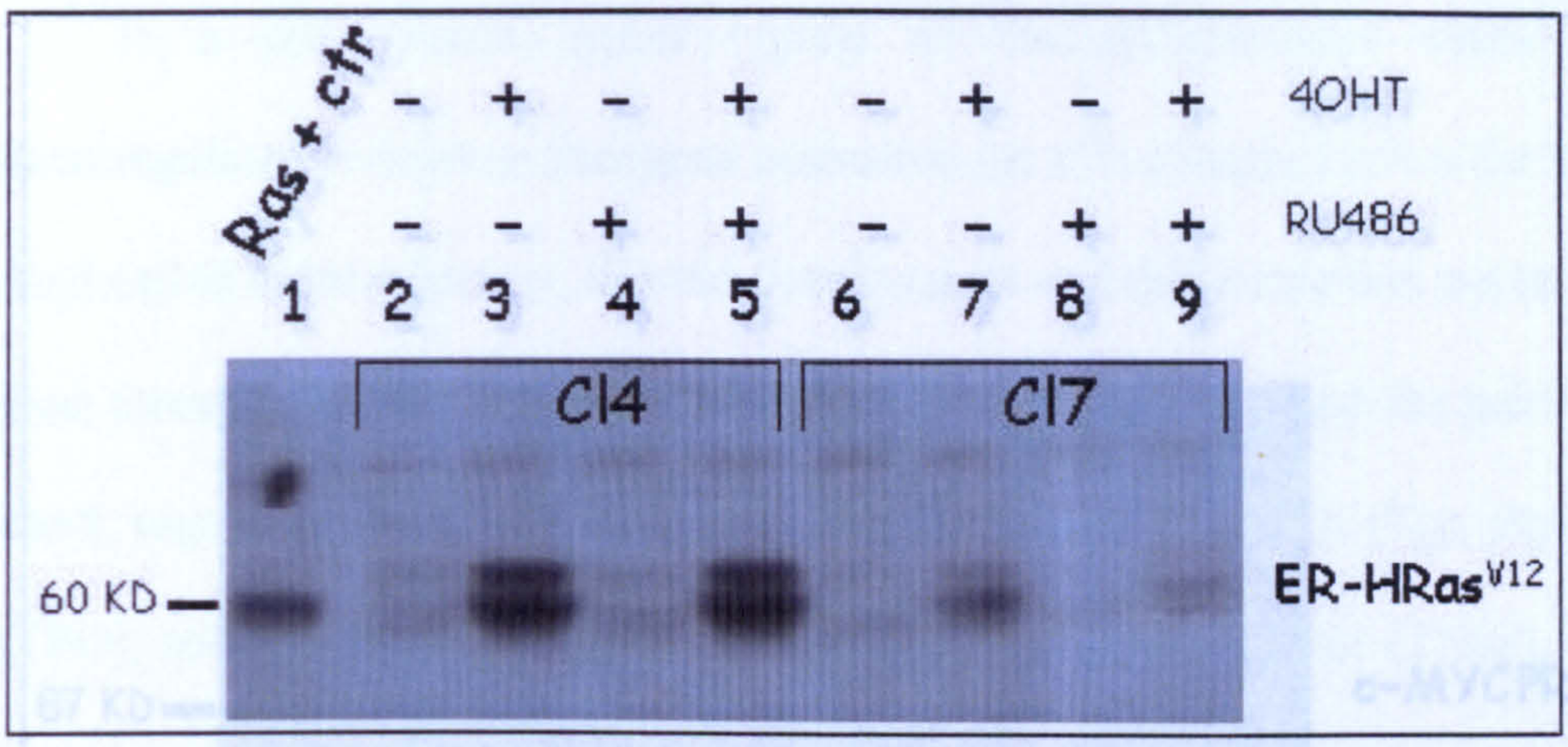

Figure 63. ER-Ras^{V12} (ER-HRas^{V12}) expression in FRTL-5 Cl4 and Cl7. Lane 1: positive control for ER-Ras^{V12} expression (Ras + ctr) (Cl11); lanes 2, 3, 4 and 5: Cl4; lanes 6, 7, 8 and 9: Cl7. Kilo Dalton (KD); 4OH-tamoxifene (4OHT); mifepristone (RU486).

The ER-Ras^{V12} protein appeared to be more stable and much more abundant after addition of 4OH-tamoxifene, as shown previously (De Vita et al., 2005) and as observed for other ER-fusion proteins (Greulich and Erikson, 1998; Samuels et al., 1993).

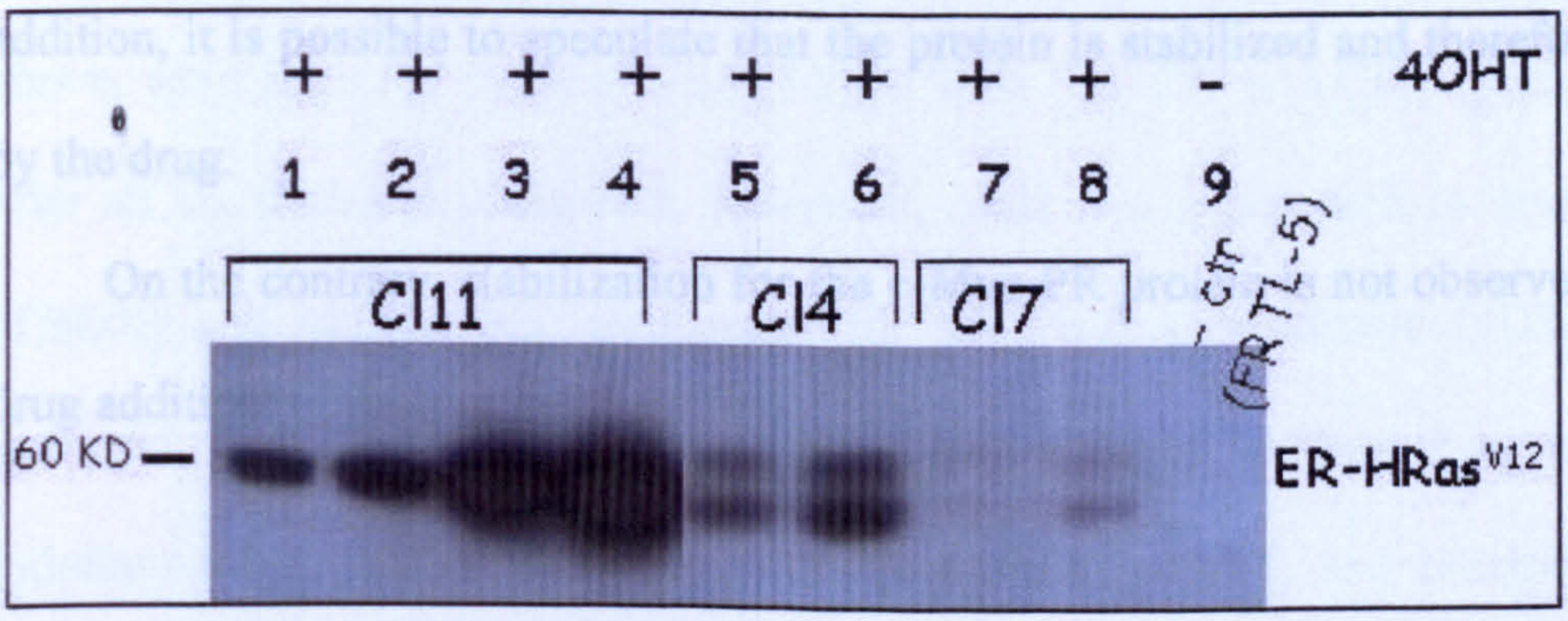

Figure 64. ER-Ras^{V12} (ER-HRas^{V12}) expression in FRTL-5 Cl11, Cl4 and Cl7. Lane 1: Cl11 0,25 µg; lane 2: Cl11 0,5 µg; lane 3: Cl11 2 µg; lane 4: Cl11 4 µg; lane 5: Cl4 7 µg; lane 6: Cl4 15 µg; lane 7: Cl7 7 µg; lane 8: Cl7 15 µg; lane 9: negative control (-ctr) for ER-Ras^{V12} expression (FRTL-5 wild type); Kilo Dalton (KD); 4OH-tamoxifene (4OHT).

Also the amount of the c-Myc-PR protein was found visibly higher in Cl4 (lanes 2 to 5) as compared to that in Cl7 (lanes 6 to 9) (Fig. 65). In this case, the stability of c-Myc-PR protein was not found to increase by the addition of hormone.

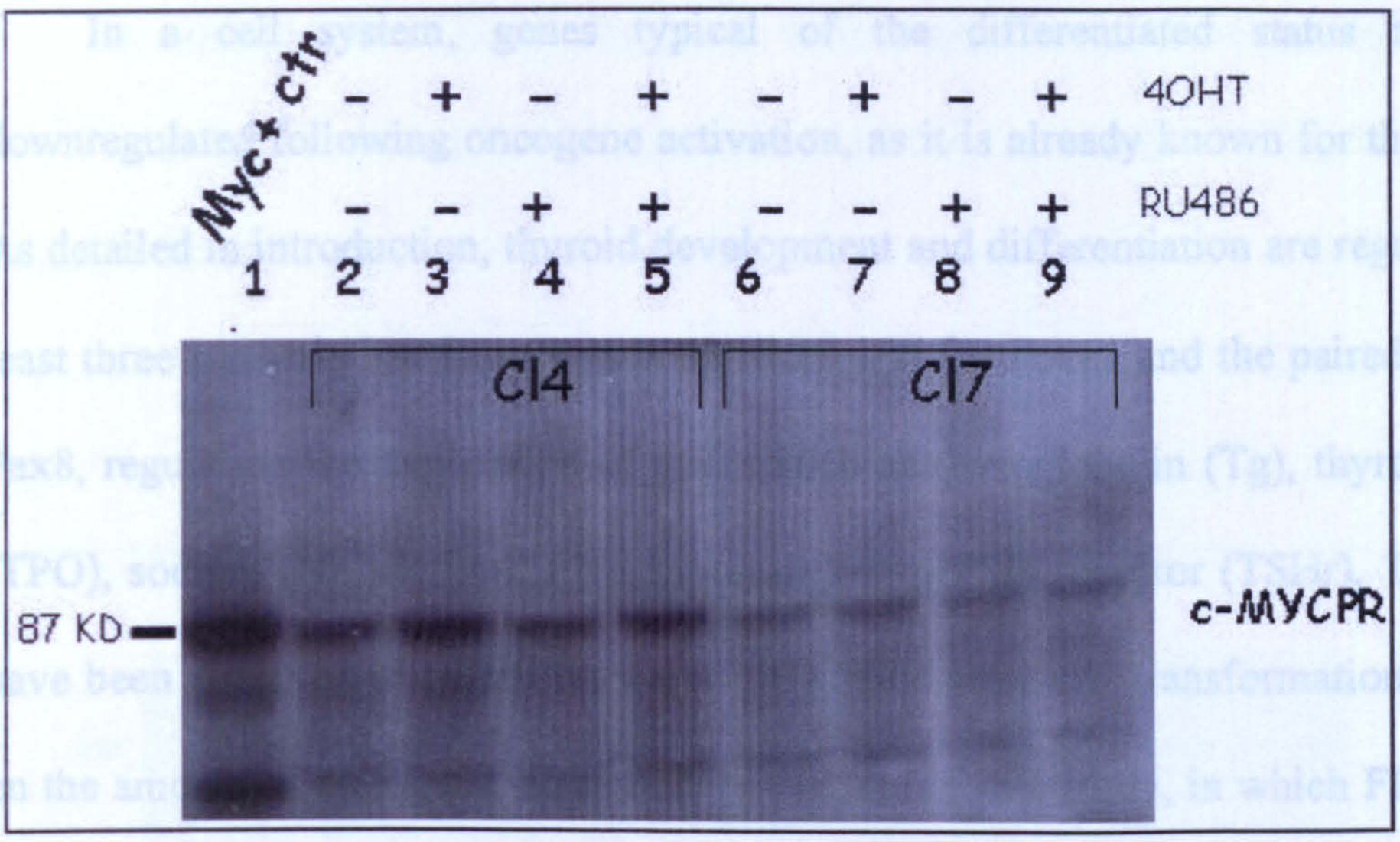

Figure 65. c-Myc-PR expression in FRTL-5 Cl4 and Cl7. Lane 1: positive control for c-Myc-PR expression; lanes 2, 3, 4 and 5: Cl4; lanes 6, 7, 8 and 9: Cl7. Kilo Dalton (KD); 4OH-tamoxifene (4OHT); mifepristone (RU486).

By this initial analysis it was possible to observe the presence and hence the correct expression of the two exogenous oncoproteins.

Since the ER-Ras^{V12} protein results more abundant after 4OH-tamoxifene addition, it is possible to speculate that the protein is stabilized and therefore activated by the drug.

On the contrary, stabilization for the c-Myc-PR protein is not observed following drug addition.

B.2.1 Analysis of genes involved in thyroid differentiation

Differentiated thyroid follicular cells are characterized by the expression of a variety of proteins that are unique for this cell type. The combined function of these genes results in the TSH-regulated synthesis of thyroid hormone.

In a cell system, genes typical of the differentiated status may result downregulated following oncogene activation, as it is already known for thyroid cells. As detailed in introduction, thyroid development and differentiation are regulated by at least three transcription factors such as Nkx2.1/Titf1, Foxe1 and the paired box factor Pax8, regulating the expression of genes such as thyroglobulin (Tg), thyroperoxidase (TPO), sodium (Na^+)/iodine (I^+) symporter (NIS), TSH receptor (TSHr). These genes have been observed to be strongly downregulated after cell transformation depending on the amount of oncogene expressed. In particular, in a study, in which FRTL-5 cells were stably transfected with the pCEFL vector carrying the ER-Ras^{V12} coding sequence, one of the G418 positively selected clones, called clone 11, expressed high levels of ER-Ras^{V12}. After 4OH-tamoxifene treatment, the levels of Tg, Pax8 and Titf1 resulted dramatically reduced in this clone (De Vita et al., 2005). Thus, we asked whether even our clone of interest, Cl4, after activation of oncoproteins and co-operation, was able to induce dedifferentiation in thyroid cells. To address this question, the levels of mRNA encoding the seven thyroid-specific proteins mentioned above, were analyzed by RealTime (RT) PCR in Cl4, Cl7 and Cl11 (positive control) after all the different treatments. Moreover, other two genes such as thyroid oxidase (THOX) and pendrin PD, responsible for the Pendred syndrome (PDS) were also analyzed. THOX catalyzes the oxidative coupling of iodotyrosines to form the iodothyronines as thyroxine (T4) and triiodothyronine (T3) and pendrin encodes a putative apical porter of iodide.

The three clones (Cl4, Cl7 and Cl11) were treated for different times: 0h, 12h, 24h and 48h with 4OH-tamoxifene or RU486 or both or ethanol (negative control), in which the hormones were dissolved. After each treatment, the proteins and the total RNA were extracted from each clone. The RNA was retrotranscribed into cDNA by using random hexamers and oligo dT in a reverse transcription reaction and analyzed.

As expected, in Cl11 all the genes were deregulated following the strong ER-Ras^{V12} expression, except Pendrin that was markedly up-regulated (Fig. 66 violet bars vs purple bars).

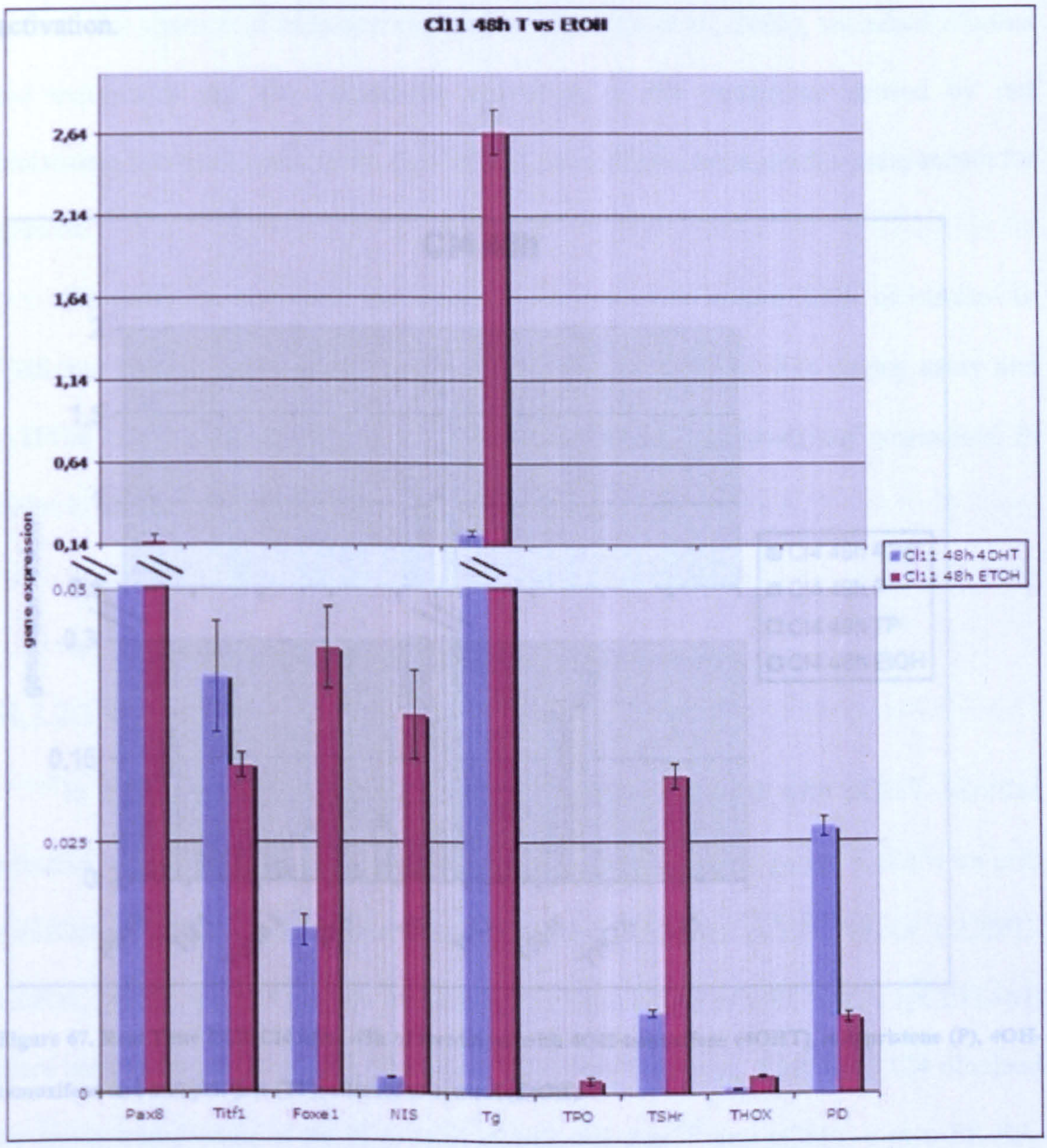

Figure 66. Real Time PCR Cl11 after 48h of treatment with 4OH-tamoxifene (4OHT), ethanol as negative control (EtOH); 48 hours of treatment (48h). For each gene, values reported were the average of triplicates normalized for the expression of α1-tubulin. That high HRas^{V12} levels lead to dedifferentiation has been observed before (De Vita et al., 2005).

Figure 67 shows the expression of thyroid-specific genes in Cl4 treated for 48 hours with the hormones. Thyroid gene expression did not show any change in Cl4 at different treatments with respect to their corresponding controls, even after 48 hours of treatment, except for thyroglobulin (Fig. 67), which reduced to after all treatments with respect to its control and this downregulation could be ascribed to the oncogenic activation.

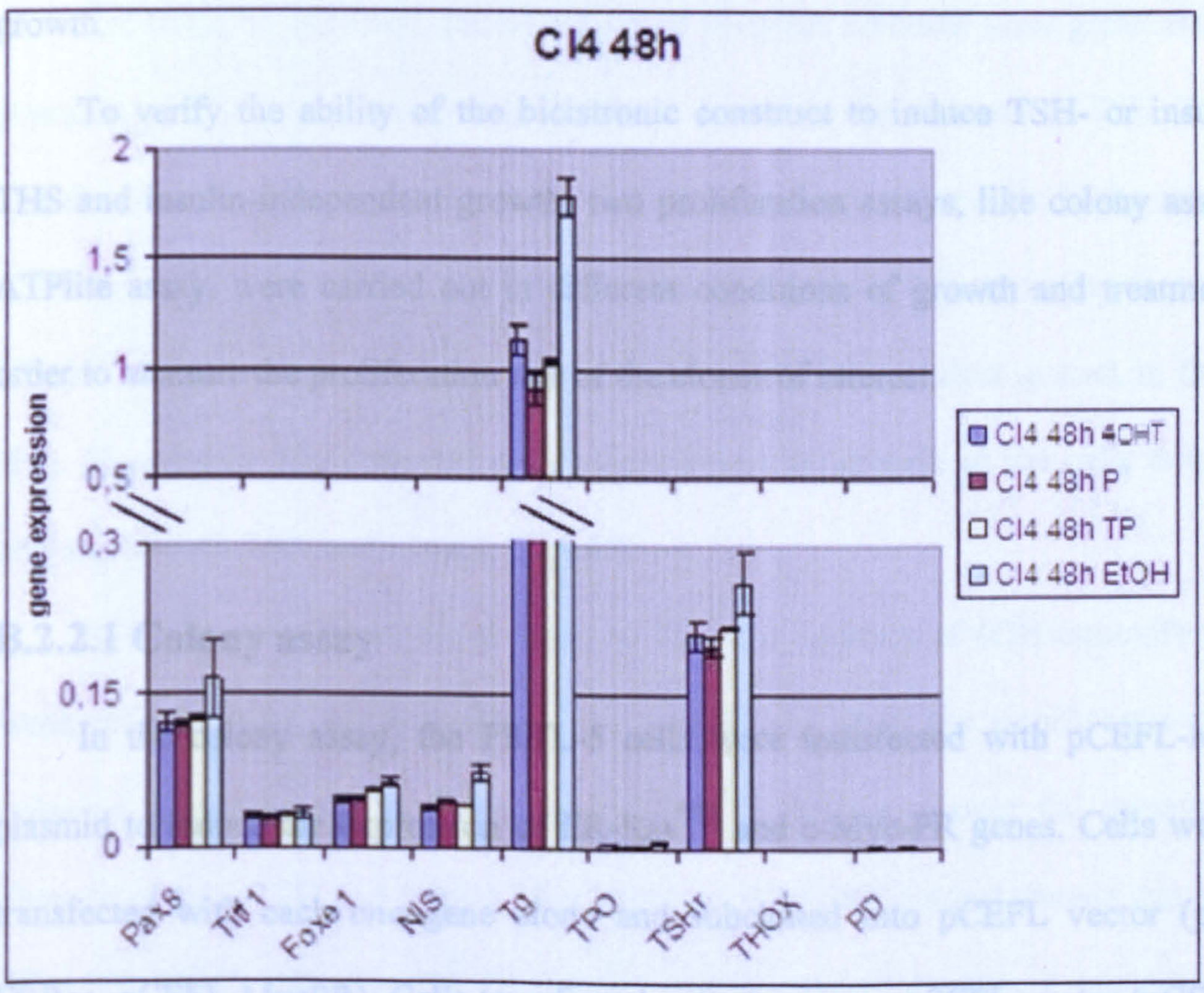

Figure 67. Real Time PCR Cl4 after 48h of treatment with 4OH-tamoxifene (4OHT), mifepristone (P), 4OH-tamoxifene and mifepristone (TP), ethanol as control (EtOH).

B.2.2 Proliferation assays

FRTL-5 cells are known to grow in the F12 coon's medium supplemented with 5% newborn calf serum and six hormones: TSH, insulin, transferrin, somatostatin, the

tripeptide Glycyl-Hystidyl-Lysine and hydrocortisol. One of the features of these cells is that they are strictly dependent on the presence of TSH and insulin, added to the culture medium for proliferation and for the maintenance of the thyroid differentiated phenotype.

Since activated oncogenes are known to deregulate cell growth by its induction even in the absence of hormone stimulation (De Vita et al., 2005), we asked whether the expression and the subsequent activation of the oncogenes carried by our bicistronic construct could make the FRTL-5 cells TSH- and/or insulin-independent for growth.

To verify the ability of the bicistronic construct to induce TSH- or insulin- or THS and insulin-independent growth, two proliferation assays, like colony assay and ATPlite assay, were carried out in different conditions of growth and treatments; in order to measure the proliferation rate of the clones of interest.

B.2.2.1 Colony assay

In the colony assay, the FRTL-5 cells were transfected with pCEFL-MycRas plasmid to induce the expression of ER-Ras^{V12} and c-Myc-PR genes. Cells were also transfected with each oncogene alone and subcloned into pCEFL vector (pCEFL-ERRas, pCEFL-MycPR). Cells transfected with the empty pCEFL vector (pCEFL-wt) were used as negative control. Moreover, Cl11 (De Vita et al., 2005) and Cl4 obtained by stable transfection of FRTL-5 with pCEFL-ER-Ras^{V12} and pCEFL-c-myc-PR-ER-Ras^{V12} respectively were used as positive controls.

After transfection, the cells were subjected to selection for G418 resistance, to allow only the transfected cells to grow and form colonies. Cells were cultered into different media, such as complete medium containing all the six hormones (6H) or

medium lacking either only TSH (5H-TSH) or only insulin (5H-INS) or both TSH and insulin (4H-TSH-INS). Each kind of medium was added with a drug: 4OH-tamoxifene (4OHT) or RU486 separately or both simultaneously and ethanol (the vehicle) as control, to activate the oncogenes.

After two weeks of continuous neomycin selection, cells were checked for their ability to grow. The colonies formed, were fixed, stained with crystal violet and counted.

Figures 68, 69, 70, 71 and 72 show the results of this assay.

For Cl11, as expected, numerous G418 resistant colonies were generated in the presence of TSH, whereas no colonies were scored in the absence of TSH (Fig. 68). The deprivation of insulin alone did not affect the growth of the cells. In the absence of TSH the addition of 4OH-tamoxifene restored the growth demonstrating that the ER-HRas^{V12} chimeric oncogene was able to induce TSH-independent growth in the clone (Fig. 68 and 69). The activated oncogene allowed the growth of the cells even in the absence of both TSH and Insulin (Fig. 69).

In the case of Cl4, in the absence of TSH, the addition of 4OH-tamoxifene had a weak effect: in fact, the drug allows the growth of a small but significant number of colonies. However, the activation of ER-Ras^{V12} did not sustain the growth in the absence of both TSH and insulin. The addition of RU486 did not change this scenario (Figs. 70, 71, 72 and table 12). Obviously, in the complete medium it was not possible to count the number of colonies and the difference, if any, between EtOH or drugs addition to the medium (data not shown).

Finally, a colony assay with cells transiently transfected with the oncogenes, was performed. However no growth was observed with any kind of selecting medium or treatment, except for the complete medium (6H) in which the number of colonies observed was comprised between 30 (for cells transfected with pCEFL-ERRas,

pCEFL-MycPR or pCEFL-MycRas) and 130 (for cells transfected with pCEFL-wt) (table 12). Thus, neither alone or both together the oncogenes were able to induce TSH-independent growth, probably because the quantity of the two proteins in this system was too low to induce the expression of the transformed phenotype such as uncontrolled proliferation in medium lacking hormones.

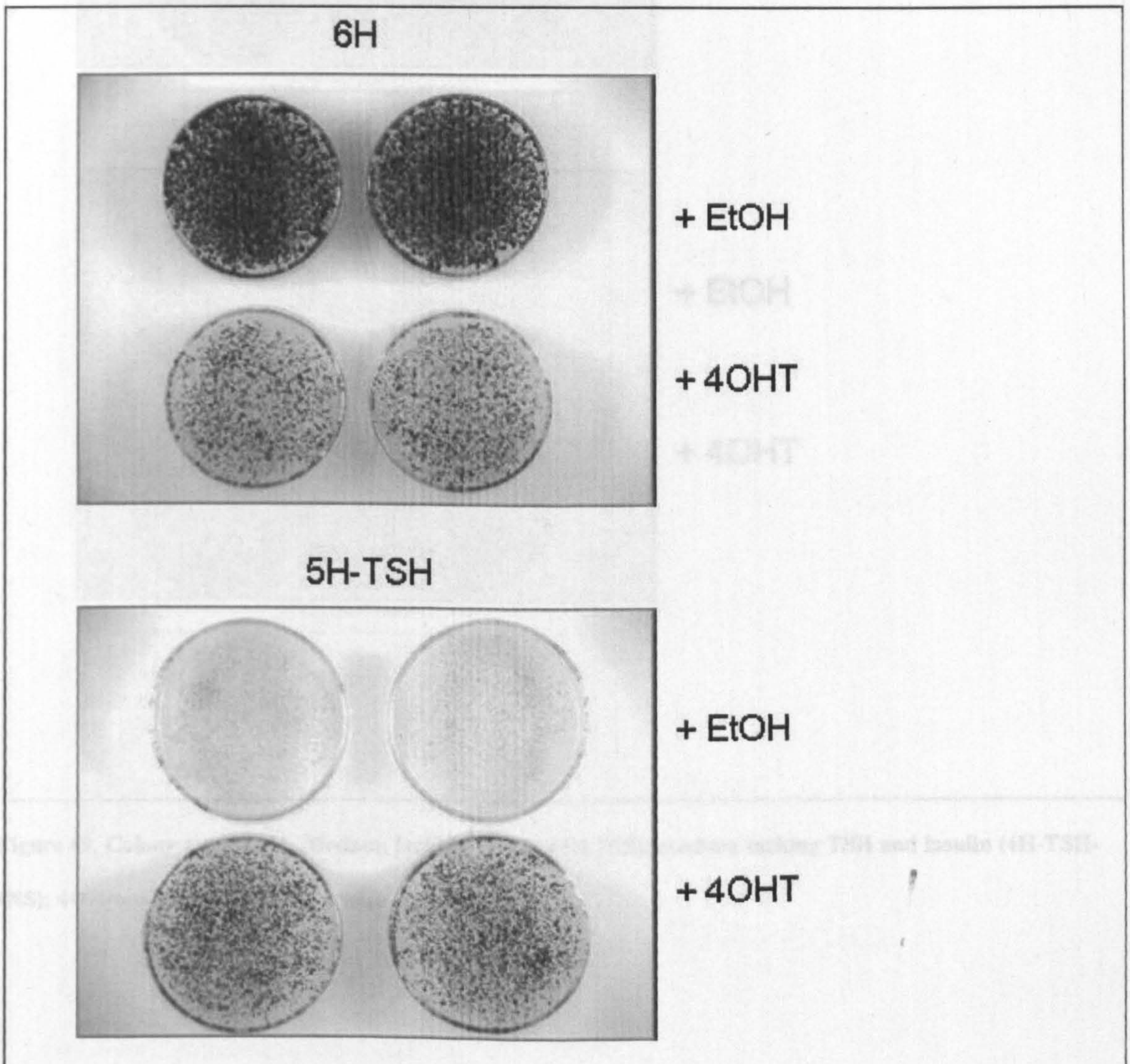

Figure 68. Colony assay Cl11. Complete medium (6H); medium lacking TSH (5H-TSH); 4OH-tamoxifene (4OHT); ethanol (EtOH).

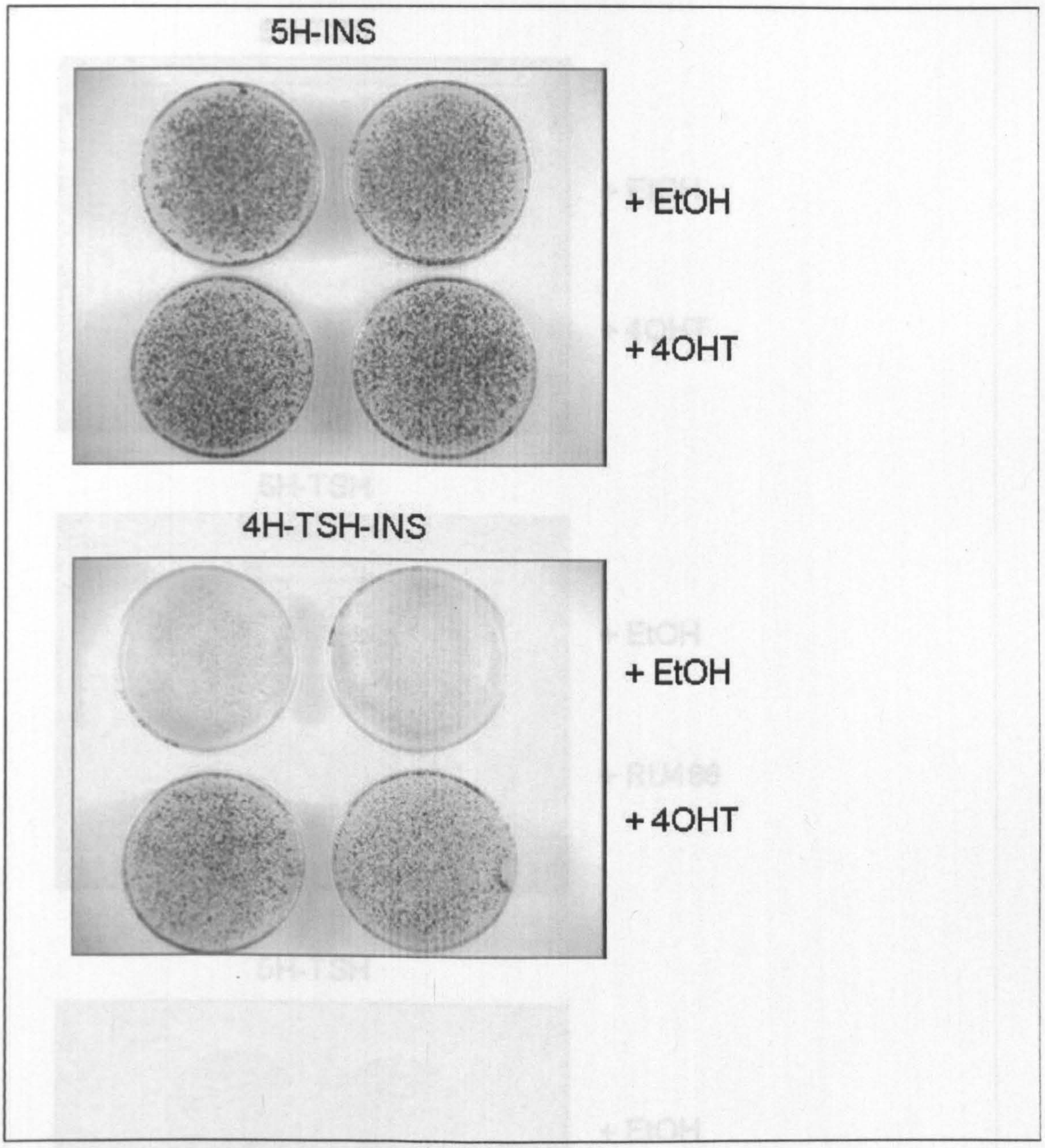

Figure 69. Colony assay Cl11. Medium lacking insulin (5H-INS); medium lacking TSH and insulin (4H-TSH-INS); 4OH-tamoxifene (4OHT); ethanol (EtOH).

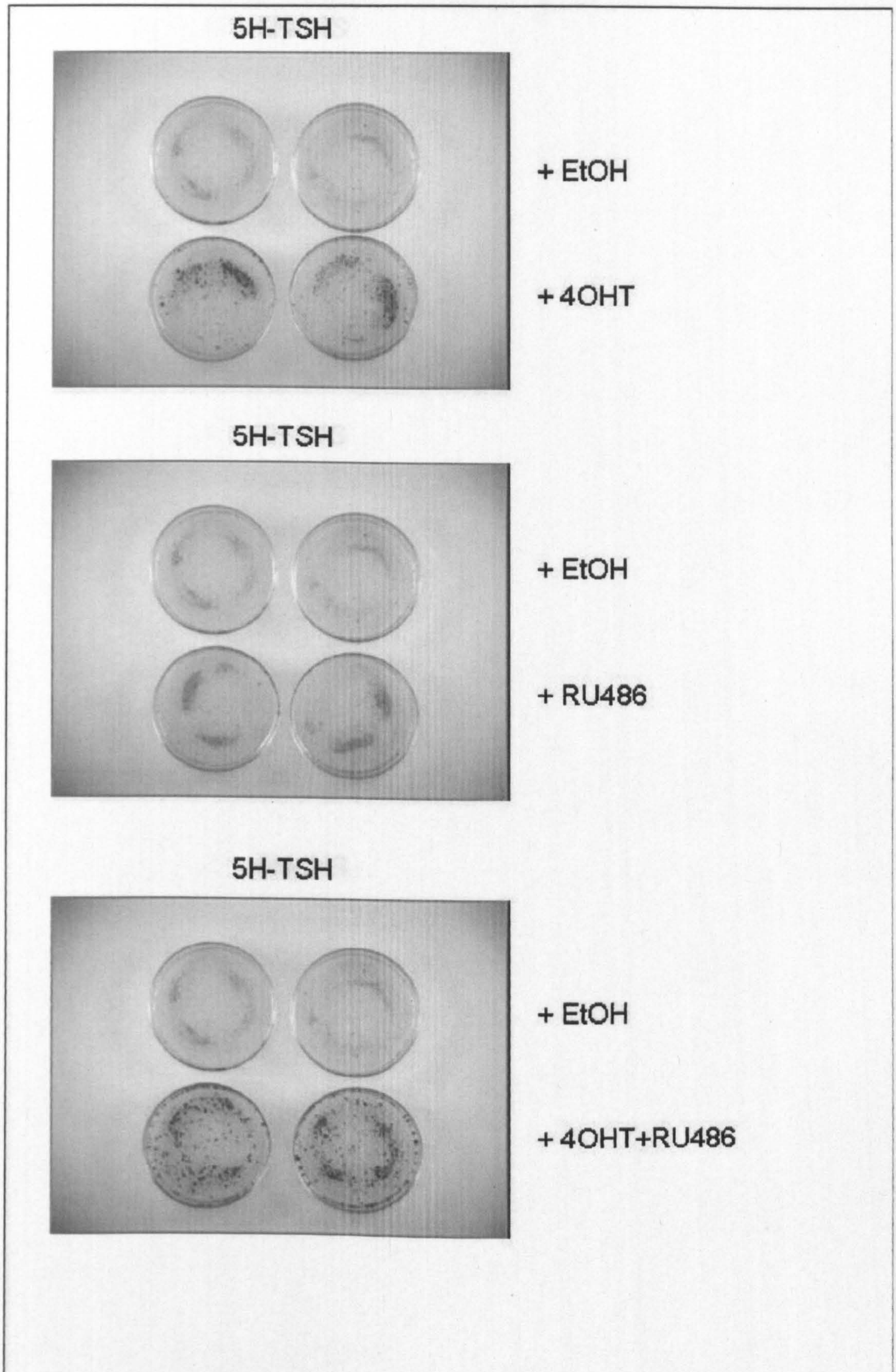

Figure 70. Colony assay Cl4. Medium lacking TSH (5H-TSH); 4OH-tamoxifene (4OHT); mifepristone (RU486); ethanol (EtOH).

5H-INS

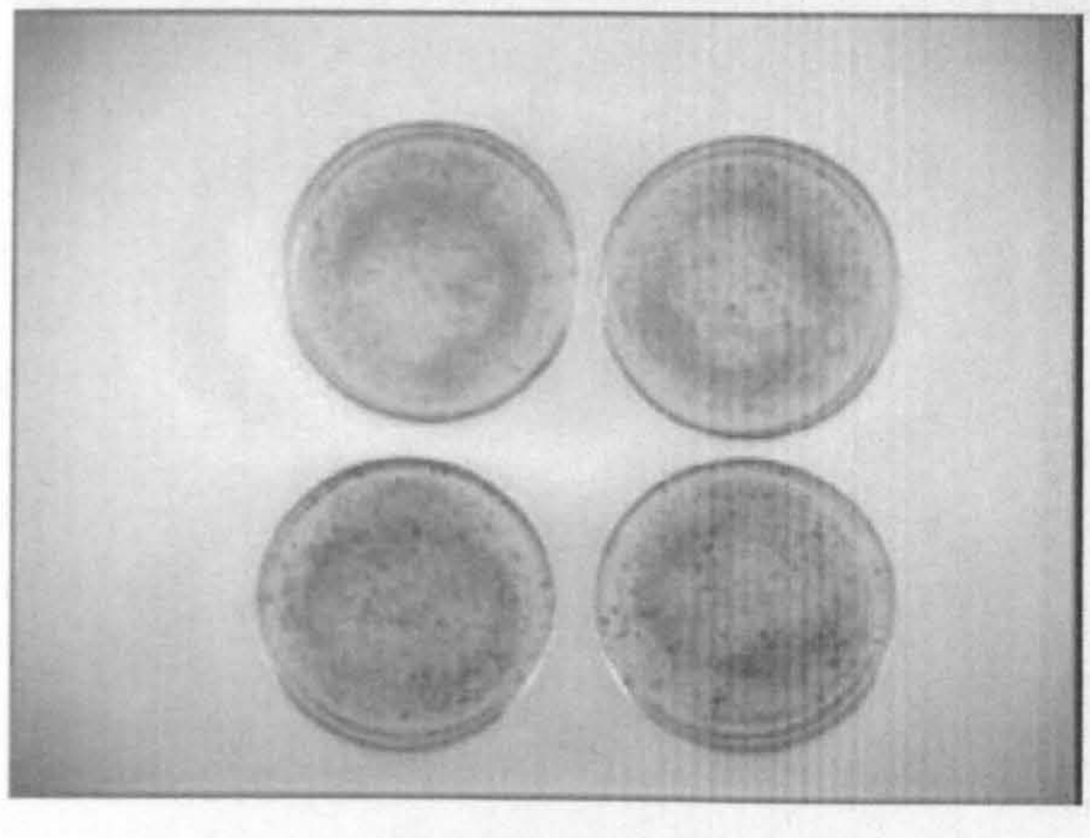

+ EtOH

+ 4OHT

5H-INS

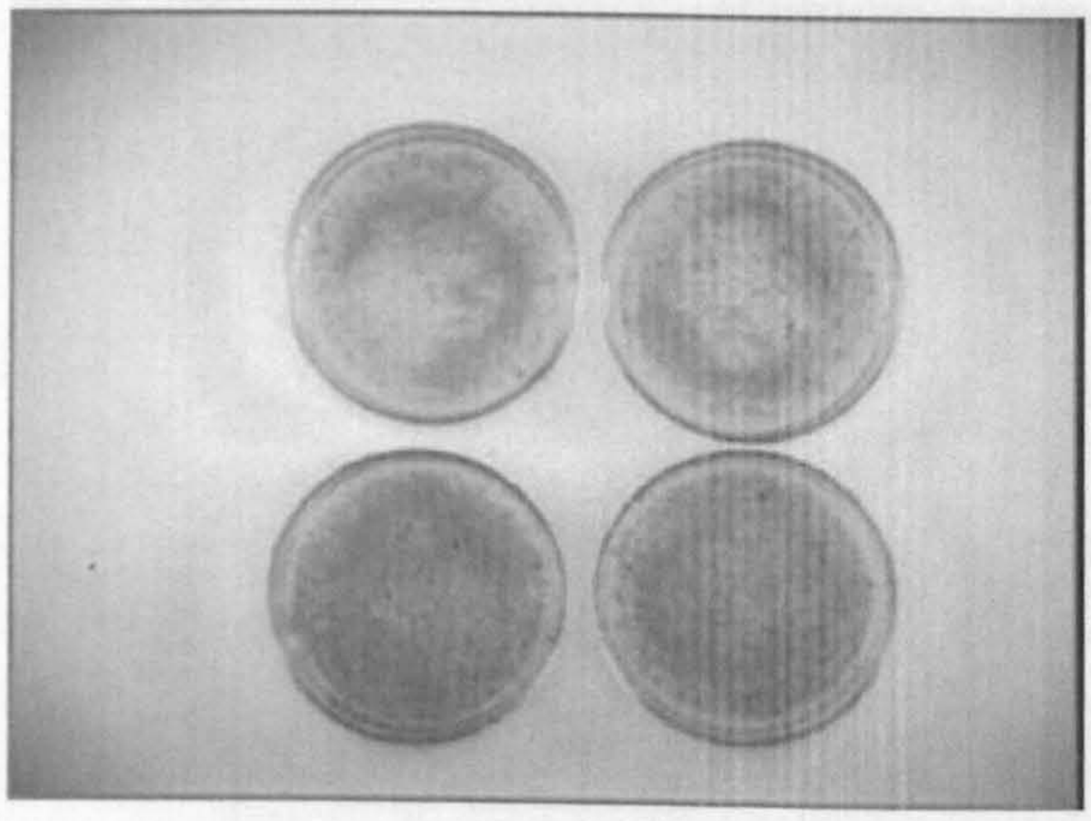

+ EtOH

+ RU486

5H-INS

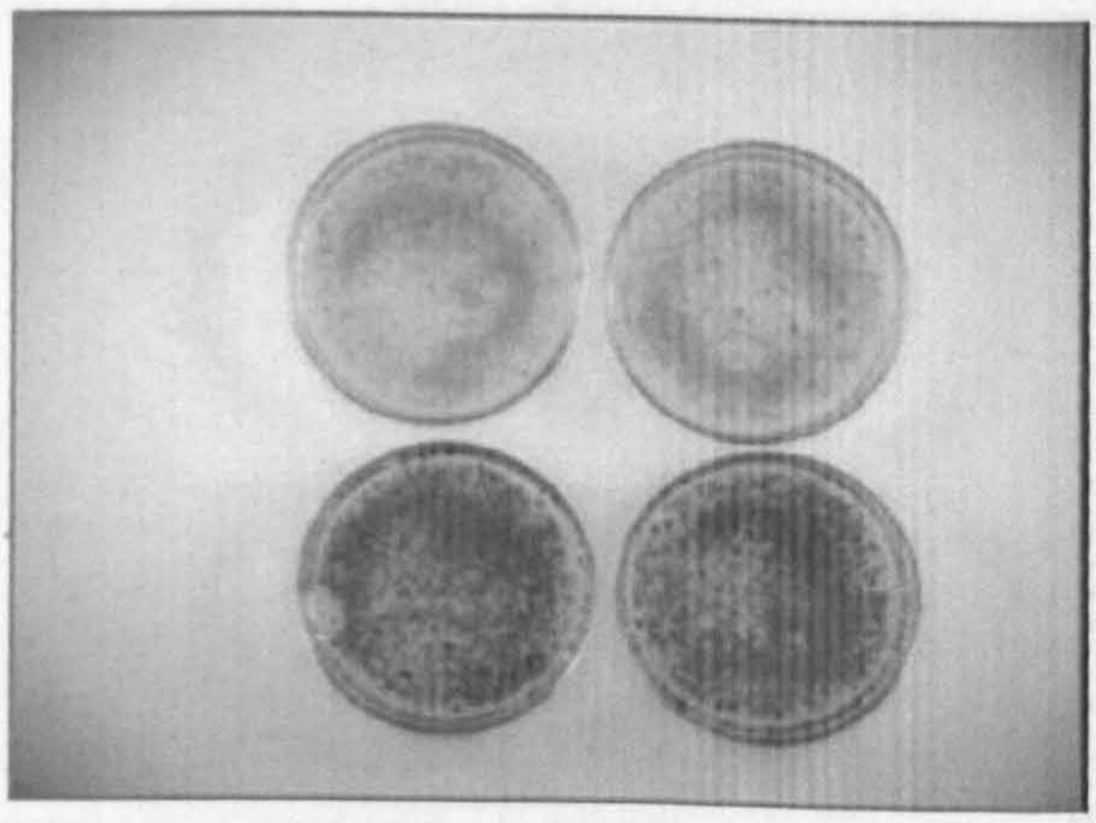

+ EtOH

+ 4OHT+RU486

Figure 71. Colony assay Cl4. Medium lacking insulin (5H-INS); 4OH-tamoxifene (4OHT); mifepristone (RU486); ethanol (EtOH).

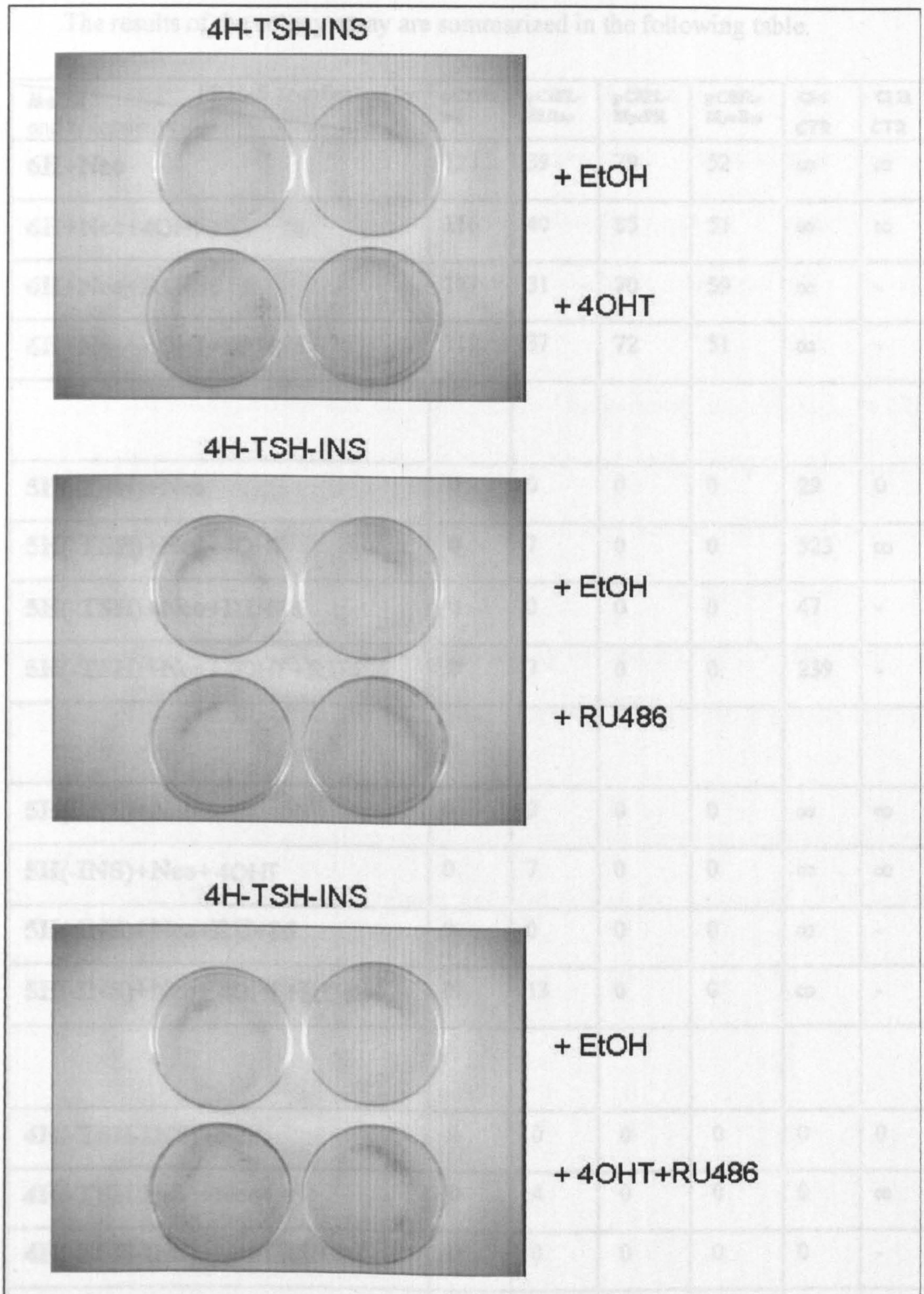

Figure 72. Colony assay Cl4. Medium lacking TSH and insulin (5H-TSH-INS); 4OH-tamoxifene (4OHT); mifepristone (RU486); ethanol (EtOH).

The results of the colony assay are summarized in the following table.

Media and treatments \ FRTL-5 tranfected by:	pCEFL wt	pCEFL-ERRas	pCEFL-MycPR	pCEFL-MycRas	Cl4 CTR	Cl11 CTR
6H+Neo	123	39	79	52	∞	∞
6H+Neo+4OHT	116	40	85	51	∞	∞
6H+Neo+RU486	117	31	70	59	∞	-
6H+Neo+4OHT+RU486	119	37	72	51	∞	-
5H(-TSH)+Neo	0	0	0	0	29	0
5H(-TSH)+Neo+4OHT	0	7	0	0	523	∞
5H(-TSH)+Neo+RU486	0	0	0	0	47	-
5H(-TSH)+Neo+4OHT+RU486	0	7	0	0	239	-
5H(-INS)+Neo	0	0	0	0	∞	∞
5H(-INS)+Neo+4OHT	0	7	0	0	∞	∞
5H(-INS)+Neo+RU486	0	0	0	0	∞	-
5H(-INS)+Neo+4OHT+RU486	0	13	0	0	∞	-
4H(-TSH-INS)+Neo	0	0	0	0	0	0
4H(-TSH-INS)+Neo+	0	4	0	0	0	∞
4H(-TSH-INS)+Neo+RU486	0	0	0	0	0	-
4H(-TSH-INS)+Neo+4OHT+RU486	0	4	0	0	0	-

Table 12. Colony assay: number of colonies after two weeks of selection growth. Cl4 and Cl11 were used as positive controls. Medium lacking TSH (5H-TSH); medium lacking insulin (5H-INS); medium lacking TSH and insulin (5H-TSH-INS); 4OH-tamoxifene (4OHT); mifepristone (RU486); ethanol (EtOH); G418 selection (NEO); infinite (∞); not done (-).

B.2.2.2 ATPlite assay

The results of colony assay were confirmed by ATPlite assay, a luminescence assay for the quantitative evaluation of proliferation and cytotoxicity of cultured mammalian cells. ATP is a marker for cell viability since it is present in all metabolically active cells and its concentration declines when the cells undergo necrosis or apoptosis.

This assay was carried out on three clones: the parental line FRTL-5, in Cl11 (ER-RAS FRTL-5) (De Vita et al., 2005) and in Cl4 (MYC-RAS-FRTL-5). The cells were grown in complete medium (6H) and medium deprived of TSH (5H) (each one supplemented with either 4OHT or RU486 or both; ethanol as negative control). The cells were maintained in culture for 6 days. Every two days (T2gg, T4gg, T6gg,) an aliquot of cells was harvested and ATP was measured and expressed as fold increase relative to time 0 (T0).

The wild type FRTL-5 cells were able to grow in the complete medium but not in the medium lacking the TSH hormone; the addition of the drugs did not interfere appreciably with the growth of the cells (Fig. 73).

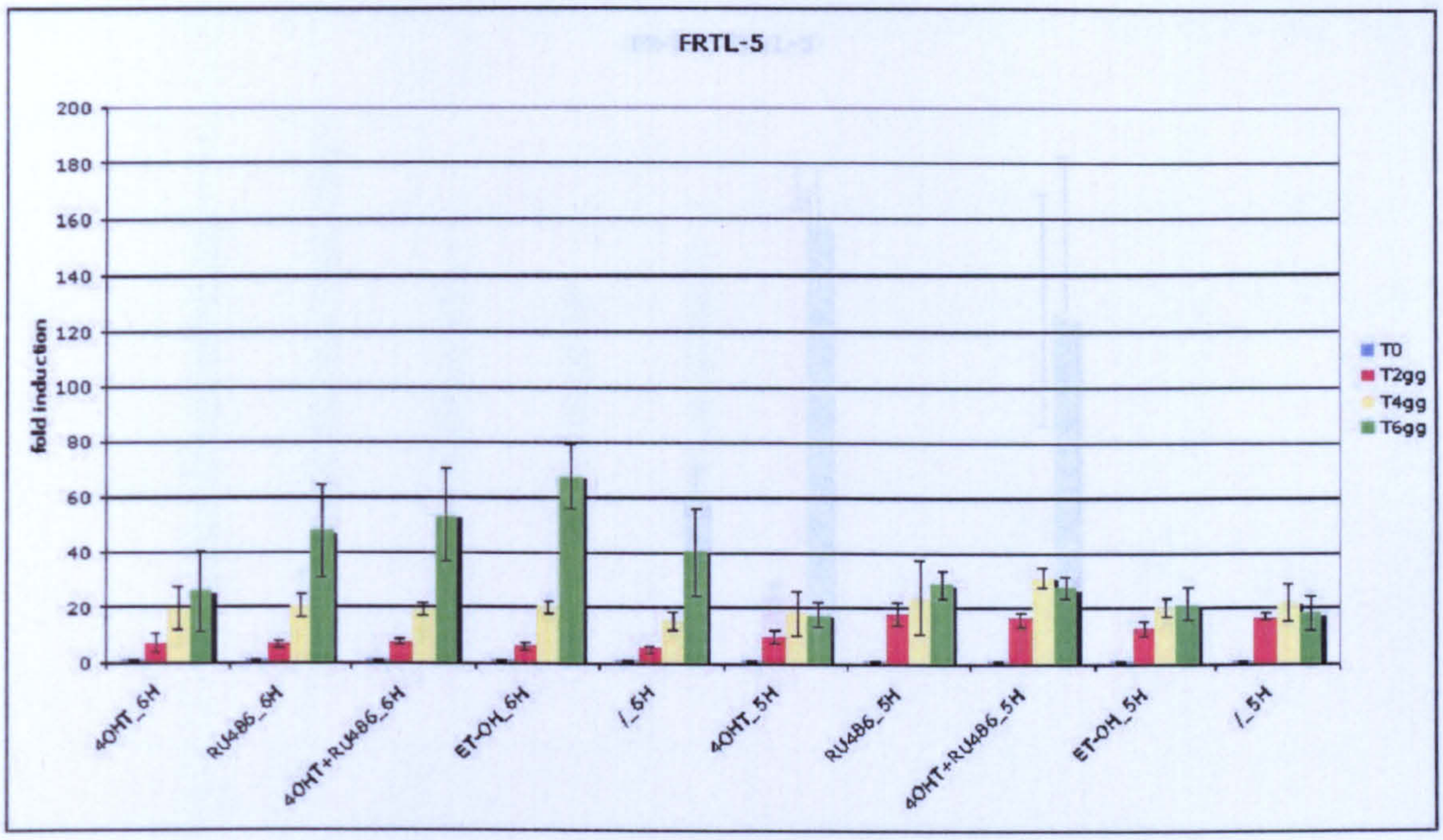

Figure 73. ATPlite Assay on FRTL-5 cells. Complete medium (6H); medium lacking TSH (5H); 4OH-tamoxifene (4OHT); mifepristone (RU486); ethanol (EtOH); no drugs (/); time 0 (T0); time 2 days (T2gg); time 4 days (T4gg); time 6 days (T6gg).

By the same ATP analysis on the stable Cl11, as previously observed (De Vita et al., 2005), the activation of ER-Ras^{V12} with 4OH-tamoxifene in 5H medium was followed by an increased proliferation rate of the clone after four days (Fig. 74).

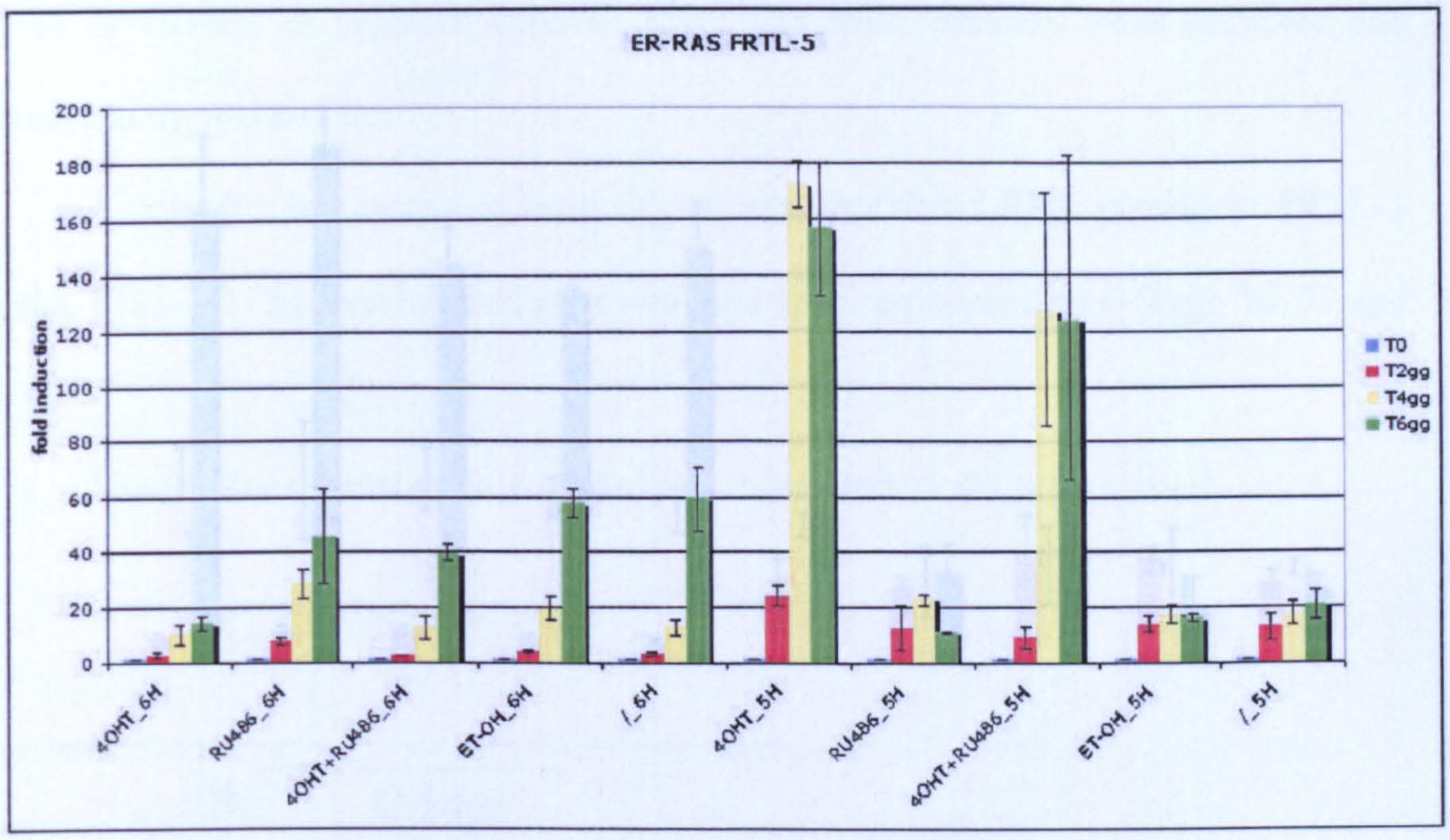

Figure 74. ATPlite Assay on Cl11 (ER-RAS FRTL-5). Complete medium (6H); medium lacking TSH (5H); 4OH-tamoxifene (4OHT); mifepristone (RU486); ethanol (EtOH); no drugs (/). time 0 (T0); time 2 days (T2gg); time 4 days (T4gg); time 6 days (T6gg).

The proliferation ability of Cl4 grown in both media 6H and 5H can be observed in figure 74. In the medium lacking the TSH hormone, its behaviour was more similar to that of wild type FRTL-5 cells than that observed for Cl11 (compare Figs. 73, 74 and 75) in the same culture conditions. According to the colony assay results, Cl4 grew normally for six days in 6H medium. After two days of culture in 5H medium its proliferation was strongly reduced and showed only a slight induction (at time four day) when treated with 4OH-tamoxifene alone or with 4OH-tamoxifene and RU486 respectively to activate the oncogenes (Fig. 75).

Moreover, it is noteworthy that the basal proliferation activity in 6H medium of this clone was higher than that of FRTL-5 or Cl11 starting from the fourth day of culture. In fact, at time 4 days the fold inductions were about 60 and 20 for Cl4 and FRTL-5 or Cl11 respectively; after 6 days the fold induction observed reached 140 in Cl4, while it was only 50 in FRTL-5 or Cl11 (compare Figs. 73, 74 and 75).

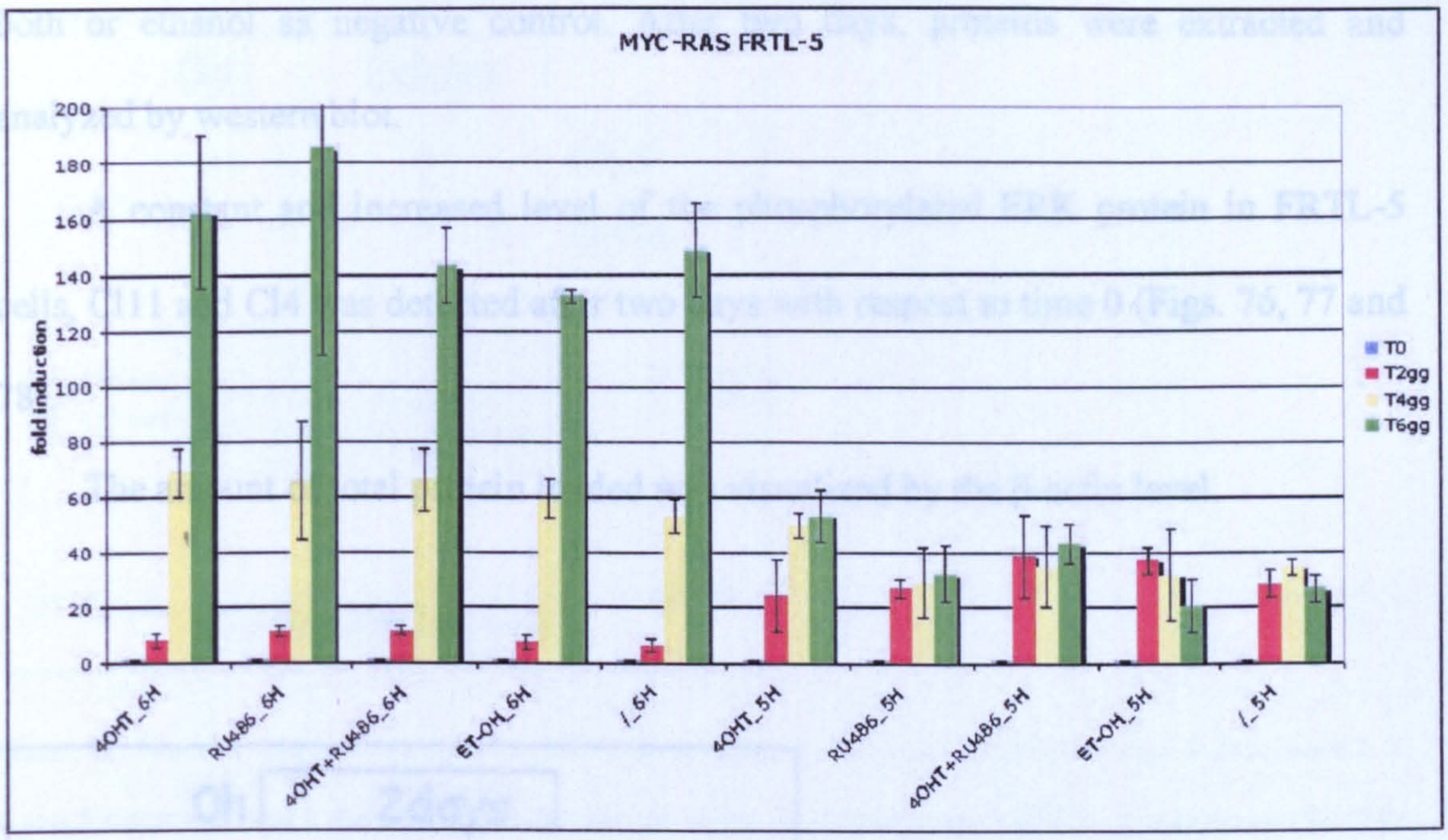

Figure 75. ATPlite Assay on Cl4 (MYC-RAS FRTL-5). Complete medium (6H); medium lacking TSH (5H); 4OH-tamoxifene (4OHT); mifepristone (RU486); ethanol (EtOH); no drugs (/). time 0 (T0); time 2 days (T2gg); time 4 days (T4gg); time 6 days (T6gg). These data were obtained by the average of triplicates and were normalized for the proliferation rate at time 0.

B.2.3 The ERK protein phosphorylation

As described in the chapter "Introduction", among the many pathways triggered by HRas, the most deeply studied is the MAP-kinase cascade in which the first effector is the protein serine/threonine kinase Raf (a MAP-kinase). Through other MAP-kinase, or MEK, that specifically phosphorylates threonine and tyrosine residues, the signal reaches the last MAP-kinase of the cascade, the ERK protein, before activating transcription factors. Thus, the phosphorylation of ERK can be studied as a tool to confirm if ER-Ras^{V12} is active.

In order to verify the activation by phosphorylation of the ERK protein in our system, parental FRTL-5 cell line, Cl11 (ER-RAS FRTL-5) and Cl4 (MYC-RAS-FRTL-5) were cultured in 6H medium supplemented with either 4OHT or RU486 or

both or ethanol as negative control. After two days, proteins were extracted and analyzed by western blot.

A constant and increased level of the phosphorylated ERK protein in FRTL-5 cells, Cl11 and Cl4 was detected after two days with respect to time 0 (Figs. 76, 77 and 78).

The amount of total protein loaded was visualized by the β-actin level.

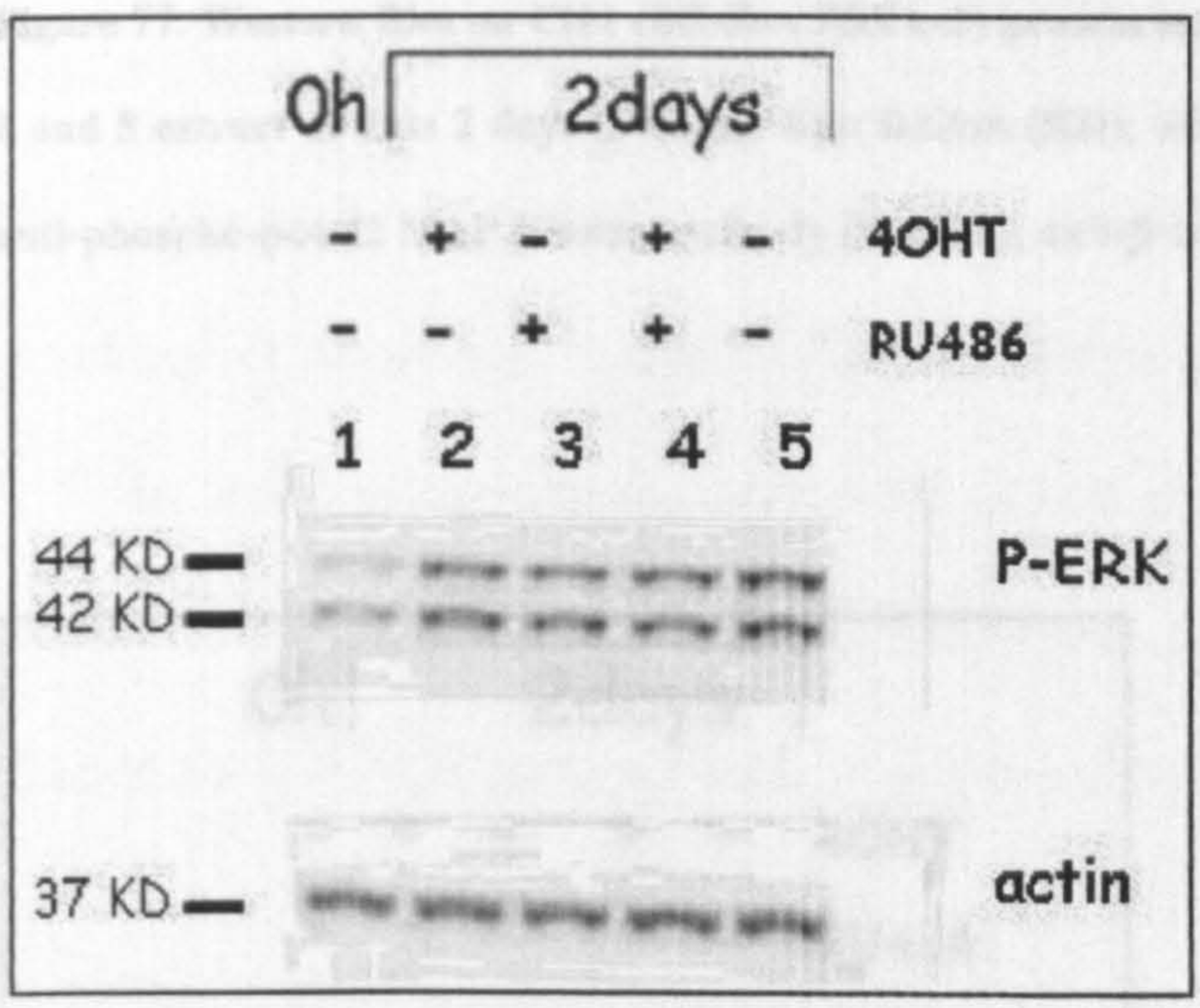

Figure 76. Western Blot on FRTL-5 protein extract. Lane 1: extract at time 0 (0h); lanes 2, 3, 4 and 5 extract at time 2 days (2 days); Kilo Dalton (KD); 4OH-tamoxifene (4OHT); mifepristone (RU486); anti-phospho-p44/42 MAP Kinase antibody (P-ERK); anti-β-actin antibody (actin).

Despite the clone (Cl11 or Cl4) or the treatments (4OHT or RU486 or both) the same trend was reflected for the ERK protein phosphorylation as observed in the parental cell line (Figs. 77 and 78).

From these results, it could be deduced that this phosphorylation course was not due to the real ERK induction, following ER-Ras^{V12} activation, but due to its basal phosphorylation in two days of culture even into the parental cell line (Fig. 76).

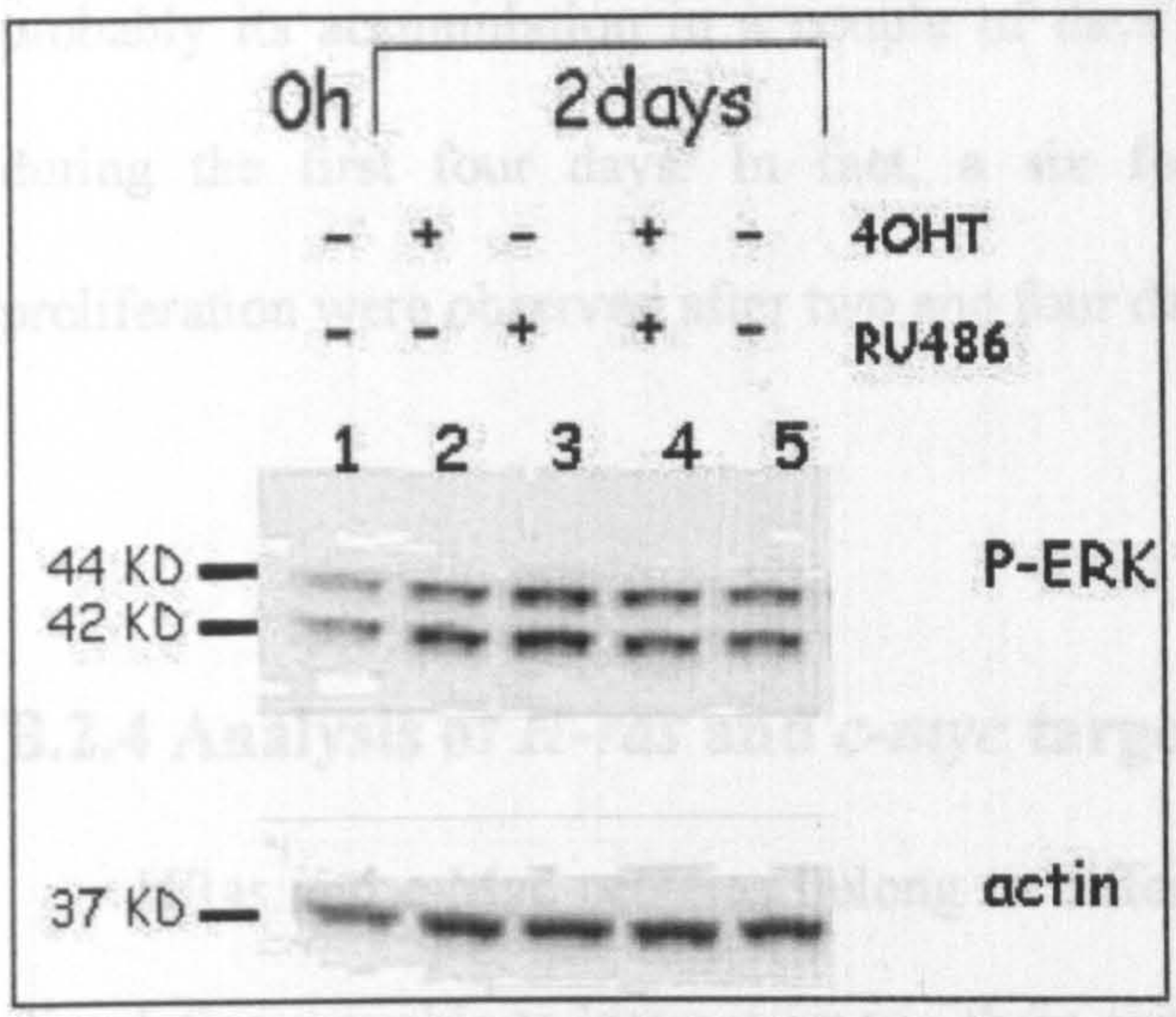

Figure 77. Western Blot on Cl11 (ER-Ras FRTL-5) protein extract. Lane 1: extract at time 0 (0h); lanes 2, 3, 4 and 5 extract at time 2 days (2 days); Kilo Dalton (KD); 4OH-tamoxifene (4OHT); mifepristone (RU486); anti-phospho-p44/42 MAP Kinase antibody (P-ERK); anti-β-actin antibody (actin).

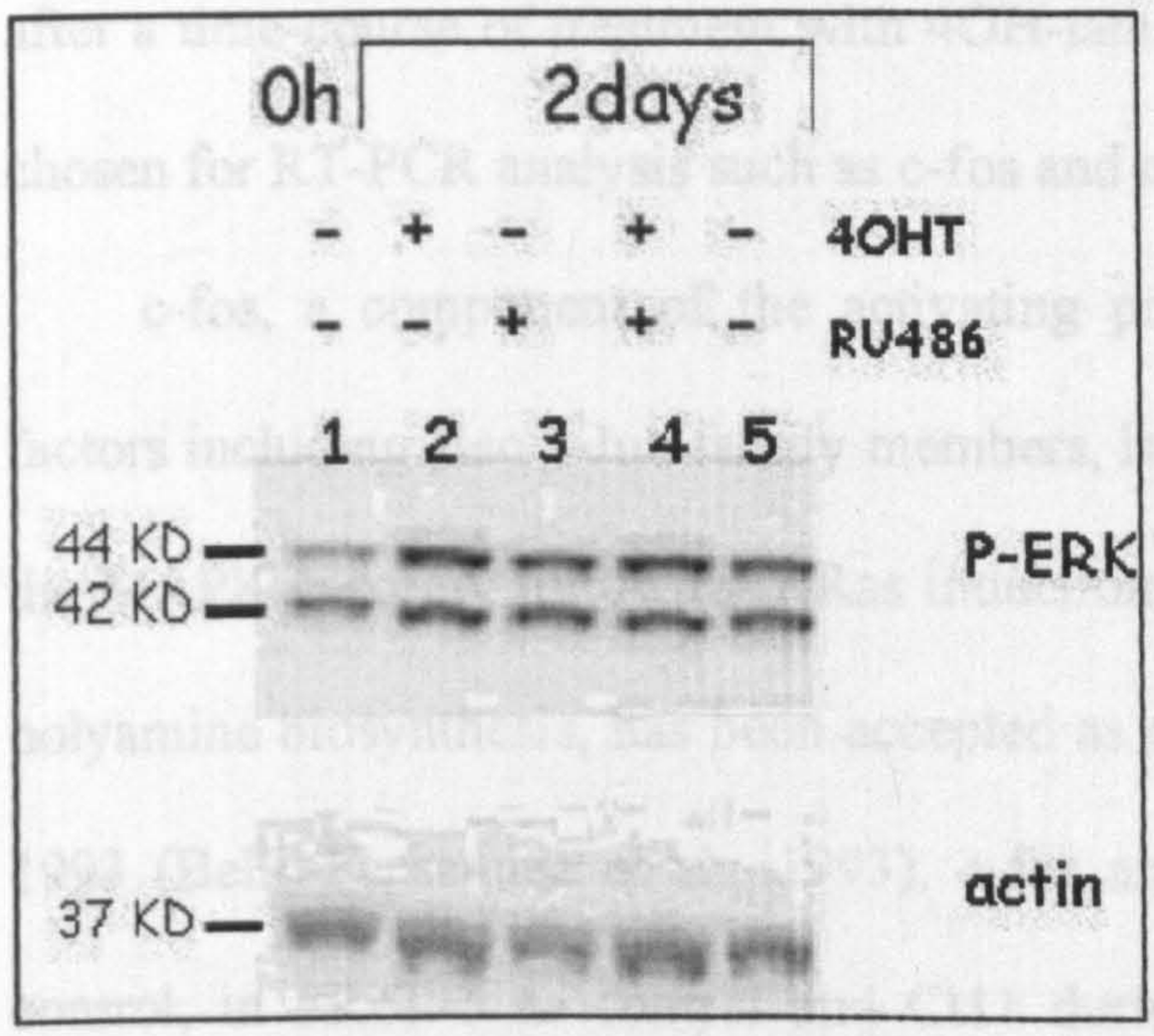

Figure 78. Western Blot on Cl4 (MYC-RAS FRTL-5) protein extract. Lane 1: extract at time 0 (0h); lanes 2, 3, 4 and 5 extract at time 2 days (2 days); Kilo Dalton (KD); 4OH-tamoxifene (4OHT); mifepristone (RU486); anti-phospho-p44/42 MAP Kinase antibody (P-ERK); anti-β-actin antibody (actin).

On comparison of the ERK phosphorylation blottings with the ATPlite assay graphs, it was possible to speculate that the increase of the ERK phosphorylation and

probably its accumulation in a couple of days could be useful for cell proliferation during the first four days. In fact, a six fold and a twelve fold inductions of proliferation were observed after two and four days of culture respectively.

B.2.4 Analysis of *H-ras* and *c-myc* target genes

HRas and c-Myc proteins belong to different networks of proteins, which upon stimulation, are able to interact among them and to determine a long-term effect at the end of the cascade by activation of many effectors. To check if also in our cells these two proteins were active after addition of drugs, it was necessary to verify the induction of proteins involved in their pathways.

In order to analyze the behaviour of the genes downstream of HRas and c-Myc, after a time-course of treatment with 4OH-tamoxifene and/or RU486, two genes were chosen for RT-PCR analysis such as c-fos and ornithine decarboxylase (ODC).

c-fos, a component of the activating protein-1 (AP-1) family of transcription factors including also c-Jun family members, is the last gene up-regulated at the end of the MAPK cascade, following HRas induction; while ODC, a rate-limiting enzyme of polyamine biosynthesis, has been accepted as c-Myc target gene in the literature since 1993 (Bello-Fernandez et al., 1993). c-fos and ODC were analyzed in Cl4 and, as control, in FRTL-5 as control and Cl11 during a time course treatment with 4OH-tamoxifene and/or RU486.

In parental cell line both genes, c-fos and ODC, showed the same trend with a gene expression increasing at 24h and going back to basal levels after 48h (Figs. 79 and 80).

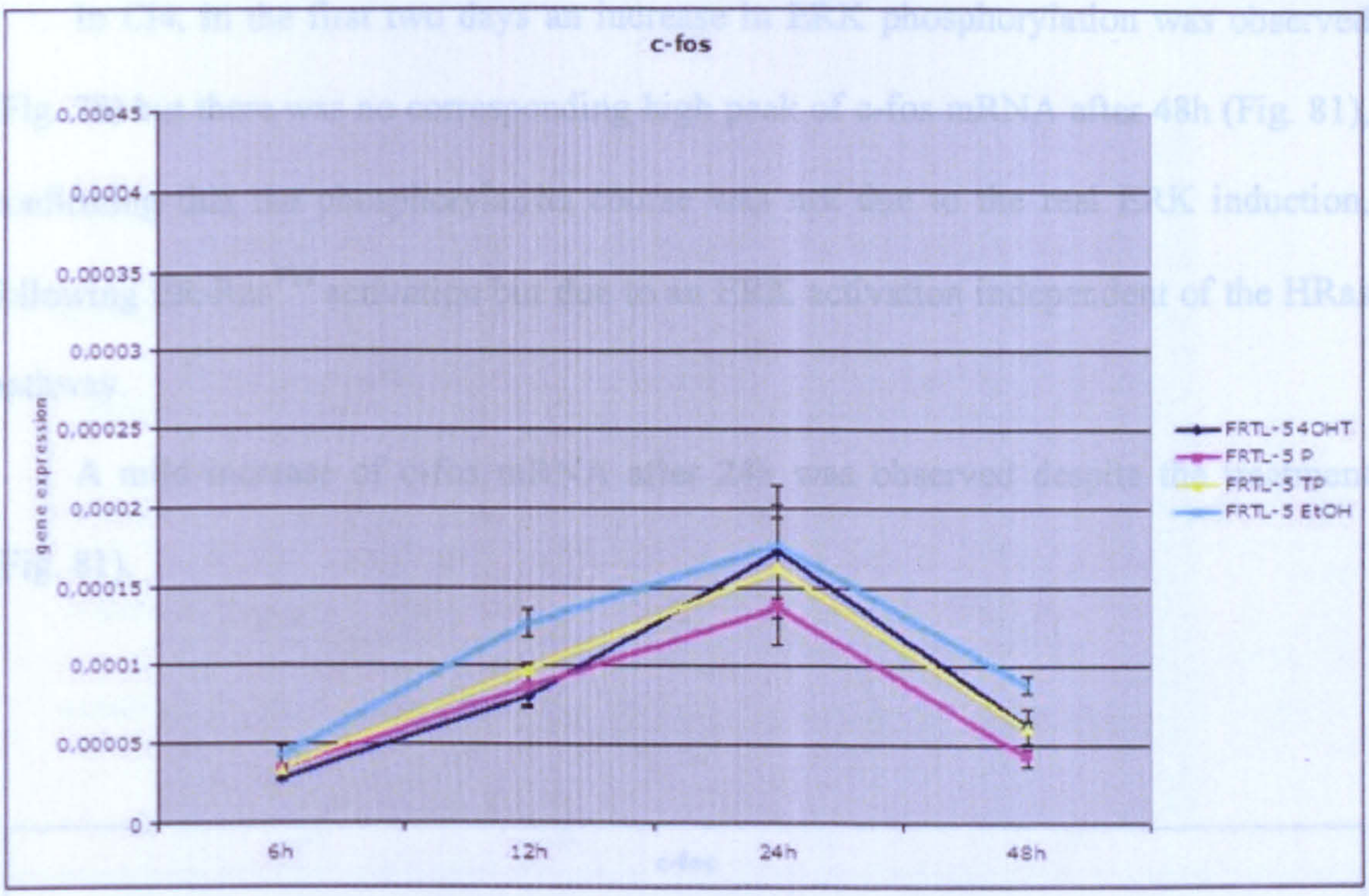

Figure 79. FRTL-5 c-fos expression. 4OH-tamoxifene (4OHT); mifepristone (P); 4OH-tamoxifene and mifepristone (TP); ethanol (EtOH).

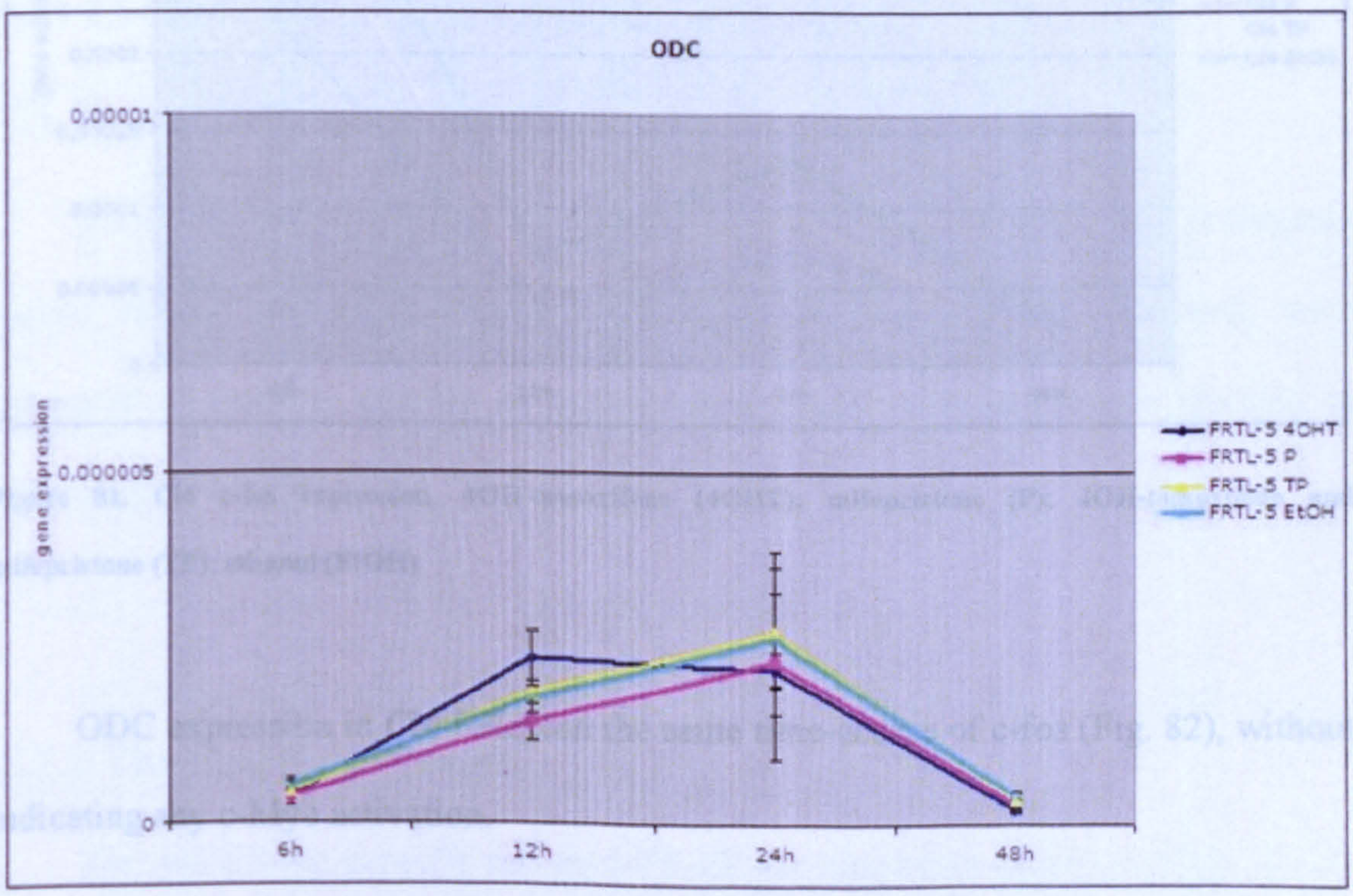

Figure 80. FRTL-5 ODC expression. 4OH-tamoxifene (4OHT); mifepristone (P); 4OH-tamoxifene and mifepristone (TP); ethanol (EtOH).

In Cl4, in the first two days an increase in ERK phosphorylation was observed (Fig. 78) but there was no corresponding high peak of c-fos mRNA after 48h (Fig. 81), confirming that the phosphorylation course was not due to the real ERK induction, following ER-Ras^{V12} activation but due to an ERK activation independent of the HRas pathway.

A mild increase of c-fos mRNA after 24h was observed despite the treatment (Fig. 81).

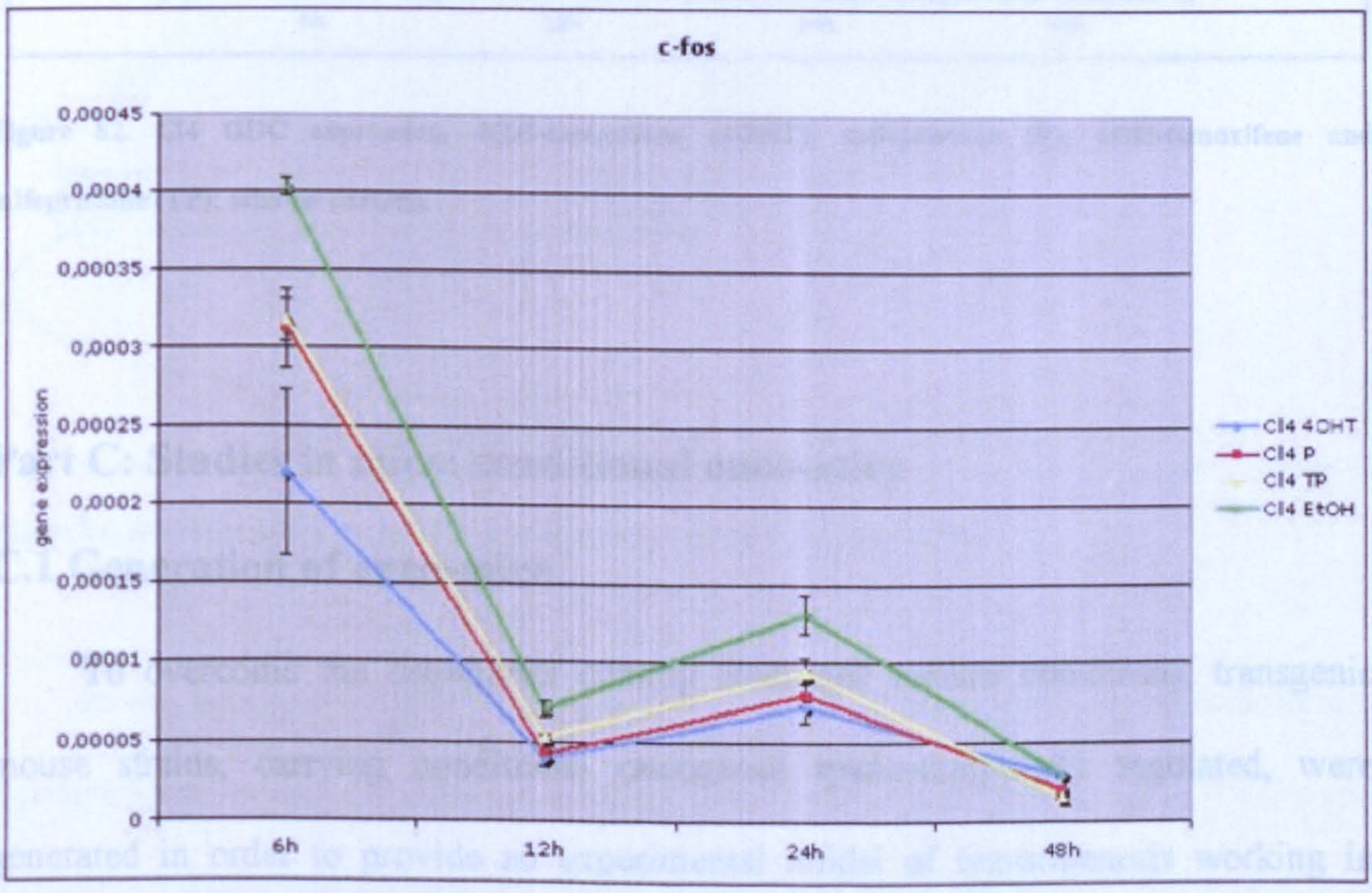

Figure 81. Cl4 c-fos expression. 4OH-tamoxifene (4OHT); mifepristone (P); 4OH-tamoxifene and mifepristone (TP); ethanol (EtOH).

ODC expression in Cl4 followed the same time-course of c-fos (Fig. 82), without indicating any c-Myc activation.

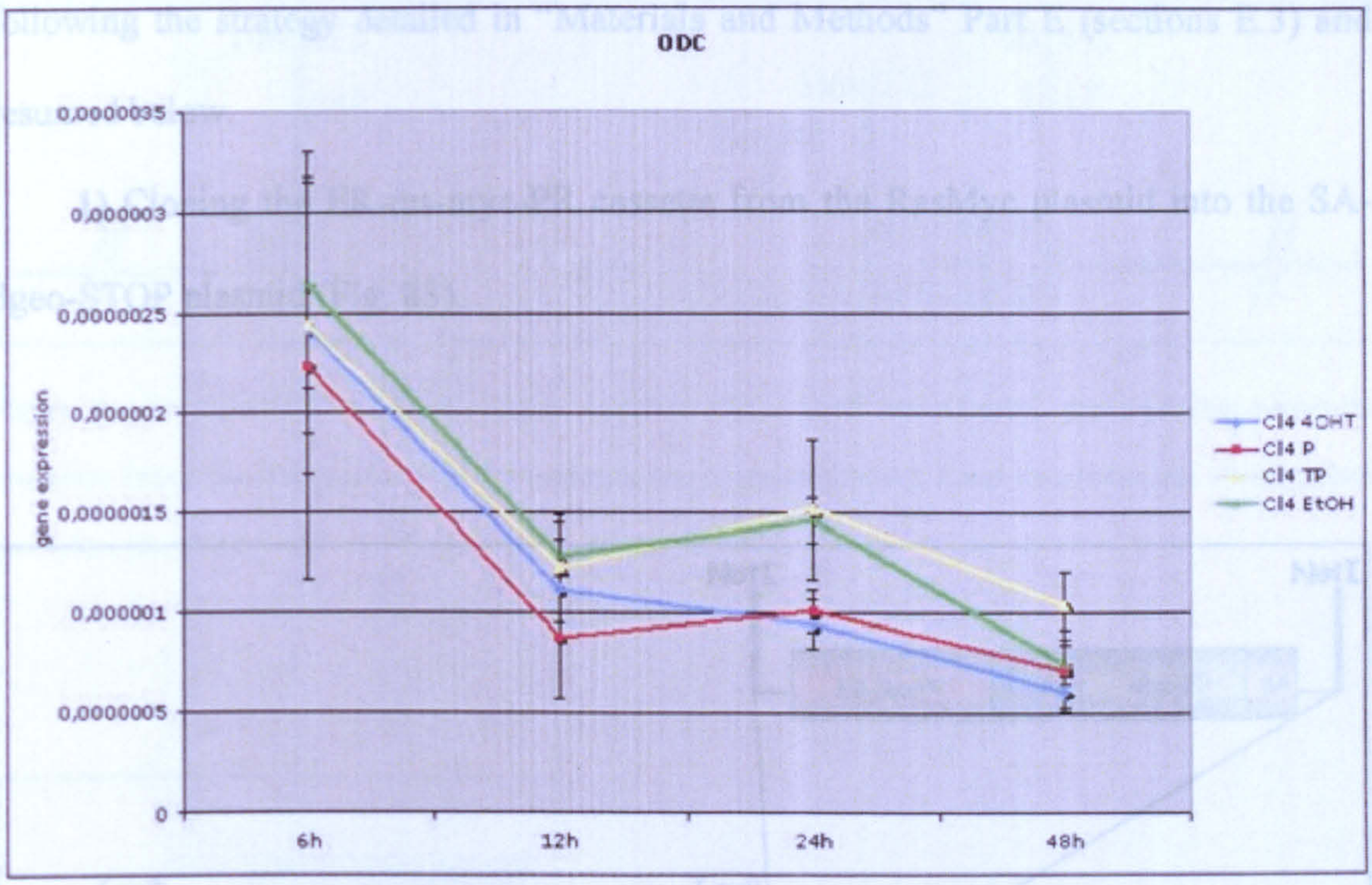

Figure 82. Cl4 ODC expression. 4OH-tamoxifene (4OHT); mifepristone (P); 4OH-tamoxifene and mifepristone (TP); ethanol (EtOH).

Part C: Studies in mice: conditional onco-mice

C.1 Generation of onco-mice

To overcome the drawbacks coming from cell culture conditions, transgenic mouse strains, carrying conditional oncogenes spatio-temporally regulated, were generated in order to provide an experimental model of tumorigenesis working in physiological conditions.

C.1.1 The targeting vectors

The two ER-ras-myc-PR and myc-PR-ER-ras bicistronic cassettes (Figs. 39 and 50) already described in "Materials and Methods" Part E (sections E.1 and E.2) and in "Results" Part A (sections A.1 and A.2), were subcloned into the targeting vector

following the strategy detailed in "Materials and Methods" Part E (sections E.3) and resumed below.

1) Cloning the ER-ras-myc-PR cassette from the RasMyc plasmid into the SA-βgeo-STOP plasmid (Fig. 83).

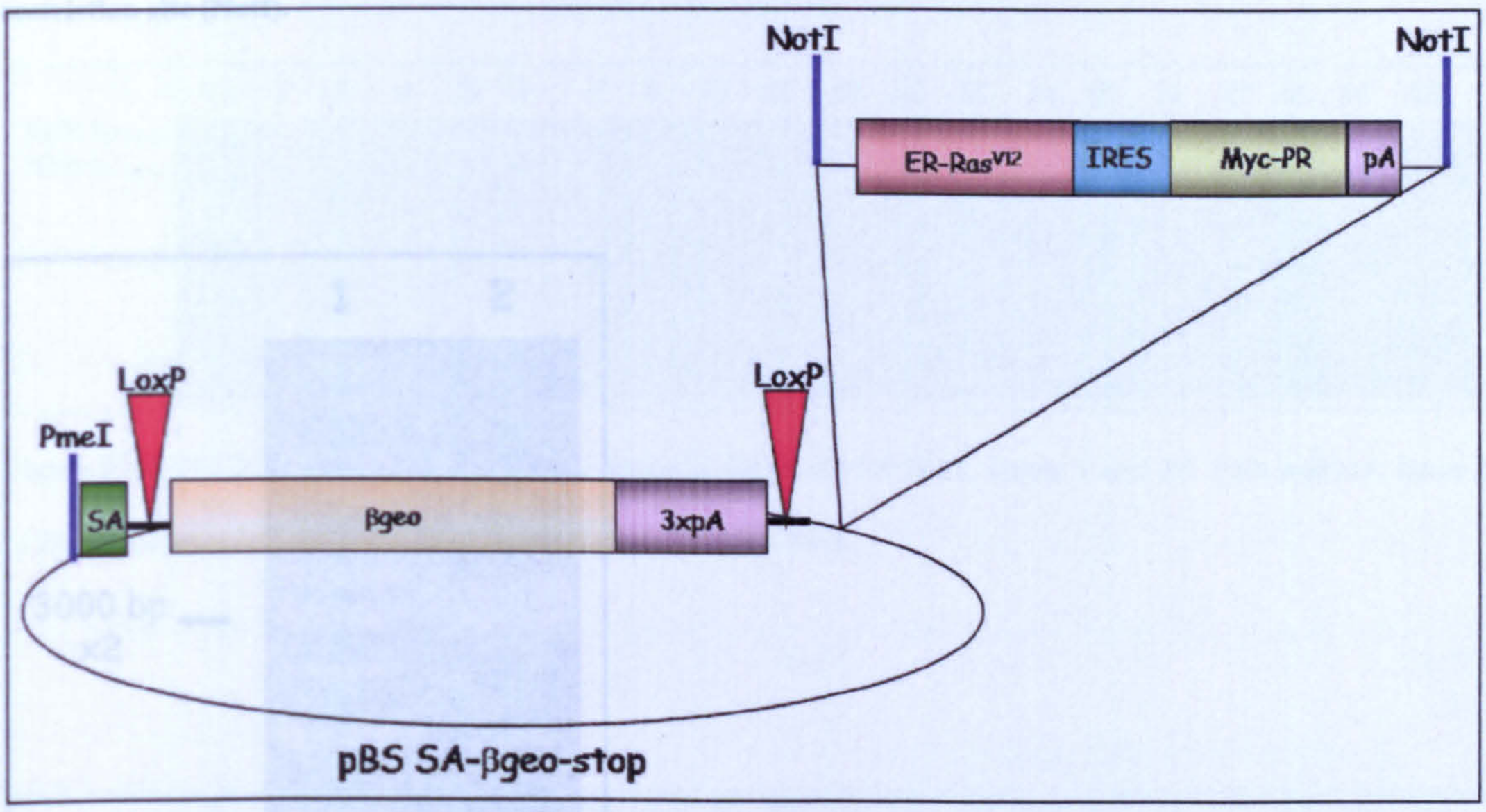

Figure 83. ER-ras-myc-PR (RasMyc cassette) cloning into pBS SA-βgeo-STOP.

In the SA-βgeo-STOP plasmid, a STOP cassette, composed of a promoterless βgalactosidase-neomycin resistance fusion protein (Friedrich and Soriano, 1991) and including a triple polyadenylation signal from SV40 large antigen T (Zambrowicz et al., 1997) was assembled. This sequence is flanked by two directly repeated LoxP sites, so that it can be removed by Cre-mediated recombination.

The BamHI-HindIII restriction, (Figs. 84 and 85), has allowed us to ascertain the presence of all the fragments subcloned into the SA-βgeo-STOP plasmid.

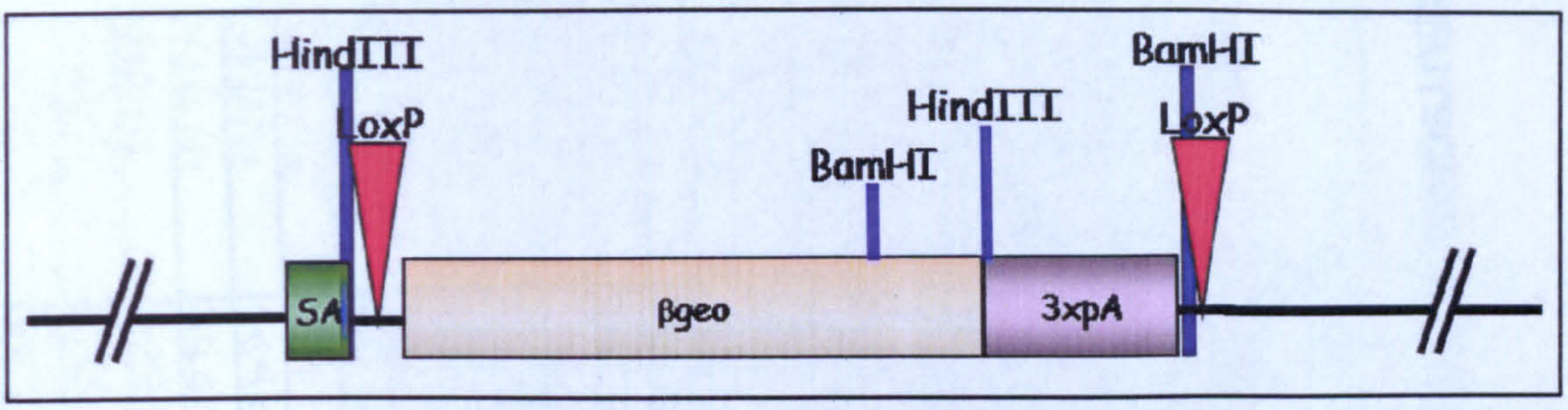

Figure 84. SA-βgeo-STOP plasmid. Splice acceptor (SA); LoxP site (LoxP); βgalactosidase-neomycin resistance fusion protein (βgeo); triple polyadenylation sequence (3xpA); PmeI restriction site (PmeI); NotI restriction site (NotI).

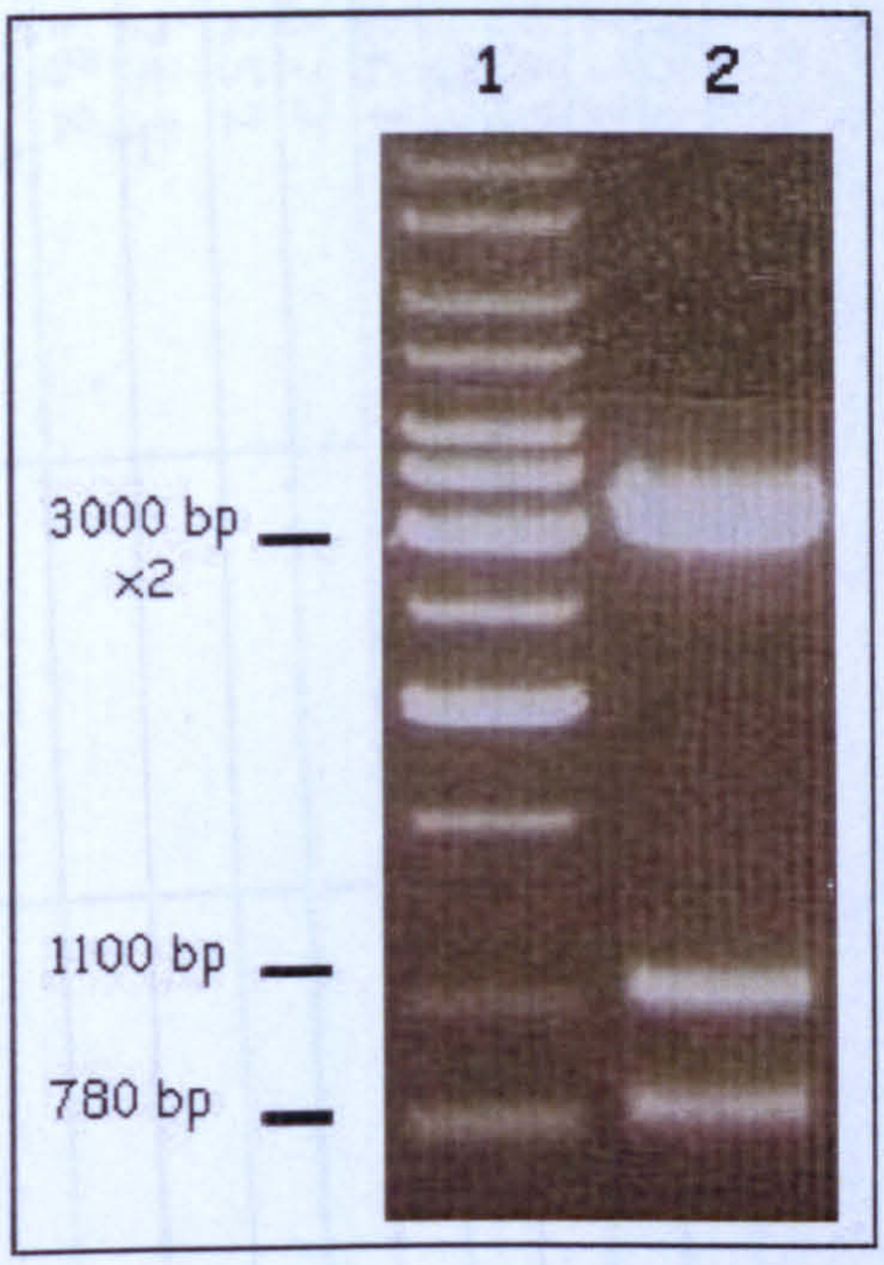

Figure 85. MINI PREP of SA-βgeo-STOP plasmid digested with BamHI and HindIII. Lane 1: 1 kb marker; lane 2: 1 positive SA-βgeo-STOP plasmid digested with BamHI and HindIII.

The SA-βgeo-RasMyc plasmid (Fig. 86) was digested with three different enzymes: NotI (Fig. 87), BamHI (Fig. 88) or HindIII (Fig. 89).

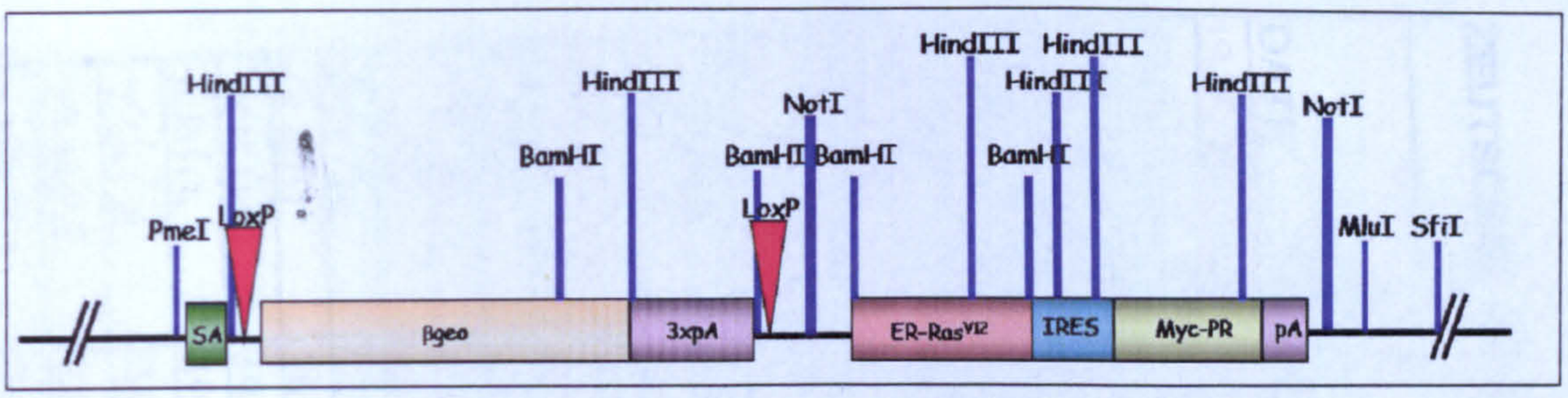

Figure 86. SA-βgeo-RasMyc plasmid

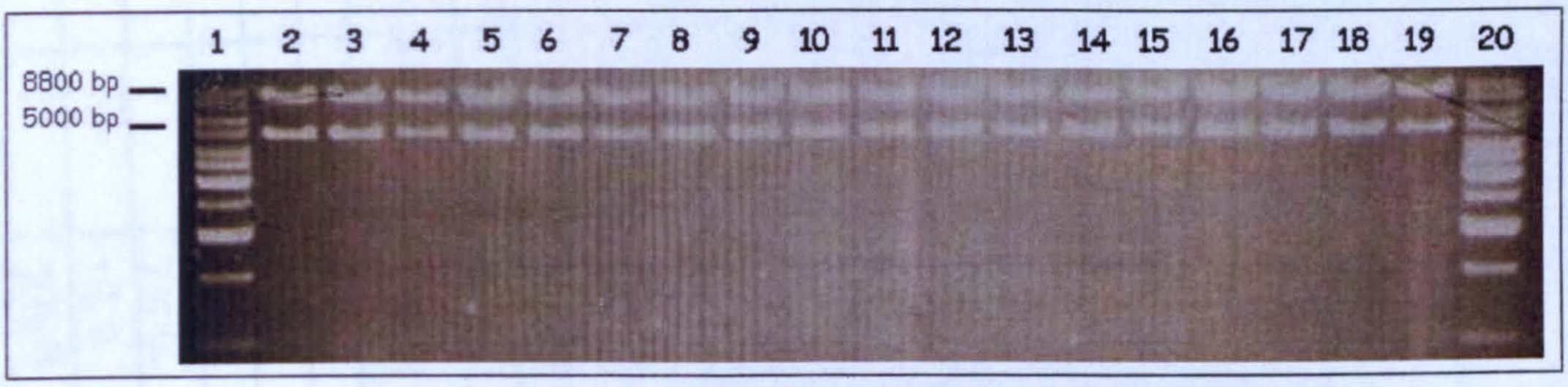

Figure 87. MINI PREP of SA-βgeo-RasMyc plasmid digested with NotI. Lanes 1 and 20: 1 kb marker; lanes 2 to 19: 18 positive SA-βgeo-RasMyc plasmid digested with NotI.

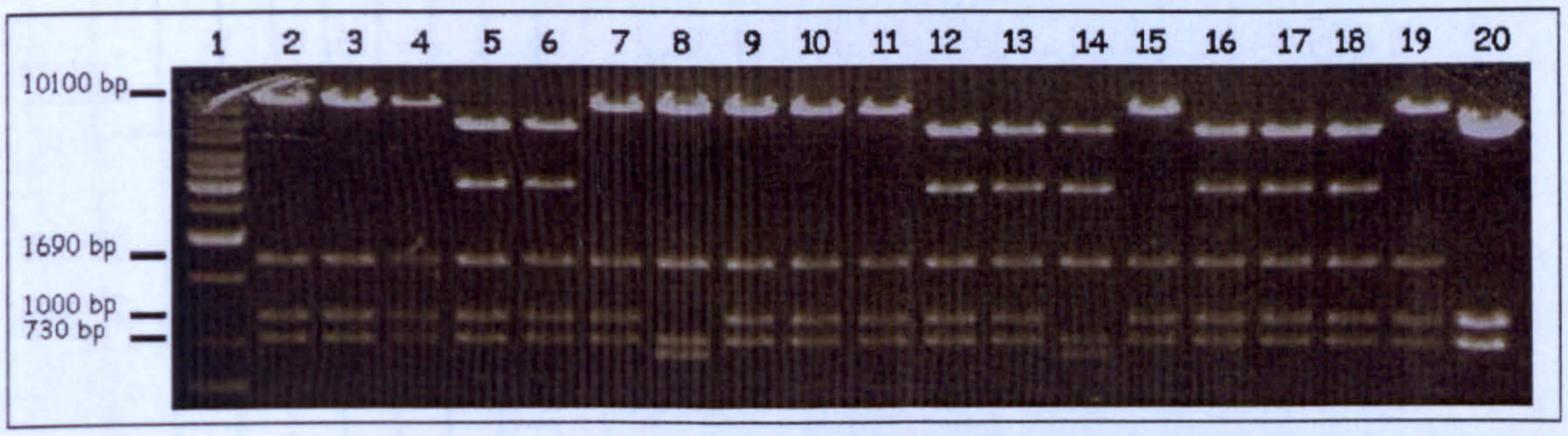

Figure 88. MINI PREP of SA-βgeo-RasMyc plasmid digested with BamHI. Lane 1: 1 kb marker; lanes 2 to 4, 7 to 11, 15 and 19: 10 positive SA-βgeo-RasMyc plasmid digested with BamHI; lanes 5 and 6, 12 to 14, 16 to 18 and 20: 9 positive SA-βgeo-RasMyc plasmid digested with BamHI.

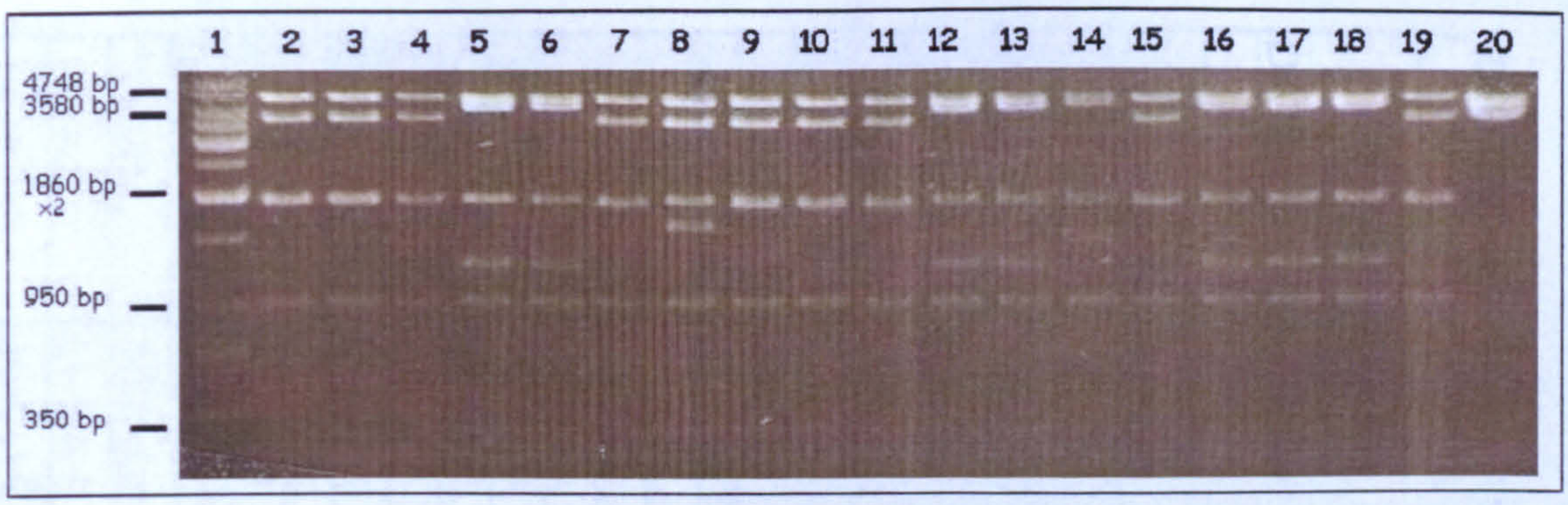

Figure 89. MINI PREP of SA-βgeo-RasMyc plasmid digested with HindIII. Lane 1: 1 kb marker; lanes 2 to 4, 7, 9 to 11, 15 and 19: 9 positive SA-βgeo-RasMyc plasmid digested with HindIII; lanes 5, 6, 8, 12 to 14, 16 to 18 and 20: 10 negative SA-βgeo-RasMyc plasmid digested with HindIII.

2) Cloning the myc-PR-ER-ras cassette from the MycRas plasmid (Fig. 50) into the SA-βgeo-STOP plasmid (Fig. 90).

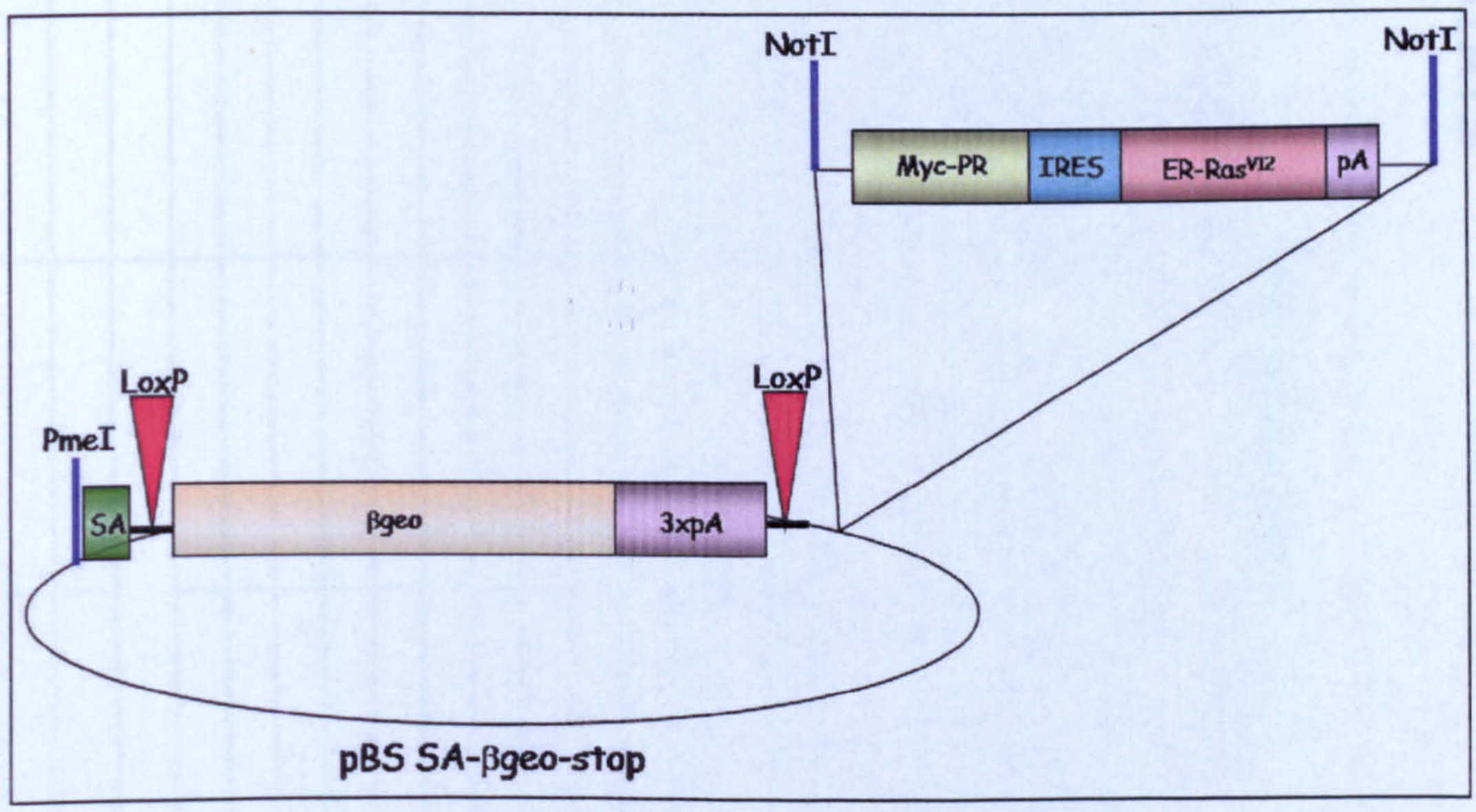

Figure 90. myc-PR-ER-ras (MycRas cassette) cloning into pBS SA-βgeo-STOP.

Then, the βglobin intron poly A sequence was inserted downstream of ER-Ras (Fig. 91). Inclusion of an intron in a transgene construct could increase the gene expression, whereas a polyadenylation signal is required for the proper termination of

transcription and stability of mRNA. In addition to these effects, poly A sequence can affect overall gene expression efficiency.

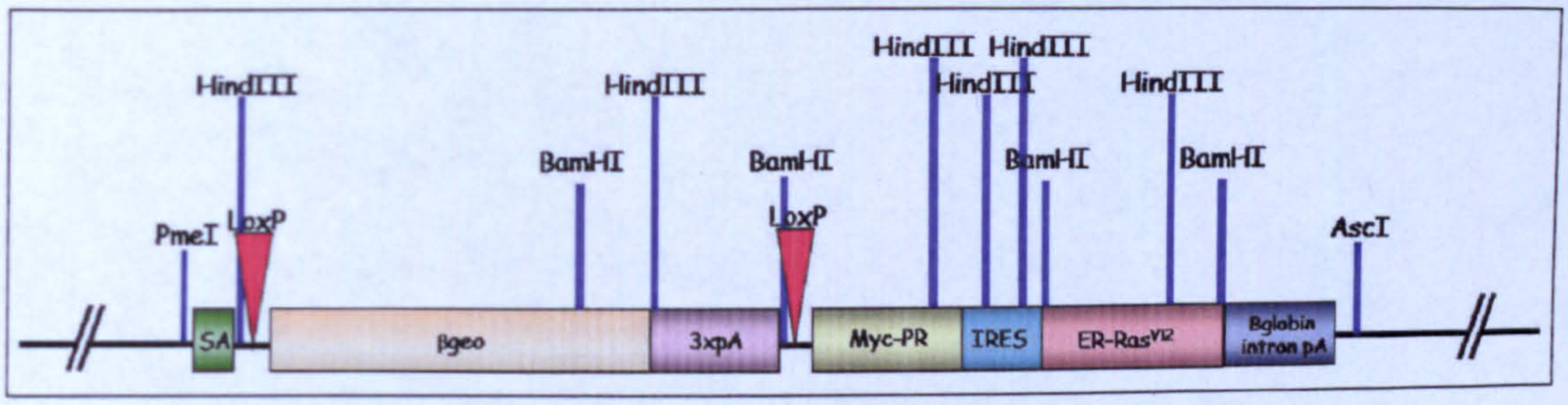

Figure 91. SA-βgeo-MycRas-βglobin intron pA plasmid

The integrity of the SA-βgeo-MycRas-βglobin intron pA plasmid was demonstrated through analysis with restriction enzymes HindIII and BamHI separately (Fig. 93) and sequencing all the cloning junctions (as schematically represented in Fig. 92) on both strands. Short pieces of some sequences are represented in figures 22, 23, 24, 25 in "Materials and Methods" chapter.

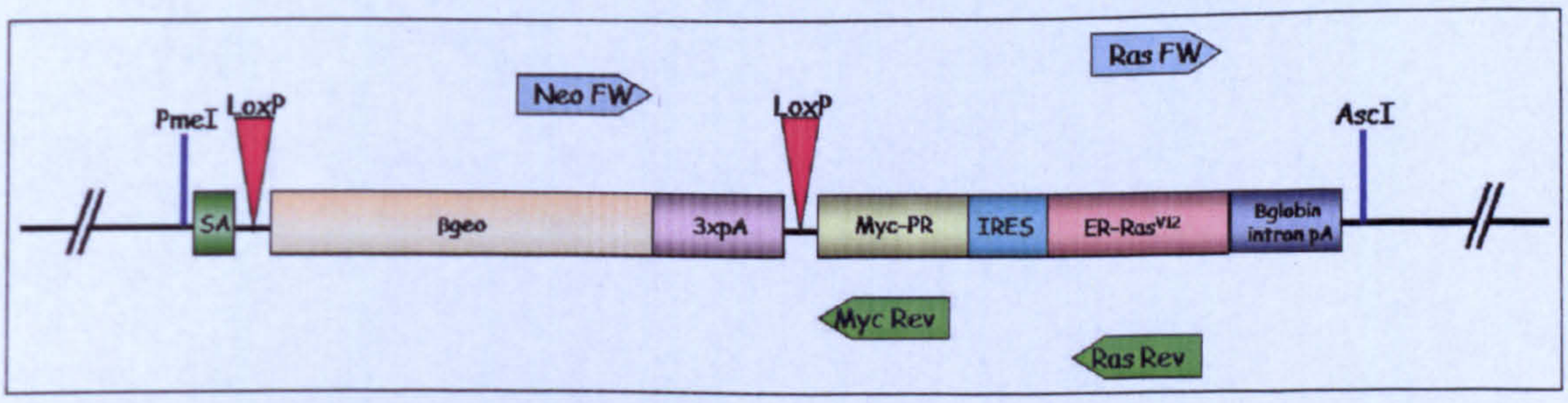

Figure 92. Schematic representation of some of the primers used for sequencing the SA-βgeo-MycRas-βglobin intron pA plasmid and their relative annealing position.

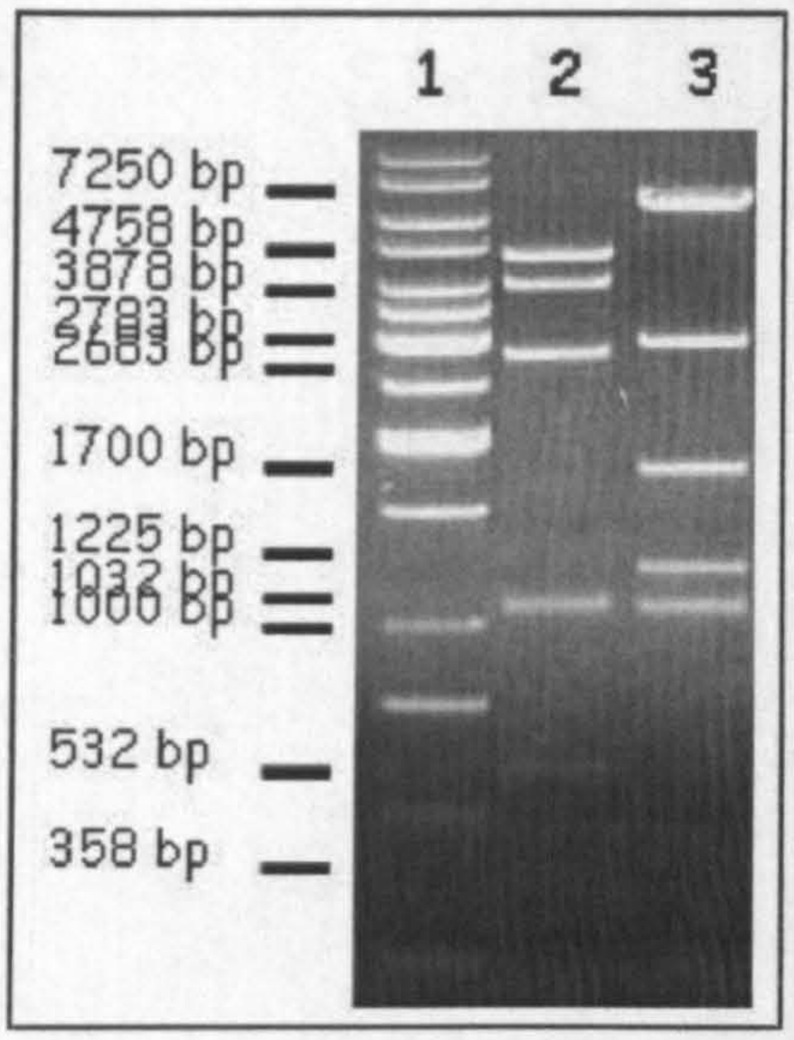

Figure 93. MINI PREP of SA-βgeo-MycRas-βglobin intron pA plasmid digested with HindIII or BamHI. Lane 1: 1 kb marker; lane 2: 1 positive SA-βgeo-MycRas-βglobin intron pA plasmid digested with HindIII; lane3: 1 positive SA-βgeo-MycRas-βglobin intron pA plasmid digested with BamHI.

In order to generate a mouse model carrying the oncogenes in all tissues and organs, two mouse strains were created through homologous recombination in ES cells, carrying the targeting vector into the two different *loci* ubiquitously expressed, ROSA26 or Eef1α1, described in paragraph 1.6.

However, the STOP cassette (described previously in this paragraph), placed before the ATG codon of the bicistronic sequence, allowed us to drive the expression of the bicistronic construct in a tissue-specific manner after its removal by Cre-mediated recombination. In particular, we wanted to observe the effects of the two oncogenes in thyroid.

Each construct, (the SA-βgeo-RasMyc plasmid and the SA-βgeo-MycRas-βglobin intron pA plasmid; figures 86 and 91), was subcloned between the arms of homology of ROSA26 and Eef1α1 *loci*, to obtain the RasMyc targeting vector and the MycRas targeting vector respectively.

The schematic structure of the targeting vector used for the homologous recombination in ES cells is shown in figure 94.

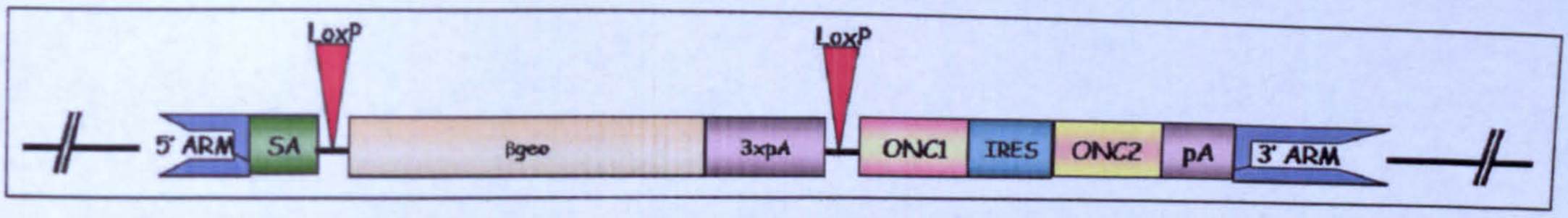

Figure 94. Targeting vector. Homology arm at 5' end (5'arm); splice acceptor (SA); LoxP site (LoxP); βgalactosidase-neomycin resistance fusion protein (βgeo); triple polyadenylation sequence (3xpA); first oncogene (ONC1); second oncogene (ONC2); polyadenylation sequence (pA); homology arm at 3' end (3'arm).

Each targeting vector was sequenced and digested with BamHI, SpeI or KpnI restriction enzymes (Figs. 95, 96, 97) before electroporation in ES cells. Figure 26, in "Materials and Methods" chapter, is part of the sequence obtained using the SA Rev primer.

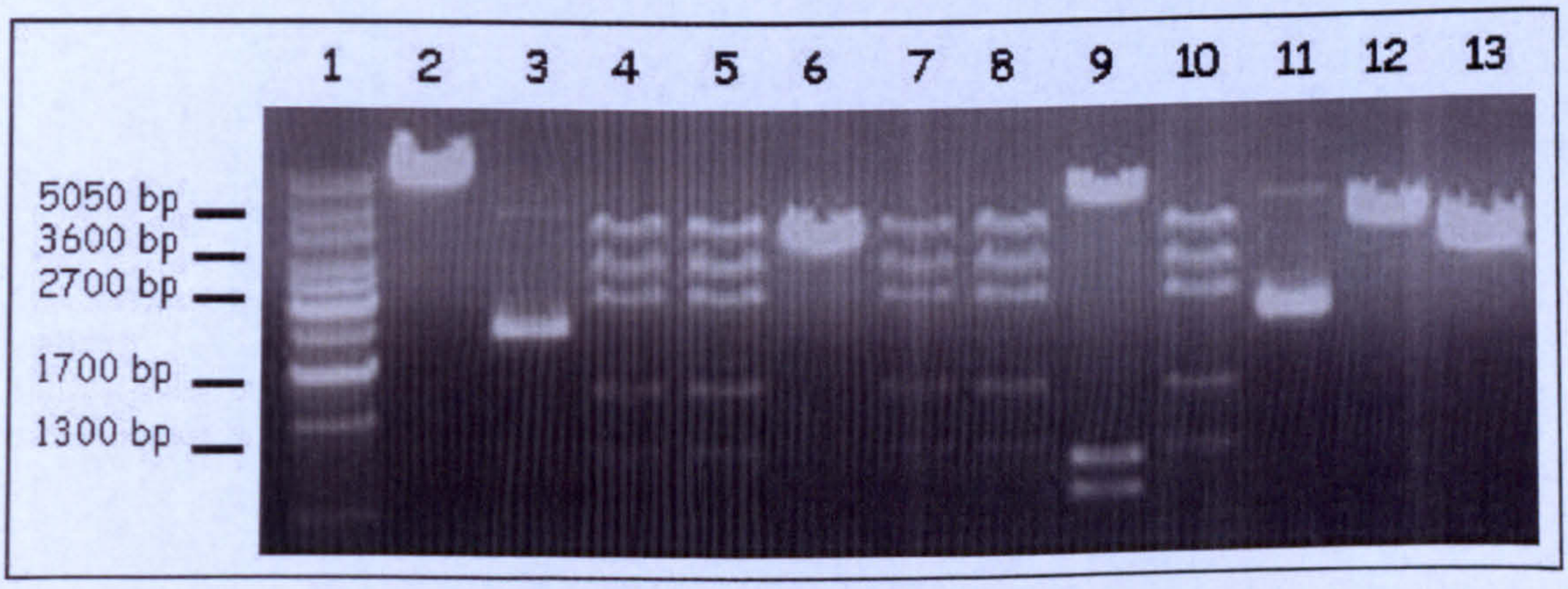

Figure 95. MINI PREP of targeting vector digested with BamHI. Lane 1: 1 kb marker; lanes 2, 3, 6, 9, and 11 to 13: 7 negative targeting vector mini preps; lanes 4, 5, 7, 8 and 10: 5 positive targeting vector mini preps digested with BamHI.

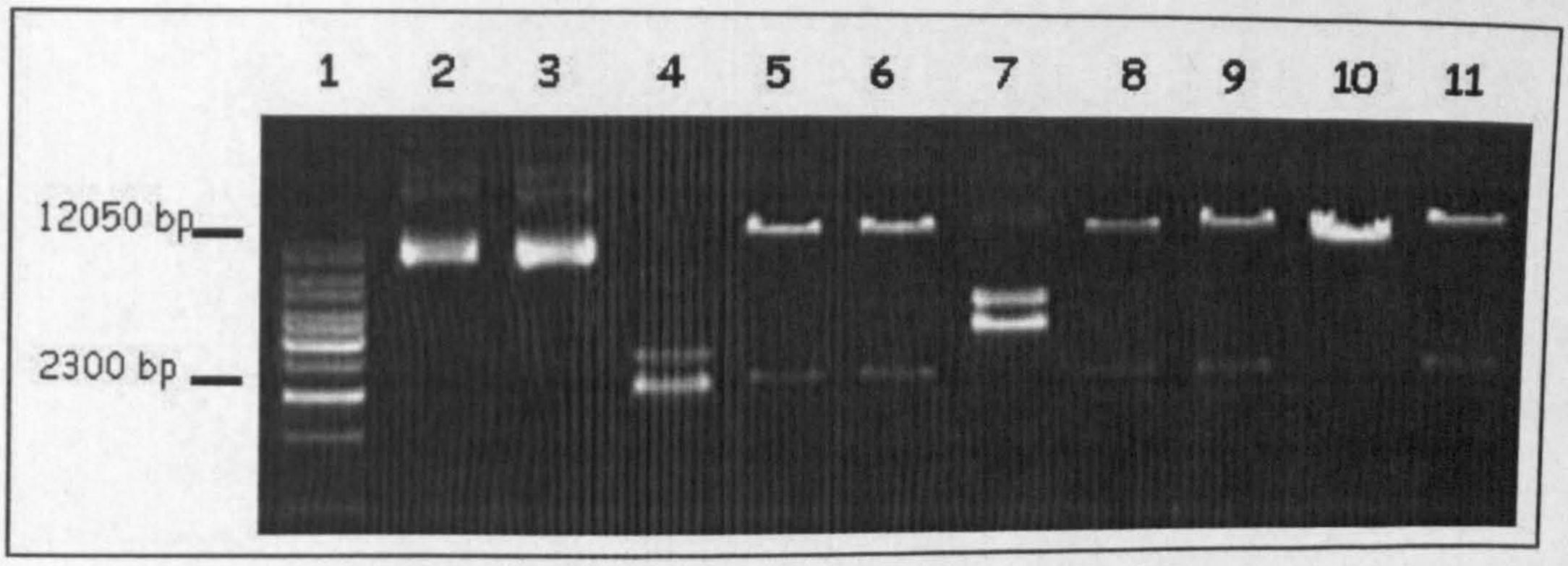

Figure 96. MINI PREP of targeting vector digested with SpeI. Lane 1: 1 kb marker; lanes 2, 3, 4, 7, and 10: 5 negative targeting vector mini preps; lanes 5, 6, 8, 9 and 11: 5 positive targeting vector mini preps digested with SpeI.

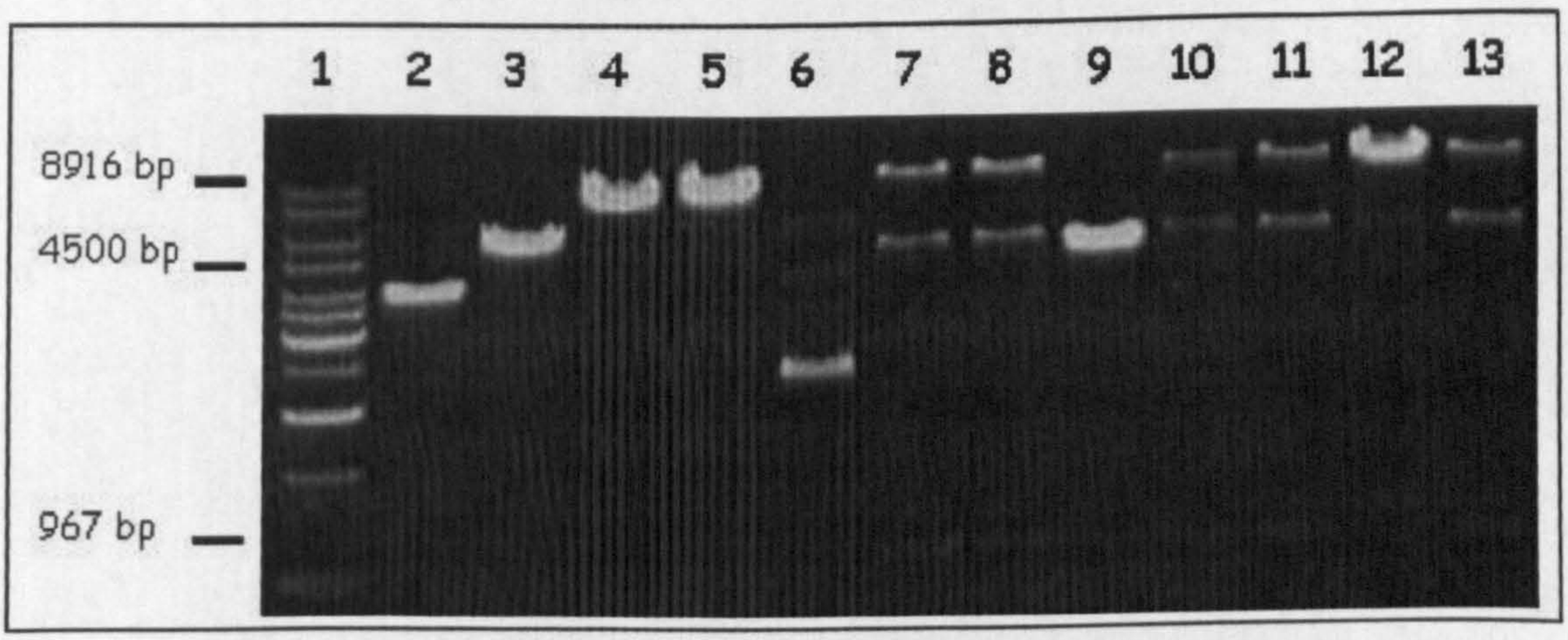

Figure 97. MINI PREP of targeting vector digested with KpnI. Lane 1: 1 kb marker; lanes 2 to 6, 9, and 12: 7 negative targeting vector mini preps; lanes 7, 8, 10, 11 and 13: 5 positive targeting vector mini preps digested with KpnI.

C.1.2 ES cells electroporation and screening

The MycRas targeting vector was electoporated into R1 Embryonic Stem (ES) cells, following the protocol described in "Materials and Methods".

The electroporated cells were fed with a medium containing the antibiotic G418. Because of the neomycin resistance carried by the vector, it was possible to select only

the clones in which the recombination had occurred. The expression of *Neomycin* promoterless cassette, driven by an endogenous promoter, did not ascertain that the targeting vector integration was a homologous recombination. Thus, to verify that the recombination event had occurred correctly, after this preliminary selection, the results were assessed by PCR.

Thus, it was possible to distinguish the wild type and the recombinant allele in each clone, following the correct homologous recombination event, based on the size of the DNA fragments produced. The PCRs for the Eef1α1MycRas/Eef1α1+ (or Eef1α1MycRas) ES clones and ROSA26MycRas/ROSA26+ (or ROSA26MycRas) ES clones were carried out as described in "Materials and Methods". The oligo primers chosen and the expected bands are drawn in the figures 98 and 99.

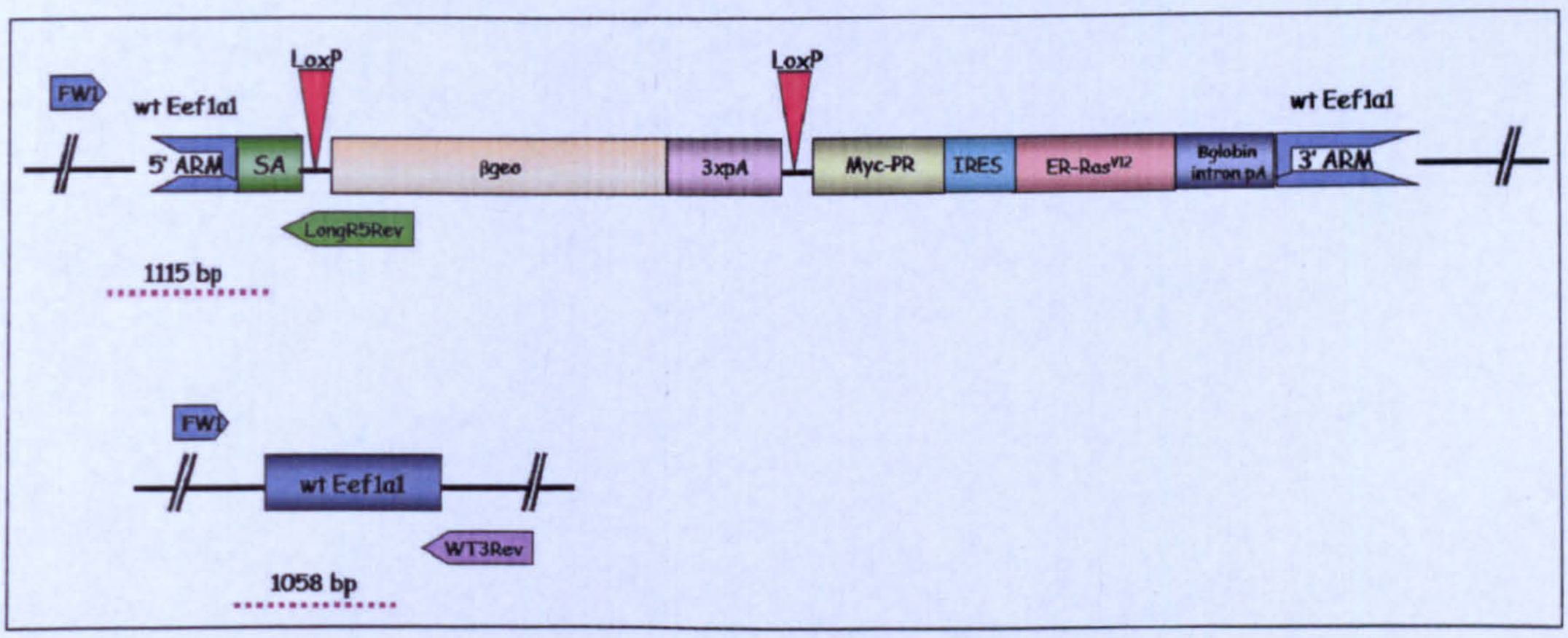

Figure 98. Eef1α1MycRas ES clones PCR screening scheme. The common FW1 forward primer was used either in combination with the LongR5Rev reverse primer to amplify a 1115 bp long PCR product on the recombinant allele or in combination with the WT3Rev reverse primer to amplify a 1058 bp long PCR product on the wt allele.

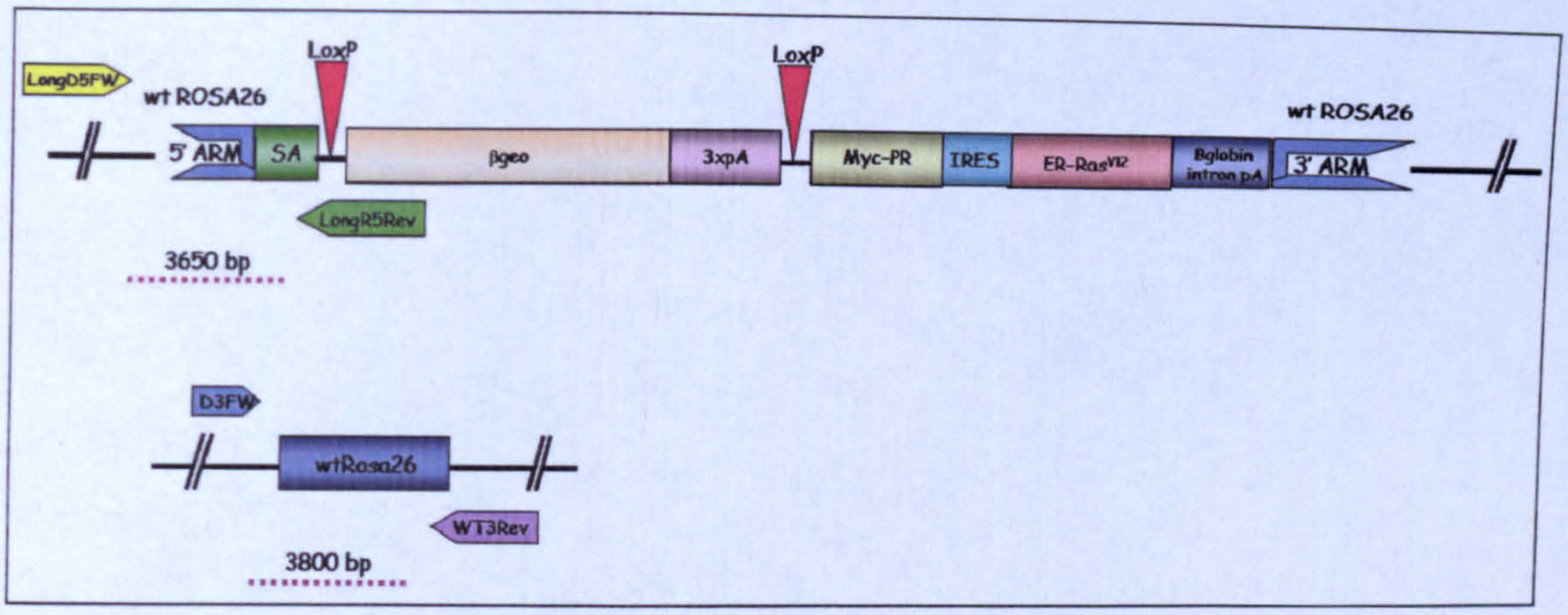

Figure 99. ROSA26MycRas ES clones PCR screening scheme. The LongD5FW forward primer was used in combination with the LongR5Rev reverse primer to amplify a 3650 bp long PCR product on the recombinant allele; the D3FW forward primer was used in combination with the WT3Rev reverse primer to amplify a 3800 bp long PCR product on the wt allele.

Eef1α1MycRas ES clones and ROSA26MycRas ES clones, which were found resistant to neomycin were picked up, at least 20 in number for each type. Further, PCR screening analysis on the 20 selected clones, led to the identification of 17 clones positive for Eef1α1 *locus* for one type and only 3 for ROSA26 *locus* for the other (Figs. 100 and 101).

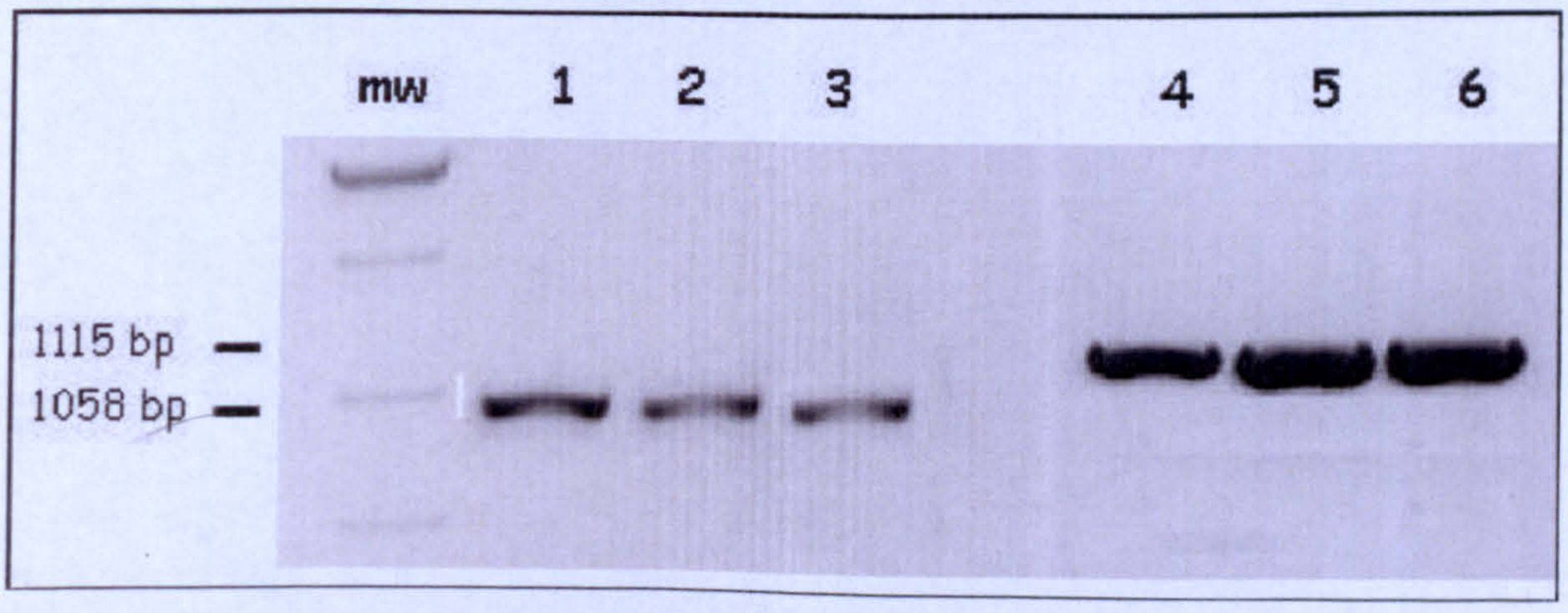

Figure 100. PCR screening Eef1α1MycRas ES clones. The 1058 bp PCR product corresponds to the wt allele; the 1115 bp PCR product corresponds to the recombinant allele; 100 bp molecular weight (mw).

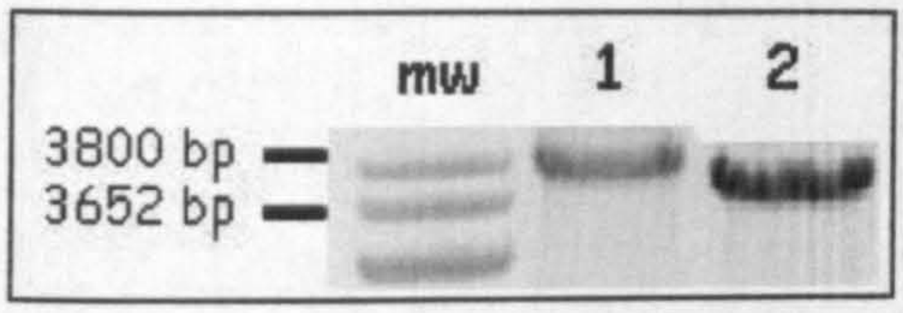

Figure 101. PCR screening ROSA26MycRas ES clones. The 3800 bp PCR product corresponds to the wt allele; the 3652 bp PCR product corresponds to the recombinant allele; 100 bp molecular weight (mw).

C.1.3 Genotyping of conditional onco-mice

Among the positive clones, one (for each *locus*) was chosen to be injected into the blastocyst picked up from a pregnant mouse. This blastocyst was then transplanted into the uterus of a substitute foster mother and several chimeras were obtained. In particular, 3 male chimeras with 100% and 1 chimera with 80% degree of chimerism were found after injection of Eef1α1MycRas ES cells and 2 male chimeras one with 100% and the other one with 80% degree of chimerism after injection of ROSA26MycRas ES cells. These chimeras with highest degree of chimerism (evaluated by coat colour) were bred with C57/BL6 wild type females to ascertain contribution of the recombinant ES cells to the germline. By this crossing, agouti mice were obtained, which were genotyped to determine the germ line transmission, by polymerase chain reaction (PCR). The PCR was set up so that in the same reaction both the wild type and the recombinant *locus* could be identified using three different primers.

The DNA was extracted from tail tips and analyzed by a triple-primer PCR method, with two forward primers and a common reverse primer to distinguish between the wild type and the recombinant allele; one of the two forward primers annealing on the wild type allele and the other one on the transgenic allele. On the basis of the size of the PCR products, it was possible to identify the homozygous wild type mice and the heterozygous mice for the targeting construct schematically

represented in figures 102 and 104 while the figures 103 and 105 show the respective PCR screening results.

Eef1α1MycRas/Eef1α1+ and ROSA26MycRas/ROSA26+ mice were thereafter referred to as E-Onc and R-Onc mice respectively.

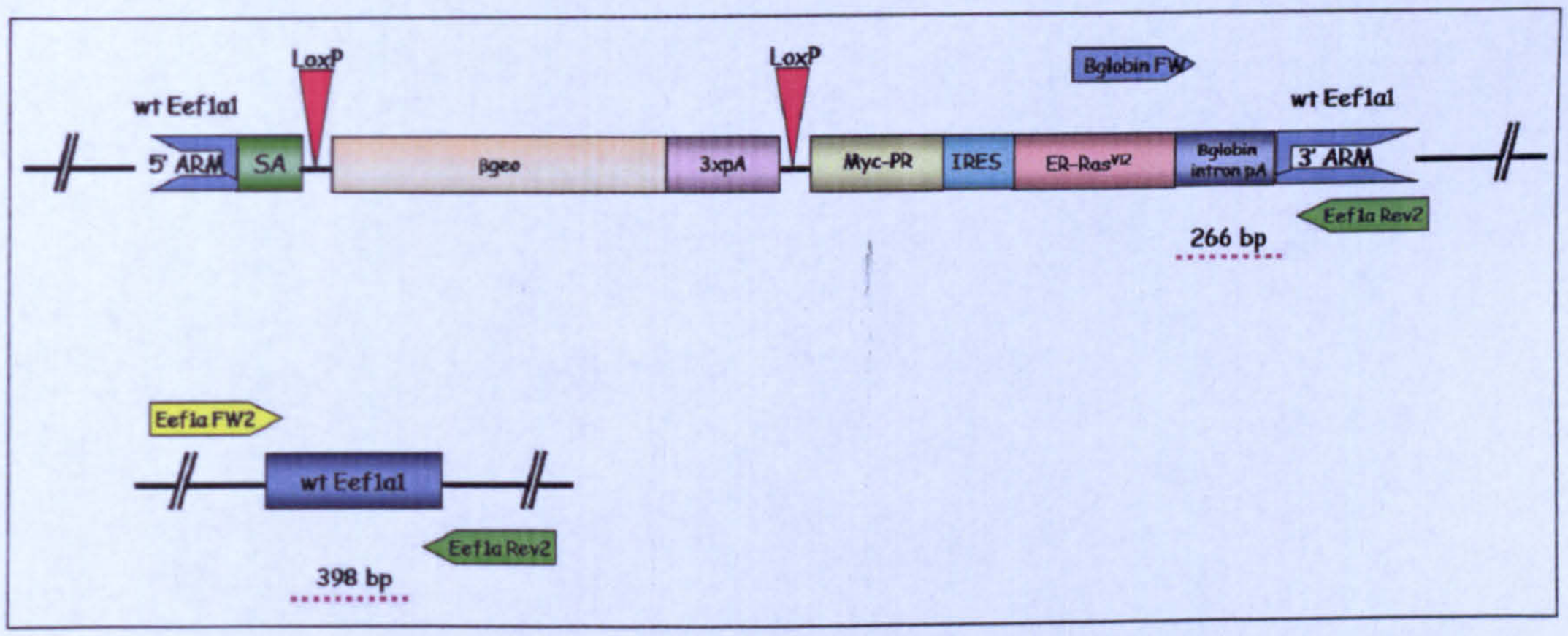

Figure 102. E-Onc mice PCR screening scheme. The common Eef1aRev2 reverse primer was used either in combination with the βglobinFW forward primer to amplify a 266 bp long PCR product on the recombinant allele or in combination with the Eef1aFW2 forward primer to amplify a 398 bp long PCR product on the wt allele.

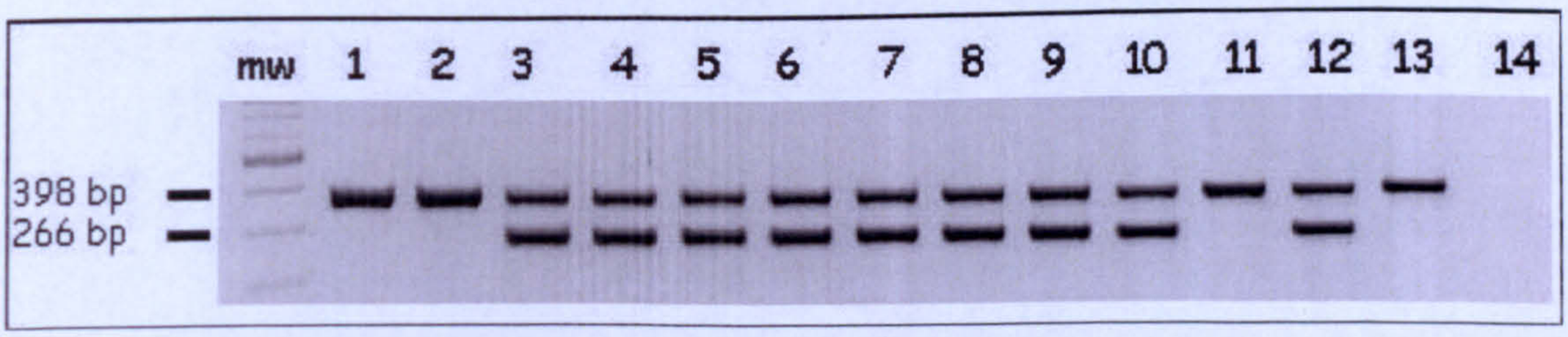

Figure 103. PCR screening of E-Onc. The 398 bp PCR product corresponds to the wt allele; the 266 bp PCR product corresponds to the recombinant allele. Lanes 1 to 11: DNA samples extracted from tail tips; lane 12: positive control; lane 13: negative control; lane 14: blank; 100 bp molecular weight (mw).

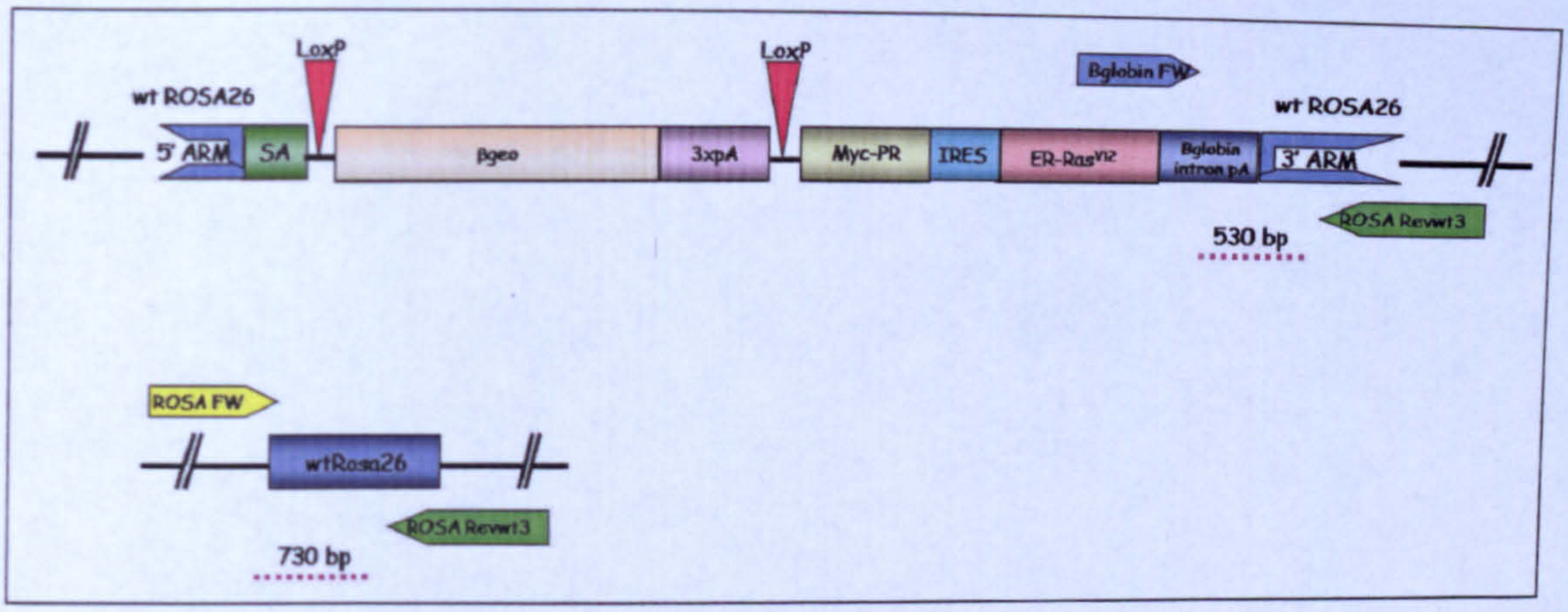

Figure 104. R-Onc mice PCR screening scheme. The common ROSARevwt3 reverse primer was used either in combination with the βglobinFW forward primer to amplify a 530 bp long PCR product on the recombinant allele or in combination with the ROSA FW forward primer to amplify a 730 bp long PCR product on the wt allele.

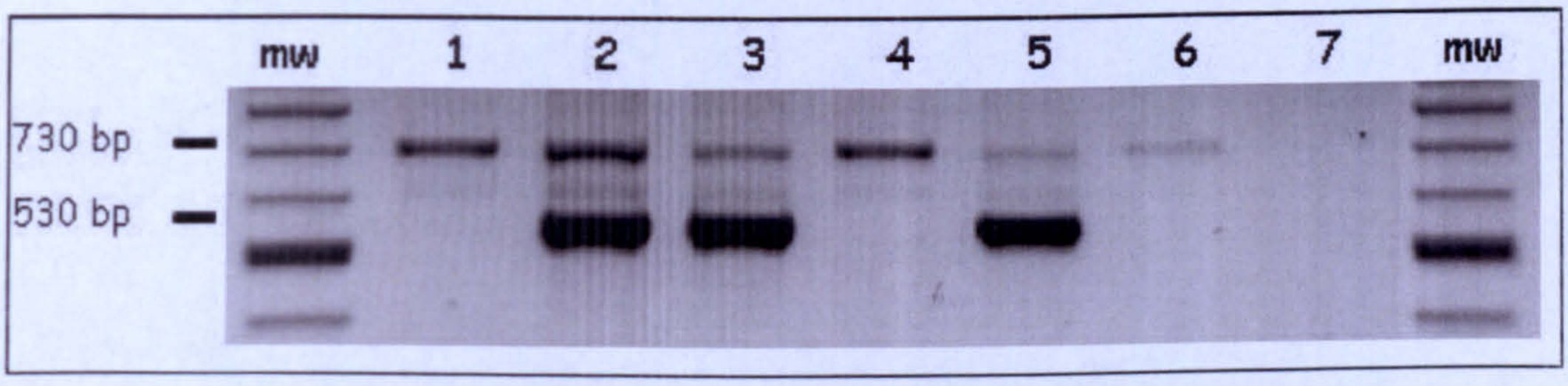

Figure 105. PCR screening of R-Onc mice. The 730 bp PCR product corresponds to the wt allele; the 530 bp PCR product corresponds to the recombinant allele. Lanes 1 to 4: DNA samples extracted from tail tips; lane 5: positive control; lane 6: negative control; lane 7: blank; 100 bp molecular weight (mw).

The recombinant strains were spread by crossing heterozygous mice (E-Onc and R-Onc) with C57/BL6 wild type females.

C.1.4 Mouse strains expressing CRE

The transgenic mice described in the previous paragraph, retained the *neo* gene and the triple polyA signal (encoded by the construct) into the recombinant *locus* to prevent the read through towards the bicistronic cassette. To allow the expression of

oncogenes in thyroid, it was necessary to generate mice in which CRE recombinase was expressed in thyroid follicular cells.

In the laboratory two mouse strains expressing *cre* in thyroid were available: the first one expressed the recombinase under the control of the *Pax8* promoter (a knock-in mouse strain) (Bouchard et al., 2004; Bouchard et al., 2002) and the second one under that of the thyroglobulin (*Tg*) promoter (a transgenic mouse strain). The main difference between *Tgcre-ER* transgene and *Pax8cre/Pax8+* was that the *cre* coding sequence under the Tg promoter is fused to the estrogen receptor to be sensitive after translation to the Tamoxifene addition (CRE-ER), while the *Pax8cre* was constitutively active after translation. Moreover, as detailed in introduction, the gene encoding for thyroglobulin during thyroid hormone production is expressed in thyroid of adult mice (E15). Whereas, *Pax8* transcription factor is involved in stimulation of thyroid genes such as Tg and TPO by binding to their promoter and determining the differentiation. Its expression is observed in thyroid and kidney by E8.5. To test the CRE-specific expression, each one of these two mouse strains was mated with the ROSA26 mouse strain. This strain carried the *β-galactosidase* (β-gal) coding sequence into the ROSA26 *locus*. To prevent its ubiquitous transcription, the coding sequence cassette was preceded by a triple polyA signal flanked by two LoxP sites (Soriano, 1999). The polyA signal excision and the β-gal transcription was possible due to the CRE expression.

The *cre* specific expression was demonstrated by the following β-galactosidase staining (Figs. 106 and 107).

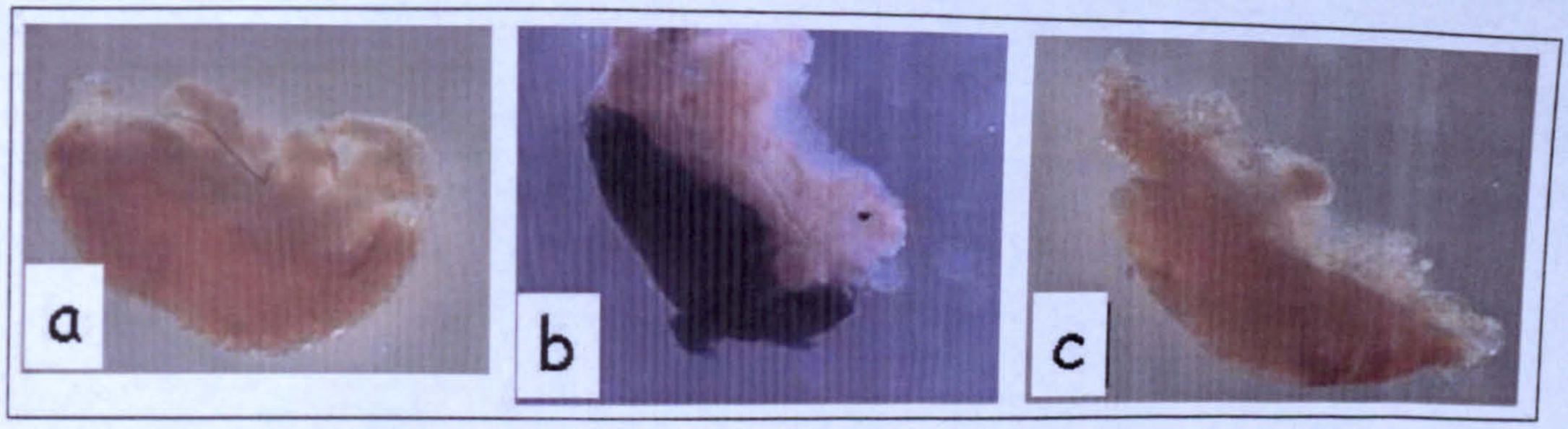

Figure 106. CRE activity in adult thyroid of *Tgcre-ER; ROSA26* mouse strain. a: *Tgcre-ER; ROSA26* mouse thyroid not treated with Tamoxifene; b and c: *Tgcre-ER; ROSA26* mouse thyroid after treatment with Tamoxifene.

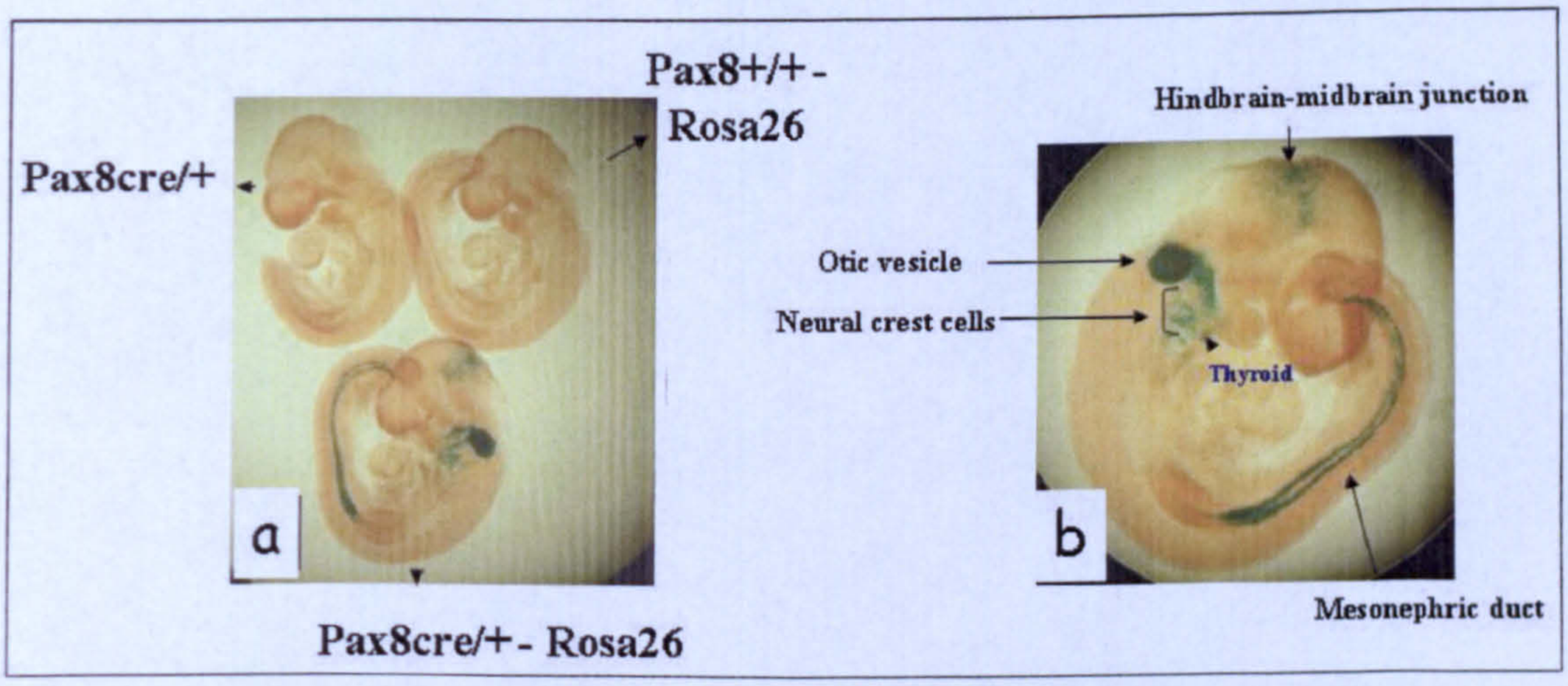

Figure 107. CRE activity in embryo mouse of *Pax8cre/Pax8+; ROSA26, Pax8+/Pax8+; ROSA26* and *Pax8cre/+* mouse strain. a: CRE activity in the three mouse strains; b: pattern of Pax8 expression in embryo.

Thus, both these two strains appeared to be amenable to allow a thyroid-restricted expression of oncogenes.

The TgCRE-ER mice were genotyped by PCR. A 450 bp PCR product was obtained using two primers annealing into the *cre* sequence (Fig. 108).

Pax8CRE/Pax8+ mice were genotyped, as described in the chapter "Materials and methods". The PCR reaction gives a 389 bp band for the wild type allele and a 700 bp product for the mutated allele (Fig. 109).

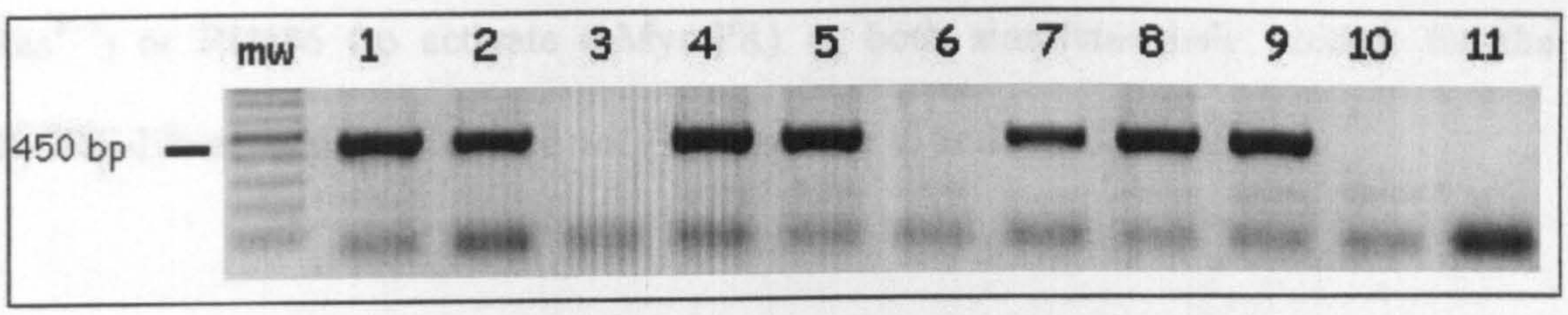

Figure 108. PCR screening TgcCRE-ER mice. The 450 bp PCR product corresponds to the recombinant allele. Lanes 1 to 8: DNA samples extracted from tail tips; lane 9: positive control; lane 10: negative control; lane 11: blank; 100 bp molecular weight (mw).

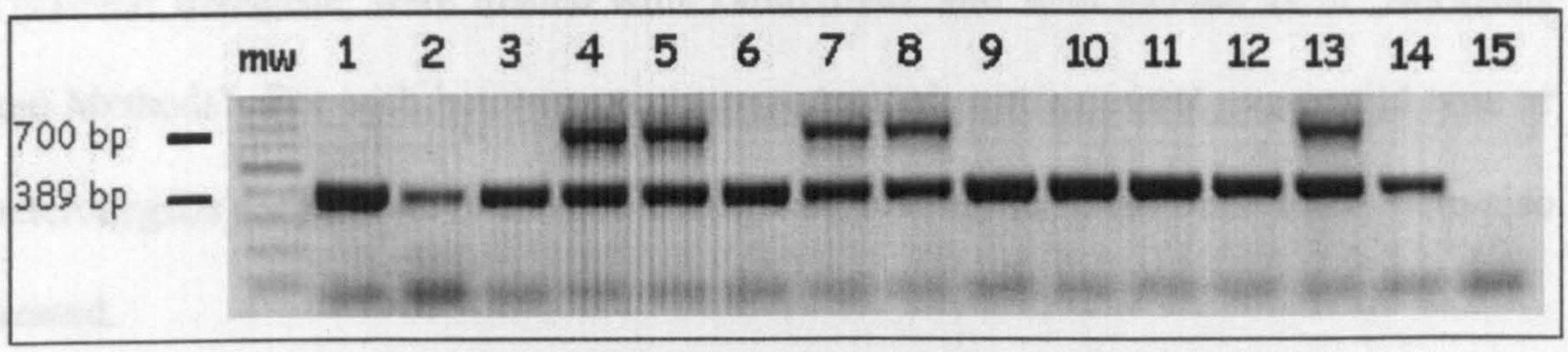

Figure 109. PCR screening Pax8CRE/Pax8+ mice. The 389 bp PCR product corresponds to the wt allele; the 700 bp PCR product corresponds to the recombinant allele. Lanes 1 to 12: DNA samples extracted from tail tips; lane 13: positive control; lane 14: negative control; lane 15: blank; 100 bp molecular weight (mw).

Both the conditional onco mice Eef1α1MycRas (E-Onc) and ROSA26MycRas (R-Onc) were crossed with TgCRE-ER transgene and Pax8CRE/Pax8+. In such a manner, four double transgenic mouse strains were generated:

- Eef1α1MycRas; TgCRE-ER (herein referred to as E-Onc/TgCRE)
- ROSA26MycRas; TgCRE-ER (herein referred to as R-Onc/TgCRE)
- Eef1α1MycRas; Pax8CRE/Pax8+ (herein referred to as E-Onc/PaxCRE)
- ROSA26MycRas; Pax8CRE/Pax8+ (herein referred to as R-Onc/PaxCRE)

The CRE action, and the Tamoxifene administration in the case of TgCRE-ER transgene, ensured the removing of the STOP cassette from each construct and the oncogenic expression in the gland.

After transcription and translation, the two oncoproteins c-Myc-PR and ER-Ras^{V12} were still inactive until the administration of either Tamoxifene (to activate ER-

Ras^{V12}) or RU486 (to activate c-Myc-PR) or both simultaneously, except for the TgCRE-ER mice already treated with Tamoxifene to activate *Tgcre-ER*.

C.1.5 Treatments with the hormones

Some of the double heterozygous mice, those with R-Onc genotype and harbouring *Tgcre-ER* transgene gene and those with E-Onc genotype and carrying *Tgcre-ER* transgene, were treated with Tamoxifene and with RU486 as in "Materials and Methods". For each heterozygous mouse treated, some control mice, wild type or heterozygous for just one of the two transgenes, belonging to the same litter, were also treated.

At the beginning the two drugs were administrated simultaneously, but almost all of the transgenic mice died in a few days and the two vehicles had not the same effect. Therefore only one drug was administered per week (each one for 5 days) and the mice were found to be alive this way (table 13).

Autopsy was performed on dead mice. They were found to have a liver containing white platelets similar to precipitate crystals and a rotten intestine.

Simultaneous treatment

Genotype	Treated mice	Died mice	Survived mice
R-Onc/TgCRE	8	7	1
R-Onc	7	1	6
E-Onc/TgCRE	2	2	0
wt	17	2	15

Single (Not simultaneous) treatment

Genotype	Treated mice	Died mice	Survived mice
R-Onc/TgCRE	6	0	6
E-Onc/TgCRE	15	0	15
R-Onc/PaxCRE	1	0	1
E-Onc/PaxCRE	3	0	3
R-Onc	3	0	3
E-Onc	15	0	15
TgCRE	16	0	16
PaxCRE	4	0	4
wt	17	1	16

Table 13. Simultaneous or single transgenic mice treatments.

C.2 Phenotype of conditional onco-mice

C.2.1 Molecular phenotype

To verify whether the thyroglobulin promoter in adult mice correctly drove the *cre* expression, the thyroid picked up from some treated mice was checked for the correct expression of the two oncogenes in the gland following the CRE action. The levels of mRNA encoding the two oncogenes after the *Neomycin* cassette excision (Fig. 110) were measured by Real Time PCR.

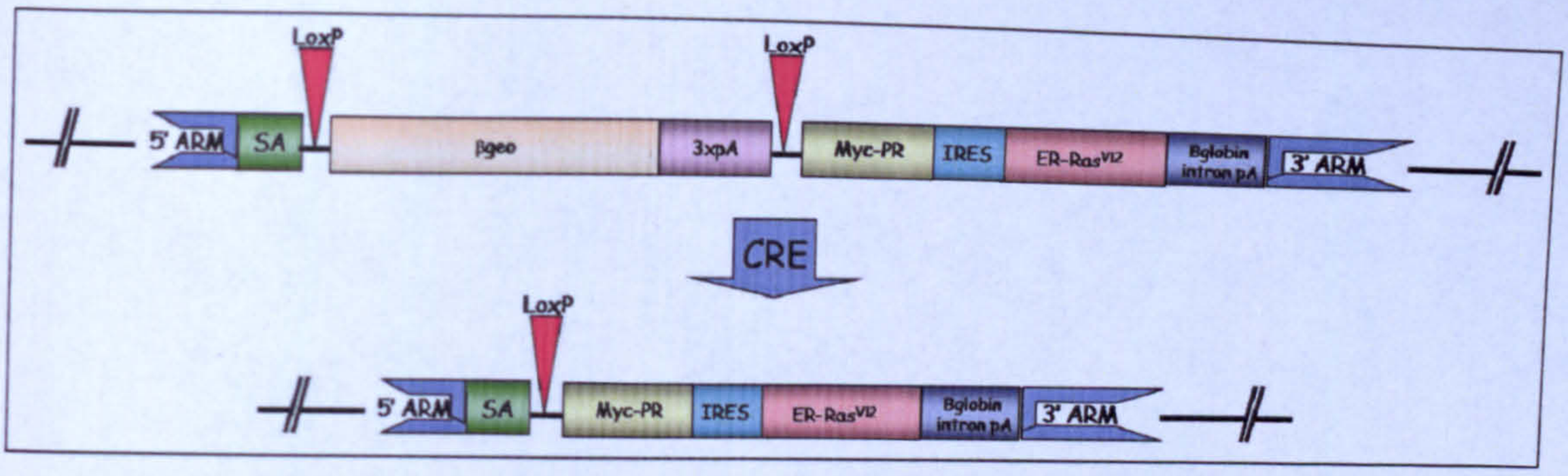

Figure 110. Schematic representation of the CRE recombinase action.

The expression of the oncogenes was analyzed in thyroids dissected from R.Onc/TgCRE mice treated with the drugs (Tamoxifene and RU486) in comparison with thyroids dissected from wild type mice belonging to the same litter of the R-onc mice. The wild type as well as mutant mice were treated with Tamoxifene and RU486 The expression values were normalized for α-1 tubulin and plotted in a graph (Figs. 111 and 112). The expression of the oncogenes was higher in untreated mice in comparison to that in wild type mice (Figs. 111 and 112). From these data, it was possible to deduce that *in vivo* the construct could function a little in a leaky manner.

However, the expression of the two oncogenes of interest in treated double transgenic mice exceeded by about 500 fold that of wild type mice used as controls (Figs. 111 and 112) indicating the correct functioning of the CRE protein under the control of the thyroglobulin promoter in thyroid. The Real Time PCR carried out on the same samples obtained in a parallel retrotanscription reaction lacking the reverse transcriptase enzyme proved that the results obtained were not influenced by the presence of contaminant genomic DNA but just due to the real oncogenic expression (data not shown). However, between the two target genes of c-Myc and H-Ras, ODC and c-fos respectively, only c-fos appeared weakly up-regulated in these treated double transgenic R.Onc/TgCRE mice (Figs. 113 and 114).

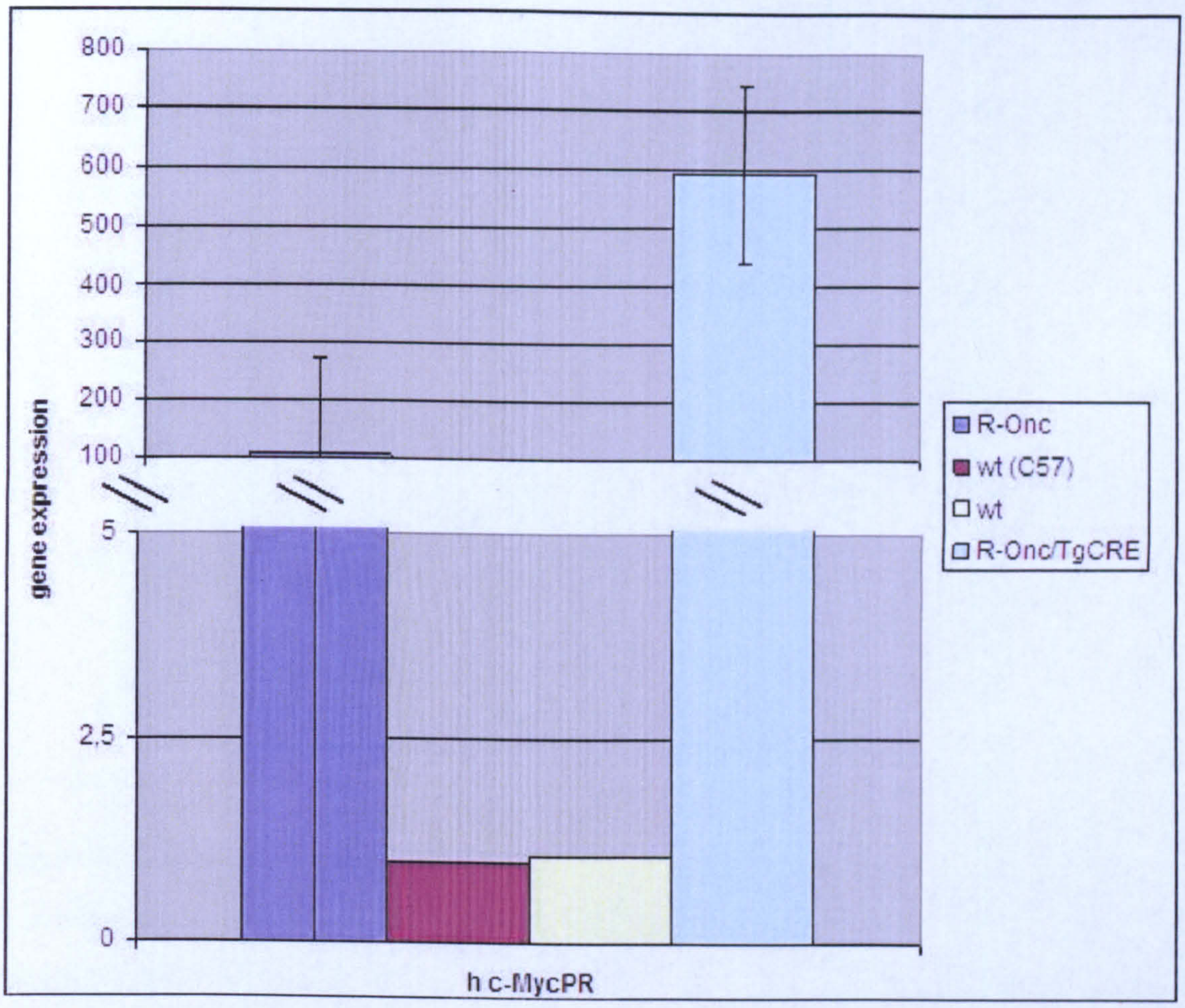

Figure 111. Real Time PCR on mouse thyroids. Blue bar indicates human c-Myc-PR (h cMycPR) expression in R-Onc mouse; purple bar and yellow bar indicate human c-Myc-PR expression in wt mice; turquoise bar indicates human c-Myc-PR expression in R-Onc/TgCRE-ER mouse. Human c-Myc-PR (h cMycPR).

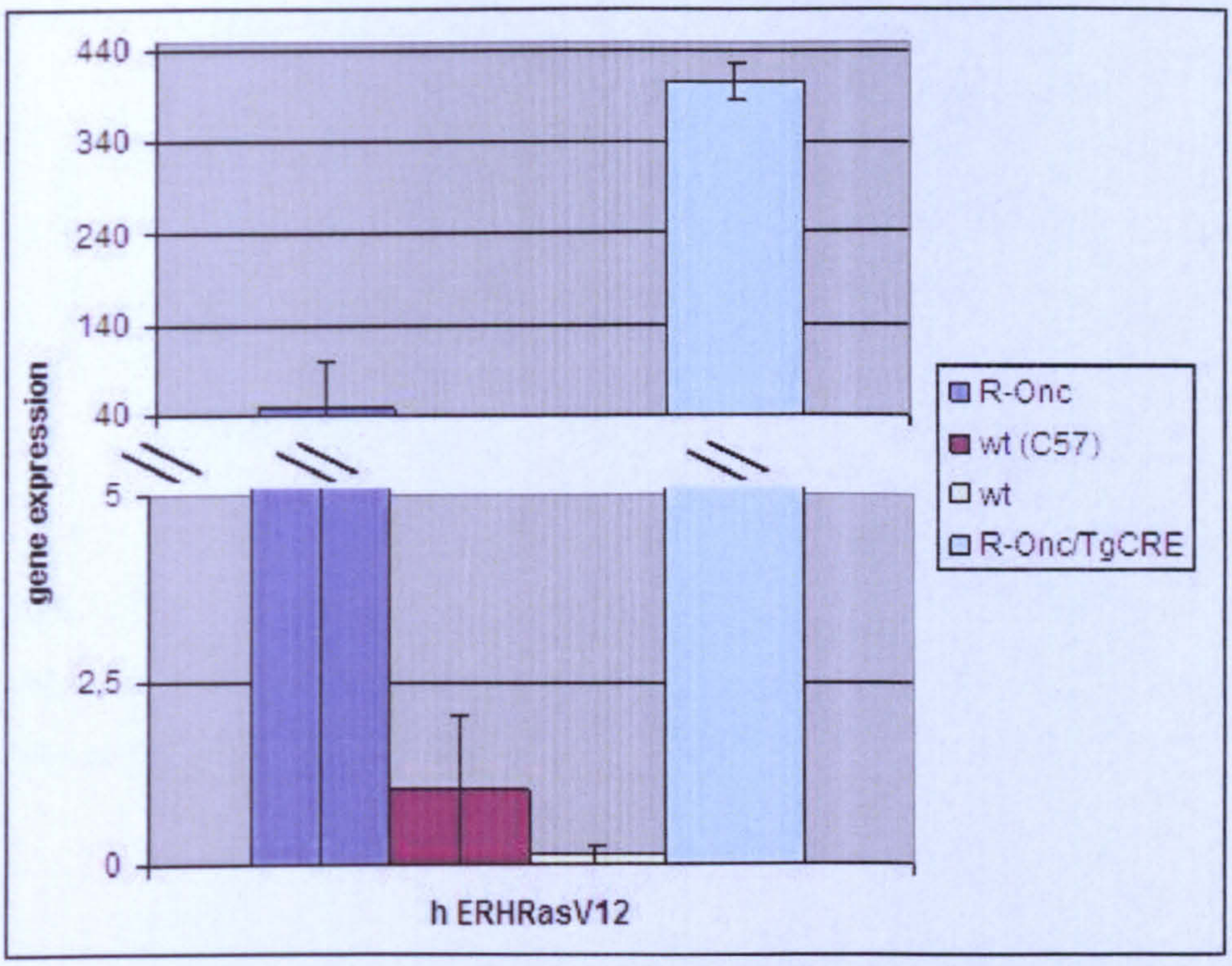

Figure 112. Real Time PCR on mouse thyroids. Blue bar indicates human ER-Hras^{V12} (h ERRas^{V12}) expression in R-Onc mouse; purple bar and yellow bar indicate human ER-Hras^{V12} expression in wt mice; turquoise bar indicates human ER-Hras^{V12} expression in R-Onc/TgCRE-ER mouse. Human ER-Hras^{V12} (h ERRas^{V12}).

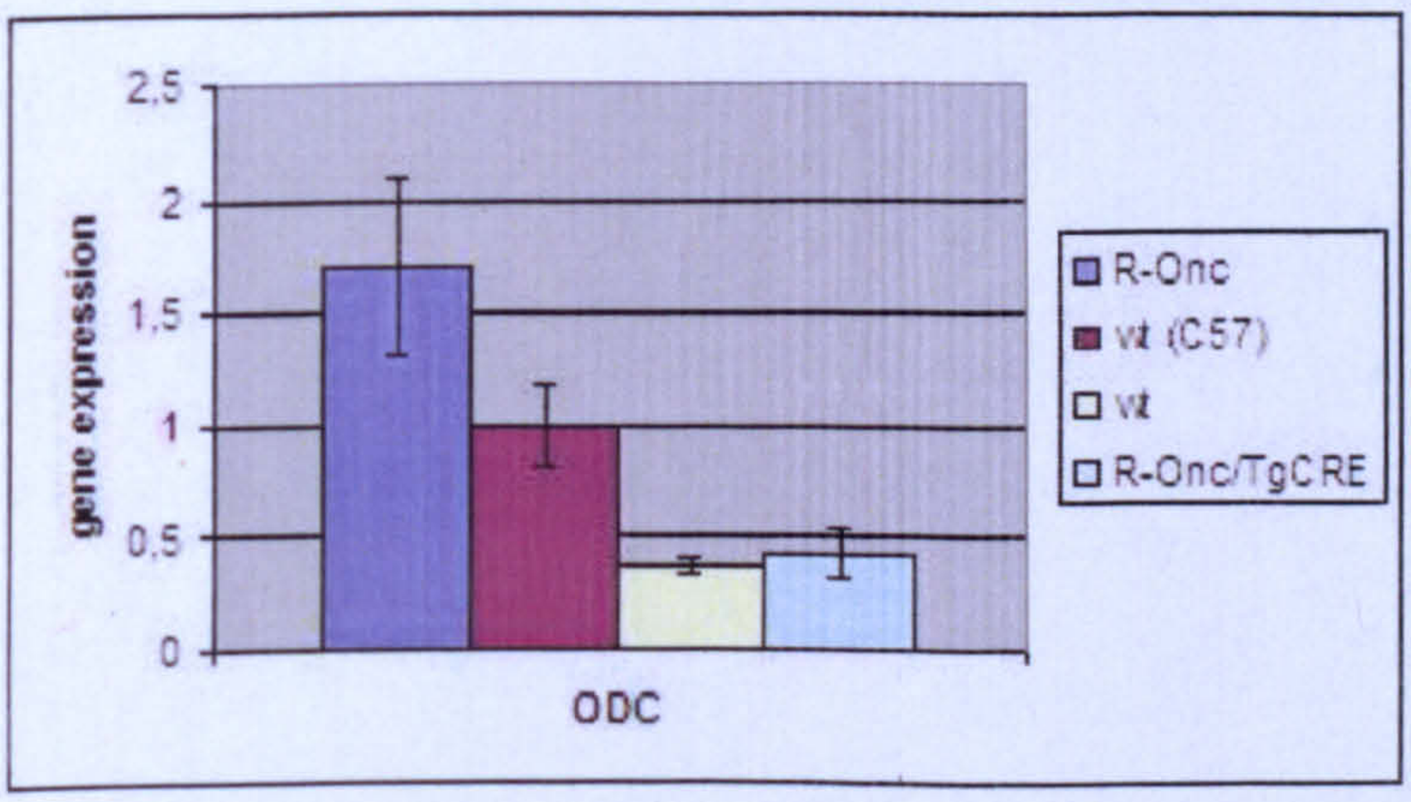

Figure 113. Real Time PCR on mouse thyroids. Blue bar indicates mouse ODC (ODC) expression in R-Onc mouse; purple bar and yellow bar indicate mouse ODC expression in wt mice; turquoise bar indicates mouse ODC expression in R-Onc/TgCRE-ER mouse. Mouse ODC (ODC).

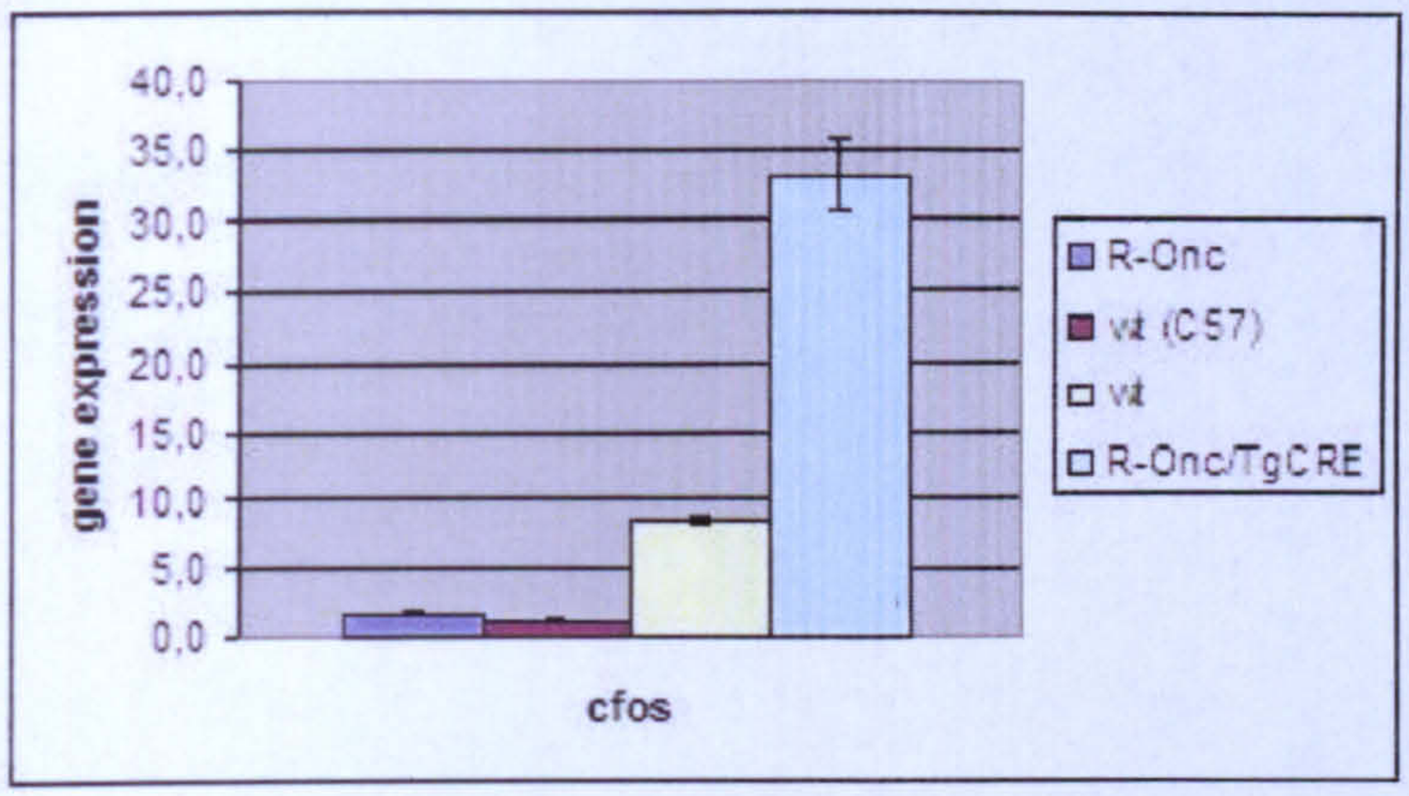

Figure 114. Real Time PCR on mouse thyroids. Blue bar indicates mouse c-fos (c-fos) expression in R-Onc mouse; purple bar and yellow bar indicate mouse c-fos expression in wt mice; turquoise bar indicates mouse c-fos expression in R-Onc/TgCRE-ER mouse. Mouse c-fos (cfos).

C.2.2 Histological phenotype

After confirming that the oncogenes of interest were expressed in thyroid following the *cre* expression pattern, we asked whether their expression could have affected the histological phenotype of the gland. To address this question, the study of the microscopic features of thyroid gland was a useful tool to define some of the mechanisms underlying the oncogenes activation.

In particular, in this case the mouse strains analyzed were:

R-Onc/PaxCRE

E-Onc/TgCRE

R-Onc/TgCRE

The figures 115 to 117 show histological sections of thyroid stained with haematoxylin/eosin. Control and mutant (double heterozygous) mice were treated with Tamoxifene and RU486 (as described in "Materials and Methods") and five months after treatments, the mice were sacrificed and thyroids picked up and fixed in 10% formalin. Paraffin embedded thyroid 5 μm sections were stained with haematoxylin/eosin.

In control as well as in mutant thyroids, the tissue was well organized in a follicular structure with the follicles appearing as a rim of flattened or cuboidal cells. Histologically the thyroids of mutant mice were indistinguishable from those of control.

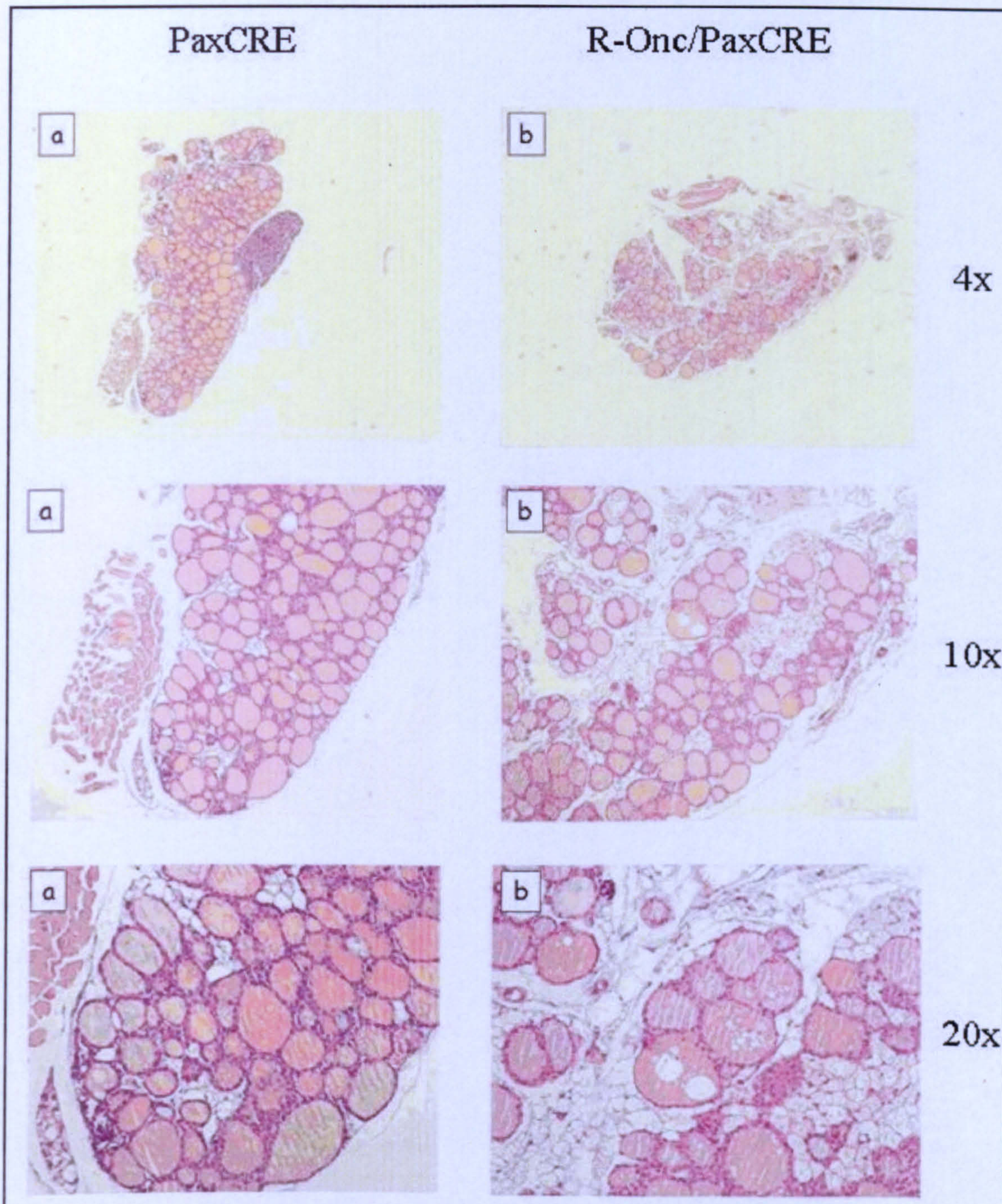

Figure 115. Histological sections of adult thyroid glands stained with hematoxylin/eosin. At the top of each image, the corresponding mouse genotype it is mentioned. a: control mouse; b: mutant mouse. Magnification: 4x, 10x and 20x.

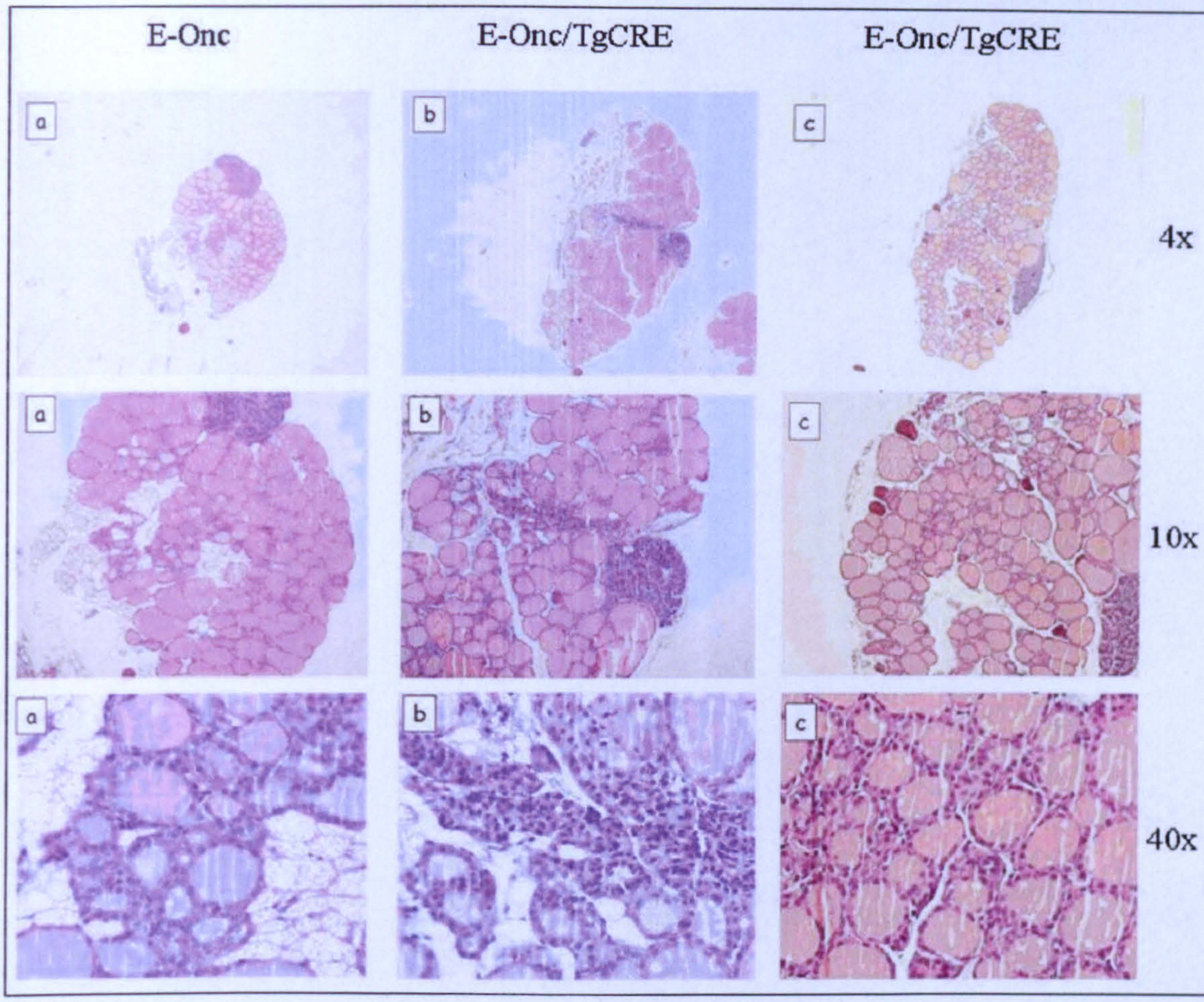

Figure 116. Histological sections of adult thyroid glands stained with hematoxylin/eosin. At the top of each image, the corresponding mouse genotype it is mentioned. a: control mouse; b and c: mutant mice. Magnification: 4x, 10x and 40x.

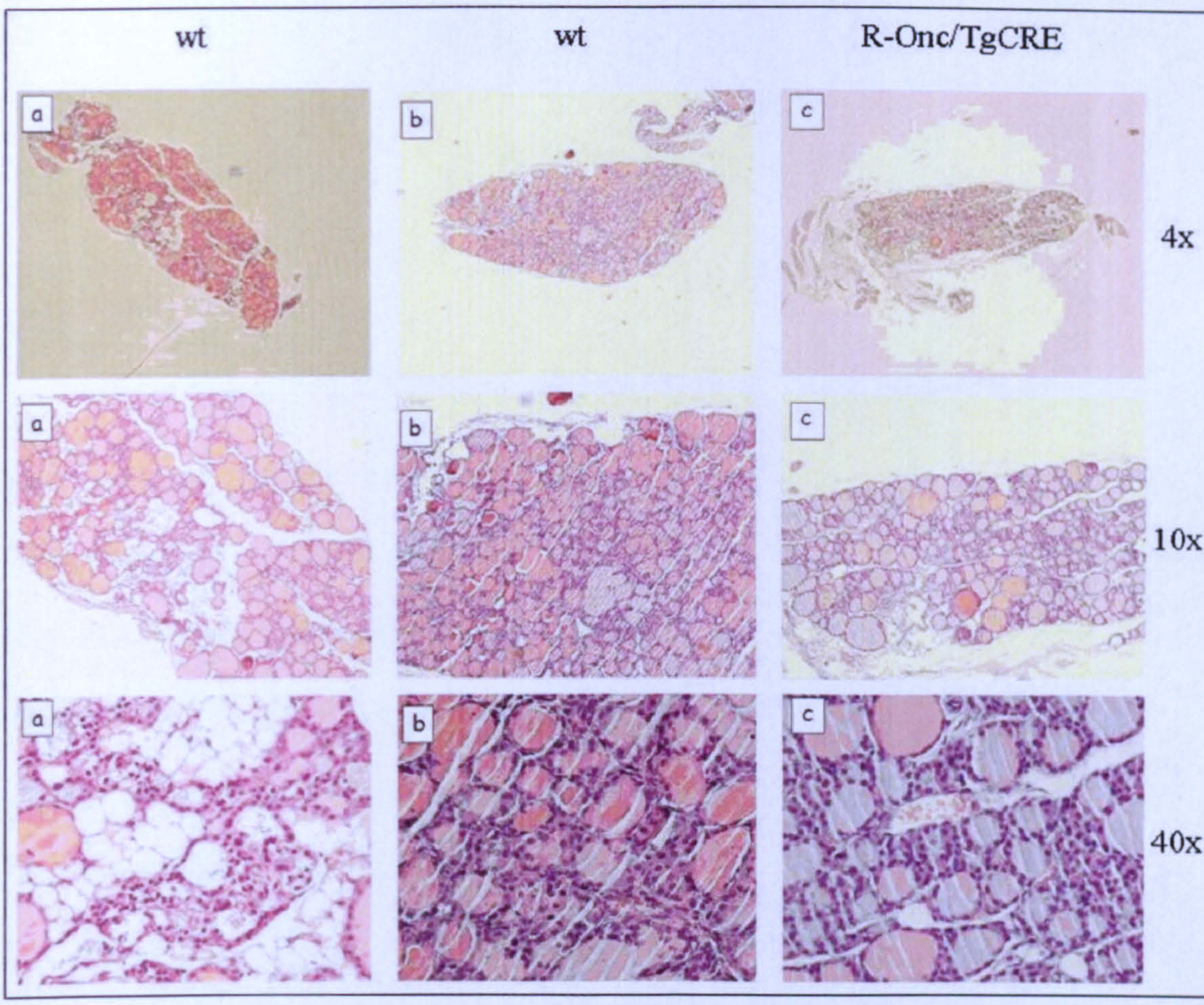

Figure 117. Histological sections of adult thyroid glands stained with hematoxylin/eosin. At the top of each image, the corresponding mouse genotype it is mentioned. a and b: control mice; c: mutant mouse. Magnification: 4x, 10x and 40x.

CHAPTER 4

DISCUSSION

Tumorigenesis has long been thought to be a multistep process. Neoplastic transformation requires numerous changes in the structure and function of cells. Malignant tumours usually arise from a protracted sequence of events in which each step creates an additional phenotypic aberration. For example, an emerging cancer cell might independently acquire the capabilities for extended proliferation, invasion of adjacent tissue and metastasis. Each step may be the manifestation of more than one new abnormality within the cancer cell.

Prolongation of cellular life span is thought to be an early event in tumorigenesis and would itself create a greater risk of cumulative mutations. The accretion of genetic damage is likely to play a role in tumour progression explaining how the malfunction of several different genes might combine to produce the malignant phenotype.

As demonstrated by several studies, colorectal tumours provide an excellent system for the study of genetic alterations involved in the development of a common human neoplasm.

These tumours seem to arise as a result of the mutational activation of oncogenes coupled with the mutational inactivation of tumour suppressor genes. For the formation of a malignant tumour mutations in at least four to five genes are necessary whereas few changes lead to benign tumorigenesis. Moreover, although the genetic alterations often occur according to a preferred sequence, the total accumulation of changes, rather than their order with respect to one another, is responsible for determining the biologic properties of the tumour (Fearon and Vogelstein, 1990).

From studies on Syrian hamster embryo (SHE) cells transfected with cloned DNA of the Harvey murine sarcoma virus (HaMSV), an oncogenic virus, it has been observed that this viral oncogene alone is insufficient to cause neoplastic transformation of normal or carcinogen-induced preneoplastic cells in culture. Following transfection with v-Ha-ras DNA, two steps are required for immortal, preneoplastic cells to become neoplastic, suggesting that, under certain conditions, for normal cells, three or more steps may be required for neoplastic progression (Thomassen et al., 1985).

Beside viral oncogenes, cellular genetic sequences, homologous to retroviral oncogenes, were identified and were proposed to have a major role in neoplastic development of certain cells.

The neoplastic transformation of primary rat embryonic fibroblasts and that of neonatal rat kidney cells has been shown to occur by two cooperating oncogenes, such as *ras* and *myc* or *ras* and the adenovirus E1a gene, whereas a single oncogene alone, could not lead to transformation (Land et al., 1983b; Ruley, 1983). In conditions in which either *ras* or *myc* alone had no obvious effect on the monolayer cultures, the two genes together could induce a dramatic alteration of the phenotype, allowing the growth of foci of morphologically altered cells. Moreover, these cotransfected cells were tumorigenic when introduced into nude mice (Land et al., 1983b).

In contrast, preneoplastic rat cells (Land et al., 1983b; Ruley, 1983) or mouse NIH 3T3 cells (Land et al., 1983a) can be neoplastically transformed by the *ras* gene alone. Similar results have been reported by Newbold and Overell (Newbold, 1983) for the transformation of preneoplastic but not normal Syrian hamster dermal fibroblasts to anchorage independence by the *ras* gene.

The observation of Land and Ruley that the *myc* and *ras* oncogenes can act cooperatively to induce the neoplastic transformation of normal cells was extended by

Thomassen also to the SHE cells. Since the *ras* oncogene can induce neoplastic transformation of immortalized cells, it is possible that *myc* oncogene induces immortality or establishment. Further studies are necessary to understand the function of *myc* oncogene activation also in other cellular systems.

The same experiments were carried out on immortalized preneoplastic cells, derived from the normal cells. It was observed that in addition to the acquisition and expression of the *ras* oncogene, further changes were needed for their transformation.

These results demonstrate the multistage nature of oncogene-induced transformation, suggesting that at least two or three steps are required for tumorigenesis of immortalized or normal cells (Thomassen et al., 1985).

On the contrary, other studies reported tumorigenic conversion by *ras* acting alone. Spandidos et al. (1984) observed that the *ras* oncogene from the human T24 bladder carcinoma cell line, carrying a substitution at amino acid position 12, alone could rescue early passage rodent cells from senescence as well as highly expressed normal *ras* proto-oncogene. The T24 oncogene, if transferred together with transcriptional enhancers, could also directly induce the malignant conversion of the same rodent cells (Spandidos and Wilkie, 1984).

Also tumorigenic conversion of rat embryo fibroblasts (REFs) by single transfected oncogene appeared to require high levels of gene expression. Clonal populations carrying high levels of the Ras protein were selectively favoured during long-term culture and they manifested the ability to seed tumours when inoculated into appropriate hosts. The Ras expression levels, analyzed in REF cultures, cotransfected with both *ras* and *myc* oncogenes, were found to decrease during *in vitro* passages. These experiment demonstrated as in the presence of a *myc* oncogene, low expression levels of a *ras* oncogene were sufficient to trigger tumorigenicity. Without the collaboration of a *myc* oncogene, the *ras* oncogene is able to convert the normal

phenotype into tumorigenic phenotype only when expressed at higher levels (>10-fold).

Furthermore, either distinct altered phenotypes or different capability to cooperate with *ras*, linked to different expression levels, were observed also for *myc* oncogene. The establishment of cell lines and the ability to cooperate with *ras* were in direct ratio to the *myc* expression levels (Land et al., 1986).

All these results lead to the conclusion that there is a threshold below which expression of a single gene has little or no consequence without the collaboration of a second alteration. This seemed to be our case, in which the ER-Ras^{V12} level in thyroid cells transfected with the bicistronic construct (carrying both c-*myc* and H*ras*^{V12} coding sequences) was about thirty fold lower than in Clone 11 (Cl11). The latter was able to dedifferentiate, as demonstrated previously in our laboratory by De Vita et al. (2005).

Although the use of cell lines has been of central importance in the development of cellular and molecular biology, their production is also linked to some problems. Transfection requires a large number of target cells to ensure that some cells of interest stably integrate the chosen DNA in a position suitable for expression. After transfection, the cells must be grown for long periods of time in culture, under selective pressure, to obtain sufficient numbers of cells expressing the gene of interest. Furthermore, the introduction of gene into cells can alter normal cellular physiology and different sites of gene integration lead to different behaviors and levels of expression of the introduced gene. Moreover, cell culture could induce selection of specific live cells to go through immortalization and can interfere with their differentiation when maintained separated from their original tissue source.

For the above reasons, our studies were aimed at investigating oncogenic cooperation *in vivo* as well as *in vitro*. Transgenic mice facilitate and ensure the presence of a conditional oncogene in all of the cells of interest at a common

integration site. By creating cohorts of mice with well-timed onsets of predictable tumours, these transgenic models would seem to provide ideal experimental models of spontaneous tumorigenesis. However, these transgenes create tissues in which virtually all the cells are expressing an activated oncogene. Hence, the transgenic model fails to address one of the most important aspects of tumorigenesis, i.e., the interactions of transformants with their normal neighbors during the early stages of this process.

The first step of this work was to create a bicistronic construct carrying H*ras*^{V12} and c-*myc* coding sequences that could be ubiquitously expressed and switched on and off in a reversible manner. Temporal and spatial control of gene activity is a fundamental tool for regulated protein expression. The "OFF/ON" gene switches allow the expression of cytotoxic and dominant negative proteins; the ability to reverse the expression of the target gene and the study of "gain of function" and "loss of function phenotypes" (De Vita et al., 2005; Jain et al., 2002; Karlsson et al., 2003; Shachaf et al., 2008; Wu et al., 2007).

Previously, a mouse strain with these characteristics was generated by Parmuit S. Jat et al. (1991). This strain harbours simian virus 40 (SV40) mutant strain tsA58 thermolabile large tumor antigen (TAg) gene under the control of the mouse major histocompatibility complex *H-2K*^{b} promoter to direct the expression to a broad range of tissues. The mice and the cells derived from them were able to survive for long time only at the permissive temperatures. It is noteworthy that determination of the amount of TAg by Western blot showed a direct correlation between the amount of TAg present and the growth potential of the cells. Cells in which only small amounts of TAg were produced showed stringent growth regulation, while cultures expressing high levels of TAg showed poor growth regulation (Jat et al., 1991).

Since the aim of this work was to investigate the multistep process of carcinogenesis as the epithelial carcinogenesis is, thyroid gland was chosen as a

suitable model for this purpose. In thyroid gland, the number and the nature of genes involved in the epithelial malignant transformation could be assayed and also the relationship between oncogene products and specific growth regulation pathways could be studied. In fact, thyroid neoplasias include a broad spectrum of tumours with different phenotypic characteristics and clinical behaviour, ranging from the highly differentiated benign adenomas through the slowly progressive, differentiated papillary and follicular carcinomas to the fatal anaplastic carcinomas (Hedinger et al., 1989). Moreover, a second characteristic of thyroid cell lines is that they retain typical biochemical markers such as thyroglobulin secretion and iodide concentration as well as a thyroid-specific combination of transcription factors as an index of their differentiated status. In addition, these cells depend on the presence of TSH for proliferation. Thus, their transformation and carcinogenesis can be related to their epithelial differentiation level. The expression of the transformed phenotype was seen to determine the block of the expression of the differentiation markers. (De Vita et al., 2005; Fusco et al., 1982)

Oncogenic mutations of Ras-family genes play an important role in malignant transformation. Their constitutive activation has been identified in tumors originating from the follicular epithelium of the thyroid gland, with variable frequencies, depending on the tumour type (Nikiforova et al., 2003; Tallini, 2002). RAS-activating mutations are associated with all types of thyroid malignancies, suggesting that they are an early event in thyroid tumorigenesis (Lemoine et al., 1989; Namba et al., 1990).

Also other studies demonstrated as after introduction of the *ras* oncogene into rat thyroid cells (FRTL-5 cells), the cells were able to grow in an anchorage-independent manner and in the absence of the six growth factors (De Vita et al., 2005; Fusco et al., 1987a). But not all thyroid cell lines behaved in the same manner. Some of them, such as PC cells, showed a fully transformed phenotype also after infection with both *ras*

and *myc* genes. They became hormone independent, grew in a semisolid medium, and were tumorigenic after injection into athymic mice. These results demonstrate that cell lines from rat thyroid gland are susceptible to one-step or two-step transformation upon infection with retroviruses bearing these two cooperating oncogenes *ras* and *myc* (Fusco et al., 1987a). Furthermore, the same authors observed also that the highest levels of *myc* were detected in the more malignant, undifferentiated thyroid cell lines. By blocking the synthesis of the Myc protein with an antisense oligonucleotide, they observed an inhibitory effect of the antisense oligonucleotide on growth of the cells and a significant reduction in their capability to grow on a semisolid medium. These results indicated that the *myc* overexpression is an important event in the process of transformation of thyroid cells and that its downregulation inhibits the proliferation of carcinoma thyroid cell lines (Cerutti et al., 1996).

The experiments described above were conducted in order to test the targeting vector in different systems: *in vitro* and *in vivo*.

In the first part of this work, we checked for the expression of proteins of the first construct (the ER-ras-myc-PR cassette) (Fig. 39 RasMyc plasmid) after transient transfections in different cell lines, such as HeLa, NIH3T3, FRTL-5 and Cos7 cells. The results showed that just in Cos7 cells, both proteins, the one upstream (ER-Ras^{V12}) and the one downstream (c-MycPR) of the IRES, were detected. It could be supposed that in the other cell lines the IRES was not able to lead the second cistron translation. This result could be explained by the fact that the activity of IRES, in spite of its maximum efficiency, remains cell-type-dependent. Moreover, in Cos7 cells, besides c-MycPR expression, even the ER-Ras^{V12} amount was much more higher than the other cell lines (Figs. 55, 57 and 59). It could be due to the fact that the same promoter (EF1α) can have different strength in different cell lines.

To induce tumorigenesis an overexpression of the c-Myc protein, was found necessary. Therefore another cloning strategy was planned to invert the two cistrons upstream and downstream of the IRES to create the myc-PR-ER-ras cassette (Fig. 50 MycRas plasmid). This MycRas construct was tested by stable transfection in FRTL-5 cells. By western blot, some clones were found expressing both oncogenes and the one with the highest ER-Ras^{V12} expression was chosen to work on.

The following experiments were carried out in the same cell system (FRTL-5) in order to analyze the genes involved in thyroid differentiation after oncogenes activation. However, by Real Time PCR it was observed that any gene, which was involved in thyroid specificity maintenance, was affected.

Moreover, on the basis of other experiments about contribution on proliferation, the concomitant activation of the two oncogenes seems to have some effect. Thus, even though we were able to reconfirm the data obtained in a previous work in which they discovered that high levels of ER-Ras^{V12} expression induced cellular dedifferentiation and TSH independent growth (De Vita et al., 2005), it was not possible to observe any contribution of the c-MycPR protein.

In our system the amount of the ER-Ras^{V12} was about thirty fold lower than that obtained in the experiments carried out by De Vita et al (2005).

The Raf-MEK-ERK kinase cascade, relaying extracellular stimuli to the nucleus, is mostly studied as Ras effector Hence also the levels of ERK phosphorylation were analyzed in our *in vitro* system. In our analysis, even though the ERK phosphorylation resulted in a constant activation regardless of the treatment to activate ER-Ras^{V12}, the downstream accumulation of c-fos was not observed. These results could be explained assuming either that this weak ERK activation could remain under the threshold to be a critical determinant of the biological response or that the observed ERK induction was not due to the Ras-Raf-MEK-ERK pathway.

Both the hypotheses would provide a relationship between the range of ERK activation and the appropriate ER-Ras^{V12} activation threshold, necessary to promote some biological effect. In fact, the magnitude of ERK activation is responsible for various outcomes. The dynamic range of ERK activation is known to be important for the determination of various cell fates, with drastically different phenotypes driven by the lower *versus* the higher range of activation. In order to control sensitivity of the cascade to stimulus and to provide a mechanism to allow adaptive behaviour of the cascade in chronic or complex signaling environments, the cells were able to develop a fine tuning system downstream of Ras. The Ras activation directly regulates the Impedes Mitogenic signal Propagation (IMP) acting as a steady-state resistor within the Raf-MEK-ERK kinase module negatively regulating ERK activation. The mechanism of inhibition appears to be through inactivation (preceded by the IMP autopolyubiquitination) of the Kinase Suppressor of Ras (KSR), the best characterized mammalian MAPK scaffold protein. KSR directly interacts with Raf-1, MEK1/2 and ERK1/2. Upon Ras activation, KSR translocates with MEK1/2 to the plasma membrane, bringing MEK1/2 in close proximity to its activator Raf-1 and downstream effectors ERK1/2. These interactions lead to the formation of Raf-MEK-ERK complex, thereby facilitating the activation of ERK1/2. By this way, it is possible to speculate how scaffolds could set the sensitivity of the system or even change the fundamental system output of the MAPK module. The relationship between the induction of Raf-MEK and the liberation of KSR provides a mechanism to tether MAPK mobilization to appropriate Ras activation threshold (Lin et al., 2009; Matheny et al., 2004; Matheny and White, 2009; Raman et al., 2007).

It has been demonstrated in the *Aspergillus nidulans* fungus that different levels of Ras regulate the order program of development (Som and Kolaparthi, 1994). Threshold levels of ERK activation, determined by different growth factors and

concentration of external stimuli, have been shown observed to drive various output and it could depend on the level and duration of activation of protein kinases (Ho et al., 2005; Traverse et al., 1992). Moreover, the kinetics of ERK induction is dependent on the subcellular localization of both ERK and its upstream intermediates. In addition to the functionally distinct plasma membrane microdomains, Ras and/or MAPK signaling has been observed on endosomes, endoplasmic reticulum, Golgi apparatus and mitocondria. This compartmentalized signaling could be accomplished by using distinct upstream pathways providing one explanation for the complexity of signaling outputs elaborated by individual signaling molecules (Mor and Philips, 2006). The amplitude of ERK activation could be modulated and might contribute to the generation of stimulus-specific biological responses. These stimuli could influence both the extent of activation and the localization (such as nuclear translocation and accumulation) of activated ERK in the same cell type, thus generating discrete phenotypic responses to distinct environmental stimuli (Whitehurst et al., 2004). Moreover, the specific cellular localization is also fundamental in imposing the sensitivity of the module to the activation (Harding et al., 2005).

Regarding c-Myc, a similar hypothesis could be done from the results observed by Felsher et al (2008). On the basis of their work, a threshold level of Myc expression exists to maintain the tumour phenotype, and the switch from a gene expression program of proliferation to a state of proliferative arrest and apoptosis depends on it (Shachaf et al., 2008). Infact, many experiments have been conducted to show how the suppression of Myc overexpression is sufficient to induce sustained tumour regression, demonstrating that following Myc inactivation even highly genetically complex tumours variously undergo proliferative arrest, differentiation, and apoptosis becoming reversible. Even if the specific consequences of Myc inactivation appeared to depend both on the type of cancer as well as the constellation of genetic events unique to a

given tumour, oncogene-induced senescence seemed to be an important mechanism by which normal cells were restrained from malignant transformation in diverse tumour types including lymphoma, osteosarcoma, and hepatocellular carcinoma (Wu et al., 2007). After prolonged Myc inactivation, some tumors exhibited a distinct propensity to relapse. However, subsequent reactivation of Myc did not always restore the cells' malignant properties but instead induced apoptosis. Thus, brief Myc inactivation appeared to cause epigenetic changes in tumour cells that render them insensitive to Myc-induced tumorigenesis (Arvanitis and Felsher, 2005, 2006; Jain et al., 2002; Karlsson et al., 2003).

Under these circumstances, it seems that a Myc threshold level could be necessary to trigger tumorigenesis.

One of the mechanisms adopted by the cell to nullify the growth advantage afforded by oncogenic activation is the coupling between tumour suppression and the program that drives cell proliferation. The Myc transcription factor is a prototypical example of this since Myc-induced apoptosis is a key intrinsic tumour suppressor mechanism that limits Myc's oncogenic potential. Hence, also the balance between apoptosis and proliferation is regulated by different amounts of the protein. Distinct threshold levels of Myc were observed to govern its output *in vivo* (Daniel J. Murphy, 2008).

Moreover, a correlation between the level of c-myc mRNA and the aggressiveness of the tumour was found, specifically in thyroid (Romano et al., 1993).

It is also plausible to imagine that thyroid cells are able to activate an unknown mechanism that regulates the coexistence of these two oncogenic proteins and consequently of their target genes to prevent the tumour formation.

BIBLIOGRAPHY

Adams, J.M., Gerondakis, S., Webb, E., Corcoran, L.M., and Cory, S. (1983). Cellular myc oncogene is altered by chromosome translocation to an immunoglobulin locus in murine plasmacytomas and is rearranged similarly in human Burkitt lymphomas. Proc Natl Acad Sci U S A *80*, 1982-1986.

Alitalo, K., Schwab, M., Lin, C.C., Varmus, H.E., and Bishop, J.M. (1983). Homogeneously staining chromosomal regions contain amplified copies of an abundantly expressed cellular oncogene (c-myc) in malignant neuroendocrine cells from a human colon carcinoma. Proc Natl Acad Sci U S A *80*, 1707-1711.

Amati, B., Frank, S.R., Donjerkovic, D., and Taubert, S. (2001). Function of the c-Myc oncoprotein in chromatin remodeling and transcription. Biochim Biophys Acta *1471*, M135-145.

Arvanitis, C., and Felsher, D.W. (2005). Conditionally MYC: insights from novel transgenic models. Cancer Lett *226*, 95-99.

Arvanitis, C., and Felsher, D.W. (2006). Conditional transgenic models define how MYC initiates and maintains tumorigenesis. Semin Cancer Biol *16*, 313-317.

Askew, D.S., Ashmun, R.A., Simmons, B.C., and Cleveland, J.L. (1991). Constitutive c-myc expression in an IL-3-dependent myeloid cell line suppresses cell cycle arrest and accelerates apoptosis. Oncogene *6*, 1915-1922.

Barbacid, M. (1987). ras genes. *Annu Rev Biochem 56, 779-827.*

Bello-Fernandez, C., Packham, G., and Cleveland, J.L. (1993). The ornithine decarboxylase gene is a transcriptional target of c-Myc. Proc Natl Acad Sci U S A *90*, 7804-7808.

Bergers, G., Hanahan, D., and Coussens, L.M. (1998). Angiogenesis and apoptosis are cellular parameters of neoplastic progression in transgenic mouse models of tumorigenesis. Int J Dev Biol *42*, 995-1002.

Birnie, K.M.R.a.G.D. (1996). *Myc* oncogenes: the enigmatic family Biochem J *314*, 713-721.

Blackwood, E.M., and Eisenman, R.N. (1991). Max: a helix-loop-helix zipper protein that forms a sequence-specific DNA-binding complex with Myc. Science *251*, 1211-1217.

Borman, A.M., Le Mercier, P., Girard, M., and Kean, K.M. (1997). Comparison of picornaviral IRES-driven internal initiation of translation in cultured cells of different origins. Nucleic Acids Res *25*, 925-932.

Bos, J.L. (1989). ras oncogenes in human cancer: a review. Cancer Res *49*, 4682-4689.

Bouchard, C., Dittrich, O., Kiermaier, A., Dohmann, K., Menkel, A., Eilers, M., and Luscher, B. (2001). Regulation of cyclin D2 gene expression by the Myc/Max/Mad

network: Myc-dependent TRRAP recruitment and histone acetylation at the cyclin D2 promoter. Genes Dev *15*, 2042-2047.

Bouchard, M., Souabni, A., and Busslinger, M. (2004). Tissue-specific expression of cre recombinase from the Pax8 locus. Genesis *38*, 105-109.

Bouchard, M., Souabni, A., Mandler, M., Neubuser, A., and Busslinger, M. (2002). Nephric lineage specification by Pax2 and Pax8. Genes Dev *16*, 2958-2970.

Brenner, C., Deplus, R., Didelot, C., Loriot, A., Vire, E., De Smet, C., Gutierrez, A., Danovi, D., Bernard, D., Boon, T., *et al.* (2005). Myc represses transcription through recruitment of DNA methyltransferase corepressor. EMBO J *24*, 336-346.

Brough, D.E., Hofmann, T.J., Ellwood, K.B., Townley, R.A., and Cole, M.D. (1995). An essential domain of the c-myc protein interacts with a nuclear factor that is also required for E1A-mediated transformation. Mol Cell Biol *15*, 1536-1544.

Burman, K.D., Djuh, Y.Y., LaRocca, R.V., Nunes, M.E., D'Avis, J.C., Nicholson, D.E., and Wartofsky, L. (1987). c-myc expression in the thyroid. I: Normal, adenomatous, and cancerous thyroid tissue. Horm Metab Res Suppl *17*, 63-65.

Campbell, P.M., and Der, C.J. (2004). Oncogenic Ras and its role in tumor cell invasion and metastasis. Semin Cancer Biol *14*, 105-114.

Capecchi, M.R. (1989). Altering the genome by homologous recombination. Science *244*, 1288-1292.

Cerutti, J., Trapasso, F., Battaglia, C., Zhang, L., Martelli, M.L., Visconti, R., Berlingieri, M.T., Fagin, J.A., Santoro, M., and Fusco, A. (1996). Block of c-myc expression by antisense oligonucleotides inhibits proliferation of human thyroid carcinoma cell lines. Clin Cancer Res *2*, 119-126.

Chang, D.W., Claassen, G.F., Hann, S.R., and Cole, M.D. (2000). The c-Myc transactivation domain is a direct modulator of apoptotic versus proliferative signals. Mol Cell Biol *20*, 4309-4319.

Cole, M.D. (1986). The myc oncogene: its role in transformation and differentiation. Annu Rev Genet *20*, 361-384.

Coller, H.A., Grandori, C., Tamayo, P., Colbert, T., Lander, E.S., Eisenman, R.N., and Golub, T.R. (2000). Expression analysis with oligonucleotide microarrays reveals that MYC regulates genes involved in growth, cell cycle, signaling, and adhesion. Proc Natl Acad Sci U S A *97*, 3260-3265.

Compere, S.J., Baldacci, P., Sharpe, A.H., Thompson, T., Land, H., and Jaenisch, R. (1989). The ras and myc oncogenes cooperate in tumor induction in many tissues when introduced into midgestation mouse embryos by retroviral vectors. Proc Natl Acad Sci U S A *86*, 2224-2228.

Conzen, S.D., Gottlob, K., Kandel, E.S., Khanduri, P., Wagner, A.J., O'Leary, M., and Hay, N. (2000). Induction of cell cycle progression and acceleration of apoptosis are two separable functions of c-Myc: transrepression correlates with acceleration of apoptosis. Mol Cell Biol *20*, 6008-6018.

Creancier, L., Mercier, P., Prats, A.C., and Morello, D. (2001). c-myc Internal ribosome entry site activity is developmentally controlled and subjected to a strong translational repression in adult transgenic mice. Mol Cell Biol *21*, 1833-1840.

Dalla-Favera, R., Bregni, M., Erikson, J., Patterson, D., Gallo, R.C., and Croce, C.M. (1982a). Human c-myc onc gene is located on the region of chromosome 8 that is translocated in Burkitt lymphoma cells. Proc Natl Acad Sci U S A *79*, 7824-7827.

Dalla-Favera, R., Gelmann, E.P., Martinotti, S., Franchini, G., Papas, T.S., Gallo, R.C., and Wong-Staal, F. (1982b). Cloning and characterization of different human sequences related to the onc gene (v-myc) of avian myelocytomatosis virus (MC29). Proc Natl Acad Sci U S A *79*, 6497-6501.

Dang, C.V. (1999). c-Myc target genes involved in cell growth, apoptosis, and metabolism. Mol Cell Biol *19*, 1-11.

Dang, C.V., O'Donnell, K.A., Zeller, K.I., Nguyen, T., Osthus, R.C., and Li, F. (2006). The c-Myc target gene network. Semin Cancer Biol *16*, 253-264.

Daniel J. Murphy, M.R.J., Laurent Pouyet, Anthony Karnezis, Ksenya Shchors, Duyen A. Bui, Lamorna Brown-Swigart, Leisa Johnson, and Gerard I. Evan (2008). Distinct threshold govern Myc's biological output in vivo. Cancer Cell *14*, 447-457.

Davis, A.C., Wims, M., Spotts, G.D., Hann, S.R., and Bradley, A. (1993). A null c-myc mutation causes lethality before 10.5 days of gestation in homozygotes and reduced fertility in heterozygous female mice. Genes Dev *7*, 671-682.

De Felice, M., Ovitt, C., Biffali, E., Rodriguez-Mallon, A., Arra, C., Anastassiadis, K., Macchia, P.E., Mattei, M.G., Mariano, A., Scholer, H., *et al.* (1998). A mouse model for hereditary thyroid dysgenesis and cleft palate. Nat Genet *19*, 395-398.

De Vita, G., Bauer, L., da Costa, V.M., De Felice, M., Baratta, M.G., De Menna, M., and Di Lauro, R. (2005). Dose-dependent inhibition of thyroid differentiation by RAS oncogenes. Mol Endocrinol *19*, 76-89.

Der, D.E., Picus, D., and Brown, D.B. (2007). Use of a hybrid fluoroscopic/three-dimensional tomographic unit to assist in targeting a hepatic metastasis for thermal ablation. J Vasc Interv Radiol *18*, 583-584.

Downward, J. (2003). Targeting RAS signalling pathways in cancer therapy. Nat Rev Cancer *3*, 11-22.

Eisenman, R.N. (2001). Deconstructing Myc. Genes & Development *15*, 2023-2030.

Eisenman, R.N., Tachibana, C.Y., Abrams, H.D., and Hann, S.R. (1985). V-myc- and c-myc-encoded proteins are associated with the nuclear matrix. Mol Cell Biol *5*, 114-126.

Escot, C., Theillet, C., Lidereau, R., Spyratos, F., Champeme, M.H., Gest, J., and Callahan, R. (1986). Genetic alteration of the c-myc protooncogene (MYC) in human primary breast carcinomas. Proc Natl Acad Sci U S A *83*, 4834-4838.

Evan, G.I., Wyllie, A.H., Gilbert, C.S., Littlewood, T.D., Land, H., Brooks, M., Waters, C.M., Penn, L.Z., and Hancock, D.C. (1992). Induction of apoptosis in fibroblasts by c-myc protein. Cell *69*, 119-128.

Facchini, L.M., and Penn, L.Z. (1998). The molecular role of Myc in growth and transformation: recent discoveries lead to new insights. FASEB J *12*, 633-651.

Fearon, E.R., and Vogelstein, B. (1990). A genetic model for colorectal tumorigenesis. Cell *61*, 759-767.

Fenske, T.S., Pengue, G., Mathews, V., Hanson, P.T., Hamm, S.E., Riaz, N., and Graubert, T.A. (2004). Stem cell expression of the AML1/ETO fusion protein induces a myeloproliferative disorder in mice. Proc Natl Acad Sci U S A *101*, 15184-15189.

Fernandez P.C., Frank S.R., Wang L., Schroeder M., Liu S., Greene J., Cocito A., and B., A. (2003). Genomic targets of the human c-Myc protein. Genes & Development *17*, 1115–1129.

Flinn, E.M., Busch, C.M., and Wright, A.P. (1998). myc boxes, which are conserved in myc family proteins, are signals for protein degradation via the proteasome. Mol Cell Biol *18*, 5961-5969.

Frank, S.R., Schroeder, M., Fernandez, P., Taubert, S., and Amati, B. (2001). Binding of c-Myc to chromatin mediates mitogen-induced acetylation of histone H4 and gene activation. Genes Dev *15*, 2069-2082.

Friedrich, G., and Soriano, P. (1991). Promoter traps in embryonic stem cells: a genetic screen to identify and mutate developmental genes in mice. Genes Dev *5*, 1513-1523.

Fusco, A., Berlingieri, M.T., Di Fiore, P.P., Portella, G., Grieco, M., and Vecchio, G. (1987a). One- and two-step transformations of rat thyroid epithelial cells by retroviral oncogenes. Mol Cell Biol *7*, 3365-3370.

Fusco, A., Grieco, M., Santoro, M., Berlingieri, M.T., Pilotti, S., Pierotti, M.A., Della Porta, G., and Vecchio, G. (1987b). A new oncogene in human thyroid papillary carcinomas and their lymph-nodal metastases. Nature *328*, 170-172.

Fusco, A., Pinto, A., Tramontano, D., Tajana, G., Vecchio, G., and Tsuchida, N. (1982). Block in the expression of differentiation markers of rat thyroid epithelial cells by transformation with Kirsten murine sarcoma virus. Cancer Res *42*, 618-626.

Garcia-Rostan, G., Zhao, H., Camp, R.L., Pollan, M., Herrero, A., Pardo, J., Wu, R., Carcangiu, M.L., Costa, J., and Tallini, G. (2003). ras mutations are associated with aggressive tumor phenotypes and poor prognosis in thyroid cancer. J Clin Oncol *21*, 3226-3235.

Gartel, A.L., and Shchors, K. (2003). Mechanisms of c-myc-mediated transcriptional repression of growth arrest genes. Exp Cell Res *283*, 17-21.

Gartel, A.L., Ye, X., Goufman, E., Shianov, P., Hay, N., Najmabadi, F., and Tyner, A.L. (2001). Myc represses the p21(WAF1/CIP1) promoter and interacts with Sp1/Sp3. Proc Natl Acad Sci U S A *98*, 4510-4515.

Ghattas, I.R., Sanes, J.R., and Majors, J.E. (1991). The encephalomyocarditis virus internal ribosome entry site allows efficient coexpression of two genes from a recombinant provirus in cultured cells and in embryos. Mol Cell Biol *11*, 5848-5859.

Gimm, O. (2001). Thyroid cancer. Cancer Lett *163*, 143-156.

Grandori, C., Cowley, S.M., James, L.P., and Eisenman, R.N. (2000). The Myc/Max/Mad network and the transcriptional control of cell behavior. Annu Rev Cell Dev Biol *16*, 653-699.

Greulich, H., and Erikson, R.L. (1998). An analysis of Mek1 signaling in cell proliferation and transformation. J Biol Chem *273*, 13280-13288.

Gulbins, E., Coggeshall, K.M., Baier, G., Katzav, S., Burn, P., and Altman, A. (1993). Tyrosine kinase-stimulated guanine nucleotide exchange activity of Vav in T cell activation. Science *260*, 822-825.

Guo, Q.M., Malek, R.L., Kim, S., Chiao, C., He, M., Ruffy, M., Sanka, K., Lee, N.H., Dang, C.V., and Liu, E.T. (2000). Identification of c-myc responsive genes using rat cDNA microarray. Cancer Res *60*, 5922-5928.

Hanahan, D. (1989). Transgenic mice as probes into complex systems. Science *246*, 1265-1275.

Hann S. R., Sears R. C., and Sealy, L. (1994). The alternatively initiated c-Myc proteins differentially regulate transcription through a noncaninical DNA-binding site. Genes & Development *8*, 2441-2452.

Hann, S.R., and Eisenman, R.N. (1984). Proteins encoded by the human c-myc oncogene: differential expression in neoplastic cells. Mol Cell Biol *4*, 2486-2497.

Hann, S.R., Sloan-Brown, K., and Spotts, G.D. (1992). Translational activation of the non-AUG-initiated c-myc 1 protein at high cell densities due to methionine deprivation. Genes Dev *6*, 1229-1240.

Hanson, K.D., Shichiri, M., Follansbee, M.R., and Sedivy, J.M. (1994). Effects of c-myc expression on cell cycle progression. Mol Cell Biol *14*, 5748-5755.

Harding, A., Tian, T., Westbury, E., Frische, E., and Hancock, J.F. (2005). Subcellular localization determines MAP kinase signal output. Curr Biol *15*, 869-873.

Hashimoto, T., Matsubara, F., Mizukami, Y., Miyazaki, I., Michigishi, T., and Yanaihara, N. (1990). Tumor markers and oncogene expression in thyroid cancer using biochemical and immunohistochemical studies. Endocrinol Jpn *37*, 247-254.

Hedinger, C., Williams, E.D., and Sobin, L.H. (1989). The WHO histological classification of thyroid tumors: a commentary on the second edition. Cancer *63*, 908-911.

Ho, W.C., Uniyal, S., Zhou, H., Morris, V.L., and Chan, B.M. (2005). Threshold levels of ERK activation for chemotactic migration differ for NGF and EGF in rat pheochromocytoma PC12 cells. Mol Cell Biochem *271*, 29-41.

Jain, M., Arvanitis, C., Chu, K., Dewey, W., Leonhardt, E., Trinh, M., Sundberg, C.D., Bishop, J.M., and Felsher, D.W. (2002). Sustained loss of a neoplastic phenotype by brief inactivation of MYC. Science *297*, 102-104.

Jang, S.K., and Wimmer, E. (1990). Cap-independent translation of encephalomyocarditis virus RNA: structural elements of the internal ribosomal entry site and involvement of a cellular 57-kD RNA-binding protein. Genes Dev *4*, 1560-1572.

Jat, P.S., Noble, M.D., Ataliotis, P., Tanaka, Y., Yannoutsos, N., Larsen, L., and Kioussis, D. (1991). Direct derivation of conditionally immortal cell lines from an H-2Kb-tsA58 transgenic mouse. Proc Natl Acad Sci U S A *88*, 5096-5100.

Juin, P., Hueber, A.O., Littlewood, T., and Evan, G. (1999). c-Myc-induced sensitization to apoptosis is mediated through cytochrome c release. Genes Dev *13*, 1367-1381.

Karlsson, A., Giuriato, S., Tang, F., Fung-Weier, J., Levan, G., and Felsher, D.W. (2003). Genomically complex lymphomas undergo sustained tumor regression upon MYC inactivation unless they acquire novel chromosomal translocations. Blood *101*, 2797-2803.

Kato, G.J., Barrett, J., Villa-Garcia, M., and Dang, C.V. (1990). An amino-terminal c-myc domain required for neoplastic transformation activates transcription. Mol Cell Biol *10*, 5914-5920.

Kato, G.J., Lee, W.M., Chen, L.L., and Dang, C.V. (1992). Max: functional domains and interaction with c-Myc. Genes Dev *6*, 81-92.

Kauffmann-Zeh, A., Rodriguez-Viciana, P., Ulrich, E., Gilbert, C., Coffer, P., Downward, J., and Evan, G. (1997). Suppression of c-Myc-induced apoptosis by Ras signalling through PI(3)K and PKB. Nature *385*, 544-548.

Kazlauskas, A., Ellis, C., Pawson, T., and Cooper, J.A. (1990). Binding of GAP to activated PDGF receptors. Science *247*, 1578-1581.

Kellendonk, C., Tronche, F., Monaghan, A.P., Angrand, P.O., Stewart, F., and Schutz, G. (1996). Regulation of Cre recombinase activity by the synthetic steroid RU 486. Nucleic Acids Res *24*, 1404-1411.

Kennedy, S.G., Wagner, A.J., Conzen, S.D., Jordan, J., Bellacosa, A., Tsichlis, P.N., and Hay, N. (1997). The PI 3-kinase/Akt signaling pathway delivers an anti-apoptotic signal. Genes Dev *11*, 701-713.

Khosravi-Far, R., and Der, C.J. (1994). The Ras signal transduction pathway. Cancer Metastasis Rev *13*, 67-89.

Kimura, S., Hara, Y., Pineau, T., Fernandez-Salguero, P., Fox, C.H., Ward, J.M., and Gonzalez, F.J. (1996). The T/ebp null mouse: thyroid-specific enhancer-binding protein is essential for the organogenesis of the thyroid, lung, ventral forebrain, and pituitary. Genes Dev *10*, 60-69.

Kimura, S., Ward, J.M., and Minoo, P. (1999). Thyroid-specific enhancer-binding protein/thyroid transcription factor 1 is not required for the initial specification of the thyroid and lung primordia. Biochimie *81*, 321-327.

Land, H., Chen, A.C., Morgenstern, J.P., Parada, L.F., and Weinberg, R.A. (1986). Behavior of myc and ras oncogenes in transformation of rat embryo fibroblasts. Mol Cell Biol *6*, 1917-1925.

Land, H., Parada, L.F., and Weinberg, R.A. (1983a). Cellular oncogenes and multistep carcinogenesis. Science *222*, 771-778.

Land, H., Parada, L.F., and Weinberg, R.A. (1983b). Tumorigenic conversion of primary embryo fibroblasts requires at least two cooperating oncogenes. Nature *304*, 596-602.

Lazzaro, D., Price, M., de Felice, M., and Di Lauro, R. (1991). The transcription factor TTF-1 is expressed at the onset of thyroid and lung morphogenesis and in restricted regions of the foetal brain. Development *113*, 1093-1104.

Lemoine, N.R., Mayall, E.S., Wyllie, F.S., Farr, C.J., Hughes, D., Padua, R.A., Thurston, V., Williams, E.D., and Wynford-Thomas, D. (1988). Activated ras oncogenes in human thyroid cancers. Cancer Res *48*, 4459-4463.

Lemoine, N.R., Mayall, E.S., Wyllie, F.S., Williams, E.D., Goyns, M., Stringer, B., and Wynford-Thomas, D. (1989). High frequency of ras oncogene activation in all stages of human thyroid tumorigenesis. Oncogene *4*, 159-164.

Leon, J., Guerrero, I., and Pellicer, A. (1987). Differential expression of the ras gene family in mice. Mol Cell Biol *7*, 1535-1540.

Levens, D.L. (2003). Reconstructing MYC. Genes Dev *17*, 1071-1077.

Li, B.Q., Kaplan, D., Kung, H.F., and Kamata, T. (1992). Nerve growth factor stimulation of the Ras-guanine nucleotide exchange factor and GAP activities. Science *256*, 1456-1459.

Li, L.H., Nerlov, C., Prendergast, G., MacGregor, D., and Ziff, E.B. (1994). c-Myc represses transcription in vivo by a novel mechanism dependent on the initiator element and Myc box II. EMBO J *13*, 4070-4079.

Li, Y., Holland, C.A., Hartley, J.W., and Hopkins, N. (1984). Viral integration near c-myc in 10-20% of mcf 247-induced AKR lymphomas. Proc Natl Acad Sci U S A *81*, 6808-6811.

Lin, J., Harding, A., Giurisato, E., and Shaw, A.S. (2009). KSR1 modulates the sensitivity of mitogen-activated protein kinase pathway activation in T cells without altering fundamental system outputs. Mol Cell Biol *29*, 2082-2091.

Luscher, B., and Eisenman, R.N. (1990). New light on Myc and Myb. Part I. Myc. Genes Dev *4*, 2025-2035.

Malumbres, M., and Barbacid, M. (2003). RAS oncogenes: the first 30 years. Nat Rev Cancer *3*, 459-465.

Mansouri, A., Chowdhury, K., and Gruss, P. (1998). Follicular cells of the thyroid gland require Pax8 gene function. Nat Genet *19*, 87-90.

Marcu, K.B., Bossone, S.A., and Patel, A.J. (1992). myc function and regulation. Annu Rev Biochem *61*, 809-860.

Marcu, K.B., Harris, L.J., Stanton, L.W., Erikson, J., Watt, R., and Croce, C.M. (1983). Transcriptionally active c-myc oncogene is contained within NIARD, a DNA sequence associated with chromosome translocations in B-cell neoplasia. Proc Natl Acad Sci U S A *80*, 519-523.

Marina Vita, M.H. (2006). The Myc oncoprotein as a therapeutic target for human cancer. Seminars in Cancer Biology *16*, 318-330.

Matallanas, D., Arozarena, I., Berciano, M.T., Aaronson, D.S., Pellicer, A., Lafarga, M., and Crespo, P. (2003). Differences on the inhibitory specificities of H-Ras, K-Ras, and N-Ras (N17) dominant negative mutants are related to their membrane microlocalization. J Biol Chem *278*, 4572-4581.

Matheny, S.A., Chen, C., Kortum, R.L., Razidlo, G.L., Lewis, R.E., and White, M.A. (2004). Ras regulates assembly of mitogenic signalling complexes through the effector protein IMP. Nature *427*, 256-260.

Matheny, S.A., and White, M.A. (2009). Signaling threshold regulation by the Ras effector IMP. J Biol Chem *284*, 11007-11011.

McMahon, S.B., Van Buskirk, H.A., Dugan, K.A., Copeland, T.D., and Cole, M.D. (1998). The novel ATM-related protein TRRAP is an essential cofactor for the c-Myc and E2F oncoproteins. Cell *94*, 363-374.

McMahon, S.B., Wood, M.A., and Cole, M.D. (2000). The essential cofactor TRRAP recruits the histone acetyltransferase hGCN5 to c-Myc. Mol Cell Biol *20*, 556-562.

Medema, R.H., de Vries-Smits, A.M., van der Zon, G.C., Maassen, J.A., and Bos, J.L. (1993). Ras activation by insulin and epidermal growth factor through enhanced exchange of guanine nucleotides on p21ras. Mol Cell Biol *13*, 155-162.

Menssen, A., and Hermeking, H. (2002). Characterization of the c-MYC-regulated transcriptome by SAGE: identification and analysis of c-MYC target genes. Proc Natl Acad Sci U S A *99*, 6274-6279.

Mor, A., and Philips, M.R. (2006). Compartmentalized Ras/MAPK signaling. Annu Rev Immunol *24*, 771-800.

Mountford, P.S., and Smith, A.G. (1995). Internal ribosome entry sites and dicistronic RNAs in mammalian transgenesis. Trends Genet *11*, 179-184.

Namba, H., Rubin, S.A., and Fagin, J.A. (1990). Point mutations of ras oncogenes are an early event in thyroid tumorigenesis. Mol Endocrinol *4*, 1474-1479.

Nesbit, C.E., Tersak, J.M., and Prochownik, E.V. (1999). MYC oncogenes and human neoplastic disease. Oncogene *18*, 3004-3016.

Newbold, R.F., and Overell, R. W. (1983). Fibroblast immortality is a prerequisite for transformation by EJ c-Ha-ras oncogene. Nature *304*, 648-651.

Nikiforova, M.N., Lynch, R.A., Biddinger, P.W., Alexander, E.K., Dorn, G.W., 2nd, Tallini, G., Kroll, T.G., and Nikiforov, Y.E. (2003). RAS point mutations and PAX8-PPAR gamma rearrangement in thyroid tumors: evidence for distinct molecular pathways in thyroid follicular carcinoma. J Clin Endocrinol Metab *88*, 2318-2326.

Packham, G., and Cleveland, J.L. (1994). Ornithine decarboxylase is a mediator of c-Myc-induced apoptosis. Mol Cell Biol *14*, 5741-5747.

Palmieri, S., Kahn, P., and Graf, T. (*1983*). *Quail embryo* fibroblasts transformed by four v-myc-containing virus isolates show enhanced proliferation but are non tumorigenic. EMBO J *2*, 2385-2389.

Parlato, R., Rosica, A., Rodriguez-Mallon, A., Affuso, A., Postiglione, M.P., Arra, C., Mansouri, A., Kimura, S., Di Lauro, R., and De Felice, M. (2004). An integrated regulatory network controlling survival and migration in thyroid organogenesis. Dev Biol *276*, 464-475.

Patel, J.H., Du, Y., Ard, P.G., Phillips, C., Carella, B., Chen, C.J., Rakowski, C., Chatterjee, C., Lieberman, P.M., Lane, W.S., *et al.* (2004). The c-MYC oncoprotein is a substrate of the acetyltransferases hGCN5/PCAF and TIP60. Mol Cell Biol *24*, 10826-10834.

Pelengaris, S., Khan, M., and Evan, G. (2002). c-MYC: more than just a matter of life and death. Nat Rev Cancer *2*, 764-776.

Penn, L.J., Brooks, M.W., Laufer, E.M., Littlewood, T.D., Morgenstern, J.P., Evan, G.I., Lee, W.M., and Land, H. (*1990*). *Domains of human* c-myc protein required for autosuppression and cooperation with ras oncogenes are overlapping. Mol Cell Biol *10*, 4961-4966.

Peukert, K., Staller, P., Schneider, A., Carmichael, G., Hanel, F., and Eilers, M. (1997). An alternative pathway for gene regulation by Myc. EMBO J *16*, 5672-5686.

Pfeifer-Ohlsson, S., Rydnert, J., Goustin, A.S., Larsson, E., Betsholtz, C., and Ohlsson, R. (1985). Cell-type-specific pattern of myc protooncogene expression in developing human embryos. Proc Natl Acad Sci U S A *82*, 5050-5054.

Plachov, D., Chowdhury, K., Walther, C., Simon, D., Guenet, J.L., and Gruss, P. (1990). Pax8, a murine paired box gene expressed in the developing excretory system and thyroid gland. Development *110*, 643-651.

Porra, V., Bernier-Valentin, F., Trouttet-Masson, S., Berger-Dutrieux, N., Peix, J.L., Perrin, A., Selmi-Ruby, S., and Rousset, B. (2002). Characterization and semiquantitative analyses of pendrin expressed in normal and tumoral human thyroid tissues. J Clin Endocrinol Metab *87*, 1700-1707.

Prior, I.A., and Hancock, J.F. (2001). Compartmentalization of Ras proteins. J Cell Sci *114*, 1603-1608.

Raman, M., Chen, W., and Cobb, M.H. (2007). Differential regulation and properties of MAPKs. Oncogene *26*, 3100-3112.

Ramsay, G., Evan, G.I., and Bishop, J.M. (1984). The protein encoded by the human proto-oncogene c-myc. Proc Natl Acad Sci U S A *81*, 7742-7746.

Romano, M.I., Grattone, M., Karner, M.P., Moiguer, S., Tetelbaum, F., Romano, L.A., Illescas, E., Padin, R., Cueva, F., and Burdman, J.A. (1993). Relationship between the level of c-myc mRNA and histologic aggressiveness in thyroid tumors. Horm Res *39*, 161-165.

Rosalie Sears, G.L., James DeGregori, and Joseph R. Nevins (1999). Ras Enhances Myc Protein Stability. Molecular Cell *3*, 169–179.

Rothberg, P.G., Spandorfer, J.M., Erisman, M.D., Staroscik, R.N., Sears, H.F., Petersen, R.O., and Astrin, S.M. (1985). Evidence that c-myc expression defines two genetically distinct forms of colorectal adenocarcinoma. Br J Cancer *52*, 629-632.

Ruley, H.E. (1983). Adenovirus early region 1A enables viral and cellular transforming genes to transform primary cells in culture. Nature *304*, 602-606.

Salghetti, S.E., Kim, S.Y., and Tansey, W.P. (1999). Destruction of Myc by ubiquitin-mediated proteolysis: cancer-associated and transforming mutations stabilize Myc. EMBO J *18*, 717-726.

Samuels, M.L., Weber, M.J., Bishop, J.M., and McMahon, M. (1993). Conditional transformation of cells and rapid activation of the mitogen-activated protein kinase cascade by an estradiol-dependent human raf-1 protein kinase. Mol Cell Biol *13*, 6241-6252.

Schmid, P., Schulz, W.A., and Hameister, H. (1989). Dynamic expression pattern of the myc protooncogene in midgestation mouse embryos. Science *243*, 226-229.

Sears, R., Leone, G., DeGregori, J., and Nevins, J.R. (1999). Ras enhances Myc protein stability. Mol Cell *3*, 169-179.

Sears, R., Nuckolls, F., Haura, E., Taya, Y., Tamai, K., and Nevins, J.R. (2000). Multiple Ras-dependent phosphorylation pathways regulate Myc protein stability. Genes Dev *14*, 2501-2514.

Semsei, I., Ma, S.Y., and Cutler, R.G. (1989). Tissue and age specific expression of the myc proto-oncogene family throughout the life span of the C57BL/6J mouse strain. Oncogene *4*, 465-471.

Seoane, J., Pouponnot, C., Staller, P., Schader, M., Eilers, M., and Massague, J. (2001). TGFbeta influences Myc, Miz-1 and Smad to control the CDK inhibitor p15INK4b. Nat Cell Biol *3*, 400-408.

Shachaf, C.M., Gentles, A.J., Elchuri, S., Sahoo, D., Soen, Y., Sharpe, O., Perez, O.D., Chang, M., Mitchel, D., Robinson, W.H., *et al.* (2008). Genomic and proteomic analysis reveals a threshold level of MYC required for tumor maintenance. Cancer Res *68*, 5132-5142.

Sherman, S.I. (2003). Thyroid carcinoma. Lancet *361*, 501-511.

Som, T., and Kolaparthi, V.S. (1994). Developmental decisions in Aspergillus nidulans are modulated by Ras activity. Mol Cell Biol *14*, 5333-5348.

Soriano, P. (1999). Generalized lacZ expression with the ROSA26 Cre reporter strain. Nat Genet *21*, 70-71.

Spandidos, D.A., and Wilkie, N.M. (1984). Malignant transformation of early passage rodent cells by a single mutated human oncogene. Nature *310*, 469-475.

Spencer, C.A., and Groudine, M. (1991). Control of c-myc regulation in normal and neoplastic cells. Adv Cancer Res *56*, 1-48.

Spitzweg, C., Heufelder, A.E., and Morris, J.C. (2000). Thyroid iodine transport. Thyroid *10*, 321-330.

Staller, P., Peukert, K., Kiermaier, A., Seoane, J., Lukas, J., Karsunky, H., Moroy, T., Bartek, J., Massague, J., Hanel, F., *et al.* (2001). Repression of p15INK4b expression by Myc through association with Miz-1. Nat Cell Biol *3*, 392-399.

Steffen, D. (1984). Proviruses are adjacent to c-myc in some murine leukemia virus-induced lymphomas. Proc Natl Acad Sci U S A *81*, 2097-2101.

Stella Pelengaris, M.K.a.G.E. (2002). c-MYC: more than just a matter of life and death. Nature Reviews Cancer *2*, 764-776.

Stewart, J., Evan, G., Watson, J., and Sikora, K. (1986). Detection of the c-myc oncogene product in colonic polyps and carcinomas. Br J Cancer *53*, 1-6.

Stone, J., de Lange, T., Ramsay, G., Jakobovits, E., Bishop, J.M., Varmus, H., and Lee, W. (1987). Definition of regions in human c-myc that are involved in transformation and nuclear localization. Mol Cell Biol *7*, 1697-1709.

Suarez, H.G., Du Villard, J.A., Caillou, B., Schlumberger, M., Tubiana, M., Parmentier, C., and Monier, R. (1988). Detection of activated ras oncogenes in human thyroid carcinomas. Oncogene *2*, 403-406.

Takai, Y., Sasaki, T., and Matozaki, T. (2001). Small GTP-binding proteins. Physiol Rev *81*, 153-208.

Tallini, G. (2002). Molecular pathobiology of thyroid neoplasms. Endocr Pathol *13*, 271-288.

Terrier, P., Sheng, Z.M., Schlumberger, M., Tubiana, M., Caillou, B., Travagli, J.P., Fragu, P., Parmentier, C., and Riou, G. (1988). Structure and expression of c-myc and c-fos proto-oncogenes in thyroid carcinomas. Br J Cancer *57*, 43-47.

Terrier P, S.Z., Schlumberger M, Tubiana M, Caillou B, Travagli JP, Fragu P, Parmentier C, Riou G. (1988). Structure and expression of c-myc and c-fos proto-oncogenes in thyroid carcinomas. Br J Cancer *57*, 43-47.

Thomassen, D.G., Gilmer, T.M., Annab, L.A., and Barrett, J.C. (1985). Evidence for multiple steps in neoplastic transformation of normal and preneoplastic Syrian hamster embryo cells following transfection with Harvey murine *sarcoma* virus oncogene (v-Ha-ras). Cancer Res *45*, 726-732.

Thompson, E.B. (1998). The many roles of c-Myc in apoptosis. Annu Rev Physiol *60*, 575-600.

Traverse, S., Gomez, N., Paterson, H., Marshall, C., and Cohen, P. (1992). *Sustained* activation of the mitogen-activated protein (MAP) kinase cascade may be required for differentiation of PC12 cells. Comparison of the effects of *nerve growth* factor and epidermal growth factor. Biochem J *288 (Pt 2)*, 351-355.

Tsai, M.H., Yu, C.L., and Stacey, D.W. (1990). A cytoplasmic protein inhibits the GTPase activity of H-Ras in a phospholipid-dependent manner. Science *250*, 982-985.

Vennstrom, B., Sheiness, D., Zabielski, J., and Bishop, J.M. (1982). Isolation and characterization of c-myc, a cellular homolog of the oncogene (v-myc) of avian myelocytomatosis virus strain 29. J Virol *42*, 773-779.

Vervoorts, J., Luscher-Firzlaff, J., and Luscher, B. (2006). The ins and outs of MYC regulation by posttranslational mechanisms. J Biol Chem *281*, 34725-34729.

Vincent, S.D., and Robertson, E.J. (2003). Highly efficient transgene-independent recombination directed by a maternally derived SOX2CRE transgene. Genesis *37*, 54-56.

Vita, M., and Henriksson, M. (2006). The Myc oncoprotein as a therapeutic target for human cancer. Semin Cancer Biol *16*, 318-330.

Vooijs, M., Jonkers, J., and Berns, A. (2001). A highly efficient ligand-regulated Cre recombinase mouse line shows that LoxP recombination is position dependent. EMBO Rep *2*, 292-297.

Wagner, A.J., Small, M.B., and Hay, N. (1993). Myc-mediated apoptosis is blocked by ectopic expression of Bcl-2. Mol Cell Biol *13*, 2432-2440.

Weinberg, R.A. (1989). Oncogenes, antioncogenes, and the molecular bases of multistep carcinogenesis. Cancer Res *49*, 3713-3721.

Westermarck, J., and Hahn, W.C. (2008). Multiple pathways regulated by the tumor suppressor PP2A in transformation. *Trends* Mol Med *14*, 152-160.

Whitehurst, A., Cobb, M.H., and White, M.A. (2004). Stimulus-coupled spatial restriction of extracellular signal-regulated kinase 1/2 activity contributes to the specificity of signal-response pathways. Mol Cell Biol *24*, 10145-10150.

Wu, C.H., van Riggelen, J., Yetil, A., Fan, A.C., Bachireddy, P., and Felsher, D.W. (2007). Cellular senescence is an important mechanism of tumor regression upon c-Myc inactivation. Proc Natl Acad Sci U S A *104*, 13028-13033.

Wyllie, F.S., Lemoine, N.R., Williams, E.D., and Wynford-Thomas, D. (1989). Structure and expression of nuclear oncogenes in multi-stage thyroid tumorigenesis. Br J Cancer *60*, 561-565.

Yamashita, S., Ong, J., Fagin, J.A., and Melmed, S. (1986). Expression of the myc cellular proto-oncogene in human thyroid tissue. *J Clin Endocrinol Metab 63*, 1170-1173.

Zambrowicz, B.P., Imamoto, A., Fiering, S., Herzenberg, L.A., Kerr, W.G., and Soriano, P. (1997). Disruption of overlapping transcripts in the ROSA beta geo 26 gene trap strain leads to widespread expression of beta-galactosidase in mouse embryos and hematopoietic cells. Proc Natl Acad Sci U S A *94*, 3789-3794.

Zannini, M., Avantaggiato, V., Biffali, E., Arnone, M.I., Sato, K., Pischetola, M., Taylor, B.A., Phillips, S.J., Simeone, A., and Di Lauro, R. (1997). TTF-2, a new forkhead protein, shows a temporal expression in the developing thyroid which is consistent with a role in controlling the onset of differentiation. EMBO J *16*, 3185-3197.

Zimmer, A. (1992). Manipulating the genome by homologous recombination in embryonic stem cells. Annu Rev Neurosci *15*, 115-137.

ACKNOWLEDGEMENTS

First of all I would like to thank Professor Roberto Di Lauro for having welcomed me in his lab and for his theoretical and practical supervision during the past years. I am grateful to him for having always trusted me and let me develop from the person I was when I arrived in the lab to what I am now. Furthermore, I wish to thank Professor Mario De Felice for his help and availability every day from the beginning and for trying to pass me its huge experience by its invaluable advices.

I would like to thank the past and present members of Professor Roberto Di Lauro's lab: Annamaria, Pratibha, Nelly, Elena, Ramona, Maria, Francesco, Marta, Paolo, Francesca, Daniela, Alessandra, Viviana, Pina, Fulvio, Henrik, Luca and Denise, for their help and many fruitful discussions. Special thanks to Professor Concetta Ambrosino for the interesting discussions we have had.

I am grateful to Professor Alfredo Fusco for having agreed to be the supervisor of my thesis work.

I am grateful to Dr. Marzia Scarfò, Dr. Andrea Affuso and all their co-workers in Biogem for their ability in mouse care.

It is important to say that the time spent in the lab has constituted an integral part of my life in the last few years. Therefore, I feel extremely lucky to have met colleagues that have become my friends and I cannot thank them enough, for all the help during the past year, for the enthusiasm they give to everything they do and for having contributed to creating the enjoyable work environment.

Finally, I am grateful to my family, for the never-ending encouragement through life.

The last but not the least, my thanks go to all the mice used and also sacrified for our work, as precious animal model.